The effects of large-scale green roof implementation on the rainfall-runoff in a tropical urbanized subcatchment

A Singapore case study

Master of Science Thesis

Faculty Civil Engineering & Geosciences

MSc. Water Resources Management

Author

Jim van Spengen

Student number: 1158007

October 07, 2010

TU Delft

singapore-delft water alliance

Author

Jim van Spengen, BSc
Delft University of Technology
Specialisation Water Resources Management
Student number: 1158007
jimvanspengen@hotmail.com

Graduation committee

Delft University of Technology

Prof. dr. ir. N.C. van de Giesen
Faculty Civil Engineering & Geosciences
Department of Water Resources Management
n.c.vandegiesen@tudelft.nl

Dr. ir. G.H.W. Schoups
Faculty Civil Engineering & Geosciences
Department of Water Resources Management
g.h.w.schoups@tudelft.nl

Dr.ir. J.A.E. ten Veldhuis
Faculty Civil Engineering & Geosciences
Department of Sanitary Engineering
j.a.e.tenveldhuis@tudelft.nl

Delft University of Technology and Deltares, Dutch research institute

Dr.ir. F.H.M. van de Ven
Faculty Civil Engineering & Geosciences
Department of Water Resources Management
Deltares: department of Urban Water Management
Frans.vandeVen@deltares.nl

ir. A.J.J. Vergroesen
Faculty Civil Engineering & Geosciences
Department of Water Resources Management
Deltares: department of Hydrology
Toine.Vergroesen@deltares.nl

Preface

"The power to transform our cities from unhealthy, stressful, overheated environments to healthier, more sustainable communities is completely within our reach - and I believe this transformation can be achieved within a generation."

Steven Peck, founder and president Green Roofs for Healthy Cities (Cantor 2008)

This thesis report is the final result of the Master of Science graduation project within the Water Resources Management specialisation study program at the Faculty of Civil Engineering & Geosciences of the Delft University of Technology. This study has been carried out with the help of the Delft University of Technology and the Singapore-Delft Water Alliance. I would like to thank both organizations for providing me the opportunity to conduct this challenging study. The experiences I have gained during the project, both in Delft and Singapore, are unforgettable. A lot of people helped and supported me during the project. In this preface, I would like to thank them.

Special thanks go out to my primary supervisor and committee member Toine Vergroesen, who gave me the opportunity to start this study at one of the Singapore-Delft Water Alliance partners: Deltares. His fundamental knowledge of the experimental set-up and modelling, helpful comments and suggestions all significantly contributed to the quality of this thesis. Without mentioning everyone's names, I would like to thank my Deltares colleagues for the pleasant formal and informal moments at the Deltares office. I would also like to extend my appreciation to my other committee members, Nick van de Giesen, Gerrit Schoups, Marie-clair ten Velduis and Frans van de Ven for their most helpful feedback during the entire thesis process. Their enthusiastic participation in the three intermediate meetings was an important motivating factor for me during the project.

Secondly, much gratitude is owed to the people who supported me during my research period in Singapore, between January and April 2010. Thanks go out to Sae'dah Ibrahim and Sally Teh, from SDWA's secretary, who organized all formal requirements for my stay in Singapore. I would like to thank SDWA employees Umid Man Joshi, who often supported me with my experimental work and Joost Buurman, who provided me with the required GIS information and organized the contacts with Singapore's Public Utilities Board. The input from the meeting with the Public Utilities Board allowed me to use Singapore as a very interesting case study, for which I am very grateful. Substantial thanks go out to John Choy and Jamilah Bte Mohd, who supported me with knowledge, experiment set-ups and early morning laughs in the Geotechnical lab of the National University of Singapore.

Furthermore, I want to thank Deltares, the University Fund Delft (UFD), the International University Fund for Promoting Partnerships (STIR) and the Parents Fund for funding my research in Delft and Singapore.

Last, but certainly not least, I would like to thank my family, girlfriend and friends, for all encouragements and support during the entire graduation process and the rest of my study.

Delft, October 2010

Jim

Executive summary

The hydrological effects of urbanization affect the rainfall-runoff regime of many cities in the world. While traditional stormwater drainage systems are often able to effectively serve the function of flood control, they increase downstream peak flows and do not provide a habitat to support a healthy aquatic ecosystem. In order to improve this situation, water managers introduced the concept of Low Impact Development. The main purpose of Low Impact Development is to mimic predevelopment site hydrology as much as possible, by reducing the volume and peak rate of flow, controlling the water quality and promoting the recharge of stormwater with decentralized, on-site detention. Green roofs are an interesting Low Impact Development measure with great large-scale implementation potential in existing urban areas as well as in areas with new housing development, because roofs account for 20-50% of the total urban land cover. This research was initiated by a lack of knowledge related to the quantitative hydrological effects of green roofs in the tropics. Singapore was chosen as a case study for this research. The main goals of the research are 1) to analyze the effects of green roofs on the rainfall-runoff in Singapore and 2) to determine the quantitative hydrological contribution of large-scale green roof implementation to sustainable stormwater drainage systems in Singapore.

Methodology

To achieve these goals a research approach is used, which combines green roof experiment measurements with green roof model simulations. First, an approach to measure and simulate the rainfall-runoff processes that occur on 1 m^2 experiment platforms has been set up. Runoff data from an extensive green roof platform, with a 12 cm soil media, and a reference roof were analyzed for 66 rainfall events in four periods of one month. Retention, peak discharge reduction, detention and base flow variables and performance indicators were used to quantify the hydrological effects of green roofs. An unsaturated zone model for the simulation of green roof rainfall-runoff was conceptualized and specified in the physically based HYDRUS-1D simulation software, which numerically solves the Richards equation for water flow in variably saturated porous media. A 9.4 ha subcatchment was used as a case study in order to quantify the hydrological effects of large-scale green roof implementation on the rainfall-runoff in Singapore. Based on a conceptualized representation of the Sunset Way subcatchment, a hydraulic routing model was build in the SOBEK software package. As in other available commercial hydraulic models, an explicit green roof modelling option is not available in the current SOBEK software. Therefore, this thesis presents a methodology that couples pre-processed green roof runoff from the HYDRUS-1D model to the SOBEK model for an accurate simulation of the scaled-up green roof effects in the case study area.

Results

Analysis of experiment measurements shows that the green roof platform retained 39% (234 mm) more rainfall than a reference roof and reduces the peak discharge with 64% compared to the reference roof. The average time to peak of the green roof hydrograph appeared 34 minutes after the reference roof peak and green roof platforms provided an average additional base flow runoff of 0.41 liters/m^2 . However, *average* experiment performance values do not give practical implications whether green roofs are an effective stormwater management solution. Individual event analysis shows that green roofs do not simply absorb water and slowly release it over a period of time. Instead, *retention* is the primary function of green roofs: rainfall is retained until the maximum storage capacity of the soil media. *Detention and peak discharge reduction* is provided by green roofs

until the moment of soil saturation. After this moment, green roof peak detention is limited to 1-2 minutes and runoff intensities closely follow the rainfall and reference roof intensities. *Base flow conservation* by extensive green roofs is not provided for rainfall events that are nearly or totally retained. If green roofs get saturated during the rainfall event, minor base flow conservation was observed for up to 3 hours after the last rainfall.

Several laboratory and field experiments were performed in order to provide a physically based initial set of parameters for the HYDRUS-1D model. Four unique optimized parameter vectors for the hydraulic functions of van Genuchten were determined with inverse modelling of transient flow experiments. It was shown that runoff at the bottom of a green roof can be described with a seepage face boundary. Runoff starts or stops when the soil water content at the bottom respectively exceeds or drops below a threshold value of 0.61. The physical background of the model provided a better understanding of the hydrological processes and the soil physics in a green roof media. Simulation results of twelve rainfall-runoff events in September, 2009 (calibration period) and December, 2009 (validation period) show that the HYDRUS-1D model gives an accurate representation of the measured green roof runoff characteristics on event scale. A limitation of the model is the over prediction of the green roof runoff when events quickly follow-up.

Scenario simulations in the Sunset Way subcatchment in Singapore show that the combined hydrological effects of large-scale roof greening on the rainfall-runoff in the main outflow canal of the area are limited. First, runoff analysis in the case study area under extreme meteorological conditions showed that extensive green roofs provide a negligible peak reduction and detention under Singapore's current design storm with a T=5 years return period. However, unilateral design requirements bias this result. Still, extensive green roofs would not have prevented flooding under the actual meteorological conditions of the November 19 flood storm. Second, negligible improvements in the reduction of non-natural water level variations were observed when the green roof scenario simulation results were compared to the base case scenario simulation results under the actual meteorological conditions of September 2009. Peak flow reduction is conditionally significant, but green roofs are particularly not suitable to provide a base flow, which can replace the natural function of groundwater during dry spells. A factor that reduces the effectiveness of green roofs at subcatchment-scale compared to experiment results, is the limited building coverage.

Conclusions and recommendations

Result analysis of this research shows that a standalone large-scale implementation of 12 cm extensive green roofs does not significantly contribute to the quantitative hydrological goals of Singapore's ABC Waters Programme. The hydrological contribution of green roofs to sustainable stormwater drainage systems in Singapore can be enhanced when the design fundamentals and implementation strategy are reconsidered and adapted to the proposed hydrological effects and site specific requirements. The presented approach which is based on model coupling of a physically based runoff generation model to an existing routing model created theoretical and practical spin-offs for the development of green roofs, as one of the LID measures that can contribute to sustainable stormwater drainage system development. Hence, the promotion and international exchange of the obtained knowledge, ideas and recommendations can contribute to the development of sustainable stormwater drainage systems in other tropical cities and the rest of the world.

Contents

List of figures

List of tables

List of symbols

a	Empirical interception constant	[L]
a_i	Empirical constant for the radiation extinction by the canopy	[-]
A	Surface area	[L^2]
$ACSF\ (t)$	Actual cumulative surface flux	[LT^{-1}]
b	Soil cover fraction or *SCF*	[-]
$\boldsymbol{b}$	Optimized parameter vector in the inverse modelling objective function	[-]
$b(x)$	Normalized distribution of the potential water uptake over a root zone	[L^{-1}]
c	Runoff factor in the surface runoff routing method	[T^{-1}]
c_p	Specific heat of moist air	[$L^2T^{-2}K^{-1}$]
C	Rational runoff coefficient	[-]
C_n	Courant number	[-]
CN	Runoff curve number in the CN method	[-]
C_r	Capillary rise	[LT^{-1}]
e_a	Saturation vapour pressure at temperature T	[$ML^{-1}T^{-2}$]
e_d	Actual vapour pressure	[$ML^{-1}T^{-2}$]
E	Evaporation	[LT^{-1}]
E_o	Open water evaporation	[LT^{-1}]
E_{NS}	Nash-Sutcliffe modelling efficiency	[-]
E_p	Potential evaporation	[LT^{-1}]
E_s	Evaporation from the soil	[LT^{-1}]
ET	Evapotranspiration	[LT^{-1}]
ET_a	Actual Evapotranspiration in HYDRUS-1D	[LT^{-1}]
Et_{aero}	Aerodynamic term of the Potential evapotranspiration	[LT^{-1}]
ET_p	Potential evapotranspiration according to Penman-Monteith	[LT^{-1}]
ET_{rad}	Radiation term of the Potential evapotranspiration	[LT^{-1}]
F	Infiltration	[LT^{-1}]
G	Soil heat flux	[MT^{-3}]
h	Water pressure head	[L]
h_a	Minimum allowed pressure head at the soil surface	[L]
h_n	Dynamic storage term in the surface runoff routing method	[L]
h_s	Non-zero minimum capillary height	[L]
h_{smax}	Maximum pressure head at the soil surface	[L]
h_{seep}	Seepage face pressure head	[L]
H	Hydraulic head	[L]
I	Interception	[LT^{-1}]
I_a	Initial abstraction term in the CN method	[L]
k	Constant for the radiation extinction by the canopy	[-]
K	Hydraulic conductivity or permeability	[LT^{-1}]
K_s	Saturated hydraulic conductivity	[LT^{-1}]
K_r	Relative hydraulic conductivity	[-]
l	Empirical pore-connectivity parameter	[-]
L	Soil column length in Darcy's Law	[L]
LAI	Leaf Area Index	[-]
m	Empirical shape parameter equal to 1-1/n in the van Genuchten equations	[-]
m_i	Empirical shape parameter for the sub curves in a dual pore-size distribution	[-]
m_y	Different sets of measurements in the inverse modelling objective function	[-]
M_{dry}	Mass of the dry soil	[M]
M_w	Mass of the wet soil	[M]
n	Pore-size distribution in the van Genuchten equations	[-]
n_i	Pore-size distribution for the sub curves in a dual pore-size distribution	[-]

n_j	Data points in a particular set in the inverse modelling objective function	[-]
P	Precipitation	[LT^{-1}]
$PCSF\ (t)$	Potential cumulative surface flux	[LT^{-1}]
$P2H$	Value of the limiting pressure head, below which roots cannot longer extract water at the maximum rate (at a potential transpiration rate of 0.5 cm/day)	[L]
$P2L$	Value of the limiting pressure head, below which roots cannot longer extract water at the maximum rate (at a potential transpiration rate of 0.1 cm/day)	[L]
$P3$	Value of the pressure head, below which root water uptake ceases	[L]
q	Specific runoff or discharge	[LT^{-1}]
q_o	Specific overland flow	[LT^{-1}]
q_{bf180}	Performance variable for the base flow 180 min after the last recorded rainfall on event scale	[L]
q_c	Performance variable for the cumulative runoff on event scale	[L]
q_i	Inflow into the drainage or sewer network in the surface runoff routing method	[LT^{-1}]
q_{int}	Interflow	[LT^{-1}]
q_{peak}	Performance variable for the peak discharge on event scale	[LT^{-1}]
q_{tot}	Performance variable for the cumulative runoff over the entire period	[L]
q_s	Specific surface runoff	[LT^{-1}]
q_{gw}	Specific groundwater seepage	[LT^{-1}]
Q	Runoff or discharge	[L^3T^{-1}]
Q_{bf180}	Performance variable for the base flow 180 min after the last recorded rainfall on event scale	[L^3]
Q_c	Performance variable for the cumulative runoff on event scale	[L^3]
Q_{peak}	Performance variable for the peak discharge on event scale	[L^3T^{-1}]
Q_{tot}	Performance variable for the cumulative runoff over the entire period	[L^3]
r_a	Aerodynamic resistance	[TL^{-1}]
r_c	Crop canopy resistance	[TL^{-1}]
R	Percolation	[LT^{-1}]
R_n	Net radiation at the earth surface	[MT^{-3}]
R_{ns}	Net solar radiation	[MT^{-3}]
R_s	Solar or shortwave radiation	[MT^{-3}]
P	Precipitation	[LT^{-1}]
P_a	Atmospheric pressure	[$ML^{-1}T^{-2}$].
S	Plant root water uptake sink term	[T^{-1}]
S_i	Sensitivity index	[-]
SCF	Soil cover fraction	[-]
S_e	Effective saturation	[-]
S_m	Potential maximum retention in the CN method	[L]
S_p	Potential water uptake	[T^{-1}]
S_t	Storage term in the water balance	[L^3]
t	Time	[T]
t_c	Time of concentration	[T]
t_d	Drain flow time	[T]
t_o	Overland flow time	[T]
tt_{peak}	Performance variable for the time to peak relative to the rainfall peak	[T]
T	Transpiration or average air temperature	[LT^{-1}], [K]
T_p	Potential transpiration	[LT^{-1}]
TT_{peak}	Performance variable for the time to peak relative to the rainfall peak	[T]
v_j	Measurement set weighing factor in the objective function	[-]
V	Flow through volume in Darcy's Law	
V_t	Volume of the total soil body	[L^3]

V_w	Volume of water	[L^3]
w_i	Weighing factors for the sub curves in a dual pore-size distribution	[-]
$w_{i,j}$	Data point weighting factor in the inverse modelling objective function	[-]
x	Vertical spatial coordinate above the reference level in the Richards equation	[L]
x_i	Value of a parameter in the sensitivity index	[any]
y_j	Simulated space-time variable in the inverse modelling objective function	[any]
y_j^*	Measured space-time variable in the inverse modelling objective function	[any]
Z	Value of a performance measure in the sensitivity index	[any]
α	Inverse air entry value or bubbling pressure in the van Genuchten equations	[L^{-1}]
$\alpha(h)$	Root-water uptake stress response function	[-]
α_i	Inverse air entry value for the sub curves in a dual pore-size distribution	[L^{-1}]
α_r	Albedo value	[-]
γ	Psychromatic constant	[$ML^{-1}T^{-2}K^{-1}$]
Δ	Slope of the vapour pressure curve	[$ML^{-1}T^{-2}K^{-1}$]
θ	Volumetric soil water content	[-]
θ_m	Extrapolated maximum soil water content	[-]
θ_r	Residual volumetric soil water content	[-]
θ_s	Saturated volumetric soil water content	[-]
θ_{seep}	Seepage face soil water content	[-]
λ	Latent heat of vaporation	[L^2T^{-2}]
ρ	Atmospheric density	[ML^{-3}]
ρ_{water}	Density of the water	[ML^{-3}]

List of abbreviations

ABC	Active, Beautiful, Clean (Singapore's Waters Programme)
ACSF	Actual cumulative surface flux
ADWP	Antecedent dry weather period
ASRPI	Additional stormwater retention performance indicator (relative to a reference roof)
BFPI	Base flow performance indicator
CN	Curve number
CSO	Combined sewer overflow
DPI	Detention performance indicator
EVAP	Evaporation experiment
GIS	Geographic Information Systems
GR1	Green roof experiment platform 1
GR2	Green roof experiment platform 2
HDB	Singapore's Housing & Development Board
IDF	Intensity-duration-frequency
IMCDS	Singapore's Inter-Ministerial Committee on Sustainable Development
LAI	Leaf area index
LID	Low Impact Development
MSO	Multi-step outflow method
NUS	National University of Singapore
OSO	One-step outflow method
PDPI	Peak discharge performance indicator
PUB	Singapore's Public Utilities Board
RefR	Reference roof experiment platform
RPI	Retention performance indicator (relative to the rainfall)
RR	Rainfall-runoff
RWU	Root water uptake
SCF	Soil cover fraction
SDWA	Singapore-Delft Water Alliance
SSQ	Value of the objective function for inverse modelling in HYDRUS-1D
TIA	Total impervious area
TDR	Time Domain Reflectrometer
WBM	Water balance model
WRC	Water retention curve
WWTP	Wastewater treatment plant

List of definitions

Detention	Delay of stormwater runoff.
Drain	Any canal, culvert, river or water course
Green roof	A roof of a building that consists of a waterproofing layer, drainage layer, filter sheet, soil media and a vegetation cover on top.
Hydraulic functions	Geophysical relationship between the soil water content, negative pressure and hydraulic conductivity curve.
Inverse modelling	A general mathematical method to determine unknown causes on the basis of observation of their effects.
Large-scale green roof analysis	Quantitative hydrological analysis of green roof effectiveness at (sub)catchment-scale.
Low Impact Development	Decentralized stormwater management measures which are designed to maintain or re-establish a natural hydrological regime.
Model calibration	Part of the model cycle that focuses on adjusting the internal model parameter values to obtain a better fit between measurements and simulations.
Model conceptualization	Part of the model cycle that addresses a mathematical description of the governing flow equations and the selected hydraulic model.
Model specification	Part of the model cycle that focuses on specifying an initial set of parameter values for the boundary conditions, the hydrological process parameters and the soil hydraulic model parameters.
Model validation	Part of the model cycle that has the aim to demonstrate whether a model simulation gives a reasonably accurate representation of real system measurements.
Model verification	Part of the model cycle that has the aim to ensure that the model does what it is intended to do (does the model implements the assumptions correctly?).
Performance indicator	Performance measure to evaluate the effectiveness of green roofs, relative to the rainfall or a reference roof. Performance indicators can be derived from performance variables.
Performance variable	Performance measure to evaluate the characteristics of green roof runoff. A variable is a static value, not relative to the rainfall or reference roof runoff (except for the time to peak, which is measured relative to the rainfall peak).
Rainfall event	A period with rain, separated to another period of rain by a 0 mm dry spell of at least 1 hour.
Retention	Abstraction of rainfall.

Routing model	Water model that describes the hydrodynamic routing towards the drainage or sewerage system, routing through devices and routing in the drainage or sewerage system (synonyms used: large-scale rainfall-runoff model or SOBEK model).
Runoff generation model	Water model that describes the losses and delays that occur in the green roof soil media or at any other (un)paved surface (synonyms used: small-scale rainfall-runoff model, unsaturated zone model, HYDRUS model).
Small-scale green roof analysis	Quantitative hydrological analysis of green roof effectiveness at experiment-scale.
Stormwater drainage system	A traditional system of drains for the conveyance or storage of stormwater.
(Sub)catchment	A separated hydrological unit where water from precipitation drains into a body of water.
Sustainable stormwater drainage system	A holistic system approach including drains and a sequence of LID measures designed to drain surface water in a manner that will provide a more sustainable way of runoff routing than what has been the conventional practice of routing run-off: through a drain to a watercourse.

1 Introduction

1.1 Urban water management problem statement and green roofs

The hydrological characteristics of urban water systems are predominantly influenced by (a) a relatively large proportion of impervious surface area and (b) the presence of man-made or hydraulically improved drainage systems (Bedient, Huber and Vieux 2008, 357). Because less pervious area is available for infiltration and because unlined natural drainage channels are being replaced by lined channels or storm sewers (Wong and Chen 1989), the response of an urban catchment to rainfall is much faster than the response of a rural area with comparable geophysical characteristics such as area and slope (Bedient, Huber and Vieux 2008). Next to this decrease in lag time between rainfall peak and discharge peak, urban development also increases the runoff volume and runoff peak. The combined effects of urbanization on the rainfall-runoff increases the exposure to the hazard of flooding (Mansell 2003) and erosion. Combined sewer overflows (CSO's) and the discharge of pollutants from roads and other hard surfaces also negatively affect the groundwater quality and the ecological state of the catchment's waterways.

(a) Houston. Source: SEMP (2005) (b) Singapore. Source: Simply Jean (2010)

Figure 1. Examples of urban flooding

Traditional urban water management practices focus on the probability reduction of floods by stormwater drainage, channelization and levee construction or improvement. Although these measures are a common traditional form of flood protection, their main disadvantage is that they merely pass the danger of flooding further downstream (Mansell 2003, p.23-24). By doing this, they could in fact increase the risk of flooding. Previously, emphasis regarding CSO solutions was placed on the so called "end of pipe" solutions. Hydraulic capacity extension of the sewer systems, flow monitoring, sewer quality sampling, dredging of contaminated soils and the construction of large underground storage tanks are example solutions that were introduced to decrease the consequences of CSO's, water on the street and sewer back-ups in homes. Low Impact Development (LID) is a relatively new concept in stormwater management. LID is a site design strategy that attempts to maintain or re-establish the predevelopment hydrological regime (EPA 2000). LID measures are based on controlling stormwater at the source (EPA 2000) by the use of micro-scale controls such as vegetated swales, permeable pavement, infiltration trenches and green roofs. An important concept of LID is emphasis on evapotranspiration from retained stormwater (Bedient, Huber and Vieux 2008, p.360). LID is unlike conventional approaches that convey and manage rainfall-runoff *at the base* of the urban catchment (EPA 2000, 1). One of the LID practises that has

high potential to reduce and detain urban rainfall-runoff are green roofs (Deutsch, et al. 2005, Carter and Rasmussen 2006). Green roofs become particularly interesting in heavily populated urban areas, where land area is unavailable for other LID practices and where defined infrastructure increases the difficulty to construct underground storage devices (Hilten, Lawrence and Tollner 2008, p.289).

Now that more and more (mega) cities develop urban water policies that do stimulate the development of green roofs, the demand for adequate understanding of the effects of green roofs is becoming vital. The research on the effects of green roofs in temperate climates, like in most parts of Europe and the US, is already reasonably developed, while research on this topic is only beginning in the tropics (Köhler, Schmidt and Grimme, et al. 2001). Especially scientific results of green roof effects in tropical countries are rather rare (Laar and Grimme 2006). This MSc thesis obliges to this particular lack of knowledge by presenting an assessment of the quantitative rainfall-runoff effects provided by green roofs in a tropical country. Therefore, a case study in Singapore will be used.

1.2 Global green roof development

Green roofs, also named vegetated roofs, are a LID measure that incorporate a soil layer with vegetation on top of traditional roofing systems. Green roofs have a long history, which apparently is in contrast with the relatively short lifetime of the LID concept of comprehensive land planning and engineering (LID-centre 2009). From 2200 until 500 before the common era, temple-towers called Ziggurats were used in Mesopotamian religions (Kjeilen 2009). It is believed that the aesthetical, distinctive sloping walls of Ziggurats were covered with trees and shrubs (Kjeilen 2009). The Hanging Gardens of Babylon, one of the seven ancient world wonders, are another example of historical garden architecture. Before 1970, green roofs were mainly constructed because of aesthetic and insulation benefits as well as their property to act as a waterproofing layer (van de Ven 2007).

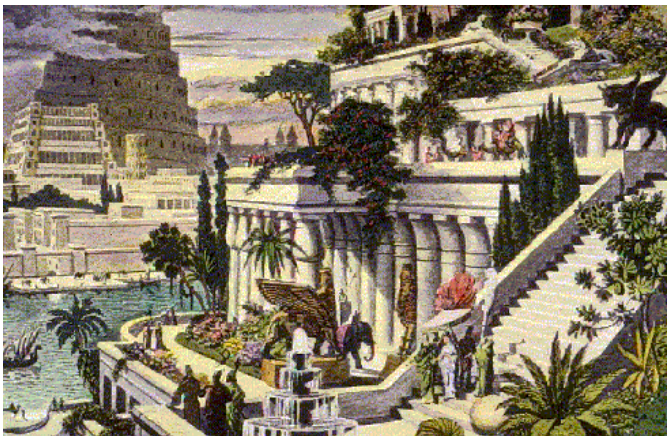

(a) Gardens of Babylon

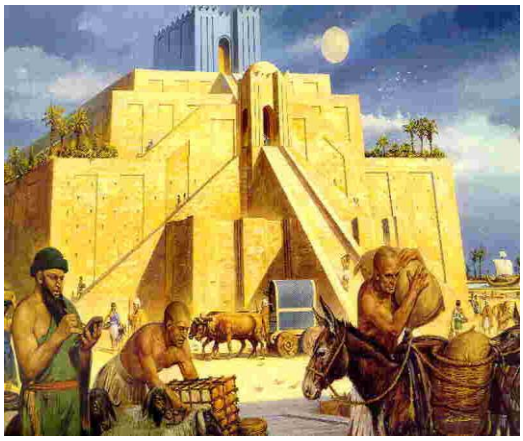

(b)Ziggurat of Ur

Figure 2. Historical green roofing

Modern green roofs were introduced in Germany in the early 1970's. Innovation of green roof technology was initiated in cooperation with private technology companies such as Optima and Bauder and studies performed by landscape architects and other researchers (Velazquez 2003). Present green roof designs evolved from study and testing of materials, development of industrial standard codes and trial and error (Velazquez 2003). These and other studies have resulted in several publications with established standards for green roof design, roofing materials, growing media, plant materials and so on (Cantor 2008). Today, green roof benefits are considered in a much

broader context. The most important advantages of green roofs are the retention and detention of rainfall-runoff in urban areas, a longer lifetime of the roofing material, insulation, reduction of the urban heat island, noise-levelling, water and air quality improvement, habitat development and aesthetic advantages (Mentens, Hermy and Raes 2002). Because of this broad scope of benefits green roofs are proposed and deployed on a small and large scale in many places. Urban areas in Germany are European trendsetters. The cities of Stuttgart (600.000 inhabitants) and München (1.3 million inhabitants) have realized 1.200.000 m^2 and 1.300.000 m^2 of green roof area respectively (Pittery and Vorstenbosch 2004). Although these cities are trendsetters, the areal contribution of green roofs is only 0.5% in Stuttgart and 0.4% in München. In the early 90's, when German green roof publications were translated in English (Cantor 2008), green roof technology transfer to the rest of the world rapidly increased. Examples of modern green roof projects are presented in Figure 3.

(a) Chicago

(b) Tokyo

(c) Stuttgart

(d) New York

Figure 3. Modern green roof practices. Source: Metropolismag.com (2006)

1.3 Application of green roofs in the tropics

Notwithstanding the adaptation of green roofs in several innovative countries in temperate climates, green roofs are still an exception in tropical climates (Laar and Grimme 2006). Meteorological characteristics of tropical climates significantly differ from those in temperate climates. They have a 12-month vegetation period, higher temperatures throughout the year, higher relative humidity, higher solar radiation and two to three times more rainfall (Köhler, Schmidt and Grimme, et al. 2001, Laar and Grimme 2006). A one-in-hundred year design storm for temperate climates, might well be an annual event in the tropics (Köhler, Schmidt and Grimme, et al. 2001). The expected advantages of green roof implementation in tropical countries might be even more important than in temperate climates. Besides the larger importance of evaporative cooling, which has the potential to decrease the urban heat island, green roofs potentially decrease the probability of flooding in tropical cities. At

present, this chance is relatively high because of frequent heavy rainstorms in absence of an efficient drainage system (Laar and Grimme 2006). Next to these additional advantages, potential green roof limitations of large-scale green roof implementation in tropical countries must be determined too. Consequently a research scope which is specifically adjusted for tropical climates, is preferable.

1.4 Scope of the research

Several earlier studies on the effects of green roofs in temperate climates show that green roofs offer great opportunities to retain, detain and reduce the peak discharge of rainfall-runoff (Berghage, Beattie, et al. 2009, Martin 2008, Kidd 2005). However, research provides little or no knowledge on the quantitative effects of large-scale green roof implementation (Joshi and Vergroesen 2010, Martin 2008), especially not in tropical regions of the world. This MSc thesis will mainly focus on the quantitative effects of green roof implementation on the rainfall-runoff in a tropical urbanized subcatchment. At the moment, experimental green roof research is being performed as a part of the Singapore-Delft Water Alliance (SDWA) research agenda. SDWA is a multinational, interdisciplinary research Centre for Water Knowledge, involving Singapore's Public Utilities Board (PUB), the National University of Singapore and Deltares (the Netherlands). This MSc thesis will be carried out within the SDWA Centre for Aquatic Science 'Pandan Canal' research programme. Green roof experiment measurements will be used to quantify the small-scale effects of green roofs on the rainfall-runoff in Singapore. The literature review will provide an overview of the established green roof knowledge, ideas and modelling techniques that can be used to quantify the effect of green roofs on the rainfall-runoff. Special attention will be given to the scientific foundation and the main advantages, disadvantages and applicability of available green roof modelling techniques. Based on this literature review, a hydrologic model of the unsaturated zone will be set up that includes the most relevant green roof rainfall-runoff predicting parameters. This runoff generation model will then be integrated into a hydraulic routing model to quantify the large-scale effects of green roof implementation in a tropical urbanized subcatchment. An urbanized subcatchment that discharges into the Sungei Ulu Pandan Canal in Singapore will be used as a case study. The research has the intention to add knowledge on the effects of large-scale implementation of green roofs in Singapore specifically, but also generically for all tropical urbanized areas. This research intention corresponds with one of the goals of the Ministry of Environment and Water Resources and the Ministry of National Development to build Singapore into an outstanding knowledge hub in the latest technology and services that will help cities to grow in a more environmentally friendly way (IMCSD 2009).

1.5 Research goals and main research question

The main goals of this research that are derived from the study context in chapters 2 and 3 are:

1. Analyze the effects of green roofs on the rainfall-runoff in Singapore;
2. Determine the quantitative hydrological contribution of large-scale green roof implementation to sustainable stormwater drainage systems in Singapore.

The research anticipates on the lack of knowledge on the quantitative effects of large-scale green roof implementation in the tropics. Because the effectiveness of solutions such as large-scale roof greening vary per location, urban water management policy is always custom made. To the fact that this study can be seen as a pilot in analyzing the effects of large-scale green roof implementation in

the tropics, a case study in Singapore is used. A final evaluation of this case study will clarify whether the promotion of Skyrise Greenery as a sustainable contribution to Singapore as a *City of Gardens and Water* (IMCSD 2009) is actually worthwhile the efforts. This research also has the intention to open up the doors for a more fundamental understanding of the effects of large-scale green roof implementation on the rainfall-runoff in tropical urbanized areas. The main research question that is coupled to the purpose of the study is:

"What is the quantitative hydrological contribution of large-scale green roof implementation to sustainable stormwater drainage systems in Singapore?"

Figure 4. Singapore offers perfect large-scale green roof implementation possibilities

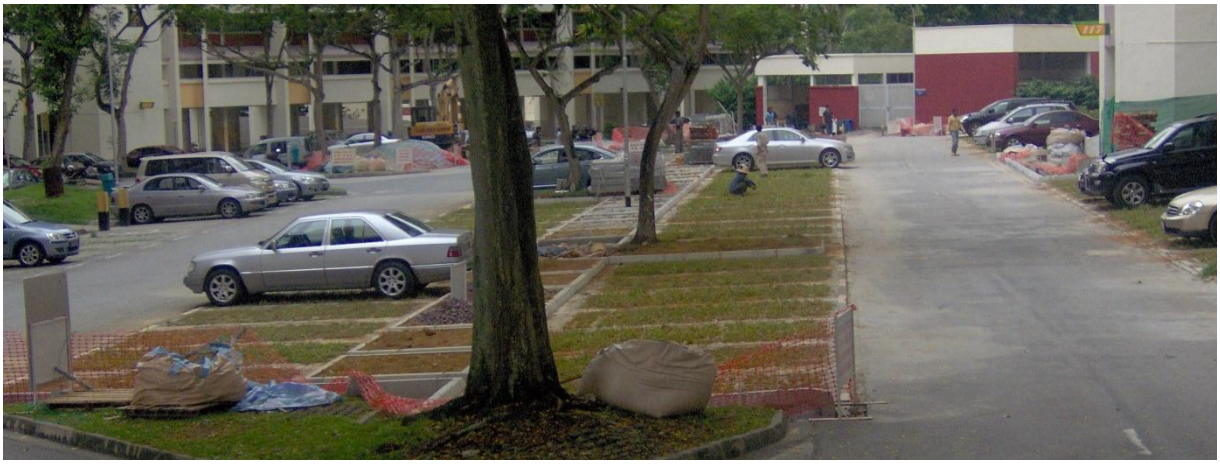

Figure 5. LID measure implementation in Singapore: porous pavement on parking lots

1.6 Research approach

A three-step research approach has been set up, in order to answer the main research question:

Introduction. The introduction consists of the problem description, green roof development, research goals, research scope, research approach and structure of the MSc research.

Step 1. The aim of the literature review is to give a critical evaluation of current green roof knowledge, ideas and hydrological modelling approaches. Singapore will be introduced as a case study.

Step 2a. The small-scale effects of green roofs on the rainfall-runoff will be analysed first. Measurements from an experimental set up will be used for this purpose. This will be done at the experimental set-up at the National University of Singapore. The combination of experimental green roof analysis results with information from the literature review has to give a better insight into the basic hydrological processes and parameters that are important for the prediction of runoff generation from green roofs in the tropics.

Step 2b. The main goal of step 2b is to create a green roof rainfall-runoff modelling tool. The goal of this model is to integrate all relevant hydrological processes and parameters, that were inventoried in step 1 and 2a. The model will be verified, calibrated and validated with measurements from the experiment set-up. The aim is to at least obtain a hydrologic model that can predict rainfall-runoff from green roofs in Singapore. Hopefully indications or recommendations for a more general applicable prediction tool or model can be given.

Step 3. The main goal of step 3 is to create a hydraulic routing model that integrates the hydrologic modelling output of step 2b and that predicts the effects of large-scale green roof implementation on the rainfall-runoff in the urban Sunset Way subcatchment in Singapore ($1^0$19'22.33"N $103^0$46'12"67"O). Hence, different scenarios have to be simulated. A base case scenario (with normal roofs) will be used to represent the current state of the system. A green roof scenario will be used to simulate the cumulative effects of large-scale green roof implementation on the rainfall-runoff characteristics of the area.

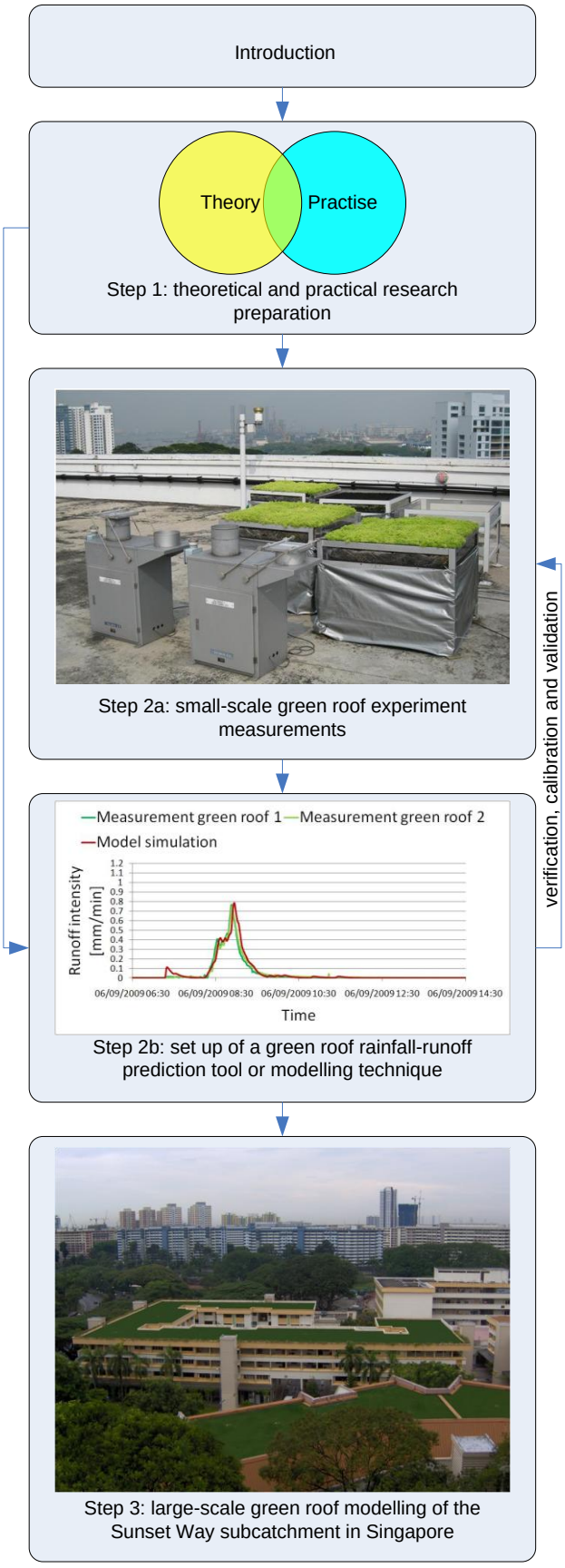

1.7 Structure of the report

The structure of the report follows the research approach that was identified in paragraph 1.6:

Part 1: theoretical and practical contextual preparation for the research

Chapter 2 of this thesis contains an exploration of the theoretical project context by means of a literature review. The literature review first aims to present an overview of the most important terms and concepts of urban water management challenges and urban water management strategies. Established ideas and knowledge about green roofs types, designs and effects will be synthesized. Secondly, a critical review of current modelling approaches that aim to simulate the effects of green roofs on the rainfall-runoff, will be presented. Final conclusions and recommendations of the literature review form the basis for the actual research of this thesis. Chapter 3 gives the practical project context. The Singapore case study will be introduced here. The main research question will be subdivided into subquestions in the end of this chapter. The sub research questions and the research objectives are derived from the theoretical and practical project context findings.

Part 2: small-scale green roof analysis

Chapter 4 starts with a description of the small-scale green roof experiments and an analysis of the available and measured rainfall-runoff data from the green roof set-up in Singapore. Chapter 5 describes the goal of the hydrologic model, the hydrologic model conceptualization, specification of input data and parameters, model assumptions and model results. The model output will be compared with real measured output. Verification, calibration and validation of the modelling tool is the last point of interest in this chapter.

Part 3: large-scale green roof analysis

Chapter 6 presents the second modelling aspect of this MSc thesis: the large-scale green roof effect simulations in Singapore. An appropriate hydraulic modelling tool combined with a GIS interface will be used to simulate the effect differences between a base case scenario and a green roof scenario. A proper link between the hydrologic modelling output and the hydraulic model input will have to be made. A description of the used methodology will include a case study area description, coverage scenarios, model schematization and meteorological test conditions. Large-scale green roof implementation results are presented first. The contribution of green roofs to a more sustainable development of stormwater draining systems in Singapore and tropical urbanized areas in general will be discussed. The last chapter, chapter 7, will present the conclusions and recommendations of the thesis research.

Part 1 Theoretical and practical contextual preparation for the research

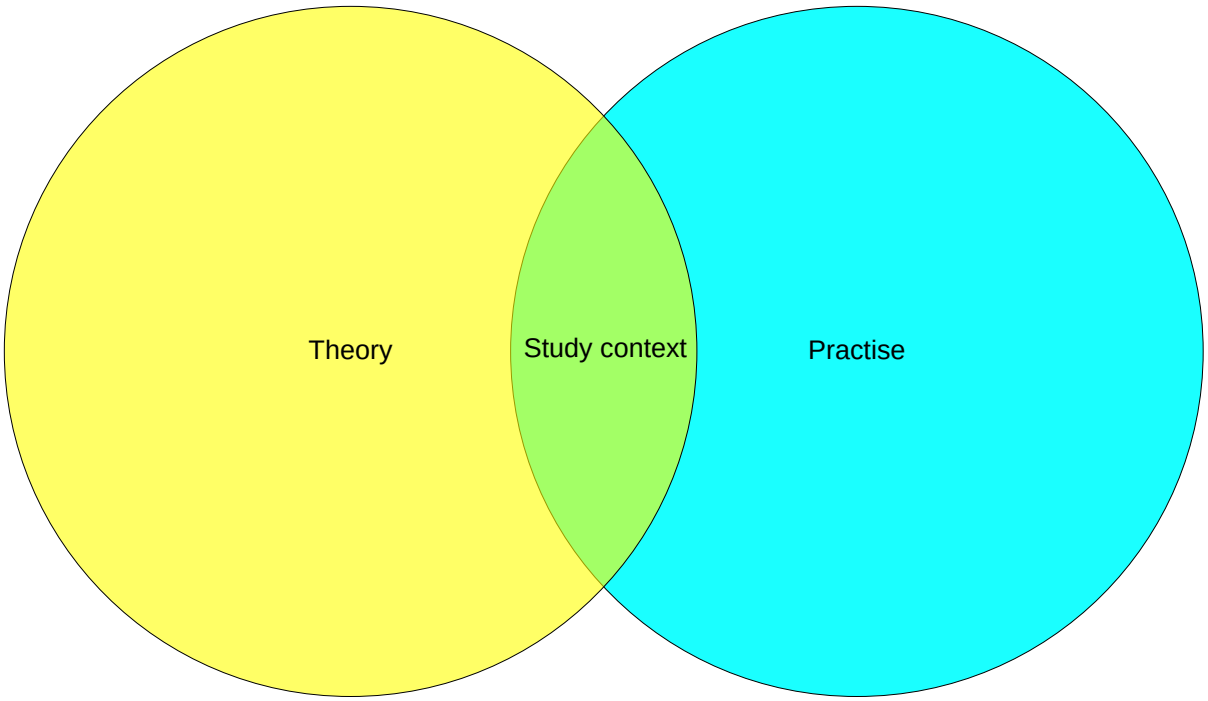

Figure 6. Theory and practice form the study context demarcation

The main objective of the first Part is to establish a study context. Research goals and research questions are then derived from this study context. The context of this green roof study is demarcated by the intersection of theoretical findings and a practical case study in Singapore. This idea is visualized in Figure 6.

Chapter 2 contains the literature review. Current arguments and ideas in the field of green roofs that are presented in articles, books, theses and dissertations will be compared, summarized and synthesized. Leads for further research will be identified. Practical relevance of the proposed study is introduced by embedding the defined study context demarcation in a particular problem situation with a real problem owner. A subcatchment in Singapore will be presented as the case study area and Singapore's Public Utilities Board will be presented as the problem owner. Relevant information about the case study in Singapore will be presented in Chapter 3. Here, Singapore's ABC Waters Programme philosophy and underlying Waters Programme Strategy will be introduced. Finally, the main research question will be specified into sub research questions and the main goals of the case study will be presented.

2 Literature review

2.1 Introduction

The purpose of this literature review is to critically analyze, compare, summarize and synthesize the current arguments and ideas from articles, books, theses and dissertations that are relevant to the scope of this research. The first underlying idea of this literature review is to provide an up-to-date overview of the basic principles concerning the topic. Second, the literature review can provide leads for further research within the area of interest. Gaps in green roof knowledge that are relevant to the scope of this thesis have to be filled in during the research part of this study. The literature review is organized around and related to the research goals and main research question of this thesis. That is to analyze the effects of green roofs on the rainfall-runoff in Singapore and to determine the quantitative hydrological contribution of large-scale green roof implementation to sustainable stormwater drainage systems in Singapore.

Basic principles and knowledge of the hydrological cycle, urban water management challenges, current urban water management policy approaches and the different Low Impact Development measures are presented in paragraphs 2.2, 2.3 and 2.4. Different green roof types and established designs are addressed in paragraph 2.5. A summary of the most important advantages and disadvantages of green roofs are presented in paragraph 2.6. With respect to the scope of this research, the main focus is on synthesizing current results and methodological approaches from researches that aim to quantify the influence green roofs have on the artificially changed rainfall-runoff relationship in urban areas. Leads for assessing the quantitative effects of green roofs in tropical areas such as Singapore, follow from an evaluation on the applicability of established green roof knowledge, ideas and analysis methodologies in paragraph 2.7. The last part of the literature review (paragraph 2.8) provides an overview of current green roof modelling techniques and the potential applicability of these models within this research. First, an overview of and a discussion on the modelling techniques that have been used in experiment-scale green roof research is given. Subsequently, the current research state in the field of large-scale green roof effect modelling will be reported. The outcome of the green roof modelling review should provide a basis for the setup of (an) appropriate green roof model(s) that can be used to simulate the hydrological effects of green roofs at experiment and subcatchment-scale in Singapore.

2.2 The hydrological cycle

Hydrology involves the study of the origin, appearance and movement of water in all her forms on top and underneath the surface level (Akker and Savenije 2006). The circulation of water over the terrestrial part of the earth's surface is often referred to as the hydrological cycle. A schematization of the hydrological cycle is presented in Figure 7. The hydrological cycle is a representation of the real stocks and processes that contains simplifications and generalizations (Ward and Robinson 1990). For the purpose of this study, the principle of the hydrological cycle and the introduced terminology, can be of great value though. It gives a theoretical foundation for later green roof research steps and understanding.

Radiation energy from the sun is one of the main force behind the hydrological cycle (Akker and Savenije 2006). It drives the cycle by *open water evaporation* (E_o) from the oceans and inland surface water. *Precipitation* (P), that reaches the *first separation point* on the earth's surface as snow, rainfall or hail, will first be temporarily stored on the ground, vegetation, buildings and paved area (Savenije

2007). Direct evaporation from this temporary surface storage is called *interception* (*I*). The remaining precipitation may replenish the soil water as *infiltration* (*F*) up until the maximum rate of infiltration. As long as the rate of water delivery to the surface is smaller than the infiltration capacity, the process is *supply controlled* (Hillel 1982). This means that water infiltrates as fast as it arrives. When the rate of water delivery starts exceeding the infiltration capacity of the soil, the process is *surface controlled or profile controlled* (Hillel 1982). Excess water that is beyond the actual rate of infiltration will flow away as *overland flow* (q_o). Infiltrated water reaches the soil moisture, that is indicated as the *second separation point*. Moisture in this *unsaturated zone* can be removed either by *evaporation from the soil* (E_s), *transpiration* (*T*) from soil to plant tissue into water vapour, by *interflow* (q_i) to the surface water or by gravity drainage to the groundwater table. This last process is called *percolation* (*R*). A hydrological expression named e*vapotranspiration* (*ET*) is often used as a collection term for the sum of all fluxes from plant transpiration and evaporation from the soil and the open water (Savenije 2007, p.39). The zone below the groundwater table is called the *saturated zone*. In the saturated zone, the pore spaces are almost completely filled with water and the pressure is equal or greater than atmospheric pressure (Ward and Robinson 1990). With this characteristics, the saturated zone distinguishes itself from the unsaturated zone, where the pores are both filled with water and air. The water pressure in the unsaturated zone is smaller than atmospheric pressure (Ward and Robinson 1990). Water can leave the saturated zone via *capillary rise* (C_r) to the unsaturated zone or via *groundwater seepage* (q_{gw}) into water bodies such as seas and oceans.

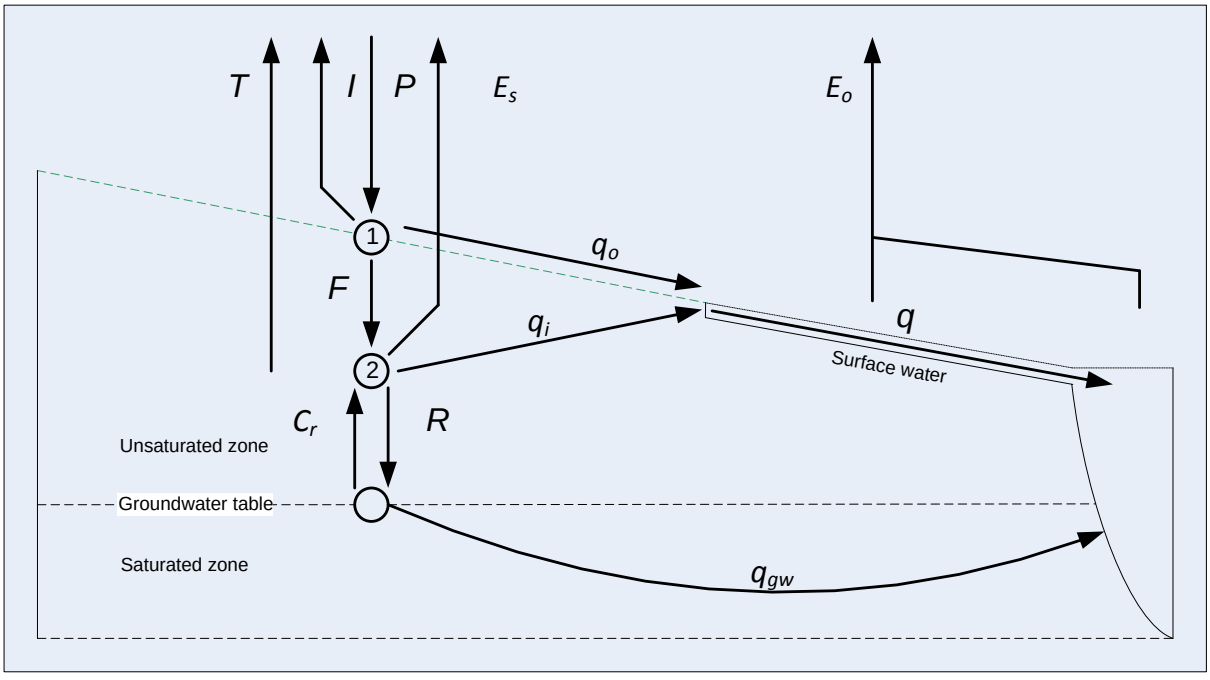

Figure 7. Hydrological cycle and relevant processes

2.3 Urbanization

The process in which the total urban population increases with 70 million people annually, while the rural area population is about static, is called *urbanization* (UN 2008). In 2001, the total world's urban population was 48% and UN (2008) predicts that in 2030, more than 60% of the total world population will live in urban areas. As a matter of fact, ongoing changes to the natural physiographic characteristics are a result of urbanization. With regard to changes in the hydrological cycle, several characteristics of urban land use will be discussed in paragraph 2.3.1. These characteristics are used in paragraph 2.3.2, to support and understand the most important hydrological effects of urban land use.

2.3.1 Relevant characteristics of urban land use

The first distinct characteristic in urban water systems is the large rate of *total impervious area* (TIA) (Bedient, Huber and Vieux 2008, Martin 2008, Mansell 2003) and deforestation. Examples of land utilization that contribute to an increased rate of imperviousness are streets, other pavements and traditional roofs. Parallel to the increasing number of people living in urban areas and the increased concentration of people living in cities (UN 2008), the TIA is continuously growing. A second main characteristic of water systems in urban areas are the different water sources and water appearances (van de Ven 2007, Mansell 2003). The five different forms of water in urban areas are precipitation, drinking water, surface water, groundwater and wastewater (van de Ven 2007).

1. Precipitation

The main inflow into the water balance of an urban system is precipitation. Several authors provided evidence that the total amount and intensity of precipitation in urban areas is larger than in rural areas. According to van de Ven (2007), a research performed by Landsberg in 1981, showed 5-15% increase in total precipitation depth and intensity in extensive urban areas. Similar results were found by Mansell (2003, p.19): "the increase in precipitation in, and downwind of, urban areas can be up to 15%". There are two main processes that account for the increase in precipitation. In the first place, the increase in precipitation is caused by higher temperatures in urban areas, because of differences in thermal balances (Marsalek, et al. 2008). This phenomenon is called the "urban-heat island" which results from several factors including (a) relatively low albedo-values and thus high energy absorbance levels of urbanized areas, (b) waste heat from buildings and means of transportation, (c) decrease of evaporative cooling due to the lack of water surfaces and vegetation subject to evaporation (Marsalek, et al. 2008). Secondly, urban areas provide up to ten times more (van de Ven 2007) solid and liquid particles, named aerosols, from combustion and industrial processes which act as nuclei in the formation of raindrops (Mansell 2003).

2. Drinking water

An important input into the urban water system is drinking water. According to van de Ven (2007, p.24) drinking water imports measured in 9 different urban areas, vary between 14-7500 mm/year, which equals 25-300% of the precipitation depths. Municipal water for drinking water supply is often imported from outside the urban area, another catchment or country (Marsalek, et al. 2008).

3. Surface waters and groundwater

The existence of surface waters in urban areas is of major importance. Surface waters provide water storage possibilities for stormwater management, ecological habitats, evaporation potential (energy balance benefits), drainage or infiltration interaction with the groundwater and are aesthetically

attractive. Surface water quality can be problematic because of combined sewer overflows and the discharge of polluted substances which are transported with stormwater (van de Ven 2007).
The effect of urbanization on the groundwater is generally characterized by changes in quantity and quality. Although van de Ven (2007, p.14) reports that paved areas still provide significant infiltration of water into the ground, lowering of groundwater tables and land subsidence (Marsalek, et al. 2008) are serious groundwater quantity issues in densely populated areas. A lot of cities experience groundwater quality deterioration via infiltration of polluted substances from the surface area and through leakage from leaky sewer conduits (van de Ven 2007).

4. Wastewater

Wastewater management and sanitation are indispensable infrastructure, which help to ensure a healthy living environment in urban areas. Wastewater management includes the collection and treatment of household wastewater and industrial wastewater. After treatment, wastewater residuals are discharged to surface water. The wastewater system consists of decentralized wastewater collection, a centralized underground sewer system and a wastewater treatment plant (WWTP). Besides wastewater, the surplus runoff from (un)paved areas is often collected in sewer systems. In general, two types of sewer systems are considered:

- Combined sewer system
- Separated sewer system

When the sewer system does collect stormwater and wastewater in the same conduit, it is called a *combined sewer* (Bedient, Huber and Vieux 2008). If the hydraulic capacity of the combined sewer system is exceeded during heavy rainstorms, the CSO will be automatically discharged via an overflow structure to adjacent surface water, which can cause surface water quality problems.
When the sewer system does collect stormwater and wastewater in separate conduits, the drainage system is called a *separated sewer* (Bedient, Huber and Vieux 2008). The wastewater or *dry weather discharge* will be directed to a WWTP. The stormwater or *wet weather discharge* will be directed into urban surface water directly. Although CSO's don't exist in separated sewer systems, surface water quality deterioration occurs as a result of pollution load brought by precipitation (wet deposition) and dry deposition of dust, traffic, corrosion from buildings, gardening pesticides etc. (van de Ven 2007, p.88). Although not explicitly explained in this thesis, both sewer systems have an improved variant which intend to decrease the negative side effects to urban surface water.

2.3.2 Hydrological effects of urbanization

Urban areas are characterized by a large rate of impervious land cover, the presence of stormwater drainage systems and five different forms of water. Leopold (1968) and Marsalek, et al. (2008) have distinguished three major effects of changed land-use on the hydrology of urban areas:

1. Changes in water quality;
2. Changes in the hydrologic amenity value;
3. Changes in the rainfall-runoff relation.

These three effect categories (Leopold 1968, p.1) will be successively discussed. With respect to the scope of this research, special attention is given to the changes in the rainfall-runoff relation.

Changes in water quality

The deteriorative effect of urban land use on the urban water quality is recognized by different authors. Urban water quality problems can be classified in three main groups. First, water quality in urban areas is influenced by many pollution sources such as combined or separated untreated sewer discharge, pollution brought by corrosion of building materials, traffic, pesticides and even treated WWTP effluent discharges on surface water (Leopold 1968, van de Ven 2007). Second, increased rates of TIA decrease infiltration rates and groundwater seepage (Marsalek, et al. 2008). This will cause higher peak discharges during rainfall periods, but lower base flow during dry spells (Savenije 2007, Leopold 1968). Strong water level variation or even dry river beds, negatively affect the ecological habitat in urban areas. The third water quality parameter, that is affected by urbanization is the water temperature. According to Leopold (1968), Pluhowski (1968) studied the effects of urbanization on water temperature. Besides a decreased proportion of stream flow originating from groundwater seepage, higher TIA rates result in an increased proportion of stream flow originating from overland flow. Changed fluxes in the hydrological cycle result in long-term urban stream flow temperatures that are 5-10 ^{0}F lower in winter and 10-15 ^{o}F higher in summer, when compared to natural stream flows (Pluhowski 1968). High temperatures in summer that result in lower oxygen concentrations could be lethal to fish and could change flora and fauna.

Changes in the hydrologic amenity value

Leopold (1968) argues that the amenity value (aesthetical attractiveness) of the hydrologic environment is negatively affected by three factors:

1. Enlargement and lining of stream channels. Humanly altered stream channels often contain little or no vegetation, are visually unnatural and can have muddy residuals during low flow;
2. Accumulation of artefacts of civilization such as beer cans, oil drums, plastic bags and furniture;
3. A change in the living or biotic environment caused by changes in non-living or a-biotic factors such as increased turbidity and reduced oxygen content.

Figure 8. Stream channel lining affect the hydrological amenity value

Changes in the rainfall-runoff relation

Perhaps the most significant effect of urbanization is a change in the rainfall-runoff relation (Mansell 2003, Carter and Rasmussen 2006, Leopold 1968, Bedient, Huber and Vieux 2008). The effect of urbanization on the volume and peak discharge of runoff will be discussed in terms of the characteristics of a hydrograph. A hydrograph is a graphical representation of the instantaneous discharge of a stream plotted versus time (Savenije 2007). Runoff represented in a hydrograph consists of discharged effective precipitation. Effective precipitation equals total precipitation minus all losses through infiltration, soil evaporation, transpiration and interception (Gribbin 2007). The time difference between the centre of mass of a precipitation event and the centre of mass of the runoff hydrograph is called the lag time (Leopold 1968).

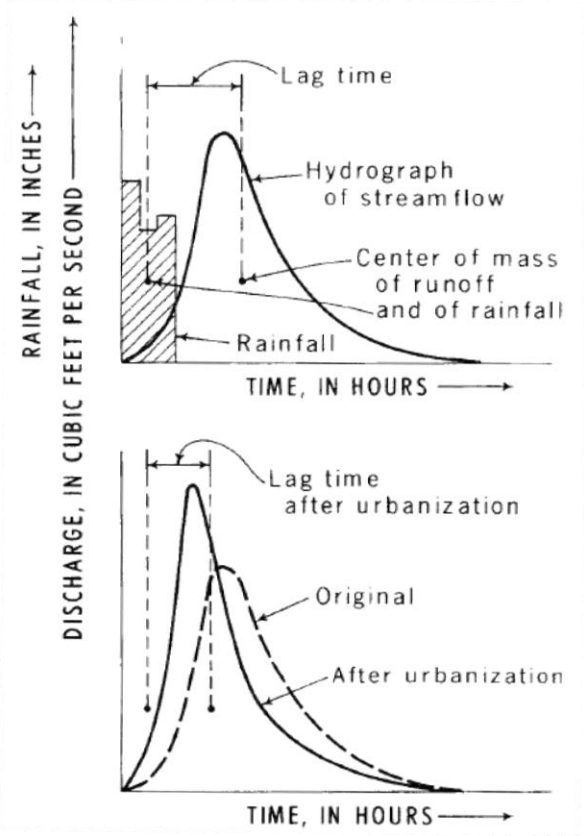

Figure 9. Effect of urbanization on the hydrograph. Source: Leopold (1968)

Marsalek, et al. (2008) provide the most complete list of the differences between rainfall-runoff response in postdevelopment and predevelopment catchments:

1.Increased runoff volumes

Runoff volumes in urban areas increase as a function of the total percentage of area made impervious (Leopold 1968). Relatively low infiltration rates combined with low plant coverage reduce both transpiration, evaporation and groundwater recharge fluxes (Marsalek, et al. 2008). The combined effects of increased input from precipitation, increased drinking water imports, decreased precipitation losses and hydraulically improved drainage systems cause an increase in urban runoff volumes of up to six times predevelopment runoff volumes, as can be concluded from Table 1. Table 1 presents the total increase in runoff volume as a result of urbanization in a standardized 1-square-mile area. This table was presented by Leopold (1968) and was based on several previous studies. More recent studies introduce the rational runoff coefficient *C*:

$$C = \frac{Runoff\ \ rate}{Rainfall\ \ rate} \qquad \text{[Eq. 2.1]}$$

This runoff coefficient incorporates all precipitation losses and is determined for several land types (Thompson 1999, p.218). Relatively large runoff coefficients in urban areas do not only increase runoff volumes during precipitation events, but do also decrease base flow runoff volumes during dry spells, because of decreased groundwater recharge (Leopold 1968).

Table 1. Increase in total runoff volume as a result of urbanization in a 1-square-mile area.
Source: Leopold (1968)

% of area served by storm sewerage	**% of area made impervious**			
	0	20	50	80
0	1	1.2	1.8	2.2
		1.3	1.7	2.2
		1.3	1.6	2.0
20	1.1	1.9	1.8	2.2
		1.4	-	-
50	1.3	2.1	3.2	4.7
		2.8	2.0	2.5
		3.7	-	-
		2.0	2.5	4.2
		1.6	-	-
80	1.6	1.9	-	3.2
100	1.7	3.6	4.7	5.6
		2.0	2.8	6.0
		-	-	3.6

2. Increased peak runoff caused by increased runoff speed

In addition to the effect on the runoff volume, hydraulically improved stormwater drainage systems decrease the lag time too (Leopold 1968). This effect is reinforced by the fact that overland flow velocities are greater in urban areas than in rural areas. The integral of a hydrograph equals the total runoff volume for a certain precipitation event or, expressed in a mathematical formula:

$$\int_o^t Q \ dt = total\ runoff\ volume \qquad \text{[Eq. 2.2]}$$

When the lag time decreases, the peak of the hydrograph must increase, in order to be mass conservative.

3. Increased peak runoff caused by reduced time of concentration

Marsalek, et al. (2008) introduces a change in the rainfall-runoff relation that has not been discerned in any other consulted literature. Hydraulic routing times in stormwater drainage systems can decrease as a function of channel shape, roughness and depth (Thompson 1999). Decreased hydraulic routing times can decrease the time of concentration *(t_c).* Time of concentration is the travel time for a water parcel that is located at the most distant part from the point of interest (Thompson 1999, p.216). For a given homogeneous catchment, the critical precipitation producing the greatest runoff is that whose duration is equal to the time of concentration of the catchment (Marsalek, et al. 2008, p.76). Since shorter precipitation events have greater rainfall intensities than longer precipitation events with the same given return period, this effect increases peak runoff in urban areas (Marsalek et al, 2008).

2.4 Stormwater management policy

Stormwater management is a definition that is used to describe all endeavours to control runoff in areas affected by urban development (Gribbin 2007, p.367). Stormwater management policy tendencies can be subdivided into two main trends:

1. Traditional stormwater management solutions;
2. Low Impact Development.

Traditional stormwater management solutions

In this thesis traditional stormwater management solutions are defined as man-made or hydraulically improved drainage systems (Bedient, Huber and Vieux 2008). Many urban areas have adopted the combined and separated sewer systems to collect both stormwater and sewage wastewater. The characteristics of both systems were addressed and explained in paragraph 2.3.1 . Some tropical countries still manage urban runoff by channelling stormwater into a system of natural or lined streams and channels. In Singapore for example, sewage wastewater is collected in an underground sewer system, while stormwater is mainly collected in non-subterranean, open channels located just below surface level. All these structures have one distinguishing feature in common: they help to convey runoff safely and efficiently away from the development (Gribbin 2007, p.367). In addition to this, sewage wastewater systems were introduced to increase public health and to decrease direct disposal of urban wastewater on adjacent surface water or groundwater bodies.

Although traditional stormwater management solutions have significant positive and proved effects, they aggravate or still do not solve (a part of) the negative effects of urbanization on the hydrologic amenity value, water quality and water quantity. Next to this, continuous costly improvements on these systems are necessary to incorporate for global climate change, the combined effects of urbanization and more strict rules for water quality and water quantity.

Low Impact Development

Instead of focussing on the conveyance of urban stormwater to adjacent areas away from the development, Low Impact Development (LID) is considered as a relatively modern stormwater management tool (Bedient, Huber and Vieux 2008, Gribbin 2007). The main goal of the LID policy is to mimic predevelopment site hydrology as much as possible, by reducing the volume and peak rate of flow, controlling the water quality and promoting the recharge of stormwater with decentralized, on-site detention (Leopold 1968, Gribbin 2007). LID policy therefore gives support to the Dutch triplet “retain, store, drain”, which is a recommendation from the Dutch Commission of Water control 21th Century (Tielrooij, et al. 2000). Examples of LID measures in urban areas are vegetated swales, permeable pavement, infiltration trenches and green roofs (Figure 10).

A good understanding of the functioning of LID measures can contribute to effective large-scale implementation and design strategies with the final goal to maintain or re-establish predevelopment site hydrology. Since roofs account for 20-50% of the total land cover in urban areas (USEPA 2008, Gromaire-Mertz, et al. 1999), green roofs are an interesting LID measure with great large-scale implementation potential in existing urban areas as well as in areas with new housing development.
This specific relevance and the limited available time of this MSc project were the main reasons to narrow the research scope to one particular LID measure: green roofs.

Figure 10. LID measures. Source: Washington County Maryland (2010), InfE'de (2010), CISC (2009)

2.5 Green roof types and design

Green roofs are roofs with a covering material which mainly exist of vegetation that may take many different forms. The adjective *green* does not refer to a colour, but to the presence of vegetation. In fact, the mix of featured plant species are not green all year around (Cantor 2008). There are several green roofs types and design strategies which will be presented in this paragraph.

2.5.1 Green roof types

Green roofs can be categorized according to their growing media thickness, vegetation type, accessibility, need for maintenance and origin. Most green roof research reports and books provide two different types of green roofs: *intensive* green roofs and *extensive* green roofs (Cantor 2008, Martin 2008, Kidd 2005). Mentens, et al. (2002) provide a subdivision in *artificially* constructed green roofs and green roofs with a *natural* origin. This leads to following categorization:

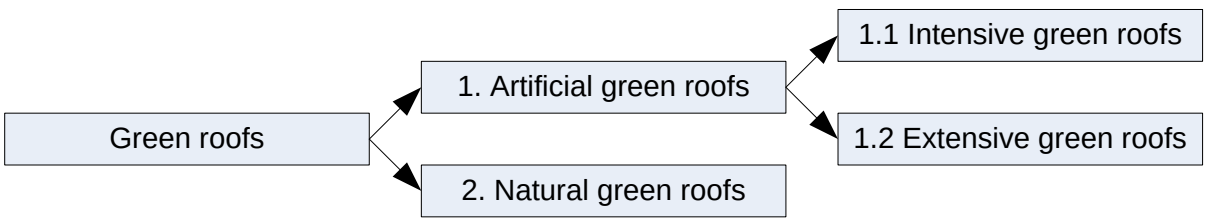

Figure 11. Green roof types

Intensive green roofs

Intensive green roofs or roof gardens are the equivalent of normal gardens, but they are placed on top of a building or an urban object. Intensive green roofs consist of a relatively thick and heavy soil layer and therefore require a specially adapted construction, foundation and building structure (WTCB 2006). Intensive green roofs are covered with grass, low plants, shrubs and (small) trees. Roof gardens have to be accessible for maintenance, but accessibility also increases the practical value of such roof types: they can be used for recreational purposes.

Extensive green roofs

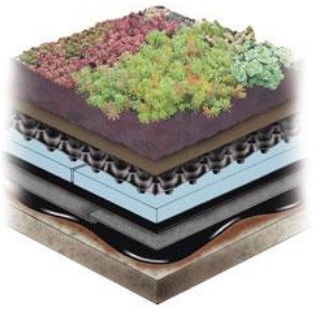

Extensive green roofs are characterized by extensive, drought tolerant and maintenance free vegetation types such as for example moss, sedum, and small shrubs. Their thickness is relatively small: between 2 and 15 cm (Martin 2008, van de Ven 2007). Because of this, extensive green roofs generally do not need additional construction modifications. Extensive green roofs require no additional irrigation or maintenance. The benefits of extensive green roofs can facilitate a widespread application in existing and new urban areas.

Natural green roofs

Natural green roofs are green roofs that have a spontaneous origin (Mentens, Hermy and Raes 2002). Natural green roofs vegetation consist of lichen and different types of moss. Natural green roofs have a development period of 10 to 20 years (Mentens, Hermy and Raes 2002), and are therefore not easily managed.

Table 2. Characteristics of different green roof types.

Characteristic	**Intensive green roofs**	**Extensive green roof**	**Natural green roof**
Origin	Artificial	Artificial	Natural
Growing media thickness	15-40 cm or more	3-15 cm	Very shallow
Wet roof load	300-1500 kg/m^2 (Cantor 2008)	50-170 kg/m^2 (Cantor 2008)	Variable
Vegetation type	Grass, plants, shrubs, trees	Moss, sedum, small shrubs	Lichen, moss
Maintenance	Generally high	Minimal	None
Irrigation	Yes	No	No
Construction costs	Up to €120,-/m^2 (Rotterdam 2008)	€40 - €65,-/m^2 (Mentens, et al. 2002)	€0,-
Applicability	At reinforced buildings	Depends on roof construction, but typically at roofs without reinforcement	Natural origin on existing flat roofs
Accessibility	Accessible	Not accessible	Not accessible

2.5.2 Green roof design

Green roofs are designed according to green roof requirements. Green roofs should provide a growing habitat for vegetation with both sufficient storage and drainage capacity while at the same time preventing any leakage of water into sub-roof spaces such as housing areas, offices or covered parking lots. Green roof design generally consists of seven different layers (Mentens, Hermy and Raes 2002, Martin 2008, WTCB 2006). From the bottom up, green roof design starts with the *roof construction*. Normally, existing roof construction is able to withstand extensive roof greening (Mentens, Hermy and Raes 2002) in green roof renovation projects. Intensive roof greening requires roof construction reinforcement in order to safely cope with the increased construction loads of a green roof. A *waterproof barrier* is placed on top of the roof construction to prevent undesired leakage. Above the waterproof barrier, a *root barrier* is placed in order to prevent the roots to penetrate through the waterproof barrier or roof construction. At present, a *protection layer* that combines the waterproof and root barrier layer is frequently used (Mentens, Hermy and Raes 2002). Subsequently, a *drainage layer* is applied on top of the root barrier. This drainage layer consists of gravel, clay grains or more sophisticated synthetic plates with bulges (WTCB 2006). Drainage layers should safeguard sufficient conveyance of water. This prevents the deterioration of the vegetation layer and leakage of water through the lower barriers (WTCB 2006). A *filter fabric* is placed on top of the drainage layer. Filter fabrics prevent the drainage layer from becoming silted up by small particles originating from the substratum. The substratum or *growing media* is a green roof layer placed on top of the drainage layer and filter fabric. It acts like a normal soil in the sense that roots settle and develop there. The growing media provides the roots with sufficient oxygen, water and nutrients. Usually garden soil improved with peat, compost and other organic materials are utilized. The most upper layer is the vegetation layer or *plant level*. Depending on the type of green roof (a combination of) sedum, different kinds of mosses, herbs, grasses, shrubs and trees can be applied (Mentens, Hermy and Raes 2002, p.9). Green roofs can be constructed using on-site prefabricating construction or prefabricated fully established vegetation mats (van de Ven 2007, p.277). Both methods have pro's and con's, but those will not be discussed here.

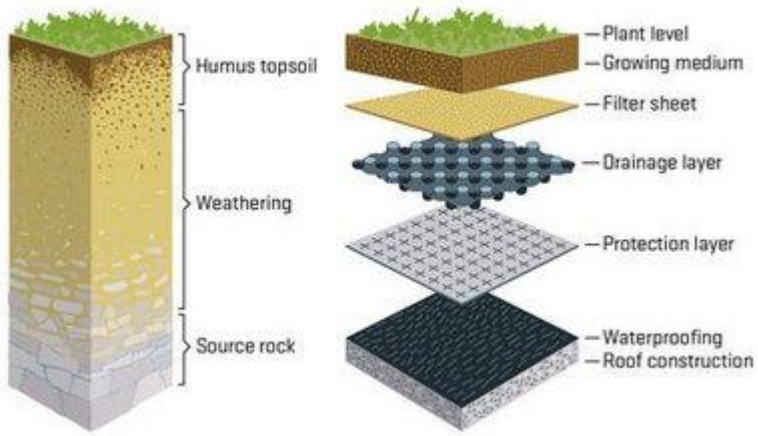

Figure 12. Characteristic cross section of a green roof. Source: Lanks (2008)

2.6 Green roof effects

This chapter will give an insight into the broad spectrum of green roof effects. With regard to the scope of this research, the main focus is on the influence that green roofs have on the artificially changed rainfall-runoff relationship in urban areas. All other relevant beneficial and detrimental green roof influences will be shortly addressed though, as these influences substantiate the overall opportunities and threats for green roof implementation.

2.6.1 Green roof advantages

2.6.1.1 Increased roof life expectancy

Green roofs increase the roof life expectancy up to two times the lifetime of an ordinary flat roof (WTCB 2006, Mentens, Hermy and Raes 2002). The longer life expectancy of green roofs is caused by:

- *Protection against infrared and UV-radiation*. Green roofs absorb infrared and UV-radiation which normally deteriorate roof materials by photochemical reactions (WTCB 2006);
- *Protection against frost, heating and large temperature variations*. Research results from WTCB (2006) show a 50 ^{0}C daily temperature variation on conventional roofs, while daily green roof temperature variation is only 10 ^{0}C.

2.6.1.2 Thermal and energy benefits

Green roofs have a positive influence on the heat regulation at a house and on an urban-scale. Because green roofs smoothen out temperature variations on a daily scale, energy (cost) savings could be established because green roof isolation characteristics decrease the desire for air conditioners in summer and radiator heating in winter periods (Cantor 2008, Mentens, Hermy and Raes 2002). Combined with other measures, green roofs have the potential to reduce the urban heat island because increased evaporation helps to cool the entire city (Cantor 2008).

2.6.1.3 Increased living comfort

The living comfort or well-being of urban population is influenced by green roofs in many ways. Examples are:

- *Increased possibilities for recreational activities*;
- *Aesthetic benefits*. A natural environment has positive influence on human's state of mind and physical well-being (Mentens, Hermy and Raes 2002);
- *Air quality improvements*. The air quality in urban areas is improved by green roofs because small airborne particles are absorbed and the humidity level of the air is kept more constantly by green roofs (WTCB 2006);
- *Noise reduction benefits.* Studies on the acoustic effects have proofed that green roofs reduce external noise levels up to 35-60 dB, while normal roofs reduce noise levels up to 30-50dB depending on the roof weight and construction type (WTCB 2006).

2.6.1.4 Habitat provision for flora and fauna

Green roofs have the potential to reintroduce nature, which can function as a home for the many species of plants and animals that disappeared during urbanization (Cantor 2008, p.9).

2.6.1.5 Urban water management advantages

One of the most important benefits of green roof implementation are the influences on urban water management (Mentens, Hermy and Raes 2002, WTCB 2006). Advantages in the field of urban water management can be subdivided in water quantity and water quality advantages.

Water quantity advantages

According to paragraph 2.3.2, urbanization increases the total imperviousness and decreases infiltration rates, resulting in both increased rainfall-runoff volumes and peak discharges. Increased rainfall-runoff and peak discharges can cause downstream flooding and can deteriorate groundwater and surface waters bodies via infiltration of polluted substances from the surface area and through leakage from leaky sewer conduits and combined sewer overflows, respectively. Some of these problems can be solved by expansion and good maintenance of the traditional stormwater drainage systems (Mentens, Hermy and Raes 2002). Typical traditional solutions are the enlargement of the hydraulic capacity of sewer systems or stormwater conveyance channels, the construction of stormwater detention basins and WWTP capacity extension (Gribbin 2007). However, these solutions are expensive, could conflict with other spatial goals and transfer the water quantity problems to downstream areas (Mentens, Hermy and Raes 2002).

Green roofs might provide a more sustainable solution against the increased runoff volumes and peak discharges. Several scientific researches prove that green roofs effectively increase rainfall retention, reduce the runoff peak and extend the delay of runoff (Berghage, Beattie, et al. 2009, Carter and Rasmussen 2006, van Woert, et al. 2005). The most important knowledge, ideas and controversies from earlier studies that aim to investigate the effects of green roofs on the rainfall-runoff will be presented and discussed here. In order to keep the overview and discussion well-organized, a subdivision is made. Subsequently, the influence of green roofs on the following changes in the rainfall-runoff relation will be examined:

1. Retention performance;
2. Peak discharge reduction performance;
3. Detention performance;
4. Base flow conservation performance.

1. Green roof stormwater retention performance

Introduction and terminology

The performance of green roofs is often expressed in terms of their capability to increase stormwater retention and hence, decrease the runoff in urban areas. Hutchinson, et al. (2003) calculate stormwater retention as “the difference between precipitation and runoff depth during the 15-month monitoring period”. Martin (2008) uses an expression from de Nardo, et al. (2005):
“retention is taken as the difference between the measured precipitation depth and runoff depth once the rainfall has stopped”. Other studies prefer to present monthly or seasonal green roof retention performance ratios in order to investigate the seasonal effect (Berghage, Beattie, et al. 2009). Van Woert, et al. (2005) present overall retention performance over a 14-month monitoring period as well as some more specified performance indicators that reveal retention characteristics for light, medium and heavy rains. To summarize, retention performance of green roofs, but also of

reference roofs, is often expressed as an absolute value or as a ratio compared to the precipitation depth. The absolute *retention performance indicator* (RPI) is expressed as:

$$RPI = precipitation\ depth - runoff\ depth \quad \text{[Eq. 2.3]}$$

If the retention performance of a roof is expressed as a *ratio* between the retention depth and the precipitation depth, the following equation can be used:

$$RPI\ ratio = \left(1 - \frac{runoff\ \ dept\ h}{precipitation\ \ \ dept\ h}\right) * 100\% \quad \text{[Eq. 2.4]}$$

Literature values of the RPI ratio can often not be directly compared. Several studies use different time intervals for assessing the retention performance of green roofs. Table 3 shows that different time intervals affect the RPI ratio. In this imaginary example the average monthly RPI ratio is 67%. This average monthly value is calculated as follows:

$$Average\ monthly\ RPI\ ratio = \frac{\sum_{Jan}^{Mar}\ \left(1 - \frac{green\ \ roof\ \ runoff\ \ \ dept\ h}{precipitation\ \ \ \ dept\ h}\right)}{3} * 100\% = 67\% \quad \text{[Eq. 2.5]}$$

The average seasonal RPI for the months of January, February and March can be calculated as 1 minus the sum of total seasonal runoff divided by the sum of total seasonal precipitation or:

$$Average\ seasonal\ RPI\ ratio = \left(1 - \frac{\sum_{Jan}^{Mar}\ runoff\ \ dept\ h}{\sum_{Jan}^{Mar}\ precipit\ ation}\right) * 100\% = 1 - \frac{180\ mm}{400\ mm} = 55\% \quad \text{[Eq. 2.6]}$$

Table 3. Effect of different time intervals on the retention performance

Month	**Precipitation [mm]**	**Runoff [mm]**	**Retention [mm]**	**Monthly RPI ratio [%]**
January	160	80	80	50%
February	40	0	40	100%
March	200	100	100	50%
Total	400	180	220	67%

The effects of different time interval choices have to be recognized when interpreting the retention performance of green roofs. The interval time should always serve the research goal. For example, when determining the urban heat island mitigation potential of green roofs, a seasonal or yearly RPI will give clear indications of cooling possibilities. When examining the effectiveness of green roofs to act as a sustainable solution against urban stormwater system capacity problems, small calculation interval times during heavy rainfall events (design events) are more purposeful. On top of this, peak discharge reduction and runoff attenuation is often far more important for stormwater management because the total rainfall volume and rainfall duration is often not the problem, it is the rate that the incoming water needs to be treated (van Woert, et al. 2005, p.1042). With this having said some literature values for retention performance indicators will be presented, compared and discussed.

Literature RPI values

Carter and Rasmussen (2006) determined green roof retention performance on a precipitation event-scale. According to this 12-month monitoring study on a 76 mm green roof in Athens GA, absolute stormwater retention varied between 2.7 mm and 41.7 mm, while RPI ratios varied between 39% and 100%, with an average retention ratio just under 78%. For light rain (<2.54 cm) nearly 88% is retained, while for medium (2.54 – 7.62 cm) and large rain events (>7.62 cm), 54% and 48% retention has been measured. Carter and Rasmussen report a reverse relationship between depth of rainfall and retention performance. Another study that is quoted very often in green roof literature is a study by van Woert, et al. (2005). Van Woert, et al. (2005) show a 61% average overall retention ratio for an extensive green roof with a growing media of only 2.5 cm and a retention fabric of 1.5 cm. 96% retention was established during light rains (<2 mm), 83% retention during medium rains (2-6 mm) and 52% retention during heavy rains (>6 mm). The largest rainfall event that was fully retained by the relatively thin green roof equalled only 5.6 mm. Rainfall categories according to Carter and Rasmussen (expressed in cm) are almost ten times larger than rainfall categories according to van Woert, et al. (expressed in mm). Because retention percentages seem to correspond to a certain degree and because Carter and Rasmussen present rainfall events of over 8 cm, it can be concluded that either Carter and Rasmussen made a large converting error between inches and cm or that they use a sum of precipitation over several days. This example reveals that one must be careful when comparing the RPI values from two different studies. Carter and Rasmussen conclude that the RPI differences from their and van Woert's research might be due to a difference in growing media depth (Carter and Rasmussen 2006, p.1267). Although this might be one reason for RPI calculation differences, rainfall differences and the categorization of rainfall classes must be considered too.

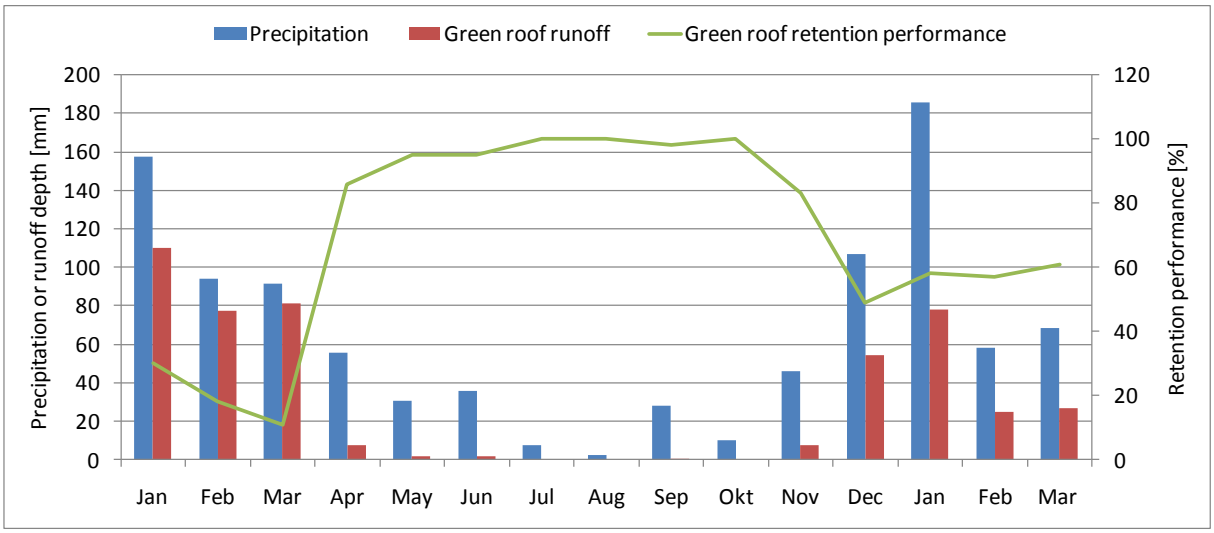

Figure 13. Monthly stormwater retention performance for a 100-130 mm green roof in Oregon. Source: Hutchinson, et al. (2003)

Stovin, et al. (2007) report a 34% average stormwater retention ratio for a 80 mm extensive green roof in Sheffield UK. This 34% is relatively low, which is probably caused by the relatively short monitoring period of 3 months and the fact that the measurements were carried out in the (wet English) spring. Hutchinson, et al. (2003) report an average rainfall volume retention for a 100-130 mm extensive green roof during a 15-month monitoring period in Oregon USA. During a 3-month winter retention comparison between January-March 2002 and 2003, 20% and 59% retention was

measured respectively (Hutchinson, et al. 2003). These results show great inter annual variability. Hutchinson, et al. explain that a 1.3 ^{0}C higher temperature, longer dry periods and vegetation maturity in 2003 did most certainly account for these inter annual differences.

Berghage, Beattie, et al. (2009) found an average stormwater retention ratio of 53% for a 85 mm extensive green roof during an 11-month monitoring period in Rock Springs USA. The RPI ratio was higher during warm weather months than during cool weather months. This study also provides an interesting addition by presenting the average stormwater retention ratio of flat asphalt roofs (14%) and roofs with growing media without vegetation (30%). These results show that it is important to look at the stormwater retention of vegetated roofs relative to a *reference roof*, since normal roofs also provide some stormwater retention. Therefore, a new PI is being introduced: the *additional stormwater retention performance indicator* (ASRPI):

$$ASRPI = reference\ roof\ runoff\ depth - green\ roof\ runoff\ depth \qquad \text{[Eq. 2.7]}$$

$$ASRPI\ ratio = \left(\frac{(reference\ \ roof\ \ runoff\ \ depth - green\ \ roof\ \ runoff\ \ depth)}{precipitation\ \ \ depth}\right) * 100\% \qquad \text{[Eq. 2.8]}$$

This PI should be used when one wants to assess the added value of green roofs on stormwater management, relative to the current situation. Figure 14 graphically illustrates the use of the ASRPI principle.

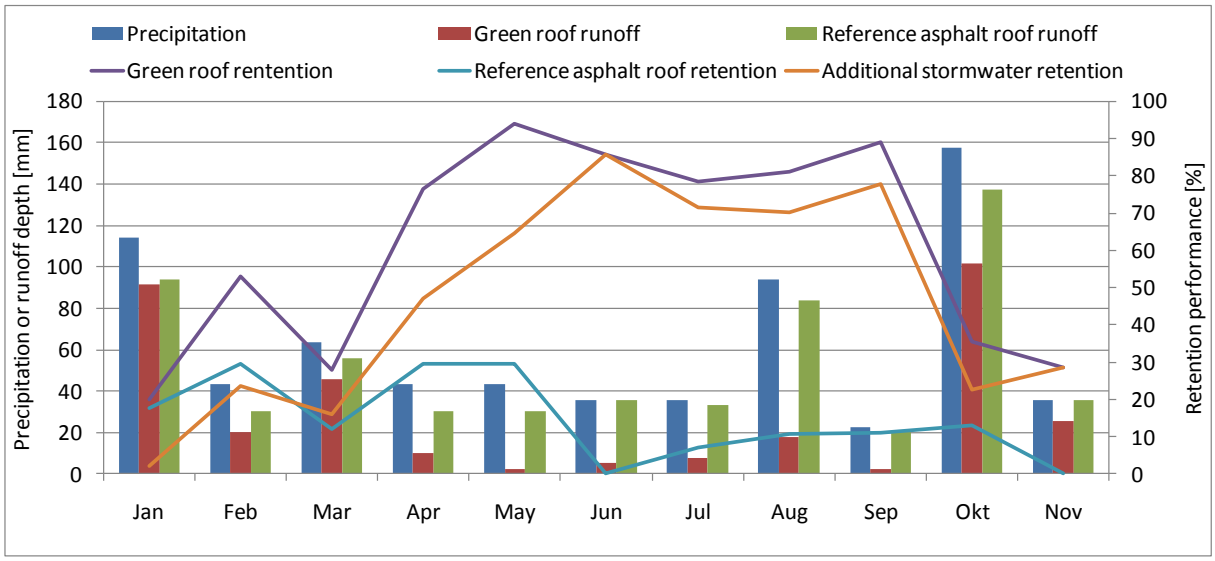

Figure 14. Monthly stormwater retention performance for a 85 mm green roof in Rock Springs. Source: Berghage, Beattie, et al. (2009)

Prowell (2006) tested the retention performance of fourteen 0.37 m^2 modular green roof blocks. These extensive green roof blocks had 100 mm of growing media and retained 43% of total precipitation during a 12-month monitoring period. The average retention for a storm event approximated 67%. This RPI difference is again caused by the different time intervals that were used (Eq. 2.5 and Eq. 2.6). The average storm event RPI (67%) is larger than the average yearly RPI ratio (43%) because relatively light rain events push up the average storm event RPI, while having almost no influence on the average yearly RPI percentage.

2. Green roof stormwater peak discharge performance

Introduction and terminology

Peak discharge reduction or hydrograph attenuation is a very important objective in stormwater management, because this could enable a size-reduction of the hydraulic structures within the stormwater drainage system, or could provide capacity for future urban development (Carter and Rasmussen 2006, p.1267). The peak discharge reduction can be expressed as an absolute discharge reduction or as a ratio and can be compared to the precipitation peak or the reference roof peak discharge. Or in formula form:

$$PDPI = precipitation\ or\ reference\ roof\ peak\ flow - green\ roof\ peak\ flow \qquad \text{[Eq. 2.9]}$$

$$PDPI\ ratio = \left(1 - \frac{Green\ \ roof\ \ peak\ \ discharge}{Precipitation\ \ \ or\ reference\ \ roof\ \ peak\ \ discharge}\right) * 100\% \qquad \text{[Eq. 2.10]}$$

Again, one should be careful when comparing the influence of green roofs on stormwater peak discharge reduction because different studies use one or more of the four possible *peak discharge performance indicators* (PDPI). Besides this, just like with the RPI, the time intervals which are used influence the peak discharge performance outcome too.

Literature values for peak discharge reduction

During a 9-month monitoring period, Moran, et al. (2004) measured a significant average PDPI ratio of 85% relative to the precipitation peak discharge for an extensive green roof in North Caroline USA. Carter and Rasmussen (2006) evaluate the PDPI ratio during their 12-month study on a precipitation event scale relative to the reference roof peak discharge . Their figures present a variable PDPI ratio of 0-80%. Carter and Rasmussen (2006, p.1268-1269) show that the PDPI ratio decreases as the precipitation depth increases, but found no significant relationship between the PDPI ratio and rainfall intensity. Stovin, et al. (2007) present a PDPI ratio and found an average peak discharge reduction of 57% relative to the precipitation peak discharge.

Berghage, Beattie, et al. (2009) do only present absolute PDPI values for eight rain events larger than 0.5 inch, but show values relative to both precipitation peak and the reference roof peak runoff. When the absolute PDPI values are converted to PDPI ratios, the average PDPI ratio relative to the precipitation peak equals 59%, while the average PDPI ratio relative to the reference roof equals 48%. Just like Berghage, Beattie, et al. and Carter and Rasmussen, Prowell (2006, p.74) defined the peak discharge reduction as the reduction in peak discharge measured in the (non)-vegetated roofs relative to the reference roof and found an average PDPI ratio of 58%.

Although a scientific comparison between literature PDPI values is hard to give, because of different locations, different green roof experiment designs, different measurement methods, differently used PDPI's and seasonal and yearly meteorological variability, all studies report major peak discharge reductions. Average PDPI ratios relative to the precipitation peak vary between 57-85% while PDPI ratios relative to a reference roof vary between 48-58%.

3. Green roof stormwater detention performance

Introduction and terminology

The detention or delay of rainfall-runoff provided by green roofs is recognized and measured in several, but certainly not all studies (Prowell 2006, van Woert, et al. 2005, Carter and Rasmussen 2006). Again, detention typology varies between green roof scientist and reports. Based on Figure 9, the detention can be characterized as the time difference between the centre of mass of a precipitation event and the centre of mass of the runoff hydrograph. This is a time-consuming and not very practical method to establish green roof detention performance. Literature *detention performance indicators* (DPI) can be split up into two categories. Carter and Rasmussen (2006) and Prowell (2006) provide a DPI as an absolute difference in time to peak between a green roof and a reference roof. Or in formula form:

$$DPI_{\Delta\ time\ \ to\ peak} = Time\ to\ peak_{green\ \ roof} - Time\ to\ peak_{reference\ \ \ roof} \quad \text{[Eq. 2.11]}$$

Van Woert, et al. (2005) use another DPI. This DPI is formulated as the time difference between the start of a precipitation event and the start of roof runoff. Or in formula form:

$$DPI_{\Delta\ time\ \ until\ \ initial\ \ runoff} = Starttime_{\ roof\ \ runoff} - Starttime_{precipitation\ \ \ event} \quad \text{[Eq. 2.12]}$$

Consequently, apart from other parameters that can influence the detention performance, just as with the RPI and PDPI, DPI values cannot be directly compared because of the use of different performance indicators in literature.

Literature values for peak discharge detention

Carter and Rasmussen (2006) found that for the observed data, the average time to peak for the reference roof was 17 minutes while the average time to peak for the green roof was 35 minutes. The average difference in time to peak amount to 18 minutes. Considerable detention variation was measured in this study. While most precipitation events were delayed between 0 and 10 minutes, a maximum time to peak difference of 120 minutes was measured. These differences in detention are explained by precipitation intensity and antecedent moisture variations (Carter and Rasmussen 2006, p.1269). Prowell (2006) found a 18 minute difference in time to peak between the modular green roof peak runoff and the reference roof peak runoff. Van Woert, et al. (2005) found a relative delay time of 15 minutes between the green roof runoff start time and the reference roof runoff start time for light rains, 5 minutes relative delay time for medium rains and less than 5 minutes relative delay time for heavy rains.

Despite of the fact that green roof stormwater detention allows for greater flexibility in designing stormwater drainage systems, a lot of studies do not mention detention characteristics of green roofs. Based on available DPI values, it can be concluded that on average initial and final green roof runoff and green roof time to peak are delayed relative to a reference roof. Astonishingly, practical consequences of these findings with regard to stormwater management are seldom explicitly addressed.

4. Green roof base flow conservation performance

Introduction and terminology

Lower base flows during dry weather periods were identified as one of the negative effects of an increased rate of imperviousness in urban areas. Together with higher peak discharges, the artificially increased water level variations negatively affect the ecological habitat in urban areas and decrease the amenity value of the stormwater drainage system. Few studies report the properties of green roofs to detain the runoff after a rain event has ended. Although a standard *base flow performance indicator* (BFPI) for LID measures is not introduced in the reviewed literature, van Woert, et al. (2005, p.1040) define the base flow performance as a relative difference in cumulative runoff between a green roof and a reference roof at certain specified points in time after the last recorded rainfall. This can be translated into the following mathematical expression:

$$BFPI_t = \int_{t_{rainfall\ \ end}}^{t} (green\ roof\ runoff\ intensity - reference\ roof\ runoff\ intensity)\, dt \qquad \text{[Eq. 2.13]}$$

Literature values for base flow conservation

Literature values of the base flow conservation properties of green roofs are very scarce. Van Woert, et al. (2005) show that the last measured green roof runoff was recorded nearly 3 hours after the rain event ended, which was only 30 minutes past the last runoff from the reference roof. An extensive green roof with a 2.5 cm media and a 1.5 cm water retention fabric was used for this part of the study. Carter and Rasmussen (2006, p.1271) report that the base flow can even be reduced for rainfall events that are (nearly) totally retained by green roofs. No other scientific evidence that demonstrates the ability of green roofs to contribute to improved base flow during dry spells has been found. In order to be sure whether green roofs can actually contribute to sustained base flows, measurements of this performance indicator will have to be collected and analyzed.

Water quality advantages

Water quality problems in urban areas were categorized into three main groups in paragraph 2.3.2. The contribution of green roofs to improve urban water quality categorized per group are:

1. Water quality deterioration because of the discharge of polluted substances

According to Berghage, Jarett, et al. (2007), the concentration of (heavy) metals (Cu, Zn, Mn and Fe) in runoff samples from green roofs were larger than runoff samples from a standard asphalt roof. Köhler and Schmidt (2003) however measured retention of lead (95%) and cadmium (88%) as a percentage of influx from experimental plots. The electronic conductivity, which is a measure of dissolved solids, was higher according to Buccola (2008), Köhler and Schmidt (2003) and Berghage, Beattie, et al. (2009). This conductivity increase is caused by plant nutrients, roots, organic matter and clay based aggregates (Berghage, Beattie, et al. 2009). Berghage, Beattie, et al. (2009) measured a reduction in nitrate runoff concentration, but a 300% increase in phosphorous and potassium concentrations. Still, due to the runoff volume reduction, green roof nutrient loadings are generally less than asphalt roof nutrient loadings (Berghage, Beattie, et al. 2009, p.iii). According to several authors the ability to remove pollutants does depend on the media depth, media type, plant cover and maturity of the green roof (Köhler and Schmidt 2003, Bucolla 2008, Berghage, Beattie, et al. 2009). Literature agrees upon the overall pH buffering capacity of green roofs: both Buccola (2008), Köhler and Schmidt (2003) and Berghage, Beattie, et al. (2009) conclude that green roofs create a

significant increase in pH. Results from green roof experiments on a roof-scale in Germany (Köhler and Schmidt 2003) and the United States (Berghage, Beattie, et al. 2009), show mean absolute pH differences of 1-3 pH points, when compared with a reference roof. In fact, green roofs normalize the pH, which effectively acts as a buffer against the deteriorating effects of acid rains in urban areas.

2. Increased water level variations because of higher TIA rates and lined waterways
Green roofs decrease the TIA since they offer infiltration and storage capacity. The water quantity advantage part of this paragraph provides results from earlier studies that focus on the retention, detention and peak discharge reduction of the rainfall-runoff. Although one could argue that green roofs try to mimic rural circumstances by smoothing out rainfall-runoff, literature provides no information about the exact effect of green roofs on ecological habitats in urban waterways.

3. Increased water temperature variations affected by a larger contribution of street runoff
It was concluded in paragraph 2.3.2 that higher TIA rates result in an increased proportion of stream flow originating from overland flow which finally results in long-term urban stream flow temperatures that are 5-10 ^{0}F (2.78-5.56 ^{0}C) lower in winter and 10-15 ^{o}F (5.56-8.33 ^{0}C) higher in summer, when compared to natural stream flows. Based on literature values that are presented in this thesis, it can be concluded that on average initial and final green roof runoff and green roof time to peak are delayed relatively to a reference roof. This would imply that green roofs act as a runoff temperature buffer. This statement was partly validated by Buccola (2008), who measured a 2 ^{0}C temperature reduction in the runoff from a 15 cm extensive green roof.

2.6.2 Green roof disadvantages

High purchase costs
The square meter price of a residential green roof depends on several variables such as the thickness of the roof, used materials, the roof angle, total green roof surface area, but also on the availability of subsidies. According to Mentens, et al. (2002) extensive green roof purchase costs will vary between €40,- to €65,-/m^2. However, in New York City the average green roof costs around €145,-/m^2 (Green-buildings.com 2008). Local authorities in the Benelux do sometimes provide subsidies in the order of €25,- to €30,- (Gemeente-Rotterdam 2009, Mentens, Hermy and Raes 2002). A full costs benefit analysis of green roofs should be provided, when one wants to assess the economic profitability of green roofs.

Building construction overload risk
Intensive green roofs, which have a weight of 300-1500 kg/m^2, require tailor made structural support for existing and new buildings (Mentens, Hermy and Raes 2002). Notwithstanding the fact that it is promoted to examine the building construction before implementing a green roof in new and existing buildings (WTCB 2006), the extra weight of a 8-15 cm extensive green roof (20-200 kg/m^2) allows for retrofit installation on most of the existing buildings, and reduces the need for additional structural support in new buildings (Berghage, Beattie, et al. 2009, p.1-1).

Fire safety issues
Normally, green roof constructions have to comply with fire regulations from national authorities. That means that the fire resistance of the individual elements, the finishing coat and the total green

roof have to be examined (WTCB 2006). Green roof fire safety solutions are a fire resistant strips on the roof-edge, compartmentalizing of large green roof surfaces and the use of fire resistant or fire delaying elements (WTCB 2006).

Increased demand for maintenance

Green roofs do need more maintenance than normal flat roofs. According to Mentens, et al. (2009) they require about the same amount of maintenance as a normal garden. Vegetation must be pruned on a yearly basis, downspouts must be regularly checked against clogging by dead plant materials and the roof media must be regularly limed against the detrimental effects of acidification (Berghage, Beattie, et al. 2009, Mentens, Hermy and Raes 2002, WTCB 2006). Special attention has to be given to the use of pesticides and fertilizers, which is still recommended often unfortunately, since those can negatively affect the runoff water quality.

Water quality problems

As was mentioned in paragraph 2.6.1.5, green roofs can negatively affect some water quality parameters. Study results by Berghage, Beattie, et al. (2009) show equal or increased hardness and ion concentration of Cu, Zn, Mn, Fe, K, and P in green roof runoff. Extra pesticides and/or fertilizers that are added to the green roof media, will have a negative impact on the runoff quality.

2.7 Implications for assessing the effects of green roofs in tropical areas

The survey on green roof effects in paragraph 2.6 of this literature review validates the conclusion of earlier scientific papers by Laar and Grimme (2006) and Köhler, et al. (2001): “scientific results on the effect of green roof implementation on the rainfall-runoff in tropical catchments are rare”. Current green roof research on the retention performance, peak discharge reduction performance, detention performance and base flow conservation generally takes place in Europe and the United States. Among others, meteorological differences in temperature, precipitation loads, precipitation intensity and antecedent moisture conditions were reported as important explanatory parameters for inter-research result differences. Because of the large differences in meteorological conditions between temperate and tropical climates, green roof performance must be assessed in the tropics itself, before any conclusions on its effectiveness for this climate type can be drawn. The two most important expected advantages of large-scale green roof implementation in tropical countries both relate to water quantity (Laar and Grimme 2006):

1. The contribution towards a sustainable stormwater drainage system: within the scope of this research this advantage refers to the potential of green roofs to (1) prevent flooding that is caused by stormwater drainage system overloads during extreme rain events and (2) to prevent high water level variations caused by increased rates of TIA;
2. The reduction of the urban heat island by evaporative cooling on roofs. Natural cooling can contribute to a more sustainable energy environment because less air-conditioning might be needed.

Based on the knowledge gap in the understanding of green roof effects in the tropics and the study discipline framework of this MSc thesis, the main focus will be on analyzing the effect of large-scale green roof implementation as a contribution towards sustainable stormwater drainage systems in a tropical urbanized catchment.

2.8 Green roof modelling review

Despite an increasing awareness and knowledge of the effects of urbanization and potential LID measures, the transition to more sustainable stormwater drainage has been slow (Elliot and Trowsdale 2005). Elliot and Trowsdale argue that the availability of effective LID modelling software, that operates effectively at the necessary range of scales, could act to encourage wider uptake of LID measures. Present studies do primarily investigate the hydrological effects of green roofs at experiment-scale. For that reason Elliot and Trowsdale (2005) recommend to investigate more on up-scaling for representation of on-site LID measures at larger spatial scales.

According to van de Ven (2007), models in the area of urban water management generally consist of two parts (van de Ven 2007, p.203). The first part or *loss model* describes the balance between input and output, while the second part or *routing model* describes the runoff retardance. Elliot and Trowsdale (2005) argue that models have to incorporate two main parts for the simulation of LID measures at catchment-scale: a *runoff generation* part and a *flow routing* part. Both modelling structures thus clearly share common features. The main difference between both structures lies in the definition of the loss model part and the runoff generation part. A direct interpretation of Elliot and Trowsdale's modelling structure better suits the modelling goals of this research, because losses *and* delays occur in the green roof soil media. Figure 15 shows the modelling structure of Elliot and Trowsdale (2005). To avoid misunderstandings, the runoff generation part is named *runoff generation model*. A runoff generation model describes the losses and delays that occur in the green roof soil media or at any other (un)paved surface. The second part or *routing model* describes the hydrodynamic routing towards the drainage or sewerage system, routing through devices and routing in the drainage or sewerage system (Figure 15).

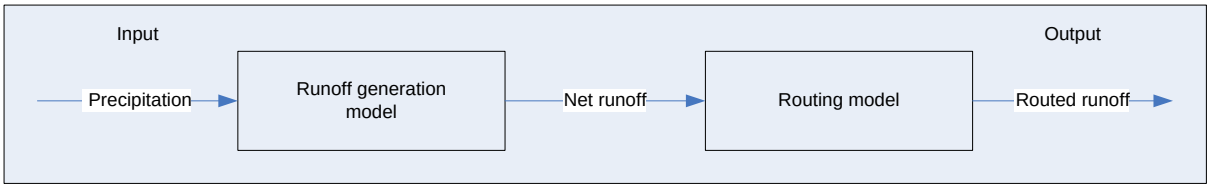

Figure 15. Model structure for the simulation of large-scale LID measure effects

Three potential runoff generation models and two potential routing models will be subsequently reviewed. It is the final goal of this review part to compare the functionality of existing stormwater models that are able to simulate the effects of green roofs to reduce the adverse hydrological effects of urbanization on an experiment-scale and on a catchment-scale.

2.8.1 Available runoff generation models

Simulation of the root zone moisture profile can be done by either empirical or physical models, which operate by solving the soil water balance equation (Mandal, et al. 2002, p.1). The former ones are based on simple bookkeeping procedures and do often only require data of soil water storage properties: the so called field capacity and the wilting point (Mandal, et al. 2002). The latter ones are based on the physics of unsaturated flow in the soil and need data of soil water storage as well as transmission characteristics (hydraulic conductivity and soil water content relationships (Mandal, et al. 2002)). Here, three potential models that have been used in antecedent green roof researches, will be reviewed. Two empirical models: the curve number method and the water balance model and

one physical model: the finite element model HYDRUS-1D. Appendix 2 gives an overview of all model characteristics and literature references.

Curve number method

The SCS curve number method (CN) is an empirical runoff generation model first issued by the Soil Conservation Service in January 1975. Technical Release 55 presents simplified procedures to calculate storm runoff volume, peak rate of discharge, hydrographs and storage volumes required for floodwater reservoirs (USDA 1986, p.i). In this model the runoff equation is:

$$q = \frac{(P-I_a)^2}{(P-I_a)+S_m} \quad ; \qquad S_m = \frac{1000}{CN} - 10 \; ; \qquad I_a = 0.2S_m \qquad \text{[Eq. 2.14]}$$

where q is the runoff depth [L], P is the rainfall depth [L], S_m is the potential maximum retention after runoff begins [L], I_a is an initial abstraction term [L] and CN is the runoff curve number [-]. The CN method is a commonly used model and is very efficient and easy to use, especially for design purposes. The CN method does only take an average antecedent moisture content into account. Besides this, the CN method is less accurate for small rainfall events, runoff output is very sensitive for CN changes and the initial abstraction term I_a was found through studies in agricultural watersheds (USDA 1986, p.2-11). These disadvantages reduce the applicability of the CN method as a successful runoff generation model. Carter and Rasmussen (2006) use the CN method to model green roof runoff for a 43 m^2 test site. They have found a CN value of 86, by using the best-fit line to the green roof runoff and precipitation data. Proposed methods to affect the shape and peak of the runoff hydrograph by combining the CN method with the rational method and graphical peak discharge method (USDA 1986) are too lumped to give an accurate description of the runoff delays that occur until the moment of inflow into the drainage network. Therefore, this model can only be applied to simulate green roof retention, not green roof runoff delays. On top of this, different green roof designs will have different CN values, which need to be individually determined. When the limitations of the CN method are taken into consideration, the accuracy and general applicability of this approach is restricted.

Water balance model

A water balance model (WBM) or reservoir model is a runoff generation model that is used in several studies that aim to investigate on the hydrological effects of green roofs (Prowell 2006, Martin 2008). A WBM is a relatively easily applicable model that can help to get a better understanding of green roof hydrological behaviour, because of it's simplicity. Water balance modelling is based on the water balance principle:

$$Input = Output + \Delta \, Storage \qquad \text{[Eq. 2.15]}$$

where for green roof modelling *Input* is the precipitation (rainfall, snow, hail), *Output* is runoff, evaporation, transpiration and interception and the *Δ Storage* term accounts for storage differences in the green roof media.

Disadvantages of using a WBM as a runoff generation model for green roofs is that a simple WBM only calculates runoff when the volume of water in the reservoir has exceeded the storage capacity,

while in reality runoff begins before maximum capacity is reached, due to preferential flow (Prowell 2006). Preferential flow can be incorporated, but will reduce the simplicity of the model thus taking away the main advantage of this type of models. Next to this a WBM does not give a true physical description of the soil water movements as they occur in unsaturated zones according to Hillel (1982), Thompson (1999) and Cuen (2004). In fact, WBM's suppose a constant root water uptake until the water storage is exhausted, while it is widely accepted and known that the volumetric water content θ [-] and the pressure head *h* [cm] have a S-shaped relation (Hillel 1982): the total available water for plants decreases exponentially with increasing suction (Berghage, Jarett, et al. 2007, p.2-6). A WBM incorporates runoff delays up until the storage is exceeded and runoff starts, but does not account for delays that are caused by flow dynamics in the unsaturated soil media. The last but not least important disadvantage of a WBM is that these models are often self-made (containing tacit modelling knowledge), difficult to transfer to a wide user public and relatively hard to adapt to other simulation conditions. It can be concluded that WBM can be a decent first model to predict green roof runoff generation. The disadvantages of the model give restrictions to its use as a model to transparently and accurately describe the losses and delays of green roofs for a wide range of applications all over the world.

HYDRUS-1D

HYDRUS-1D is a physically based model for the simulation of one-dimensional vertical flow of water in variably saturated porous media (Simunek (c), et al. 2008). The software program numerically solves the Richards equation for saturated-unsaturated water flow. Richards equation for transient, vertical water flow equals:

$$\frac{\partial \theta}{\partial t} = \frac{\partial}{\partial x}\left[K\left(\frac{\partial h}{\partial x} + 1\right)\right] - S \qquad \text{[Eq. 2.16]}$$

where θ is the volumetric water content [-], *t* is time [T], *x* is the vertical spatial coordinate (positive upward) [L], *K* is the hydraulic conductivity [LT^{-1}], *h* is the water pressure head [L] and *S* is a sink term [$L^3\ L^{-3}\ T^{-1}$] to account for water uptake by plant roots. The program solves the Richards equation by obtaining a water retention function θ*(h)*, which describes the relationship between the water pressure head, *h* [L] and soil water content, θ [-] and a hydraulic conductivity function *K(h),* which describes the relationship between the hydraulic conductivity *K* [LT^{-1}] and the water pressure head *h* (Assouline and Tartakovsky 2001). Both hydraulic model functions are obtained by the input of six soil hydraulic parameters. These parameters can be determined with inverse modelling of transient flow experiments (Durner (c), Jansen and Iden 2008) or by using the Neural Network Prediction tool in HYDRUS. HYDRUS-1D is a scientifically verified and public-domain, freely available model. HYDRUS can be adopted and used in a variety of locations, since geographical and meteorological parameters can be modified easily. Another advantage of HYDRUS is the open bottom boundary option, which enables the simulation of water flow in unsaturated zones without an underlying saturated zone. A possible lack in total insight in the functioning of the model, model assumptions and computational programming can be seen as a disadvantage of this model. Still, the source code is freely available on the internet (PC-PROGRESS 2008). Hilten, et al. (2008) conclude that, based on their measurement results, HYDRUS appears to over predict green roof runoff during heavy rains. This relationship was found not to be statistically significant though (Hilten, Lawrence and Tollner 2008). Nonetheless, Hilten, et al. recommend additional observations of heavy rains.

As a conclusion to this runoff generation model review, the physically based HYDRUS-1D model has the largest potential to accurately simulate runoff generation from green roofs, since it is suitable to describe both losses and delays that occur in an unsaturated soil media without an underlying saturated zone. The physical background offers the opportunity to better understand the green roof functioning. On top of these advantages the software is freely available and scientifically verified.

2.8.2 Available routing models

In order to create a green roof modelling tool that operates effectively at (sub)catchment-scale, routing processes of flows in the drainage network have to be represented in a routing model (Elliot and Trowsdale 2005). Final output of such a routing model are the discharge and different water levels over time. Based on this output the effect of large-scale green roof implementation on rainfall-runoff in urbanized catchments can be modelled. Green roof scenarios can finally be evaluated and compared to the existing situation with standard roofs (Busiek, et al. 2007).

Elliot and Trowsdale (2005) reviewed ten existing stormwater models in relation to attributes relevant to modelling LID. They gave a clear indication which of the ten reviewed models could be utilized to model relevant routing processes for green roofs. Of all ten models only MOUSE and SWMM included full spectrum hydraulic routing methods (Elliot and Trowsdale 2005, p.398). According to Elliot and Trowsdale, only WBM addressed modelling of green roof devices so far. Based on this paper from 2005, it can be concluded that a green roof modelling tool that operates effectively at (sub)catchment-scale still does not exist. Stovin, et al. (2007, p.17) also conclude that no commercial stormwater management tool (they quote US EPA's, SWMM and Wallingford InfoWorks model) incorporates any capability to explicitly model green roof performance at catchment-scale. However, an implicit green roof modelling option in Mike Urban was found in an analysis report for roof greening in Washington (Busiek, et al. 2007). This model and the possibility to incorporate implicit green roof simulation options in the Dutch SOBEK model will be reviewed.

Mike Urban

Busiek, et al. (2007) quantified the benefits of green roofs and trees by using the hydraulic model Mike Urban to estimate the combined effects of large-scale rainfall-runoff reductions on the stormwater drainage system in Washington D.C. This model builds from the basic runoff equation (Busiek, et al. 2007):

$$Runoff = precipitation - potential\ evapotranspiration - infiltration - storage \quad \text{[Eq. 2.17]}$$

Storage amounts for trees and green roofs were added to the model as a storage component:

$$Storage = Interception\ storage * coverage\ area \quad \text{[Eq. 2.18]}$$

A storage amount of 1 inch (2,54 cm) for 3-4 inch (7.62-10.16 cm) of soil media was assumed, based on average literature review values. The model evaluates greening scenarios by integrating GIS land cover data and hydrologic processes using rainfall storage and coverage areas for trees and green roofs (Busiek, et al. 2007, p.iv). Scenarios were run for an average rainfall year continuous simulation, and a 1-year 6-hour design storm, which has been derived from the local intensity-duration-frequency curve. Since Mike Urban doesn't provide a standard green roof model option, the green

roof infrastructure area was separated from the existing “grey” watershed. Each area was then governed by a different set of parameter values, and summed to get the total runoff from the existing grey and green infrastructure sub sheds (Busiek, et al. 2007, p.B-15). This modelling methodology corresponds to the recommendations from Elliot, et al. (2005): hydrological implications of LID can be represented either explicitly or implicitly by adjusting the catchment routing parameters and by increasing the depression storage in the runoff generation sub-model. The Mike Urban model has been calibrated with monitoring data from along the Anacostia River that drains one of Washington D.C.’s watersheds.

SOBEK

SOBEK is a 1D/2D water model developed by Delft Hydraulics Software. SOBEK can be used for the simulation of water flow processes in networks such as irrigation systems and drainage or sewer systems (Deltares 2009). Catchment areas can be modelled in a lumped or detailed manner. SOBEK can be used to analyze the effects of measures that have the potential to prevent drainage congestion, street flooding and water pollution from sewer overflows (van de Ven 2007, p.226). SOBEK is composed of several modules. The rainfall-runoff (RR) module has the property to act as a runoff generation model for several types of land use. In the RR module, standard losses and delays are incorporated. The runoff delays that take place on a roof-scale until the moment of inflow into the drainage network can be modelled by using the incorporated surface runoff routing method, which is defined as (Deltares 2009):

$$q_i = c * h_n \qquad \text{[Eq. 2.19]}$$

where q_i is the inflow into the drainage or sewer network [LT^{-1}], c is a runoff factor [T^{-1}] and h_n is the dynamic storage of net runoff [L] on the surface. Hydraulic routing in the drainage network is schematized in the SOBEK one-dimensional flow module (1DFLOW) by the Delft-scheme, that solves the De Saint-Venant equations by means of a staggered grid (Deltares 2009).

As in other available commercial hydraulic models, an explicit LID or green roof modelling option is not available in the current SOBEK modelling package. Implicit green roof modelling in Mike Urban, showed that large-scale simulation of green roof effects can be made possible in present water models. Green roof simulation accuracy can be improved when the static storage amount for the simulation of green roof losses is replaced by a runoff generation model that incorporates both losses and delays that occur on a green roof-scale. This can either be done by the introduction of a new software component, or by coupling of an existing runoff generation model to an existing routing model. A physically correct representation of large-scale green roof implementation effects can finally lead to improved LID design, implementation strategies and decision making. The modelling work that is introduced in this report has the aim to contribute to the development of an appropriate green roof modelling tool.

2.9 Literature review summary

Urban water management challenges and solutions

Several researches identify that ongoing urbanization have changed several characteristics of water systems in urban areas. Deforestation, streets, pavements and traditional roofs have increased the rate of total impervious area. A second main characteristic of water systems in urban areas is the presence of stormwater and wastewater drainage systems, a change in the quantity and quality of precipitation, surface waters and groundwater and an additional input into the hydrological cycle: drinking water imports. An important hydrological effect that results from these changed characteristics are changes in the rainfall-runoff relation. First, the combined effect of increased input from precipitation, increased drinking water imports, decreased precipitation losses and hydraulically improved drainage systems cause an increase in urban runoff volumes of up to six times predevelopment runoff volumes. Second, an increase in total impervious area and hydraulically improved drainage systems respectively reduce the overland flow times and drain flow times. This effect results in higher runoff peaks during a precipitation event and lower base flows during dry spells.

A relatively modern management policy that aims to re-establish or maintain predevelopment site hydrology is called Low Impact Development. Green roofs are a Low Impact Development measure with great large-scale implementation potential in existing urban areas as well as in areas with new housing development, because roofs account for 20-50% of the total land cover in urban areas. Different types and designs of green roofs exist. Because of its small thickness (2-15 cm) and the choice of a drought tolerant vegetation type, extensive green roofs do generally not need additional construction modifications and are maintenance free. Trends towards sustainable urban development have increased the emphasis on the large range of green roof benefits, which among others consist of hydrological benefits, insulation and cooling advantages, increased living comfort, habitat provision and increased roof life time expectancy. A combination of this trend and green roof benefits suggest that a widespread application in existing and new urban areas can be made possible, but high purchase costs, building construction risks, fire safety issues, maintenance demand and water quality problems also have to be considered.

Quantitative hydrological green roof research

The ability of green roofs to re-establish or maintain the predevelopment rainfall-runoff relation has been investigated in many studies. The relevance of extensive green roofs is reflected in these studies, because they merely address the effects of thin layered roof designs. Green roof performance has been organized into four categories:

1. Retention performance;
2. Peak discharge reduction performance;
3. Detention performance;
4. Base flow conservation performance.

It follows from this literature review that several researches identify positive effects of green roofs on the first three performance classes. It is hard to synthesize the results of these researches into a general understanding of the quantitative hydrological effects of green roofs, because their performance is often presented in averages and/or differently formulated percentages. Additionally,

green roof performance varies between studies because of different designs, different measurement strategies, different measurement locations with corresponding meteorological conditions and normal inter-annual meteorological variations. Present scientific work contains little or no information on the base flow conservation performance or green roofs, while this characteristic can provide improvements towards a more natural hydrological regime. Next, the hydrological effects of green roofs are often only determined on experiment-scale while potential benefits for stormwater management should be assessed at (sub)catchment-scale. Last, existing green roof studies were performed in temperate climates. Because of the large differences in meteorological conditions between temperate and tropical climates, additional research is necessary to quantify the effects of green roofs on the rainfall-runoff in the tropics. This can be achieved by abstracting and analyzing the retention, peak discharge reduction, detention and base flow conservation performance from green roof rainfall-runoff response measurements on experiment-scale. Performance indicator values can be presented as an absolute value or a ratio, preferably relative to a reference roof.

Green roof modelling

The second aim of this research is to determine the quantitative hydrological contribution of large-scale green roof implementation to sustainable stormwater drainage systems in Singapore. Hydrological losses and delays and hydraulic routing processes of flows in the stormwater drainage system have to be represented in a simulation model. With this simulation model, green roof scenario's can finally be evaluated and compared to an existing situation. Elliot and Trowsdale (2005) and Stovin, et al. (2007) conclude that a commercial green roof modelling tool that operates effectively at (sub)catchment-scale still does not exist. An approximate way to model the large-scale hydrological implications of green roofs was found in an analysis report for roof greening in Washington. Here, green roof runoff retention was represented by increasing the storage on roofs to 2.54 cm in the spatially distributed Mike Urban model. The same methodology can be applied within the Dutch SOBEK water model, which has the advantage that it is freely available within this research, locally developed and used. The presented methodology can suit the modelling goals of this research, but the static storage amount of this model does not represent real hydrological processes that occur on a green roof. Simulation accuracy can be improved when the static storage amount on roofs is replaced by an alternative runoff generation model. The empirical curve number method and water balance model as well as the physically based HYDRUS-1D model have been used to simulate the hydrological effects of green roofs on experiment-scale in earlier researches. From these three models, HYDRUS-1D potentially gives the physically most correct description of the real processes in unsaturated soils. Compared to the reviewed empirical models, the HYDRUS-1D model has the theoretical advantage that it is suitable to accurately describe both losses and delays that occur in an unsaturated soil media without an underlying saturated zone. The physical background also offers an opportunity to better understand the green roof functioning. On top of these advantages, the software is freely available and scientifically verified.

The identified implicit green roof modelling option, which is based on model coupling of an existing physically based runoff generation model to an existing routing model, has the aim to contribute to improved green roof design, implementation strategies, decision making and the development of an appropriate explicit green roof modelling tool or node. Chapter 5 and 6 of this research will elaborate on the methodology and results of the green roof models.

3 Singapore case study context

3.1 Introduction to the Singapore case study

The city-state island country Singapore, officially the Republic of Singapore, is located just above the equator at $1^0$18'N $103^0$51'E and has a tropical rainforest climate according to the climate classification of Köppen. Temperatures are quite constant around the year. Daily variations are minimal: the average temperature is 31 ^{0}C during daytime and temperatures hardly ever drop below 24 ^{0}C during the night. The average annual rainfall is 2400 mm and the average monthly rainfall, which is controlled by the monsoon seasons, varies between 150 - 270 mm (Figure 16).

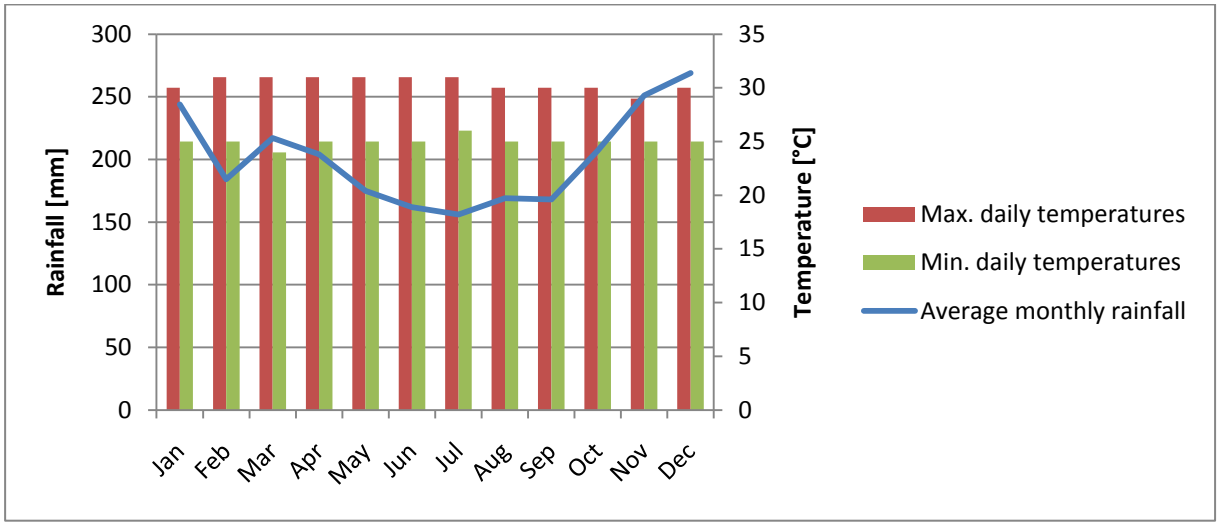

Figure 16. Rainfall and temperature averages for Singapore.
Source: Klimaatinfo.nl (2010), Worldclimate.com (2008)

With its land area of 710 km^2, Singapore is the smallest country in Southeast Asia (Singapore Government 2009). In 2009 the total population measured 4.987.600 million people and the yearly growth rate was 3.1% (Singapore Government 2009). Consequently Singapore's population density for 2009 was 6925 persons per square kilometre. Singapore is subdivided in three main catchment areas: the Central Catchment, Western Catchment and Eastern Catchment. Singapore's catchments include 17 artificial reservoirs, 27 rivers and a complex urban stormwater drainage system (PUB Singapore (d) 2008). A subcatchment of the Western Catchment that discharges to the Sungei Ulu Pandan River will be used later on in this research for the simulation of the large-scale effects of green roofs on the rainfall-runoff. Hydrological research in this demarcated area combines the goals of SDWA to perform hydrological research activities in the Pandan area (SDWA 2010) with PUB's goal to introduce and stimulate LID measures in the Western Catchment (PUB Singapore (b) 2007), within the allowable time and interests of this research.

Urban Water Management Challenges

The hydrological effects of urbanization, which were identified in the literature review, also affected Singapore's hydrological regime (PUB Singapore (b) 2007). Flooding, stream erosion, sedimentation, water quality problems and a reduced amenity value all "perfectly" apply to this case study, as can be concluded from Singapore's Active Beautiful Clean (ABC) Design Guidelines (PUB Singapore (e) 2009), Catchment Master Waterplan (PUB Singapore (b) 2007) and the Singapore Green Plan 2012 (Hoong 2002). The following quote from the ABC Design Guidelines (PUB Singapore (e) 2009), perfectly

summarizes the hydrologic problem Singapore is facing: “While concrete waterways are able to effectively serve the function of flood control, they increase downstream peak flows, and do not provide a habitat to support a healthy aquatic ecosystem”. This quote resembles some major earlier findings from the literature review. Heavy downpours that caused flash floods in Marina Parade and Chai Chee Road on April 5, 2009 (Cheney 2009) and in the Bukit Timah area on November 19, 2009 (Channelnewsasia.com 2009) prove that the effectiveness of Singapore’s present stormwater drainage system is somewhat disputable however.

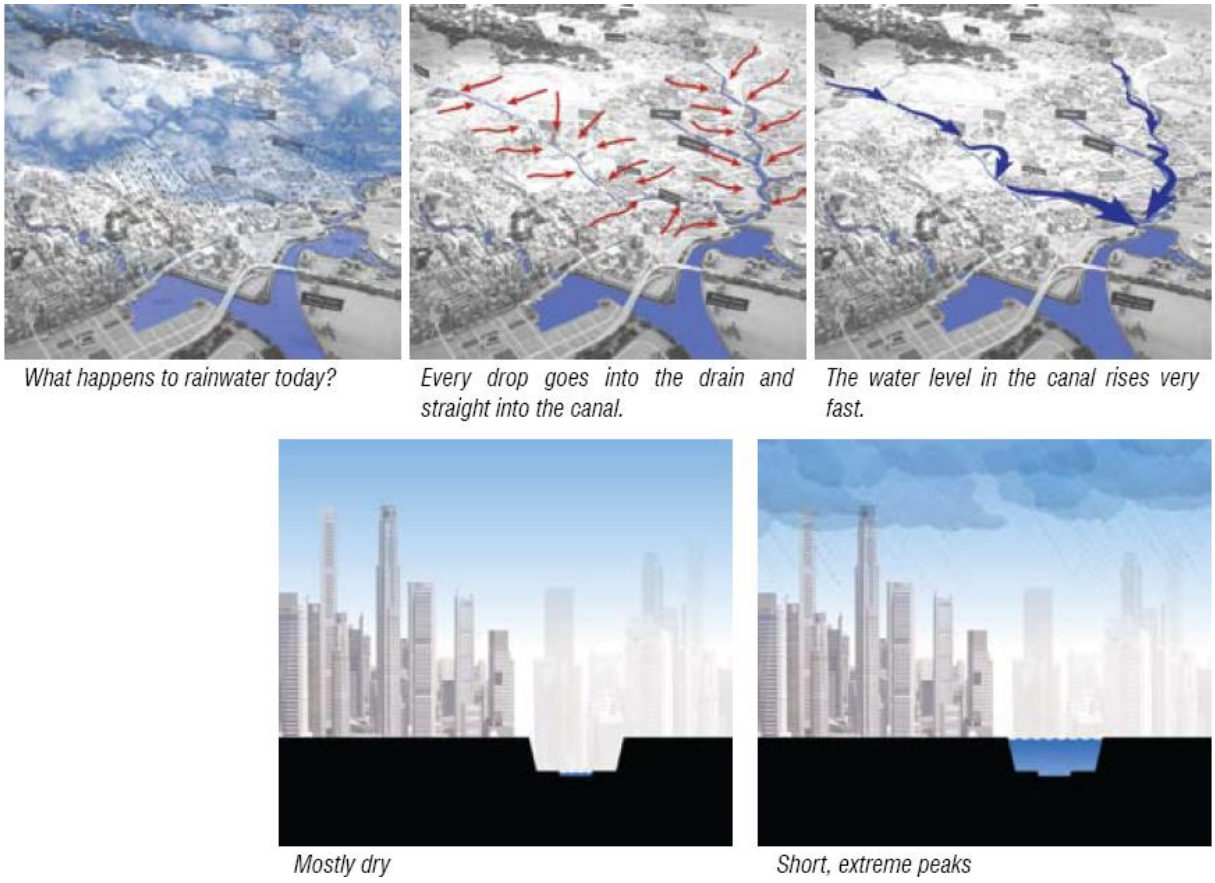

Figure 17. Hydrologic effects of present urban water management strategies in Singapore.
Source: PUB Singapore (e) (2009)

Another major urban water management challenge in Singapore is the drinking water supply. Singapore wants to decrease their reliance on Malaysian fresh water imports by ensuring greater sustainability in the future (Hoong 2002, p.45). Practices in this field are desalination plants, the NEWater wastewater recycling project and an increase of water supply catchments from 50% to 67% of Singapore’s land surface (Hoong 2002). This last strategy that focuses on catching, channeling and storage of rainwater via reservoirs, drains and canals, can contrast with Singapore’s policy to strongly encourage the use of LID measures (PUB Singapore (b) 2007) because evaporation and transpiration of retained water in LID measures decrease the inflow of runoff into reservoirs. Unfortunately, this dilemma is suppressed in present reports and water plans. Nevertheless, both effects have to be taken into account when decisions are made about the implementation of green roofs.

Singapore's present and future urban water management strategy

Singapore's national water agency, the Public Utilities Board, is responsible for the collection, production and reclamation of water in Singapore (PUB Singapore (f) 2008). As stated in the Sewerage and Drainage Act (Attorney-General's Chambers 2010), Singapore's water infrastructure consists of a separated stormwater drainage and sewerage system. Singapore's traditional *stormwater drainage system* consists of a 7000 km network of rivers, canals and drains. This system was designed to quickly and efficiently convey stormwater runoff to the sea or the nearest water body (PUB Singapore (e) 2009, p.8). Disadvantages of this traditional strategy, with respect to the scope of this research were illustrated in Figure 17.

Singapore's future urban water management strategy, the ABC Waters Programme, has been developed by PUB in partnership with the people-public-private (3P) sectors (PUB Singapore (c) 2008). Under the ABC Waters Programme, the existing waterways and water bodies are expected to serve beyond their functional and utilitarian needs. They will be transferred into clean, aesthetic, recreational, cultural and life style amenities (PUB Singapore (b) 2007, p.20) by synergistically integrating Singapore's reservoirs and waterways (blue), parks (green) and recreational infrastructures and facilities (orange) into a more sustainable urban environment named the *City of Gardens and Water* (PUB Singapore (c) 2008, p.2). This philosophy is visualized in Figure 18.

.

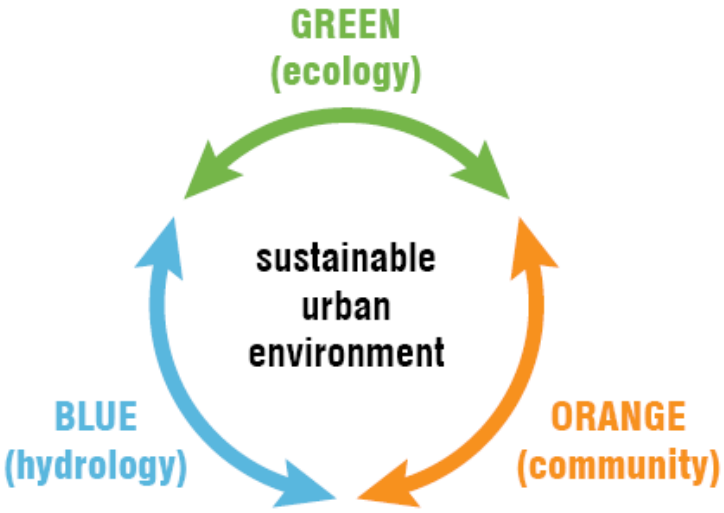

Figure 18. ABC Waters Programme philosophy. Source: PUB Singapore (e) (2009)

Implementation of LID measures is encouraged in order to mitigate the impact of development on the quality and the quantity of water bodies downstream (PUB Singapore (e) 2009, p.9). The provision of green roofs within public and private developments to filter, reduce and delay the release of stormwater to the drainage system are one of the measures promoted in PUB's Western Catchment Masterplan (PUB Singapore (b) 2007, p.43). In fact, Singapore's public housing authority, the Housing & Development Board (HDB), piloted extensive green roofs to reduce heat build up on exposed concrete roof surfaces, and to help slow down stormwater discharge (PUB Singapore (e) 2009, p.27). According to PUB, green roof advantages could be expected in the blue, green and orange systems of the ABC Waters Programme. This research focuses on the quantitative hydrological effects of green roofs in the blue system. Effects of green roofs in the green and orange systems as well as qualitative and aesthetical effects of green roofs in the blue system are

recognized, but are not part of the main research focus. Finally, the combined contribution of large-scale implementation of LID measures has to lead to a more *sustainable stormwater drainage system* in Singapore. A sustainable stormwater drainage system is defined here as a holistic system approach including drains and a sequence of LID measures designed to drain surface water in a manner that will provide a more sustainable way of runoff routing than what has been the conventional practice of routing run-off (SEPA 2010). This approach is graphically visualized in Figure 19.

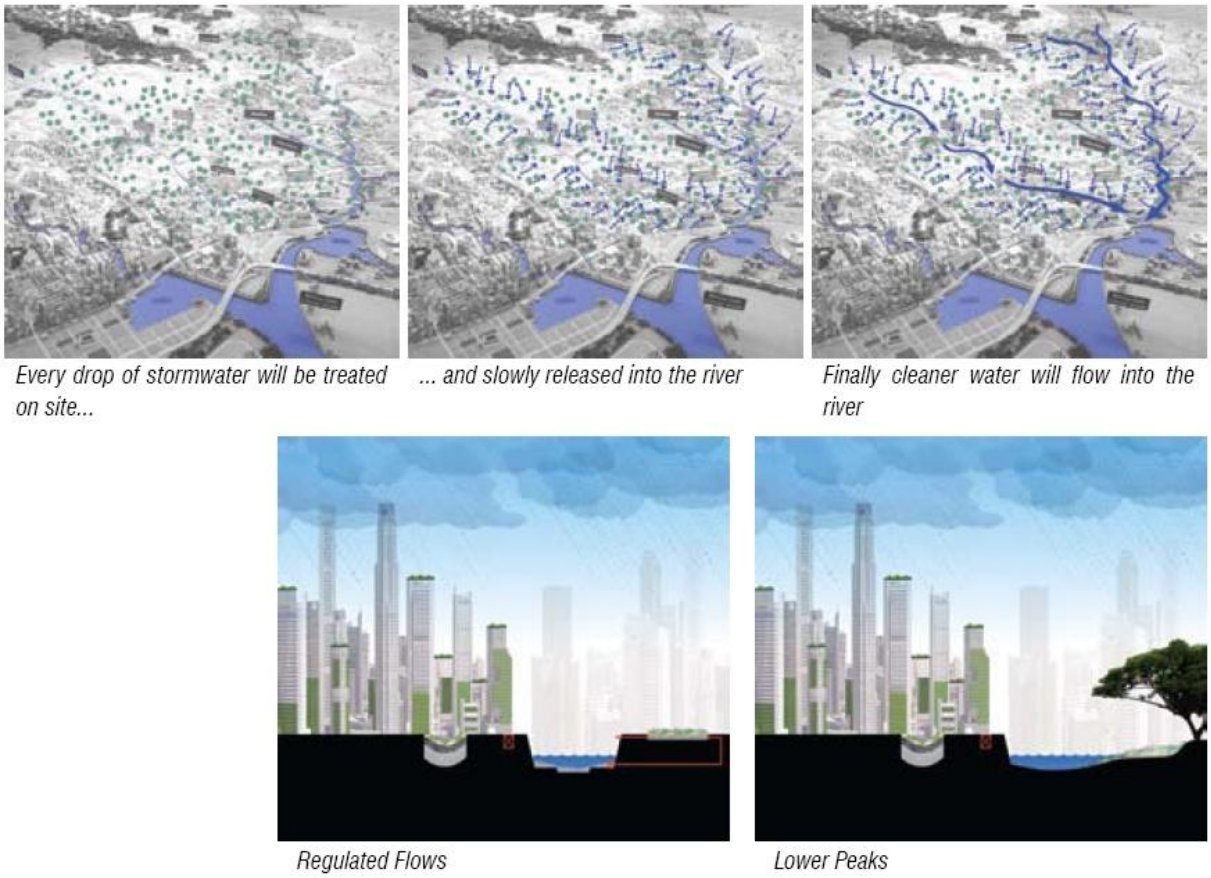

Figure 19. Hydrologic goals of future ABC Waters Management Strategy.
Source: PUB Singapore (e) (2009)

3.2 Specification of the main research question into sub research questions

The first main goal of the further research is to analyze the effects of green roofs on the rainfall-runoff in Singapore. Second, it is the aim to determine the quantitative hydrological contribution of large-scale green roof implementation to sustainable stormwater drainage systems in Singapore. In the end, a final evaluation of this case study will clarify whether the promotion of Skyrise Greenery within Singapore's ABC Waters Programme is actually worthwhile the efforts. Because this research has the intention to open up the doors for a more fundamental understanding on the effects of large-scale green roof implementation on the rainfall-runoff in tropical urbanized catchments, an evaluation will be given on the applicability and opportunities for green roofs in tropical urbanized catchments. The possibility to realize these goals and intensions can be derived from the answer to the main question of this research:

"What is the quantitative hydrological contribution of large-scale green roof implementation to sustainable stormwater drainage systems in Singapore?"

With respect to the case study and the literature review conclusions, the sub research questions that result from this main research question are:

1 **"What are the effects of green roofs on the rainfall-runoff on experiment-scale and how can we model them?"**
   a. *What is the retention, peak discharge reduction, detention and base flow conservation of green roofs in Singapore based on available experiment measurement data?*
   b. *How can one simulate the green roof performance?*
      i. *Understand the leading processes of a green roof;*
      ii. *Create a model that is able to simulate green roof rainfall-runoff processes;*
      iii. *Verification, calibration and validation of the model with experiment measurements;*
      iv. *Use of the model to simulate the performance of an individual 1m^2 green roof platform.*
   c. *What are the abilities and limitations of the green roof rainfall-runoff model?*

2 **"What are the effects of large-scale green roof implementation on the rainfall-runoff in the Sunset Way subcatchment in Singapore?"**
   a. *What are the relevant catchment characteristics?*
   b. *How can one transform the individual green roof runoff simulations to large-scale green roof runoff simulations?*
   c. *Given different coverage scenarios, what are the scaled-up effects of green roofs on:*
      i. *Peak discharge and canal water levels during extreme (design) conditions;*
      ii. *Regulation of canal flows during average meteorological conditions.*

3 **"Which green roof strategy and programme should Singapore choose?"**
   a. *What are the capabilities and limitations of large-scale green roof implementation in Singapore?*
   b. *Which implementation and design strategy is recommended?*
   c. *How can the case-study results contribute to a more sustainable development of stormwater drainage systems in tropical urbanized areas?"*

The answers to these (sub) research questions will be provided as the research progresses to the following research chapters.

Part 2 Small-scale green roof analysis

Figure 20. Green roof experiment set-up

In order to be able to facilitate the hydrological analysis of large-scale green roof implementation at subcatchment-scale, Part 2 presents an approach to model the rainfall-runoff processes which occur on a small-scale green roof experiment platform. Hydrological measurements from the green roof experiments that are located on the rooftop of the National University of Singapore will be collected and interpreted. A model for the simulation of transient, vertical water flow in unsaturated media will be set up to predict the runoff generation from extensive green roofs in Singapore over a range of measured meteorological conditions. A good understanding of the hydrological processes and the soil physics in the green roof media is an urgent necessity in order to end up with a reliable and good model that fits the purpose of this research: formalizing knowledge on the effects of large-scale green roof implementation. Finally, this knowledge can help to improve implementation strategies and design considerations for green roofs. In turn, this can enhance the contribution of green roofs towards more sustainable stormwater drainage systems in the future.

Chapter 4 presents a methodology and analysis of the green roof measurements, which were performed on an experimental site at the National University of Singapore. Green roof rainfall-runoff of four monthly series, including 66 precipitation events, will be analyzed and evaluated based on the performance indicators that were introduced in the literature review. After that, the contents of chapter 5 will focus on designing and testing an unsaturated zone model for the simulation of green roof rainfall-runoff. This chapter will be structured around the iterative model cycle. The conceptualization and initial specification of the input for the unsaturated zone model will be described. Sequentially, the internal model parameters will be calibrated against the green roof measurement results. Once the final set of model parameters has been specified, the green roof runoff simulations will be validated, but for a set of hydrological events that were not used for model calibration. Within this framework several quantitative and qualitative performance measures for every individual measured vs. simulated rainfall-runoff event will be determined and compared. This chapter ends with a discussion and conclusions regarding the first subquestion of this research.

4 Experimental analysis of small-scale green roof rainfall-runoff measurements in Singapore

4.1 Introduction

Green roof rainfall-runoff measurements that are analyzed in this research originate from the green roof experiment set-up that is part of SDWA's Aquatic Science Centre 'Pandan Canal' experimental initiatives. The green roof platforms were installed in order to obtain a better understanding of their internal rainfall-runoff processes and their use in water quantity and water quality management. This research focuses on examining the water quantity side of the green roof rainfall-runoff interests of this experiment set-up. Data logging started in July, 2009 and includes continuous small time scale measurements of the rainfall-runoff from five roof platforms with different treatments. Regarding the scope of this research only three of these treatments were observed and analyzed: a reference roof and two green roof platforms.

First, the green roof measurement materials will be described (paragraph 4.2). Here, the site location, design of the different platform treatments and the available measurement periods will be outlined. Next, the methodological framework for the small-scale green roof performance analysis will be provided (paragraph 4.3). The result section (paragraph 4.4) of this chapter will give an overview of the small-scale green roof rainfall-runoff analysis results. This analysis includes 66 rainfall events during four monitoring periods of one month. Finally, conclusions will be drawn on the outcome of the experimental analysis (paragraph 4.5). The conclusions will be completed with important leads and recommendations for further green roof rainfall-runoff modelling in chapter 5.

4.2 Green roof measurement materials

4.2.1 Description of the experiment set-up

Site location

The five green roof experiment platforms are located on top of the Engineering Auditorium (EA) building on the campus of the National University of Singapore at coordinates $1^0$18'01.02"N and $103^0$46'13"E (Figure 21). This location was selected because of the ease of accessibility, small distance from the SDWA office and educational purposes. Next to this, the site cannot be entered by unwanted "guests" that could manipulate or destroy the experiment set-ups (except for birds) and monitoring instruments. The Engineering Auditorium is a seven-story high building and is not directly bordered by any other (higher) buildings that could influence rainfall or wind speeds. Nevertheless, the platforms were closely placed to some industrial constructions and an air-conditioning fan. These structures might influence meteorological conditions (wind speed and rainfall) at the set-ups. This has to be accepted, but when one wants to deduce conclusions from hydrological measurements in urban areas, these influences have to be taken into account in the end.

Figure 21. Location of the green roof experiments, SDWA office and NUS meteorological station. Source: Google (2009)

Experiment set-up

The total experiment set-up consists of five 1 m^2 green roof platforms with different treatments. On February 2010, the set-up consisted of the following treatments:

- A reference roof;
- Two extensive green roofs;
- Two platforms with extra drainage block treatments to asses extra detention possibilities.

Based on the research demarcation, that was established earlier, this research primarily focuses on comparing the rainfall-runoff from the reference roof and the extensive green roofs. The two remaining platforms with extra drainage blocks are used in other SDWA green roof studies and will not be considered in further detail.

Platform design

The platform construction is identical for all treatments and consists of a solid metal frame with a 100 X 100 x 21 cm soil storage tray made of PVC plastic. The total height of the frame, which has a typical 1^0 roof slope towards the drain, is 84 cm. The identical platform design allows for good comparison between different treatment runoff results.

Reference roof design

The reference roof platform consists of a standard platform design with a 2 cm thick *concrete base layer*. Rainfall that falls on the reference roof is able to flow to the drain, which is depicted on the right side of Figure 22. The collected runoff flows from the drain via a pipe to the runoff tipping bucket that collects the runoff water from the platforms.

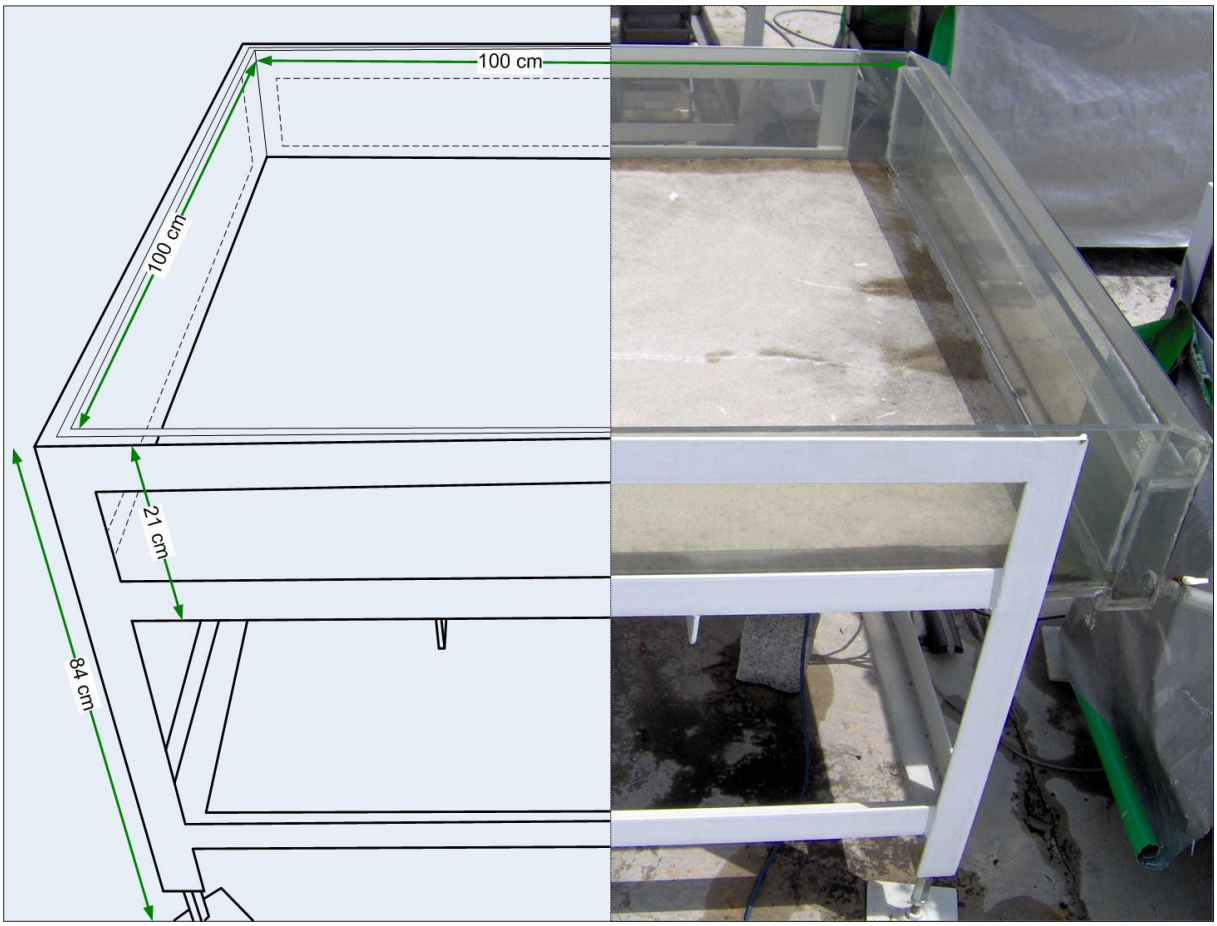

Figure 22. Platform design of the reference roof

Extensive green roof design

Both extensive green roof platforms are build in a similar way. On top of the 1 cm *PVC plate*, which forms the bottom of the storage tray, lies a 2 cm thick *concrete base layer*. This layer is the same as the one on the reference roof platform. On top of the concrete base layer lies a 3 cm thick *drainage layer* of clay marbles. This drainage layer allows for easy drainage as soon as the runoff drips out of the soil media of the green roof. A synthetic *filter fabric* between the growing media and the drainage layer has a thickness of approximately 0.1 mm and prevents the soil from flushing out of the storage tray. A 12 cm thick *growing media* is used in both green roof experiment platforms. The growing media consists of standard potting soil. The potting soil is a mixture of white peat, black peat and clay and has additional fertilizers. Finally, the *vegetation layer* consists of sedum plants, with an average height of 5 cm. The sedum species that is used is *Sedum Mexicanum*. This sedum species has a very high drought tolerance (Greenroofplants.com 2010) and has great potential for tropical green roof applications. Appendix 3 shows the vegetation development of the green roof platforms. No maintenance (irrigation and/or weed removal) was performed on the green roof platforms. The design of the extensive green roof platforms is graphically illustrated in Figure 23 and Figure 24.

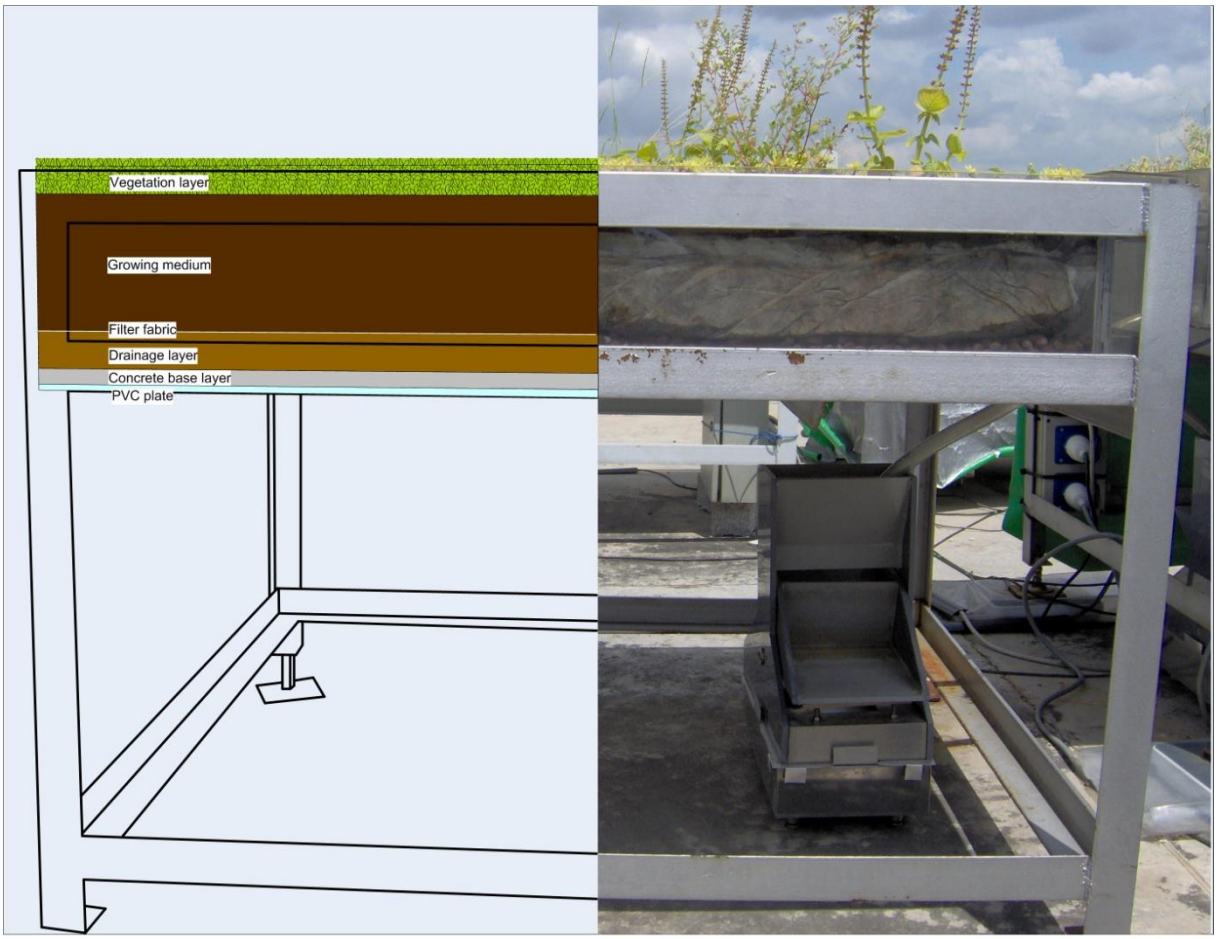

Figure 23. Platform design of the extensive green roof

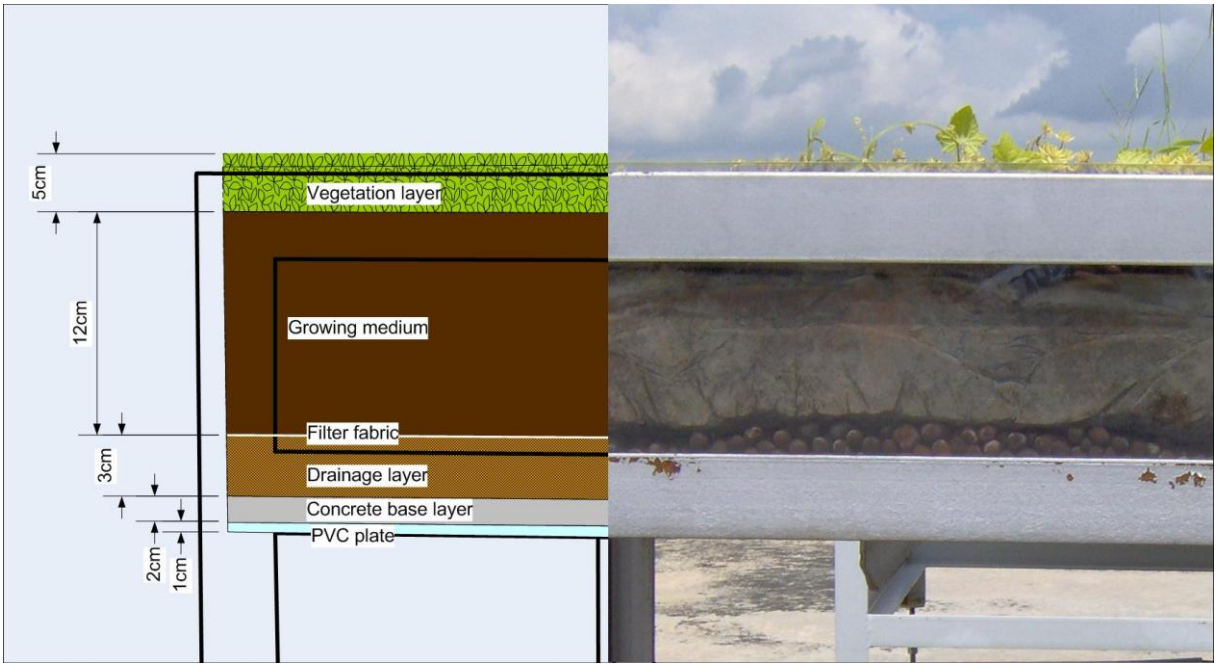

Figure 24. Dimensions of the extensive green roof platform design

4.2.2 Description of available data

The green roof measurement dataset used within the analysis consists of two components:

1. Runoff data from the reference roof and the extensive green roofs;
2. Meteorological measurements.

The measurement devices, measurement interval, measurement period and several other relevant characteristics of the dataset will be discussed briefly.

Runoff data from experiment set-ups

Runoff from all platform designs accumulate in the drainpipes. A rubber hose connects the downstream side of each 1 m long drainpipe with the tipping buckets. The tipping buckets have a volume of 1 litre, which equals 1 mm of rain on a 1 m^2 roof platform. The size of the buckets increase the accuracy due to a lower tip frequency at high outflow rates compared to a standard rainfall tipping bucket with a tip for every 0.2 mm (or the relatively similar 0.01 inch tip). Tipping bucket rain gauges have been recommended by Prowell (2003) in order to avoid fluctuating water levels during storm events caused by runoff falling into collection containers. Tipping buckets also eliminate the need to empty the collection containers after every rain event. This enables continuous runoff data logging. All tipping buckets are placed on a balance with an accuracy of 1 gram. Balance measurements are logged onto a PC on a 2-second time interval since November 2008. In this research four runoff series of about one month, including a total number of 66 storm events with P>0.5 mm, were recorded. These four series took place during the following periods:

1. July 5-20, 2009;
2. September 1-22, 2009;
3. December 2-31 2009;
4. March 10 - April 10, 2010.

Either rainfall tipping bucket problems or roof platform balance logging failures decreased the available measurements in 2009. Moreover, Singapore experienced a 1:100 year dry spell in January and February 2010, resulting in only one runoff event in those two months and a reduced and changed green roof vegetation cover (Appendix 3). This dry spell narrowed the available measurements in 2010 up to a one month period between March 10 and April 10. In this fourth period, only measurements from green roof 2 are available.

Meteorological measurements

Meteorological measurements include rainfall [mm], atmospheric pressure [kPa], air temperature [^{0}C], relative humidity [%], wind speed [m/s], and incoming radiation [W/m^2]. Rainfall was measured at a 1-minute interval with a 0.2 mm RG600 Global Water Tipping bucket rain gauge and a GL500-2-1 data logger which has been placed next to the experiment platforms on the rooftop of building EA. The tipping bucket rain gauge was calibrated for different rainfall intensities, because the accuracy of the tipping bucket decreases when the tipping frequency increases. All other meteorological data were obtained from the NUS weather station. These measurements were available at a 5-minute time interval. More details of the meteorological measurements are presented in Appendix 4.

4.3 Green roof measurement analysis methodology

The green roof measurement analysis consists of three basic research steps:

1. Collection and determination of the measurement series;
2. Processing of the measurements into a dataset and finally into performance indicators;
3. Reporting the measurement results (paragraph 4.4).

The four measurement series of July, September, December 2009 and March/April 2010 were selected as a manageable and sufficiently representative set of rainfall-runoff events. All relevant characteristics of these events were analyzed and combined into an extensive dataset with hydrograph characteristics. Because these hydrograph characteristics vary from event to event, each performance indicator will be calculated on an event based-scale. The performance indicators of interest are all expressed relative to the reference roof except for the RPI-values:

- Retention performance indicator relative to rainfall (RPI) and a reference roof (ASRPI);
- Peak discharge performance indicator (PDPI);
- Detention performance indicator (DPI).
- Base flow performance indicator (BFPI).

Mathematical expressions for all performance indicators can be found in Eq. 2.3 - Eq. 2.13. The methodology is illustrated with hydrograph analysis calculations in the box below. A 13.59 mm rain event, which took place on September 19, 2009, is used as a hydrograph analysis example.

Hydrograph analysis example

The rainfall-runoff event of September 19, 2009, with first recorded rainfall at 10:15, will be used as an example to illustrate the green roof measurement analysis. Performance indicator calculations for the stormwater retention, peak discharge reduction, detention and base flow conservation will be treated successively. Like all other rainfall-runoff events, raw event data can be found in Appendix 5.

Stormwater retention

The 13.59 mm rainfall event resulted in 13.14 mm runoff for the reference roof (RefR), while green roof 1 (GR1) and green roof 2 (GR2) produced 10.06 and 10.39 mm of runoff respectively. The retention performance indicator (RPI) relative to the rainfall depth and the additional stormwater retention performance indicator (ASRPI) relative to the reference roof are calculated as follows:

$$RPI\ RefR = 13.59 - 13.14 = 0.45\ mm$$
$$RPI\ RefR\ ratio = 1 - \left(\frac{13.14}{13.59}\right) * 100\% = 3.31\%$$

$$RPI\ GR1 = 13.59 - 10.06 = 3.53\ mm$$
$$RPI\ GR2 = 13.59 - 10.39 = 3.20\ mm$$
$$RPI\ GR1\ ratio = 1 - \left(\frac{10.06}{13.59}\right) * 100\% = 25.97\%$$
$$RPI\ GR2\ ratio = 1 - \left(\frac{10.39}{13.59}\right) * 100\% = 23.55\%$$

$$ASRPI\ GR1 = 13.14 - 10.06 = 3.08\ mm$$
$$ASRPI\ GR2 = 13.14 - 10.39 = 2.75\ mm$$
$$ASRPI\ GR1\ ratio = \frac{(13.14 - 10.06)}{13.59} = 22.66\%$$
$$ASRPI\ GR2\ ratio = \frac{(13.14 - 10.39)}{13.59} = 20.24\%$$

Peak discharge reduction

The peak discharge of the reference roof was 0.77 mm/min, while the peak discharge of green roof 1 and green roof 2 was 0.48 and 0.46 mm/min respectively. The peak discharge performance indicators relative to the reference roof are calculated as follows:

$$PDPI\ GR1 = 0.77 - 0.48 = 0.29\ mm/min$$
$$PDPI\ GR2 = 0.77 - 0.46 = 0.31\ mm/min$$
$$PDPI\ GR1\ ratio = \left(1 - \frac{0.48}{0.77}\right) * 100\% = 37.66\%$$
$$PDPI\ GR2\ ratio = \left(1 - \frac{0.46}{0.77}\right) * 100\% = 40.26\%$$

Peak discharge detention

The peak of the reference roof coincided with the peak of the rainfall leading to a peak delay of 0 minutes. The two green roofs both had a peak delay of 16 minutes. The detention of the green roofs relative to the reference roof can be calculated as follows:

$DPI\ GR1 = 16 - \ 0 = 16\ minutes$ and $DPI\ GR2 = 16 - \ 0 = 16\ minutes$

Base flow conservation

Base flow conservation calculations will be extracted from the cumulative base flow depths between the last recorded rainfall, 60 minutes after the last recorded rainfall and 180 minutes after the last recorded rainfall. Generally, green roof runoff was rare after 180 minutes past the last recorded rainfall. This finding does not apply for overlapping rainfall events. The base flow of the reference roof and green roof 1 are 0.07 and 0.36 mm (or l/m^2) and don't further increase between one and three hours after the last recorded rainfall. The 0-60 min base flow and 0-180 min base flow for green roof 2 are 0.98 and 1.49 mm respectively. The base flow performance indicators are:

$BFPI_{60}\ GR1 = 0.36 - 0.07 = 0.29\ mm$ and $BFPI_{60}\ GR2 = 0.98 - 0.07 = 0.91\ mm$

$BFPI_{180}\ GR1 = 0.36 - 0.07 = 0.29\ mm$ and $BFPI_{180}\ GR2 = 1.49 - 0.07 = 1.42\ mm$

The associated hydrographs for the reference roof and both green roofs as well as the cumulative rainfall are graphically depicted in Figure 25.

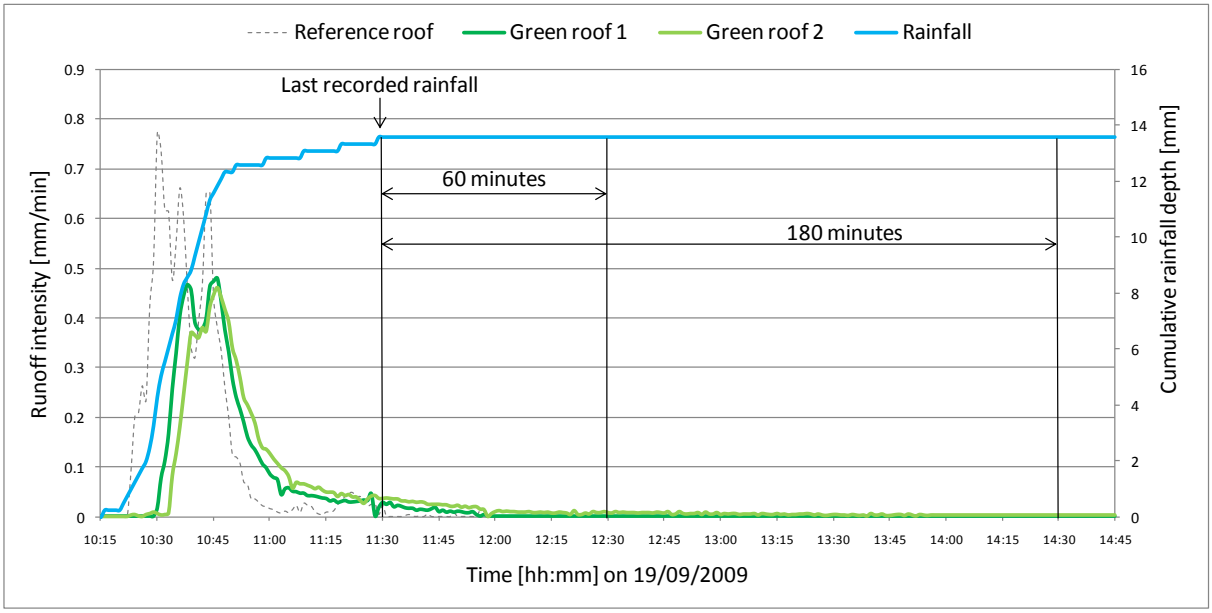

Figure 25. Hydrograph and cumulative rainfall for a storm event on September 19, 2009

4.4 Green roof measurement results

The aim of this chapter is to provide an overview of the 1 m^2 platform green roof experiment measurement results. For analysis purposes, measurement results will be classified first (4.4.1). In a quartet of sub-paragraphs the retention performance (4.4.2), peak discharge reduction (4.4.3), peak discharge detention (4.4.4) and base flow conservation (4.4.5) properties of the green roof platforms versus the reference roof will be examined. Presented results were derived from platform measurements of green roof 2. Because measurements from platform 1 are not available for the period in March and April 2010, the available number of events for this platform is reduced with 24 events to 42 events. Next, a tilted tipping bucket at the GR1 platform in September introduces data recording errors. In order to avoid a bias in the comparison of the performance indicators, because of measurement errors or a different number of events in both datasets, GR1 is purely used to assess the differences between both green roof platform results. These differences can give indications for experiment heterogeneity and hence will have to be taken into account as well (4.4.6).

4.4.1 Measurement results classification

Green roof measurement results were analyzed for four periods of about one month. Nine events were analyzed in July, 2009 of which only three events resulted in green roof runoff. In September, 2009, ten events were analyzed and out of these ten events nine events produced green roof runoff. For December 2009 and March/April 2010 respectively 17 out of 23 and 11 out of 24 rainfall events generated green roof runoff. A *rainfall event* is defined as a period with rain, separated to another period of rain by a 0 mm dry spell of at least 1 hour. For further analyses purposes, all 66 rainfall events are ranked in classes. Small rainfall events, with a rainfall depth of between 0.5-2.5 mm are ranked in the first class. Medium events have a rainfall depth of between 2.5-10 mm and large events have a rainfall depth of between 10-20 mm. The last extreme class, contains rainfall events with a total depth exceeding 20 mm. This classification has been based on the idea to obtain classes which all contain a reasonable number of events. In the end, this classification is still arbitrarily though.

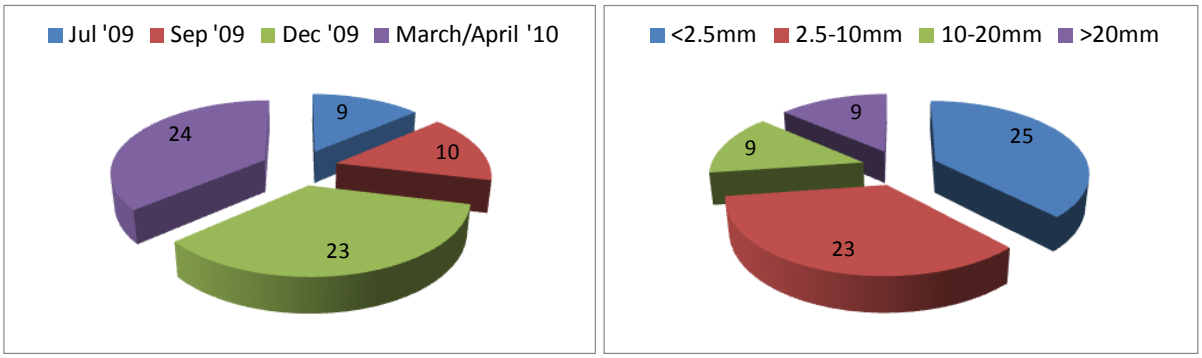

Figure 26. Number of rainfall events per period and classification of rainfall events

4.4.2 Stormwater retention

The overall rainfall depth in the four observed periods equals 595 mm. Total reference roof runoff equals 490 mm while green roof 2 has a total runoff of 256 mm. The total absolute retention of the green roof platform is 339 mm, while the retention of the reference roof still adds up to a total of 105 mm. The average of the sum of all event based RPI ratios for green roofs equals 75% while the average total RPI ratio equals 57%. Differences in both performance indicator ratios clearly indicate a high number of small rainfall events without green roof runoff (RPI ratio=100%), while these small events have a relatively low influence on the total runoff sum. This dissimilarity almost disappears

when we look at the additional stormwater retention, relative to the reference roof runoff. The green roof provides an additional water retention of 234 mm. The average sum of all individual event ASRPI ratios show an additional retention of 38% while the average total ASRPI ratio equals 39%. These results show that the reference roof retention for small events is quite high as well. Normally, reference roof retention volumes equal at least 0.5 mm, but can increase up to over 5 mm for long drizzling events, where evaporation regenerates the storage capacity continuously. The rest of this subparagraph will be structured around two hypotheses:

1. Green roof retention performance decreases with increasing rainfall depths;
2. Green roof retention performance increases with longer antecedent dry weather periods.

Rainfall depth vs. retention performance

Absolute retention performance of the green roof platform is visualized in the two topmost graphs of Figure 27. The left top graph shows that there is a weak positive relationship (R^2=0.44) between the absolute amount of retained rainfall by the green roof and the rainfall depth. Small as well as some larger events are totally retained by the green roof. These events are located on the red 100% RPI line. The largest event, which is totally retained, is the 24 mm rain event of July 15, 2009. An even weaker relationship (R^2=0.29) is found between the absolute ASRPI and the rainfall depth. Some negative absolute ASRPI values occur, which indicate that the amount of retained rainfall from a reference roof can be conditionally higher than for a green roof. This only happens when events quickly follow up: green roof base flow from a previous event "artificially" decreases the retention of the new event. The left bottom graph of Figure 27, shows a weak relationship (R^2=0.27) between the retention performance ratio and the rainfall depth. While some of the larger events are totally retained by the green roof (RPI ratio=100%), some small events are only partially retained.

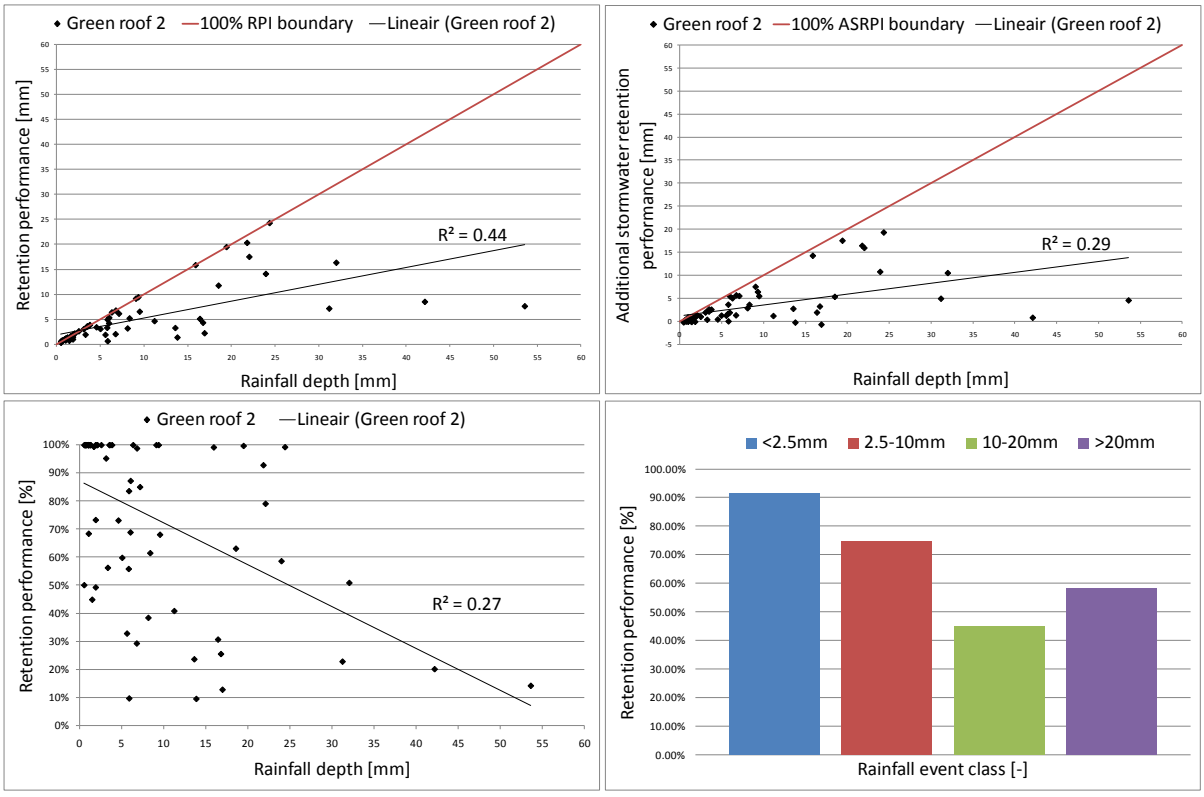

Figure 27. Retention performance of green roofs vs. rainfall depth

The right bottom graph of Figure 27 shows the average event based RPI ratio as a function of the four rainfall classes. The average RPI ratio for the 25 small rainfall events exceeded 90%. Declining RPI ratios were found for the medium (2.5-10 mm) and large (10-20 mm) events: 75% and 45% respectively. However, the RPI ratio for extreme events (>20 mm) was 58% and exceeds the ratio of the large event class. This might be caused by natural variance and the relatively small sample size of each class. It is more likely though, that the antecedent number of dry weather days does account for this irregularity in measurement results.

Antecedent dry weather period vs. retention performance

Based on green roof hydrological processes it can be hypothesized that the *antecedent dry weather period* (ADWP) influences the retention performance of green roofs. Measurement analysis shows that most of the rainfall events occur after a relatively short ADWP (average ADWP is 1.32 days for all events). Figure 28 (a) visualizes the weak relationship (R^2=0.23) between the ADWP and the absolute ASRPI values, which are defined as the extra retention of the green roof relative to the reference roof. Fitted curves in Figure 28 are logarithmic, because of the exponential decrease of transpiration during increased antecedent dry weather prolongation (Berghage, Jarett, et al. 2007, p.2-6). If only the rain events with more than 10 mm of rainfall depth are selected, the relationship between ADWP and ASRPI becomes more pronounced. From this analysis it becomes clear that the ADWP is not a good predictor for the retention as well: the green roof retention capacity can still be high when the ADWP is low because of a small antecedent rain event after a long dry weather period. Instead of the ADWP, which is easy to measure, the antecedent soil water content is probably a better predictor for the retention performance. To conclude: retention performance is not solely a function of the antecedent dry weather period as well. This means that both hypotheses have to be rejected: the retention of green roofs is complex and dynamic.

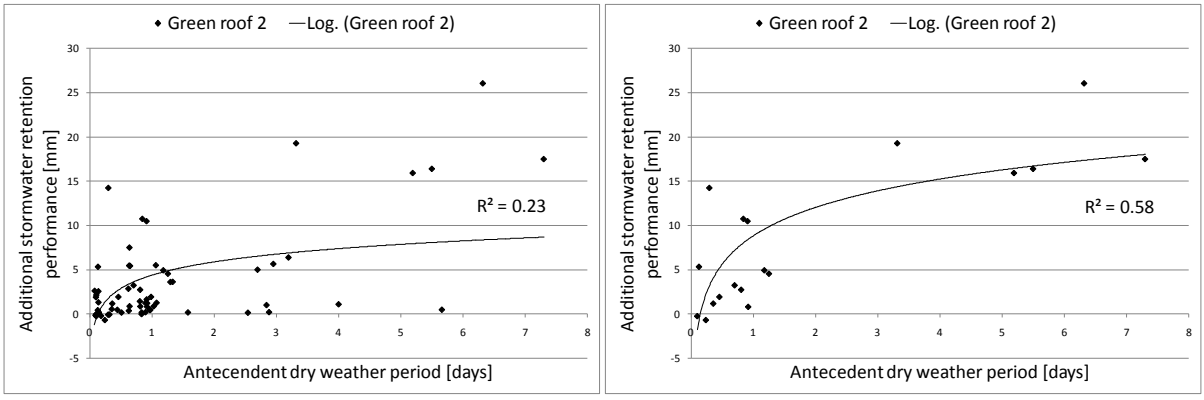

(a) All events (b) All events with P>10 mm

Figure 28. Additional stormwater retention performance vs. antecedent dry weather period.

4.4.3 Peak discharge reduction

Peak discharge reduction or hydrograph attenuation is a very important objective in stormwater management, because this could reduce the environmental impact, could enable a size-reduction of the hydraulic structures within the stormwater drainage system, or could provide capacity for future urban development. The average peak discharge reduction (PDPI) ratio, relative to the reference roof, over the four periods equals 77.5%. This average value is higher than the PDPI-value from Prowell (2006) who measured a peak discharge reduction relative to a reference roof of 64%. A large number of small storms without any green roof runoff in this research and the shallower media in

Prowell's work (10 cm) might be a cause for this difference. To prevent performance indicator biasing, three negative PDPI values were neglected in this analysis, because associated intensities are very small (20/03/2010), which is sometimes caused by the base flow of a previous rainfall event (04/12/2009 and 10/03/2010). The rest of this subparagraph will be structured around two hypotheses:

1. Green roof peak discharge reduction decreases with increasing rainfall depths and intensities;
2. Green roof peak discharge reduction increases with lower antecedent soil water contents.

Rainfall depth and intensity vs. peak discharge performance

The individual PDPI ratios of the green roof, relative to the reference roof, varied between 0 and 100%. The largest absolute peak reduction equals 2.21 mm/min for the rainfall event of September 17, 2009 10:11. During this event the peaks of the rainfall, reference roof runoff and green roof runoff were 2.40, 2.23 and 0.02 mm/min respectively. The average and median PDPI ratios decrease for rainfall events with increasing depths (Figure 29 (a)). The extremes of the same graph show that even large and extreme event peak discharges can sometimes be fully reduced. On the other hand, the minimum PDPI ratio reduces for large and extreme events to 26 and 24% respectively. Reduced peak discharge reduction reliability for larger (design) storms is an important disadvantageous feature of green roofs with respect to stormwater management practise. It is concluded that the rainfall intensity is not a good predictor for the green roof runoff peak intensity. Two extremes, which are highlighted in the right graph of Figure 29, illustrate this. Dry antecedent roof conditions can fully omit green roof peaks (15.91 mm rain event of 17/09/2009), while peak intensities are hardly reduced under initially wet green roof conditions (53.60 mm rain event of 21/03/2010).

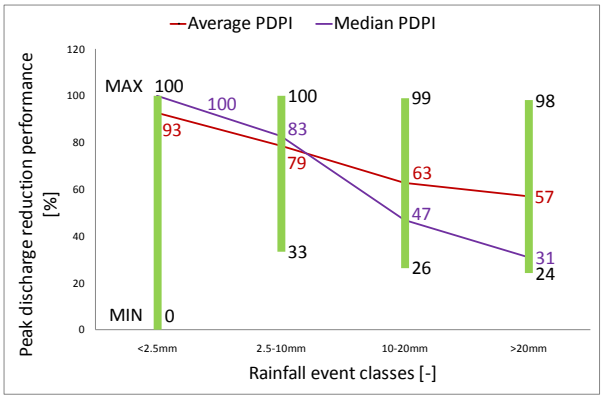

(a) PDPI per rainfall event class

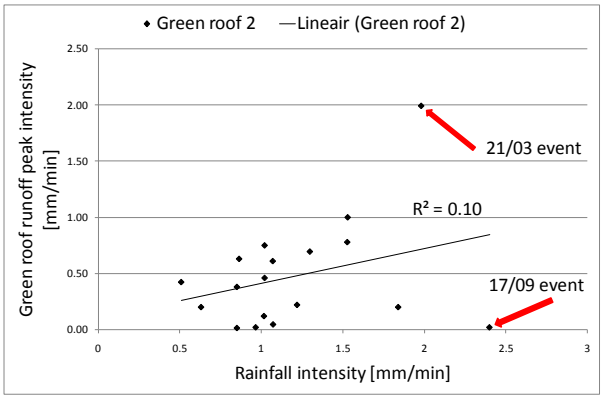

(b) PDPI vs. rainfall intensity with P>10 mm events

Figure 29. Peak discharge reduction performance

Antecedent soil water content vs. peak discharge performance

Antecedent soil water contents affect the peak discharge performance. Hydrograph analysis of a 15.91 mm rainfall event (17/09/2009) and a 53.60 mm (21/03/2010) clearly illustrate the effect of the green roof antecedent soil water content. The relatively dry/unsaturated green roof on September 17 almost totally retains the rainfall, which resulted in a 99.1% peak reduction. This smoothing effect rapidly decreases when the green roof becomes saturated, as can be observed in the reference and green roof hydrograph of the March 21, 2010 rainfall event (Figure 30). This example also illustrates that the peak discharge reduction performance decreases when a large

volume of rainfall saturates the soil, before the actual rainfall or reference runoff peak occurs. The dynamic complexity of rainfall depth and intensity distribution over time as well as the antecedent soil water content of the green roof determine the peak discharge performance. Therefore, just as with the retention performance, both hypotheses cannot be unilaterally accepted.

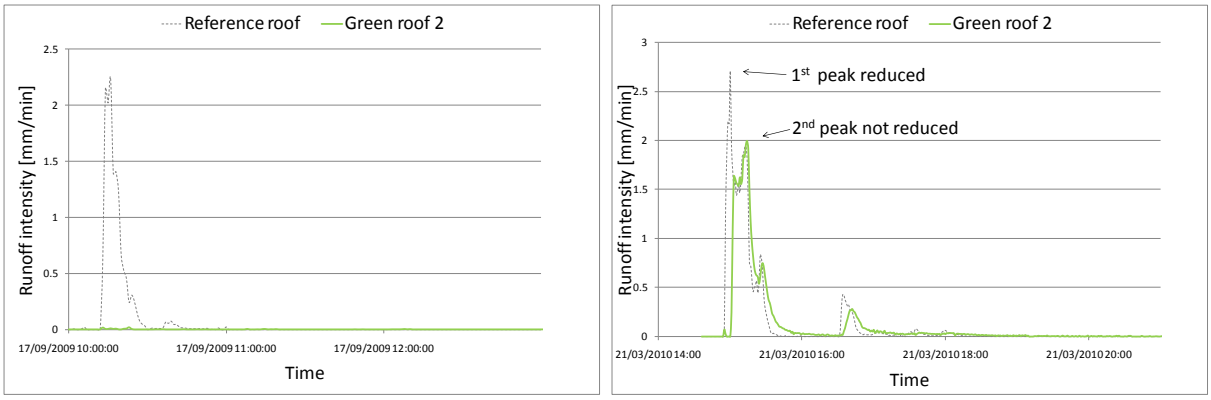

Figure 30. Rainfall-runoff event hydrographs of September 17, 2009 and March 21, 2010

4.4.4 Peak discharge detention

On top of a peak discharge reduction, practical advantages of green roofs with regard to stormwater management can be increased by desynchronizing runoff flows in an urbanized catchment. Again, a combination of both the rainfall characteristics as well as the antecedent green roof conditions determine the detention performance. Apart from preferential flow, peak discharge detention can only be observed when the total rainfall depth exceeds the available retention storage. Within the observed periods, 41 out of 66 events produced runoff and thus a potential runoff delay. Three peaks of the green roof preceded the peaks of the reference roof. Preferential flow paths and measurement equipment accuracy errors at very low intensities (<0.08 mm/min) are likely the cause for this. The average time to peak of the green roof is 37 minutes, while the average time to peak of the reference roof is only 4 minutes. The 34 minutes peak delay between the green roof and rainfall peak corresponds with the 35 minutes literature value from Carter and Rasmussen (2006). Average detention performance decreases with increasing rainfall event classes, for the small, medium and large events (Figure 31, left graph). The average detention performance for the extreme event rainfall class is higher than all other classes: 54 minutes.

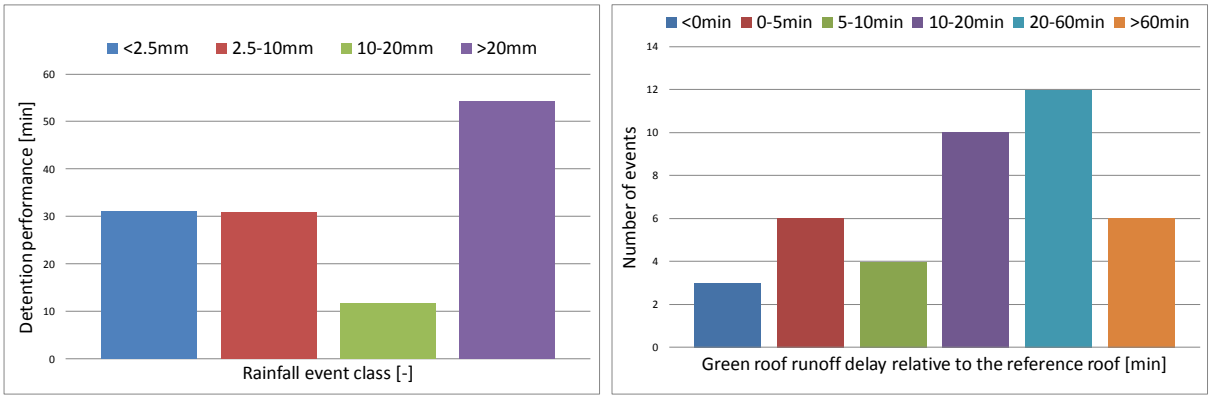

Figure 31. Detention performance per rainfall event class and number of events per delay class

The small sample size (9 events) in this class and six events with relatively high delays in March and April, 2010 could explain the unforeseen high detention performance in this class. More than half of all remaining runoff events can be categorized in the 10-20 min and 20-60 min classes, while 32% of all events have a delay of less than 10 minutes (Figure 31, right graph).

Influence of rainfall characteristics

Next to the influence of infrequent data points, variations in rainfall characteristics between individual events introduce additional complexity. An example of this complexity is illustrated in Figure 32. Hydrographs of two events on September 6, 2009 (P=31.2 mm) and March 14, 2010 (P=32.0 mm) show that the green roof almost totally retain the first peak of the reference roof. After soil saturation, the green roof intensity and delay of the second peak follow the reference roof much closer in both events. Because the first peak of the September 6 event is smaller than the latter one, the peak delay is only 3 minutes here. The first peak of the March 14 event is bigger than the second peak, which results in a peak delay of 130 minutes. Based on the given definition of a rain event, these results are formally correctly calculated values of the detention performance. The formalization however covers the real functioning of the green roof detention. It can be concluded that a static performance indicator is not able to account for all dynamic processes that actually occur. This limitation should always be considered when addressing the performance of green roofs.

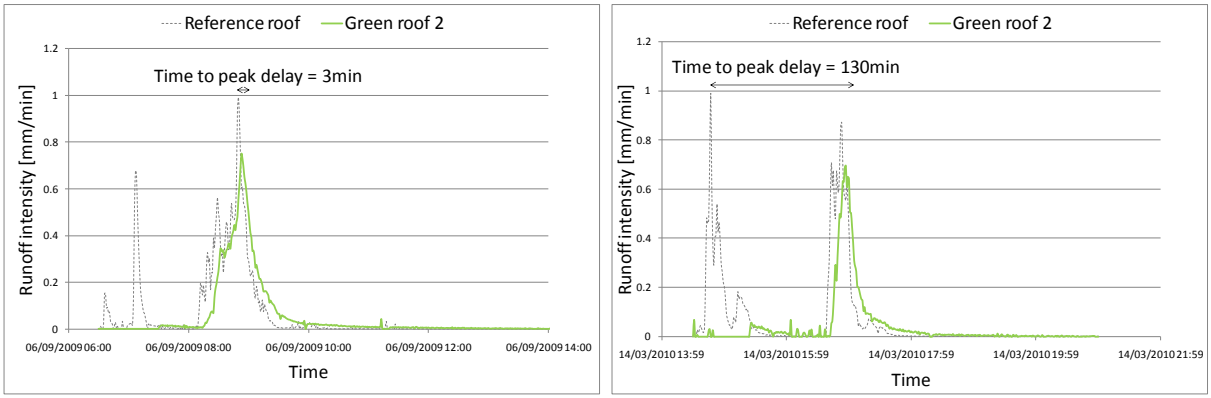

Figure 32. Rainfall-runoff event hydrographs of September 06, 2009 and March 14, 2010.

4.4.5 Base flow conservation

One of the future hydrological goals in PUB's ABC Waters Program strategy is to regulate canal base flows with onsite treatment of rainfall. To test whether green roofs could potentially contribute to this goal, the base flow of the green roof platforms was examined. The cumulative runoff depths at 60 and 180 minutes after the last recorded rainfall were analyzed for the reference and green roof platform. Compared to the reference roof runoff, the green roofs provide an extra 0.2 mm of base flow 0-60 minutes after the last rainfall measurement. On top of this, green roofs provide an average additional 0.21 mm of base flow in between 60 and 180 minutes after the last rainfall. Base flow from the reference roof is only provided for up to 60 minutes after the last recorded rainfall. Unlike a reference roof, green roofs do not provide base flow for most small and medium events, since most of those rainfall events do not result in green roof runoff at all (Figure 33). Green roof base flow advantages start to get interesting in the large and extreme event cases. For the large events they provide an extra 1.16 mm of base flow, up to three hours after the last rainfall (Figure 33). $BFPI_{180}$ results of the extreme events give an average extra base flow of 0.76 mm (Figure 33). Over the whole measurement period, the maximum $BFPI_{60}$ was 1.79 mm, while the maximum $BFPI_{180}$ was 2.63 mm.

Based on the measurement results analysis it can be concluded that the extensive green roof base flow performance is conditional. Most of the base flow is discharged within 1 hour after the last recorded rainfall and continues for up to 3 hours after the last rainfall. The examined extensive green roof design is able to delay the runoff and provide some extra base flow (<3 litres/m^2) directly after a large or extreme rainfall event, but they cannot provide continuous base flow in between rainfall events with long dry spells. This analysis shows that extensive green roofs cannot replace the natural function of groundwater, which provides the total flow of the recession curve until the next period of rainfall in natural situations (Savenije 2007).

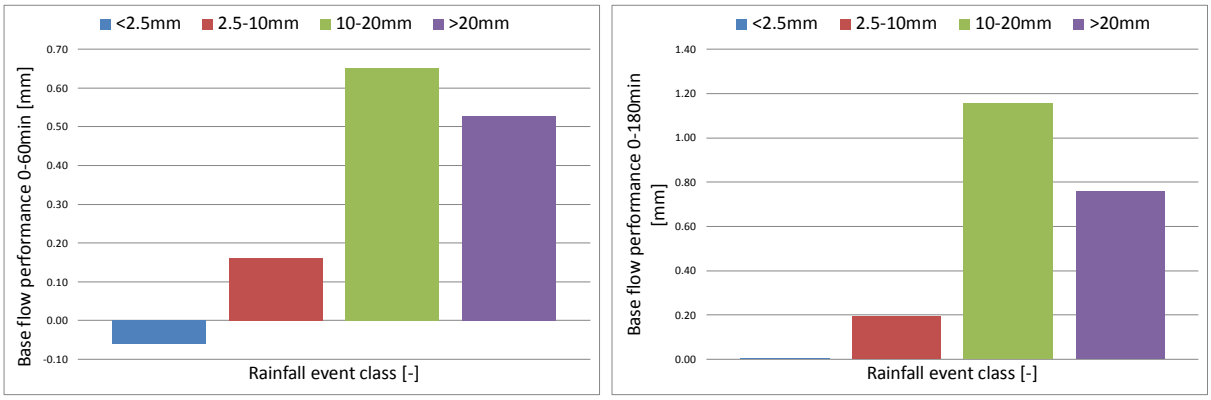

Figure 33. Base flow performance vs. rainfall event classes

4.4.6 Green roof performance heterogeneity

The experiment results of green roof 2 relative to a reference roof were analyzed in paragraphs 4.4.1-4.4.5. For future modelling goals (calibration and validation with the measurement results), the results of green roof 1 were roughly examined as well. A data summary of the measurements from green roof platform 1 and 2 as well as the reference roof are presented in Appendix 5. Generally, both green roofs show similar response during the periods in July, September and December, 2009. Apart from small irregularities, two major response differences will be addressed here:

1. Differences in retention performance;
2. Differences in base flow performance.

Differences in retention performance

Cumulative rainfall in the three measurement periods in July, September and December, 2009 adds up to a total of 356 mm. Cumulative runoff of green roof 1 and 2 in these periods add up to 124 mm and 161 mm respectively. A first possible reason for the higher retention performance of green roof 1 is the position of the roof relative to an air-conditioning fan (Figure 34). Artificially increased wind speeds induced by the fan could increase evaporation rates and thus accelerate regeneration of potential storage in the green roof media. Cumulative rainfall retention for the July, 2009 and September, 2009 period are (almost) similar for both roofs however: 82 mm (GR1) and 76 mm (GR2) in July and 65 mm (GR1) and 65 mm (GR2) in September. The retention difference between both roofs arises almost totally from the December, 2009 period. Data recording errors, induced by a tilted tipping bucket at platform 1, are almost certainly the cause of this. Small differences in media depth, which result from manual preparation of the platforms, and vegetation differences between both roofs can also account for (part) of the retention deviations between both platforms.

Figure 34. Positioning of green roof 1 (top) and green roof 2 (bottom)

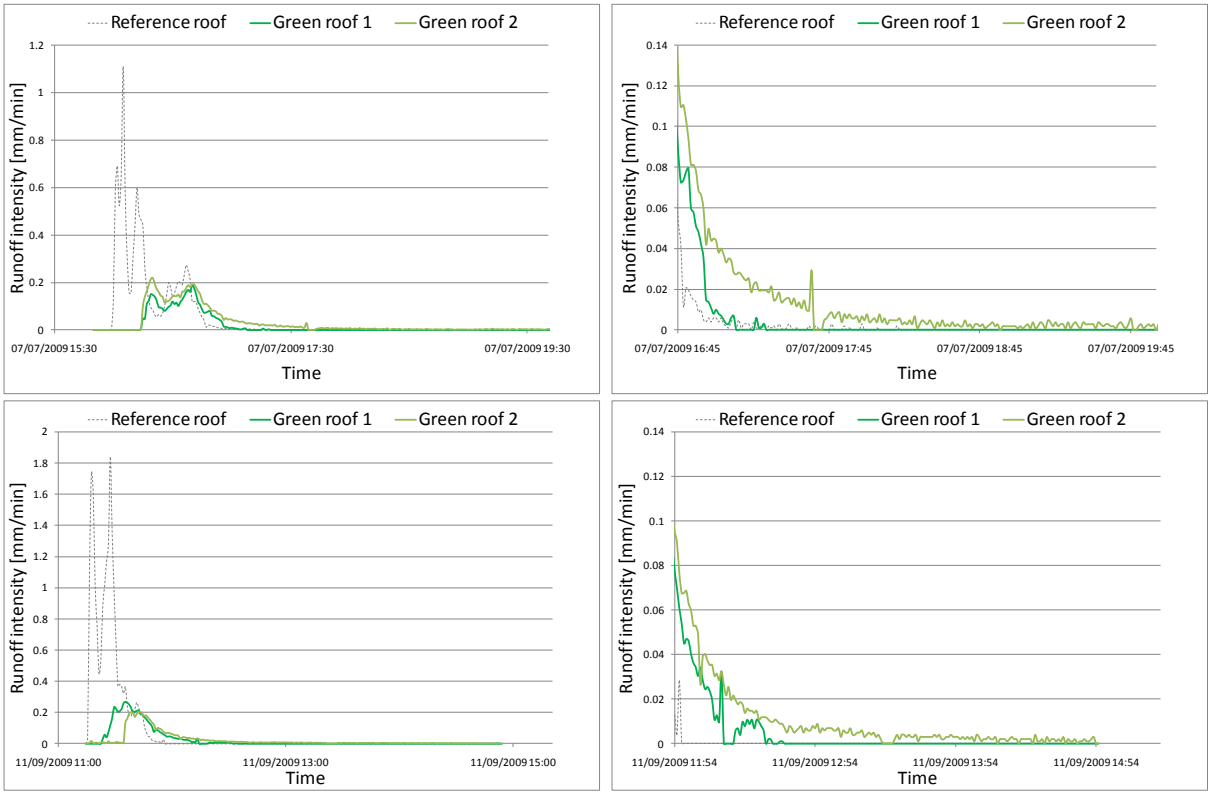

Figure 35. Base flow rainfall-runoff event hydrographs of July 07, 2009 and September 11, 2009.

Differences in base flow performance

Base flow runoff after the last recorded rainfall appeared to be higher for green roof 2 compared to green roof 1 for almost all (36 out of 42) events in the months of July, September and December, 2009. Figure 35 illustrates this measurement result for the events of July 7 and September 11, 2009. The graphs on the right side zoom in on the base flow of both hydrographs up to three hours after the last recorded rainfall. The runoff hydrograph of green roof 2 continuously lies above the hydrograph of green roof 1 and clearly shows the prolonged base flow runoff time of up to 3 hours, while the base flow from green roof 1 generally stops 1 hour after the last recorded rainfall. This base flow difference is probably caused by clogging of the lower media part, the filter fabric or a small blockage in the drainage layer of the green roof 2 platform.

4.5 Small-scale green roof experiment conclusions and discussion

Experiment materials and methods

The quantitative effects of 1 m^2 extensive green roof platforms on the rainfall-runoff were analyzed during four monthly periods in July, September and December, 2009 and March/April, 2010 at the National University of Singapore. The green roof platforms consist of a 5 cm drainage layer and a 12 cm potting soil media that is planted with the drought resistant Sedum Mexicanum. For research purposes the green roof runoff of 66 rainfall events were measured and compared with the runoff from a reference roof. Therefore, runoff data and rainfall data were automatically logged on small time intervals of 2 seconds and 1 minute respectively. A *rainfall event* has been defined as a period with rain, separated to another period of rain by a 0 mm dry spell of at least 1 hour. The quantitative effects of green roof runoff reduction, peak discharge reduction, peak discharge detention and base flow conservation were expressed as performance indicators to allow for a comparison between green roof platforms and a reference roof. Because the additional effects of green roofs compared to standard reference roofs are of major interest for stormwater management purposes, all performance indicators, except for the RPI, were expressed relative to the reference roof. The retention performance relative to the reference roof (ASRPI) was also examined.

Experiment results, discussion and conclusions

It was shown in the measurement result section that on average, extensive green roofs score well on all four performance indicators. The green roof platform retained 339 mm out of the 595 mm rainfall (57%) over the four measurement periods. Compared to the reference roof, this means an additional retention of 234 mm. The average peak discharge of the green roof rainfall-runoff events was reduced 64% compared to the reference roof, and the average time to peak of the green roof hydrograph appeared 37 minutes after the rainfall peak and 34 minutes after the reference roof peak. The green roof platforms provided small extended base flow amounts for up to three hours after the last recorded rainfall. In the first hour after the rainfall stopped, green roofs provide 0.20 liters/m^2 of additional base flow. An extra 0.21 liters/m^2 of base flow is provided between one and three hours after the last recorded rainfall. It was shown that because of the given definition of a rainfall event, values of the (AS)RPI, PDPI and DPI do sometimes not give a physically correct representation of the actual retention, peak discharge reduction and detention functioning of a green roof. The extra retention and peak discharge reduction relative to a reference roof, is underestimated now and then because of base flow from a previous rainfall event. A more severe effect occurs when green roofs retain one or more peaks, of which one is the maximum reference

roof peak during the event, in a multiple-peak rainfall event. In this case the peak discharge detention can be highly overestimated, as was graphically illustrated in Figure 32. Because of this effect, individual event analysis should also be included when one wants to *understand the green roof functioning*. The *average* experiment performance indicator values often do not give practical implications whether green roofs can act as an effective stormwater management solution in the tropics and Singapore specifically. Unfortunately, practical conclusions are frequently drawn based on these averages. In order to be able to draw valid conclusions, one should considerer that:

1. Practical effectiveness of green roofs should be based on individual event analysis rather than on an average performance;
2. Green roof experiment performance cannot be directly translated into overall catchment performance.

Based on analysis of individual, more extreme events, it can be concluded that the effectiveness of the investigated green roof design is conditional. The green roof is able to abstract rainfall until its maximum storage potential. After saturation of the media, green roof hydrographs follow the reference hydrographs closely. To a large extent the rainfall depth and intensity as well as the antecedent wetness of the roof influence this event-based performance of green roofs. Especially in tropical countries, like Singapore, initial abstraction can be large because of high evaporation rates. On the other hand, green roof effectiveness can be reduced in those areas, because tropical design storm rainfall depths quickly saturate the media, after which peak discharge reduction is limited. Green roof base flow conservation performance is conditionally as well. For small and medium events, green roofs generally retain all rainfall, resulting in no runoff at all. Nevertheless, for large and extreme events the base flow can be prolonged for up to three hours. Although green roofs generate a base flow volume of up to 3 litres/m^2 after the last recorded rainfall, they cannot replace the natural function of groundwater. Still, stormwater management benefits can be expected because green roofs increase the time to peak. A variety of statistical options are available to summarize and formalize the performance of green roofs for individual events. Min/median/max values, mean values with standard deviation and exceedance probabilities are recommended for future green roof experiment-scale data analysis. Longer time series will then have to be available as well. Additionally, extra research is necessary in order to analyze the influence of a changing vegetation cover density and plant diversity on the effectiveness of extensive green roofs in the tropics. Maintenance (irrigation and weed removal) is suggested, in order to reduce plant mortality and the entry of invasive plant species.

Second, practical stormwater management advantages of the peak discharge reduction and peak desynchronizing effect of green roofs have to be examined on (sub)catchment-scale, since green roof surface area and other catchment characteristics dynamically influence the scaled-up runoff hydrograph. The practical contribution of green roofs to partly re-establish regulated flows within Singapore's stormwater drainage system has to be examined on (sub)catchment-scale as well.

5 Small-scale green roof rainfall-runoff modelling

5.1 Introduction

A modelling approach for the simulation of green roof rainfall-runoff will be presented in this chapter. From a theoretical point of view, this modelling approach is purely carried out for research purposes. It is the aim to understand the hydrological processes and the soil physics in a green roof media. Like many other modelling demonstrations, this could potentially contribute to the development of knowledge within an area of science (Beven 2001). From a practical point of view, the modelling part of this research aims to improve decision-making and drainage system design of sustainable stormwater drainage systems in Singapore. This chapter mainly focuses on the theoretical purpose of the unsaturated zone model, while the large-scale analysis in Part 3 of this research focuses on the practical application of this model in a catchment-scale rainfall-runoff simulation.

The physically based HYDRUS-1D model was chosen as a tool to simulate the hydrological behaviour of green roofs on experiment-scale. HYDRUS-1D version 4.13 was used in this research (PC-PROGRESS 2008). The HYDRUS program numerically solves the Richards equation for water flow in variably saturated porous media. The process that starts with the set-up of the unsaturated zone model and ends with final simulations of small-scale green roof rainfall-runoff events, will be structured around the iterative model cycle. The used model cycle (Figure 36) is an adapted combination of model cycle theories used in hydrological modelling (Beven 2001) and discrete system modelling (Verbraeck 2003).

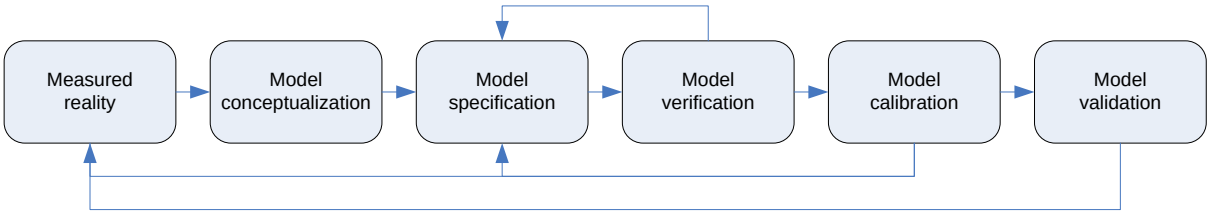

Figure 36. Schematic representation of the model cycle

The model conceptualization in paragraph 5.2 will address a mathematical description of the governing flow equations and the selected hydraulic model. The concept of boundary conditions, which are controlled by the internal and external state of the system will be addressed here too. An initial specification of the boundary conditions, the hydrological process parameters and the soil hydraulic model parameters will be presented in paragraph 5.3. In order to ensure that the model does what it is intended to do (Etessami and Gilmore 2008), the implementation of the initial specification in the model will be verified in paragraph 5.4. After this, the internal model parameters will be calibrated (paragraph 5.5). In the final validation phase (paragraph 5.6) of the model cycle, green roof model simulations will be compared to green roof measurements outside the calibration period in order to demonstrate whether the model gives a reasonable representation of the reality (Etessami and Gilmore 2008). The following research hypothesis will be tested:

"The physically based HYDRUS-1D model can better predict the green roof rainfall-runoff performance than the simple regression equations that were used in Chapter 4"

An overview of the conclusions and a discussion about green roof rainfall-runoff modelling in HYDRUS-1D is provided in the end of this chapter.

5.2 Model conceptualization

In absence of a groundwater table, the green roof soil media can be characterized as an unsaturated zone. The water balance for the unsaturated zone in the green roof is expressed as:

$$\frac{dS_t}{dt} = (P - I - q_s - E - T - q) * A \qquad \text{[Eq.5.1]}$$

where dS_t/dt [L^3T^{-1}] is the change in soil water storage in the unsaturated zone, P is the precipitation [LT^{-1}], q_s is the specific surface runoff [LT^{-1}], I is the interception [LT^{-1}], E is the evaporation [LT^{-1}], T is the transpiration [LT^{-1}] and q is the specific runoff rate out of the unsaturated zone bottom [LT^{-1}]. All terms can be expressed in the correct units by multiplying the hydrological fluxes on the right side with the surface area A [L^2]. It is then assumed that these fluxes are homogenous in space and can be linearly scaled-up to any green roof surface area. The conceptualization phase of the model cycle addresses three main components:

1. Conceptualization of the internal state of the unsaturated zone;
2. Conceptualization of the green roof boundaries;
3. Conceptualization of the hydrological processes.

The green roof is conceptualized according to the water balance principle where the runoff flux at the bottom depends on two internal state variables of the unsaturated zone: the soil water content, which is a measure of storage, and the unsaturated permeability. The governing flow equations and the hydraulic model choice will be described in paragraph 5.2.1. The internal state of the unsaturated zone in turn can be obtained by integrating the change in soil wetness over depth and time. The change in storage depends on the fluxes at the upper and lower boundaries. At the upper boundary, hydrological processes are driven by atmospheric conditions (external state) such as wind, temperature, humidity and radiation. Again, just like for the lower boundary, the upper boundary and the internal state are mutually dependent, since the surface runoff, evaporation and transpiration are influenced by the antecedent storage conditions of the soil. The conceptualization of the green roof boundaries and hydrological processes are given in paragraphs 5.2.2 and 5.2.3.

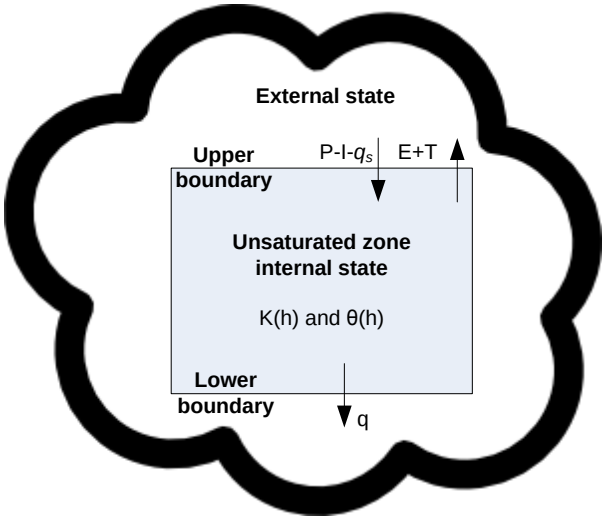

Figure 37. Green roof model concept

5.2.1 Conceptualization of the internal state of the unsaturated zone

5.2.1.1 Derivation of Richards equation for water flow in the unsaturated zone

The HYDRUS computer code numerically solves the Richards equation for variably-saturated flow (Simunek (c), et al. 2008). Richards equation (Eq. 2.16) can be derived by substitution of the continuity equation into the differential form of Darcy's equation, that was derived by Slichter in 1899 (Hillel 1982, p.94):

$$q = -K_s \nabla H \quad \text{[Eq. 5.2]}$$

where q is the specific discharge rate or flux [LT^{-1}], K_s is the saturated hydraulic conductivity [LT^{-1}] and ∇H is the gradient of the hydraulic head in 3-dimensional space (Hillel 1982). Though originally used for saturated flow, Richards has extended Darcy's law to unsaturated flow, with the provision that the unsaturated hydraulic conductivity is a function of the water pressure head h (Hillel 1982, p.95). K_s now becomes K and:

$$q = -K \nabla H \quad \text{[Eq. 5.3]}$$

In the case that only vertical flow of water (1-dimensional) is considered, Eq. 5.3 can be written as:

$$q = -K \frac{dH}{dx} \quad \text{[Eq. 5.4]}$$

Since the hydraulic head H [L] is the sum of the negative water pressure head h [L} and x [L], the vertical distance (positive upward) above the reference level, this can be transformed into:

$$q = -K \frac{d}{dx}(h + x) \quad \text{[Eq. 5.5]}$$

Which can be simplified in two steps:

$$q = -K \frac{dh}{dx} - K \frac{dx}{dx} = -K \frac{dh}{dx} - K \quad \text{[Eq. 5.6]}$$

When we combine this formulation of Darcy's law with the continuity equation (conservation of mass) $\partial\theta/\partial t = -\partial q/\partial x$, where θ is the volumetric soil water content [-], this gives (Hillel 1982, p.220):

$$\frac{\partial \theta}{\partial t} = -\frac{\partial}{\partial x}\left[-K \frac{\partial h}{\partial x} - K\right] = \frac{\partial}{\partial x}\left[K \frac{\partial h}{\partial x} + K\right] \quad \text{[Eq. 5.7]}$$

When this equation is further simplified and by incorporating a sink term S that accounts for water uptake by plant roots [T^{-1}], the Richards equation that is used in HYDRUS-1D to describe the water movement in an unsaturated porous media (Simunek (c), et al. 2008, p.11) has been fully derived:

$$\frac{\partial \theta}{\partial t} = \frac{\partial}{\partial x}\left[K\left[\frac{\partial h}{\partial x} + 1\right]\right] - S \quad \text{[Eq. 5.8]}$$

5.2.1.2 Hydraulic model options

The differential form of the Richard's equation (Eq. 5.8) shows that the hydraulic conductivity, moisture content and water pressure head are mutually dependent. When one wants to numerically solve the Richards equation which has three unknown variables *K,* θ and *h,* two more equations are required. Several scientists have attempted to develop analytical solutions for the relationship between the hydraulic conductivity, moisture content and water pressure. The relationship between the moisture content and the water pressure head θ*(h)* is called the *soil water retention function.* The relationship between the hydraulic conductivity and the water pressure head *K(h)* is called the *hydraulic conductivity function***.** HYDRUS allows their users to choose between six types of hydraulic

models for the soil hydraulic properties (PC-PROGRESS 2008). These hydraulic models can be split up into two main groups (Durner (a), et al. 1999):

1) Unimodal, single-porosity models
2) Bimodal, dual-porosity models

Unimodal descriptions of the hydraulic functions imply that soils have equivalent pore-size distributions (Durner (a), et al. 1999). The pore-size distribution quantifies the volumes of different classes of pore-sizes (Hillel 1982). Based on this assumption, single-porosity models conceptualize the physical flow profile as one region (Simunek (c), et al. 2008). Single-porosity models describe the soil water retention function and hydraulic conductivity function by a sigmoidal or S-shaped function, which requires at least four parameters (Durner (a), et al. 1999). The HYDRUS-1D code allows users to select five different types of single-porosity models for the soil hydraulic properties. Among those, the van Genuchten-Mualem model (van Genuchten (a) 1980) is set as the standard hydraulic model. Van Genuchten's unimodal pore-size distribution model is based on the following set of equations (van Genuchten (a) 1980):

$$S_e = \frac{(\theta - \theta_r)}{(\theta_s - \theta_r)} = [1 + (\propto |h|)^n]^{-m} \qquad \text{[Eq. 5.9]}$$

where S_e is the effective saturation [-], θ is the volumetric soil water content [-], θ_r and θ_s are the residual and saturated volumetric soil water content respectively, α is an empirical shape parameter which frequently has been referred to as the inverse air entry value or bubbling pressure [L^{-1}] (van Genuchten (b) and Nielsen 1985), n is an empirical shape parameter which is an indicator for the pore-size distribution [-] and m [-] is an empirical shape parameter that is equal to 1-1/n.

A *bimodal* description of the hydraulic functions has been derived by Wolfgang Durner in 1994 and was used to determine the hydraulic parameters of soils in several papers (Durner (a), et al. 1999, Durner (c), Jansen and Iden 2008). The bimodal description conceptualizes soil flow profiles as a two-region, dual pore-size distribution (Durner (a), et al. 1999). To describe retention curves of soils with bimodal pore-size distributions, a linear superposition of the van Genuchten-type sub curves is used (Durner (a), et al. 1999, p.819):

$$S_e = \frac{(\theta - \theta_r)}{(\theta_s - \theta_r)} = \left[\sum_{i=1}^{2} w_i \, [1 + (\propto_i |h|)^{n_i}]\right]^{-m_i} \qquad \text{[Eq. 5.10]}$$

where the integer 2 denotes the bimodality of the model (the number of pore-size distributions), w_i [-] are the weighing factors for the sub curves, subject to the constraints $0<w_i<1$ *and* $\sum w_i=1$ and where α_i, n_i and m_i are empirical shape parameters of the sub curves, as in the unimodal description of van Genuchten's unimodal pore-size model (Durner (a), et al. 1999, p.819).

Hysteresis

One of the limitations that arises when describing the water retention curve with a soil water retention function results from the phenomenon that is named hysteresis (Ward and Robinson 1990). The equilibrium soil water content at a given water pressure head is not only a value of the that water pressure head, but also upon whether the soil is drying or wetting (Hillel 1982, Ward and

Robinson 1990). The equilibrium soil water content at a given water pressure is larger in desorption (drying curve) than in sorption (wetting curve) (Hillel 1982, p.79). Hysteresis can be caused by (a combination of) entrapped air and swelling and shrinking , but the most important contribution is caused by the so called “ink bottle” and “contact angle effect” (Hillel 1982). Both effects are caused by the fact that many pores are larger than their openings. This characteristic shape causes higher negative pressures necessary to enable air to enter the narrow pore neck and drain the pore, than is necessary during wetting of the bulkier pore body (Ward and Robinson 1990, p.136). The contact angle effect results from the fact that the contact angle of fluid interfaces on the soil solids tends to be larger during wetting than during drying (Marshall, Holmes and Rose 1999). These effects result in two separate water retention curves for wetting and drying where, at a given negative pressure, the soil water content is larger on the drying curve than on the wetting curve. Figure 38 graphically represents this hysteresis effect. The HYDRUS-1D model incorporates hysteresis by using an empirical hysteretic model that was introduced by Kool and Parker in 1987 (Simunek (b), Sejna and van Genuchten 2005). In HYDRUS, This model can only be implemented in the Van Genuchten’s unimodal pore-size distribution model (Eq. 5.9).

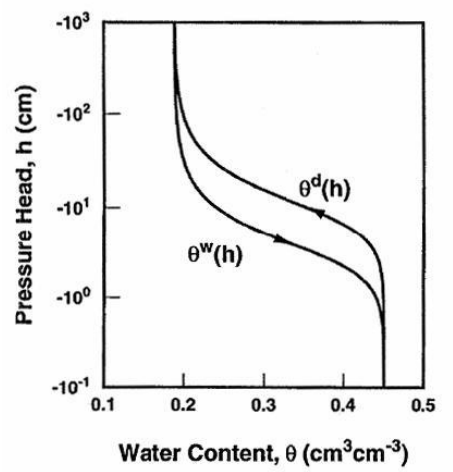

Figure 38. Hysteresis effect in the water retention curve. Source: Simunek (c), et al. (2008)

5.2.1.3 Hydraulic model choice

Basically three choices have to be made when it comes down to selecting the soil hydraulic model:

1. Which *single-porosity* model fits the purpose of the analysis best?
2. Do we choose a *single-porosity* or *dual-porosity model*?
3. Is it relevant to incorporate the *hysteresis effect*?

Five single-porosity models are available in HYDRUS-1D. These are 1&2) the van Genuchten-Mualem model (with and without an air-entry value of -2 cm), 3) a modified van Genuchten model, 4) the Brooks-Corey model and 5) the Kosugi log-normal model (Simunek (c), et al. 2008). Despite or just because its relative simplicity , the van Genuchten-Mualem model is widely used by soil physicists around the world (Kodesova 2003, Durner (a), et al. 1999, Hopmans, Simunek, et al. 2002). Its popularity has resulted in many scientific papers that analyze and evaluate the ability to describe the unsaturated hydraulic properties of soils by determining values for the hydraulic parameters in van Genuchten’s hydraulic model (Parker, Kool and van Genuchten 1985). This gives certain advantages over the use of Kosugi’s model that was developed in 1996 (Simunek (b), Sejna and van Genuchten

2005) since one can consult many papers during the research for help and comparison. Van Genuchten derived a new model over the older Brooks-Corey model, because numerical convergence problems sometimes occurred in saturated-unsaturated flow problems (van Genuchten (a) 1980, p 892). Moreover, the accuracy of this model was lower than one of the alternative models by that time (van Genuchten (a) 1980). Out of the three van Genuchten models, the standard model fits best to the soil type used for the green roof experiments. The van Genuchten-Mualem model with a -2 cm air-entry value option is a special case of the modified van Genuchten model (Simunek (c), et al. 2008). This model that was developed in 1988 by Vogel and Cislerova allows for a non-zero minimum capillary height, h_s [L], by replacing θ_s from Eq. 5.9 by a fictitious (extrapolated) parameter θ_m [-], which is slightly larger than θ_s (Simunek (c), et al. 2008, p.24). The -2 cm air-entry value option is a special case of this modified van Genuchten model with h_s = -2 cm. These modified models are recommended for fine/heavy textured soils with a relatively small pore-size distribution when n is relatively small ($1.0<n<1.3$ (Simunek (c), et al. 2008)). According to Hillel (1982) the expression fine/heavy textured soils is an attribute of clayey soils, which perfectly corresponds to the low standard value for the parameter n in the HYDRUS model software (n=1.25 for clay). Since the used potting soil is not fine/heavy textured but rather light/course, this option is not favourable. This demonstrates that the standard van Genuchten-Mualem model is the favourable single-porosity model for further research.

In the choice between a single-porosity model and a dual-porosity model one has to observe the purpose of the final analysis according to Durner (a), et al. (1999). In several papers Durner, et al. determined the differences in performance between van Genuchten's single-porosity model and his own dual-porosity model (Durner (a), et al. 1999, Durner (b), Schultze and Zurmuhl 1999, Durner (c), Jansen and Iden 2008). Based on inverse modelling of several soil types, Durner, et al. conclude that more flexible hydraulic functions, such as dual-porosity retention models can fit the retention curves of natural undisturbed soils better than less parameterized functions such as the single-porosity models (Durner (b), Schultze and Zurmuhl 1999, p.673). The drawback of more flexible hydraulic functions is the larger number of parameters, which is 1) generally not desired in parameter estimation procedures and 2) it becomes more and more difficult to individually interpret them (Durner (b), Schultze and Zurmuhl 1999, Durner (a), et al. 1999). Based on Durner's recommendation to stick to a relatively simple, less-parameterized model for field use purposes, it is the single-porosity model that will be initially used for further analysis in this research.

Now that we have chosen the single-porosity model of van Genuchten, only the last of the three choices remains: *do or can we incorporate the hysteresis effect?* Though HYDRUS-1D allows to incorporate the hysteresis effect in van Genuchten's single-porosity model, this will be disregarded in the unsaturated zone modelling part of this work. Because of the complexity that comes along with individual determination of the two *main branches* (drying and wetting branch) of the water retention curve, hysteresis is normally disregarded in practice (Hillel 1982, p.80, Ward and Robinson 1990). The water retention curve, which is generally reported, is the *drying curve* since it is easier to experimentally measure this branch (Hillel 1982). On top of this, an attempt to describe the inflow and outflow simultaneously with the hysteretic model of Kool and Parker during inflow/outflow experiments in an earlier research (Durner (b), Schultze and Zurmuhl 1999, p.669) did lead to much worse results than when van Genuchten's model was used without the hysteretic model. However, disregarding the hysteretic effect means disregarding proved dissimilarities in the soil water

retention and hydraulic conductivity function of the two main branches, which probably has a negative influence on the accuracy of unsaturated zone modelling results.

5.2.1.4 Derivation of van Genuchten's hydraulic model functions

Now that we have chosen to use the van Genuchten's non-hysteretic, single-porosity hydraulic model, the water retention function and hydraulic conductivity function will be derived.

Water retention function

When we rewrite the two equations on the left hand side of Eq. 5.9 we obtain:

$$S_e(\theta_s - \theta_r) = (\theta - \theta_r) \qquad \text{[Eq. 5.11]}$$

And thus,

$$\theta = \theta_r + S_e(\theta_s - \theta_r) = \theta_r + \frac{(\theta_s - \theta_r)}{S_e{}^{-1}} \qquad \text{[Eq. 5.12]}$$

When Eq. 5.9 is substituted in Eq. 5.12 van Genuchten's water retention function has been found. In this function θ becomes a function of the empirical parameters and the water pressure head only:

$$\theta(h) = \theta_r + \frac{(\theta_s - \theta_r)}{[1+(\propto|h|)^n]^m} \qquad \text{[Eq. 5.13]}$$

Hydraulic conductivity function

The total derivation of the hydraulic conductivity function has been described by van Genuchten (a) (1980). The first important step in the derivation is the substitution of van Genuchten's equation for the effective saturation, S_e (Eq. 5.9), into the relative hydraulic conductivity function K_r [-] that was derived by Mualem in 1976 (van Genuchten (a) 1980, p.892):

$$K_r = S_e^l \left[\int_0^{S_e} \frac{1}{h(x)}\,dx \Big/ \int_0^1 \frac{1}{h(x)}\,dx\right]^2 \qquad \text{[Eq. 5.14]}$$

where the newly introduced parameters *l* [-] is an empirical shape parameter which accounts for tortuosity and correlation between pore sizes (Durner (a), et al. 1999) and *h* is the water pressure head [L]. The pore-connectivity parameter *l* was estimated to be about 0.5 as an average for many soils (Simunek (c), et al. 2008, p.23). Van Genuchten (a) (1980) derives that, including *l=0.5* and the parameter constraint *m=1-1/n*, the relative hydraulic conductivity expressed in terms of the effective saturation becomes:

$$K_r(S_e) = S_e^{0.5}\left[1 - \left(1 - S_e{}^{1/m}\right)^m\right]^2 \qquad \text{[Eq. 5.15]}$$

When $K_r(S_e)=K(h)/K_s$ (van Genuchten (a) 1980, p.893) is substituted in the left side of Eq. 5.15, and both sides are multiplied with K_s then the following hydraulic conductivity function is found:

$$K(h) = K_s S_e^{0.5}\left[1 - \left(1 - S_e{}^{1/m}\right)^m\right]^2 \qquad \text{[Eq. 5.16]}$$

This unsaturated hydraulic conductivity function is used in the source code of the single-porosity model in HYDRUS-1D as can be found in the manual (Simunek (c), et al. 2008, p.23). The hydraulic conductivity as a function of the soil water content, $K(\theta)$, can be derived from substitution of the water retention function $\theta(h)$ into Eq. 5.16. Figure 39 shows $\theta(h)$ and $K(\theta)$ functions for sand, loam and clay soils up to h=-15000 cm (wilting point). The vertical axes of both graphs are plotted on a logarithmic scale. Parameter values for sand, loam and clay were taken from HYDRUS' Neural Network Prediction tables (Simunek (b), Sejna and van Genuchten 2005). Similar parameter values for potting soil are not included in the Neural Network Prediction tables and therefore have to be determined in the specification phase of the model cycle.

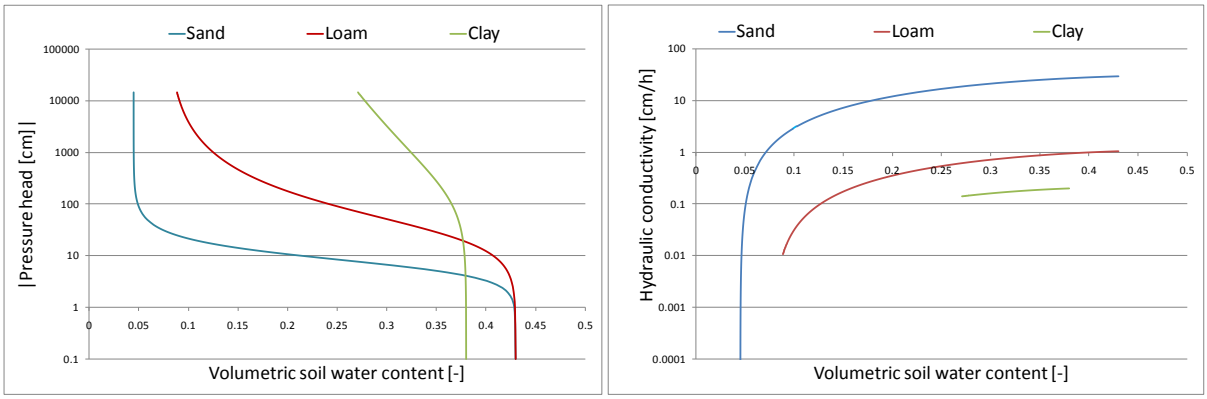

Figure 39. Soil water retention and hydraulic conductivity functions for sand, loam and clay soils.

5.2.2 Conceptualization of the green roof model boundaries

The green roof platform is conceptualized as a system with an internal and external state, hydrological processes and boundaries. The internal state is connected with the external state by two boundary conditions:

1. Upper boundary condition;
2. Lower boundary condition.

Fluxes at the upper boundary are driven by hydrological processes. The incoming flux is the infiltration and the outgoing fluxes are evaporation from the bare soil, interception and transpiration from the green roof vegetation. These fluxes are driven by the external state (atmospheric conditions) and the current condition of the internal state (soil water content and hydraulic conductivity) of the green roof.

At the lower boundary of the green roof, runoff has to be initiated when a certain storage threshold value θ, with corresponding water pressure threshold h, of the soil media (internal state) is exceeded. Runoff intensities will depend on the unsaturated hydraulic conductivity at this threshold value. After runoff has passed this lower boundary, it will quickly drain from the drainage layer into the green roof platform tipping bucket. The runoff time from the moment of outflow at the lower boundary to the tipping bucket is assumed to be negligible. The storage threshold value will be determined in the specification phase of the model cycle.

5.2.3 Conceptualization of the hydrological processes

Fluxes at the upper boundary are driven by hydrological processes. It follows from the water balance (Eq. 5.1) that the incoming flux equals the total precipitation minus the abstraction terms for plant interception and surface runoff. In fact P - I - q_s add up to the total water quantity that infiltrates into the soil media and thus increases the soil water content. The outgoing hydrological fluxes are the evaporation from bare soil and the transpiration from plant vegetation. Transpiration fluxes are driven by water uptake in the root zone while evaporation fluxes occur via the top soil layer of the green roof media. The precipitation solely depends on atmospheric conditions. Abstraction from interception is a function of the total plant leaf area and antecedent interception. The surface runoff, evaporation and transpiration are all a function of both internal and external state conditions: they are not only a function of the atmospheric conditions, but also on the antecedent soil water content of the green roof media. Evaporation at the lower boundary is assumed to be negligible. Specification of the hydrological processes is given in the specification phase of the model cycle.

5.3 Model specification

Now that the unsaturated zone model of a green roof platform has been conceptualized, an initial specification of the boundary conditions, the hydrological process parameters and the soil hydraulic model parameters will be presented in this paragraph. This paragraph starts with a specification of the boundary conditions of the model (5.3.1). Then, an overview an overview of the most important hydrological processes will be specified (5.3.2). Special research interest goes out to the determination of the soil hydraulic parameters for the van Genuchten functions by inverse modelling in paragraph 5.3.3.

5.3.1 Specification of the green roof model boundary conditions

Two boundaries have to be specified in the representation of the green roof platform in the model:

1. Upper boundary condition;
2. Lower bounary condition .

The upper boundary condition will be described by an *atmospheric boundary condition* with possible surface runoff. The potential fluid flux across the upper soil-air interface is controlled by external conditions and the antecedent soil water content near the surface (Simunek (c), et al. 2008). The external conditions are specified as variable boundary conditions (precipitation), meteorological parameters (specification of the evapotranspiration model) and meteorological conditions (radiation, temperature, relative humidity and wind speed). Meteorological measurements that were used as input for the atmospheric boundary conditions can be found in Appendix 4. More information on the upper boundary condition is given in the actual evaporation section (Eq. 5.27 and Eq. 5.28).

The lower boundary will be modelled by using a *seepage face boundary condition*. Simunek (c), et al. (2008) recommend this type of boundary condition for laboratory soils or lysimeters when the bottom of the soil is exposed to the atmosphere. The condition assumes that the lower boundary flux (where green roof runoff occurs) will remain zero as long as the pressure head is negative. One can specify a value h_{seep} [L] other than h=0 cm to trigger the flux across the seepage face. In situ soil water content measurements were performed on the green roof experiments in Singapore with a Time Domain Reflectrometer (TDR) and soil sample oven drying directly after a rainfall-runoff event.

Experiment results confirm that gravity drainage across the bottom of the soil media does occur before the soil becomes saturated. Oven drying experiments of fully saturated soil samples showed that θ_s values of the potting soil vary between 0.78 and 0.89, while oven drying experiments and TDR measurements of drained out soil samples show that the measured values for θ_{seep} vary between 0.52 and 0.65, with an average of 0.61. Differences in θ_{seep} can be caused by heterogeneity of the soil or preferential flow paths. A full description of the experiment materials, theory and θ_{seep} measurement results can be found in Appendix 6. When the water retention function parameters have been determined, θ_{seep} can be coupled to h_{seep} in order to obtain the required seepage face head boundary condition.

5.3.2 Specification of the hydrological processes

The hydrological processes were conceptualized in Eq. 5.1. This paragraph will provide an overview of all governed equations that account for the precipitation, interception, evaporation and transpiration terms in the conceptual water balance. A description of the data input and initial parameter values are specified.

Precipitation

Precipitation data is used as a direct input for the model. Since the precipitation has been measured every minute with a tipping bucket on location, 60 precipitation values per hour are imported.

Interception

Precipitation that is temporarily stored on a natural (vegetation) or artificial (roads, buildings, pavement) soil cover in the form of interception is computed according to the following equation:

$$I = a \cdot LAI \left(1 - \frac{1}{1+\frac{bP}{a \cdot LAI}}\right) \quad \text{[Eq. 5.17]}$$

Where *I* and *P* are the interception [L] and precipitation [L] over the time step *t, a* is an empirical interception constant [L], *b* [-] is the soil cover fraction (*SCF*), *P* is the precipitation [L] and *LAI* is the leaf area index [-]. *LAI* is a function of the average measured crop height on the green roof platforms (5 cm):

$$LAI = 0.24 \cdot crop\ height = 0.24 \cdot 5 = 1.2 \quad \text{[Eq. 5.18]}$$

The soil cover fraction is calculated according to (Simunek (c), et al. 2008, p.217):

$$SCF = 1 - \exp(-a_i \cdot LAI) = 0.43 \quad \text{[Eq. 5.19]}$$

where a_i is an empirical constant for the radiation extinction by the canopy [-]. The standard value for a_i is set to 0.463. Although not explicitly mentioned in the HYDRUS-1D manual, the source code reveals that the interception depends on the antecedent interception or:

$$I_n = I_m - I_e \quad \text{[Eq. 5.20]}$$

where I_n is the "new" interception [L], I_m is the maximum interception storage [L] and I_e is the excess or "old" interception [L] from previous rainfall, which has not yet evaporated back into the atmosphere (Simunek (b), Sejna and van Genuchten 2005). HYDRUS assumes that the total intercepted water storage decreases at the potential transpiration rate, which is calculated with the

Penman-Monteith equation described in Eq. 5.22 - Eq. 5.26. The maximum interception value in a certain time step can be found by calculating the limit of Eq. 5.17 as *P* approaches infinity. Or in formula-form:

$$I_m = \lim_{P\to\infty} a \cdot LAI\left(1 - \frac{1}{1+\frac{bP}{a\cdot LAI}}\right) = a \cdot LAI \qquad \text{[Eq. 5.21]}$$

With this having said and with an estimated interception constant a of 1.5 mm, the modelled maximum interception storage I_m of the green roof platforms is 1.8 mm. This maximum interception lies in between the 1 mm green roof interception which was estimated by Berghage, Jarett, et al. (2007) and an average measured interception from mature grass of 3 mm (Corbett and Crouse 1968). A bug in the interception calculations according to Eq. 5.17 is discussed in paragraph 5.5.4.1.

Potential evaporation and transpiration

Potential evaporation and transpiration values are calculated with the Penman-Monteith equation in Eq. 5.22 - Eq. 5.26. Actual evaporation rates are calculated as a function of the antecedent soil water conditions, according to Eq. 5.27 and Eq. 5.28. Actual transpiration is accounted for in the root water uptake term S [T^{-1}], which is a function of the potential transpiration rate and water availability over the root zone depth according to Eq. 5.29 and Eq. 5.30.

Evapotranspiration is incorporated into the model by the Penman-Monteith equation:

$$ET_p = ET_{rad} + ET_{aero} = \frac{1}{\lambda}\left[\frac{\Delta(R_n - G)}{\Delta+\gamma(1+r_c/r_a)} + \frac{\rho c_p (e_a - e_d)/r_a}{\Delta+\gamma(1+r_c/r_a)}\right] \qquad \text{[Eq. 5.22]}$$

where ET_p is the potential evapotranspiration rate [LT^{-1}], ET_{rad} is the radiation term [LT^{-1}], ET_{aero} is the aerodynamic term [LT^{-1}], λ is the latent heat of vaporation [L^2T^{-2}], R_n is net radiation at the earth surface [MT^{-3}], G is the soil heat flux [MT^{-3}] (HYDRUS assumes G≈0), ρ is the atmospheric density [ML^{-3}], c_p is the specific heat of moist air [$L^2T^{-2}K^{-1}$], $(e_a\text{-}e_d)$ is the vapour pressure deficit [$ML^{-1}T^{-2}$], e_a is the saturation vapour pressure at temperature T [$ML^{-1}T^{-2}$], e_d is the actual vapour pressure [$ML^{-1}T^{-2}$], r_c is the crop canopy resistance [TL^{-1}] (r_c=200/*LAI*) and r_a is the aerodynamic resistance [TL^{-1}]. Equations to calculate the variables in the Penman-Monteith equation are presented in the HYDRUS manual (Simunek (c), et al. 2008). The slope of the vapour pressure curve, Δ [$ML^{-1}T^{-2}K^{-1}$] and the psychromatic constant, γ [$ML^{-1}T^{-2}K^{-1}$] are defined as (Simunek (c), et al. 2008):

$$\Delta = \frac{4098 e_a}{(T+237.3)^2} \qquad \text{[Eq. 5.23]}$$

$$\gamma = 0.00163\frac{P_a}{\lambda} \qquad \text{[Eq. 5.24]}$$

respectively, where T is the average air temperature [K] and P_a is the atmospheric pressure [$ML^{-1}T^{-2}$]. The Penman-Monteith method to calculate ET_p only requires four standard meteorological parameters. These are (Akker and Savenije 2006):

1. Radiation data;
2. Wind speed data;
3. Relative humidity data;
4. Air temperature data.

All four parameters have been measured on a 5-minute time interval on the rooftop of the E2 building at the National University of Singapore, approximately 100 m from the experiment location. The location of the meteo station is depicted in Figure 21. More information on the meteorological measurements can be found in Appendix 4. While the potential reference evapotranspiration ET_p depends only on crop and atmospheric conditions, the actual total flux ET_a [LT^{-1}] through the soil surface (upper boundary of the model) and the plants is limited by the availability of soil water and the ability of the soil matrix to transport water (Feddes, et al. 1988, p.85). Or (Akker and Savenije 2006):

$$ET \leq ET_p \qquad \text{[Eq. 5.25]}$$

In order to account for these limitations, HYDRUS separates the potential evapotranspiration into a potential evaporation and potential transpiration term. According to the HYDRUS source code:

$$E_p = ET_p e^{-k \cdot LAI} = ET_p(1 - SCF) \qquad \text{[Eq. 5.26]}$$

$$T_p = ET_p\left(1 - e^{-k \cdot LAI}\right) = ET_p \cdot SCF$$

where E_p is the potential evaporation [LT^{-1}], T_p is the potential transpiration [LT^{-1}], k is a constant governing the radiation extinction by the canopy [-], *LAI* is the leaf area index [-] and *SCF* is the soil cover fraction [-]. The two latter terms were introduced in the interception section. The actual evaporation calculations will be discussed in the upcoming section, while the actual transpiration via plant water uptake will be presented in the actual transpiration section.

Actual evaporation

One has to account for limitations in the ability of the soil matrix to transport water to the soil surface which is actually available for evaporation. Therefore, the actual surface flux across the upper boundary of the model is calculated by maximizing the following absolute surface flux that accounts for antecedent soil water conditions near the surface (Feddes, et al. 1988, Neuman, et al. 1976):

$$\left|-K\frac{dh}{dx} - K\right| \leq E_p \quad at\ x = L \qquad \text{[Eq. 5.27]}$$

and:

$$h_a \leq h \leq h_{smax} \qquad at\ x = L \qquad \text{[Eq. 5.28]}$$

where the left hand side of Eq. 5.27 is the actual upward flux at the soil-air interface, as was found earlier in Eq. 5.6. h_a in Eq. 5.28 is the minimum allowed pressure head at the soil surface [L]. It can be interpreted as the pressure head at θ_r or wilting point (Neuman, et al. 1976). h_{smax} is the maximum pressure head at the soil surface [L]. The value for h_{smax} has been set to zero. This means that surface runoff q_s is initiated when the soil becomes saturated. However, in practise the green roof soil media never reaches the saturated soil water content, as was concluded in paragraph 5.3.1.

Actual transpiration

Actual plant transpiration is accounted for in the root water uptake sink term S [T^{-1}] in HYDRUS (Simunek (c), et al. 2008). We already introduced this sink term in Eq. 5.8. The sink term is defined as (Neuman, et al. 1976):

$$S(h) = \alpha(h) S_p \qquad \text{[Eq. 5.29]}$$

where *α(h)* is the root-water uptake stress response function [-] and S_p is the potential water uptake rate [T^{-1}]. The model calculates the actual transpiration flux [LT^{-1}] by integration of *S(h)* over the depth *z*. Several distributions for *α(h)* give relationships between the potential water uptake rate and the actual root-water uptake sink term *S(h)*. Neuman, et al. (1976) introduced a relationship between the sink term as a function of the water pressure head, which will be used in this research. The potential water uptake rate S_p can be expressed as a function of the potential transpiration T_p (Simunek (c), et al. 2008):

$$S_p = b(x) T_p \qquad \text{[Eq. 5.30]}$$

Where *b(x)* is a normalized distribution of the potential water uptake over a root zone of arbitrary shape [L^{-1}]. This function describes the spatial variation of the potential root water uptake over the root zone. An illustration of Feddes' stress response function *α(h)* (Neuman, et al. 1976) and an example of a non-constant potential root-water uptake distribution function *b(x)* in the root zone of the soil (Simunek (c), et al. 2008) is given in Figure 40. Within this research, the water uptake distribution *b(x)* is assumed to be constant with depth and in time.

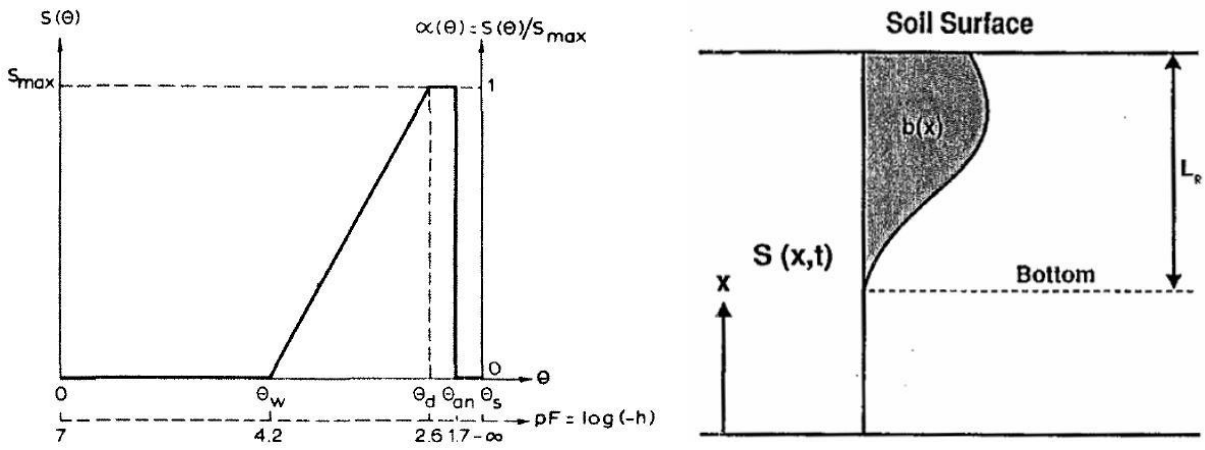

Figure 40. Schematic representation of the root-water uptake processes.

5.3.3 Determination of parameters for the hydraulic functions

The contribution of the change in storage over time, dS_t/dt, can be considered as the most important component of the water balance calculations in the green roof model. The change in storage over time equals all incoming minus outgoing fluxes. The change in storage over time, and thus the soil water content over time, is calculated by a numerical solution of the Richards equation for variably saturated water flow (Eq. 5.8). The finite difference scheme which is used to discretize the Richards equation is given in the HYDRUS-1D manual (Simunek (c), et al. 2008, p.95), and will not be presented here. The specification of the discretization in time and space have to be provided by the user. For the time discretization, the initial time, final time, initial time step, minimum time step and maximum time step have to be provided. For the spatial discretization, one has to specify the soil profile. This includes the nodal density (vertical distance between nodes), initial values of the water content or pressure head, sub regions when the domain consists of more than one soil type and observation points for the model output (Simunek (b), Sejna and van Genuchten 2005). The spatial discretization is presented in Appendix 7. All hydrological fluxes, except the rainfall, and the storage term depend on the defined soil water retention function θ*(h)* and the hydraulic conductivity function *K(h)*. A good

description of the green roof runoff can only be obtained when these two functions give a sufficiently good representation of the real soil hydraulic properties in the unsaturated zone. The soil hydraulic properties are expressed by several parameters for the soil water retention and hydraulic conductivity function. Simulation accuracy of the green roof rainfall-runoff on experiment-scale depends, to a large extent, on the accuracy of parameter determination. In paragraph 5.2.1.3 the van Genuchten's non-hysteretic, single-porosity hydraulic model has been chosen. The soil water retention function and hydraulic conductivity function (Eq. 5.13 and Eq. 5.16) require six soil hydraulic parameters: θ_r, θ_s, α, n, K_s and l. Parameter identification by inverse modelling of transient flow experiments is an attractive way to simultaneously estimate the soil hydraulic parameters of the soil water retention function and hydraulic conductivity function (Hopmans, et al. 2002). This section gives an overview of the inverse modelling experiments that were carried out to determine the soil hydraulic parameters for the green-roof experiment potting soil in Singapore.

5.3.3.1 Inverse modelling theory

According to a definition by Hopmans, et al. (2002, p.964), *inverse modelling* is "a general mathematical method to determine unknown causes on the basis of observation of their effects, as opposed to modelling of direct problems whose solution involves finding effects on the basis of a description of their causes". When we translate this to the particular case of unsaturated water flow, inverse modelling is a method to determine the soil hydraulic properties on the basis of water pressure head, soil water content and/or boundary flux observations (evapotranspiration, outflow volume measurements).

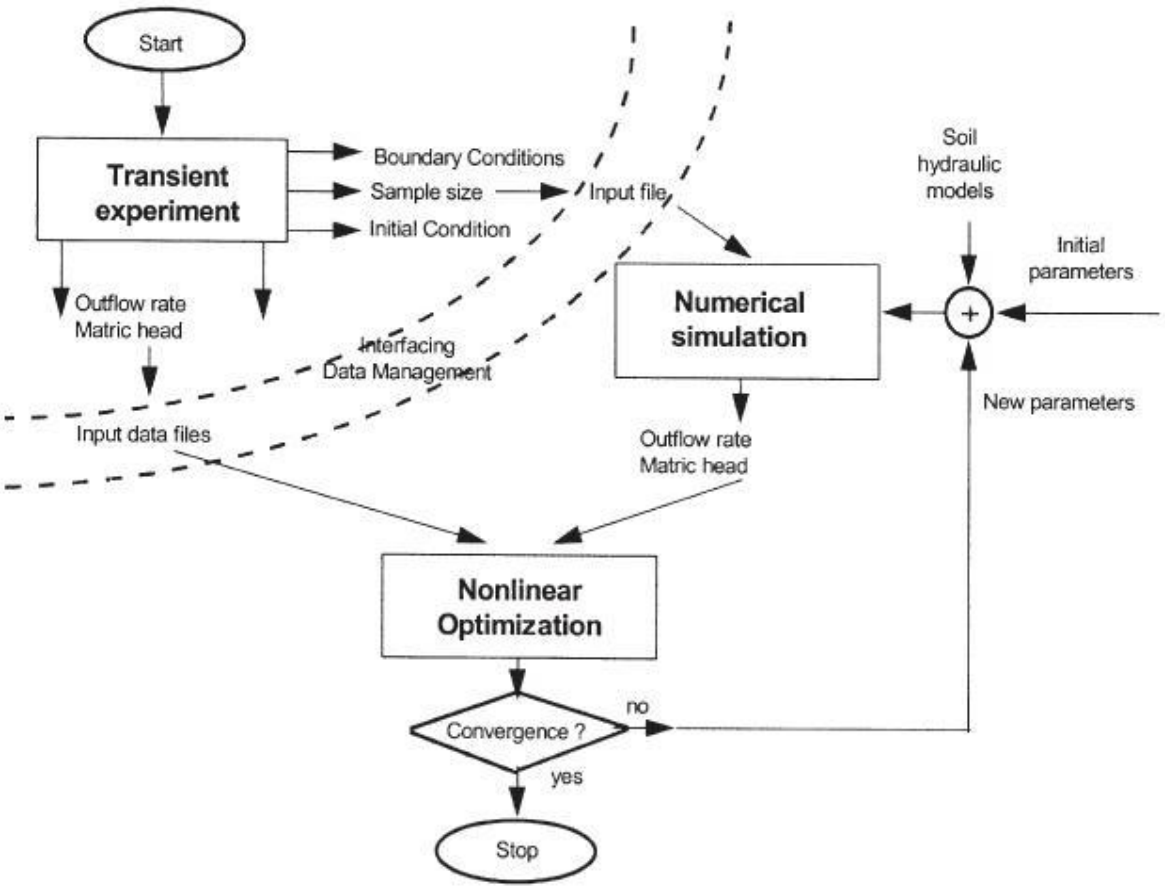

Figure 41. Flow chart of the inverse modelling theory. Source: Hopmans, et al. (2002)

The flow chart in Figure 41 by Hopmans, et al. (2002) gives an overview of the inverse modelling theory. Inverse modelling consists of three functional parts:

1. A controlled transient flow experiment;
2. A numerical flow model for the simulation of transient flow experiments;
3. An optimization algorithm.

Controlled transient flow experiment
The first "component" of inverse modelling is a controlled transient flow experiment for which the initial and boundary conditions are prescribed and where several effects are observed. Effects that are often observed in transient flow experiments are the water pressure head *h* and/or the water content θ and/or (cumulative) evaporation and/or (cumulative) runoff. Several experiments have been proposed and used for inverse parameter optimization. Experiment design examples are given in papers by Hopmans, et al. (2002), Simunek (c), et al. (2008) and Durner (a), et al. (1999). Hopmans, et al. (2002) give the most complete overview with inverse modelling experiment descriptions, results and discussions from evaporation, infiltration and drainage experiments and several outflow methods. The experiment method choice and set-up design will be presented in paragraph 5.3.3.2.

Numerical flow model for the simulation of transient flow experiments
A numerical model is an important part in inverse modelling, since this model will be used to simulate the transient flow regime of the experiment given certain specified initial and boundary conditions. The HYDRUS-1D model will serve as the numerical model for simulation of transient flow experiments to determine the soil hydraulic parameters in this research.

Optimization algorithm
The two unimodal hydraulic model functions of van Genuchten are defined by the parameter vector **b**={ θ_r, θ_s, α, n, K_s, l }^{T}. The saturated volumetric water content θ_s can normally be determined with an oven-dry test, where an experiment soil sample with known volume V [L^3] is weighed before and after 24 hours of drying at 105 ^{0}C. In practise this gives a maximum number of 5 remaining variable parameters that needs to be optimized with inverse modelling (Durner (a), et al. 1999). For optimization purposes, an objective function is defined which expresses the deviations between the measured data and the simulated data as a function of the unknown parameter vector **b** (Durner (a), et al. 1999). This objective function is defined as (Simunek (c), et al. 2008, Hopmans, Simunek, et al. 2002):

$$E(\boldsymbol{b}, y) = \sum_{j=1}^{j=m_y} v_j \sum_{i=1}^{i=n_j} w_{i,j} \left[y_j^*(z, t_i) - y_j(z, t_i, \boldsymbol{b}) \right]^2 \qquad \text{[Eq. 5.31]}$$

where $E(\boldsymbol{b},y)$ is the objective function that expresses the deviations between measured (y_j^*) and simulated (y_j) space-time variables using the soil hydraulic parameters of the optimized parameter vector **b** (Hopmans, et al. 2002). The first term on the right hand side sums the residuals for all different sets of measurements m_y. The second summation sums up all residuals between measured and simulated data in a particular measurement set. Here n_j represents the number of data points in a particular set. v_j and $w_{i,j}$ are weighting factors. A solution of the inverse problem is attained by minimization of the objective function by a Levenberg-Marquardt nonlinear minimization method (Simunek (c), et al. 2008). This method is based on the least-squares approach. Initial estimates of

the optimized parameter vector **b** are iteratively improved during the optimization process, until a predetermined convergence criterion (reduction of *E(**b**,y)* between two consecutive iterations) has been achieved (Simunek (c), et al. 2008, Hopmans, Simunek, et al. 2002).

The "success" of an inverse soil hydraulic parameter determination depends on whether the inverse problem is "correctly posed" (Durner (b), Schultze and Zurmuhl 1999). Success is related to convergence and parameter uniqueness of the final optimized parameter vector (Simunek (c), et al. 2008). It is the final goal to reach the global minimum of the objective function. In order to obtain convergence and parameter uniqueness the following recommendations where given in inverse modelling literature (Hopmans, Simunek, et al. 2002, Durner (b), Schultze and Zurmuhl 1999):

- Minimize measurement errors of the measured data in *E(**b**,y)*;
- Aim for a minimum number of parameters to be optimized;
- Apply an appropriate hydraulic model;
- Apply suitable boundary conditions and weighting factors;
- Choose the correct type of measured data;
- Provide well-constrained initial parameter estimates;
- Experiment design should cover a wide water content range.

In order to test for (non)uniqueness of the optimized parameter vector **b**, Simunek (c), et al. (2008) recommend to solve the inverse problem repeatedly using different initial parameter estimates. If most of the runs converge to the same optimized parameter vector, one can assume that this parameter vector represents the global minimum and therefore is unique (Durner (a), et al. 1999).

5.3.3.2 Experimental options for inverse modelling

Available inverse experiment designs
According to Durner (b), Schultze and Zurmuhl (1999), inverse experimental set-ups can be categorized into three classes:

1. One-step outflow method
2. Multi-step outflow method
3. Continuous outflow method

Of these three design classes, the *one-step* and *multi-step outflow method* generally require the same experimental set-up. These methods are based on determining the parameter vector **b** for the hydraulic functions with the use of a Tempe Pressure Cell (Figure 42). Standard Tempe Pressure Cell set-ups are distributed by the Soilmoisture Equipment Corporation (SEC 1995). Tempe Pressure Cell outflow experiments are based on a stepwise change in the pressure head on the top of the soil sample (upper boundary condition). The one-step outflow method is based on a single pressure head change at the beginning of the experiment, while the multi-step outflow method includes several small pressure head changes in one experiment (Durner (b), Schultze and Zurmuhl 1999). When the pressure head on top of the soil sample is raised above atmospheric pressure, the higher pressure within the Tempe Cell forces water out of the initially saturated soil pores, through the ceramic plate into a tube that siphons the outflow to a leveling bulb that is placed on a balance (SEC 1995).

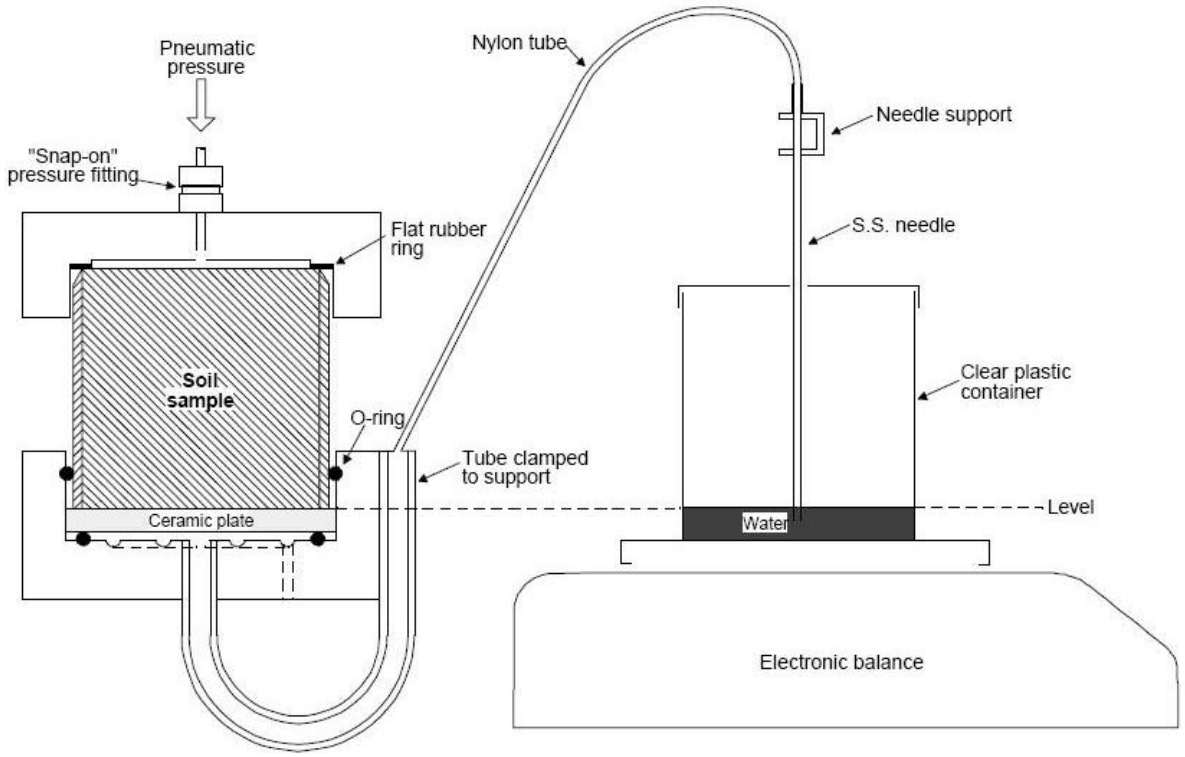

Figure 42. Tempe Pressure Cell experimental set-up. Source: Green, et al. (1998)

The measurement sets m_y in the objective function generally consists of (a combination of) measured water contents, pressure heads and/or cumulative outflow across the lower boundary of the soil column. Notwithstanding the ease of its experimental design and the relatively accurate results that were presented by Parker, et al. (1985), several researchers demonstrated that the Multi-step outflow method is superior to the One-step outflow method (Durner (a), et al. 1999). The quick change of the boundary condition in the One-step method does not represent natural conditions and contact problems at the interface between the soil and the porous plate occur as a result of this large pressure changes (Durner (b), Schultze and Zurmuhl 1999). Because of this, a very thin drained soil layer next to the porous plate unnaturally controls the total outflow rate. However, uniqueness problems in one-step outflow experiments can be minimized if pressure head data is included in the objective function (Hopmans, Simunek, et al. 2002). The Multi-step outflow method has been introduced and recommended because earlier work shows that this method requires less different measurement sets to obtain a unique set of hydraulic parameters (Hopmans, Simunek, et al. 2002).

The *continuous outflow method* varies from the One-step and Multi-step outflow method in the sense that it entails a continuous smooth change of the boundary pressure head instead of a discrete pressure head step (Durner (b), Schultze and Zurmuhl 1999). The continuous outflow method can be performed with an automated, computer controlled Tempe Cell set-up (Durner (b), Schultze and Zurmuhl 1999), but this is a rather expensive and complex experiment. Another continuous outflow method is the Wind Method (Simunek (a), Wendroth and van Genuchten 1998). In this laboratory experiment, an undisturbed sample is saturated on a ceramic plate before the start of each run. At the beginning of the experiments, evaporation is initiated by using a fan to blow air away from the soil surface at room temperature. The measurement sets m_y, in the objective function consisted of pressure heads (from tensiometer readings), evaporation fluxes (from regular soil sample weighing) and a soil water content measurement at the end of each experiment (Simunek (a), Wendroth and

van Genuchten 1998). Simunek (a), Wendroth and van Genuchten (1998) conclude that this parameter estimation technique can be successfully used to predict the soil hydraulic parameters for a wide range of soils.

5.3.3.3 Materials of selected experimental set-ups

Multiple One-step and Multi-step outflow experiments were performed in the geotechnical lab of the University of Singapore to determine the soil hydraulic properties of the potting soil that is used as a green roof media at the 1 m^2 platforms. Next to these laboratory experiments, an evaporation experiment was carried out under field/atmospheric conditions. These three methods were individually performed, measured and simulated.

One-step and Multi-step outflow experiments

Several soil samples of 3 cm height and 8.5 cm diameter were prepared at approximate mean density of the green roof platform soil. Next to this, two undisturbed samples from the green roof platform were collected with a core sampler for laboratory testing as well. It was not feasible to use undisturbed samples from the roof top experiments only, because the high number of samples would have destroyed these experiment set-ups that were still operational at the time of the inverse modelling experiments. Soil samples were contained in a brass cylinder and assembled in a Tempe Pressure Cell, with a 5.7 mm thick , -10 m air-entry ceramic plate. The high air entry-value of the ceramic plate ensures that the ceramic plate will remain saturated for all applied pressure heads lower than this air-entry or bubbling pressure of -10 m. The reproducibility of the optimized parameter vector per method was evaluated by performing several double/backup experiments. Outflow from the soil samples was initiated in all outflow experiments by (stepwise) increasing the pressure head on top of the soil. After initial saturation, soil samples were unsaturated by lowering the bulb level to the top of the ceramic plate before starting the experiment. This has been recommended in previous studies because it was shown that flow from an initially saturated soil sample is not according to Richards equation (Durner (b), Schultze and Zurmuhl 1999). Cumulative outflow $q(t)$ [LT^{-1}] was measured as a function of time by weighing a bulb on top of an electronic balance that was automatically logged onto a PC at a 1-min time interval. For some experiment runs, the pressure was measured with a pressure transducer and logged onto a PC at a 5-min time interval. After each experiment the final soil water content was determined by oven-drying. The final soil water content was used as a reference point for calculation of the initial water content and other equilibrium water contents (applicable for Multi-step experiments) during the same experiment run. A detailed description of the experimental set-up and the experiment input for the numerical simulation is given in Appendix 9.

Evaporation experiment

Next to the One-step and Multi-step outflow experiments, a 12-day evaporation experiment was performed. This evaporation experiment is based on the Wind Method that was mentioned earlier. The main difference between both experiments is that the Wind Method is a laboratory inverse experiment while the evaporation experiment in this research was carried out under field conditions: on the same rooftop as the green roof platforms. The set-up consists of a tray with a 5 cm drainage layer and a 10 cm potting soil layer. Both layers are separated by a thin filter fabric. No plants are grown on the soil. After initial wetting of the soil until runoff occurred (at θ_{seep}), the sample was placed on two balances which were connected to a PC. Evaporative water loss from the top was

determined by weighing the total experiment on a 2-sec time interval. The progress of the water pressure over time was measured with two tensiometers, which were placed at z = 1.5 cm and z = 5.5 cm above the soil bottom (Figure 44). Meteorological data from the NUS meteo station (Appendix 4) was used for calculation of the hydrological fluxes. A detailed description of the experimental set-up and the experiment input for the numerical simulation is given in Appendix 10.

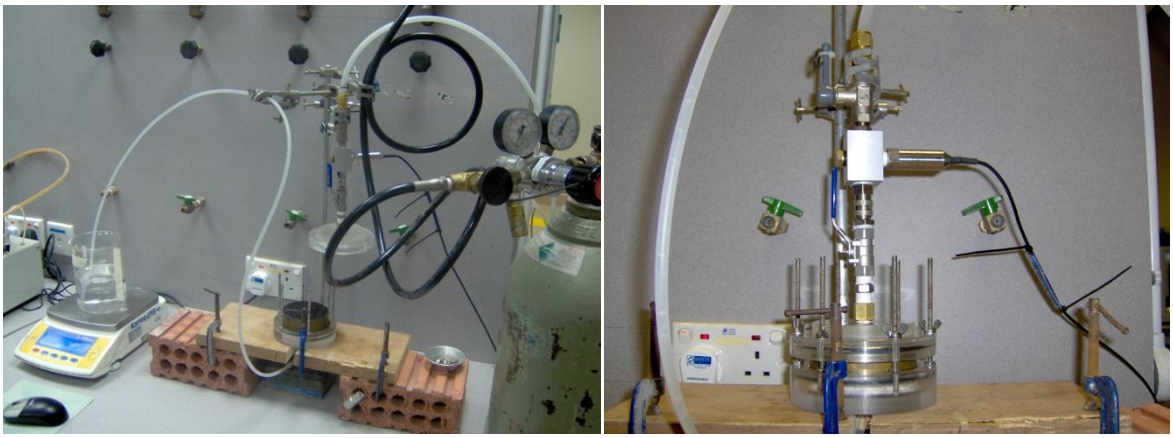

Figure 43. One-step and Multi-step outflow experimental set-up

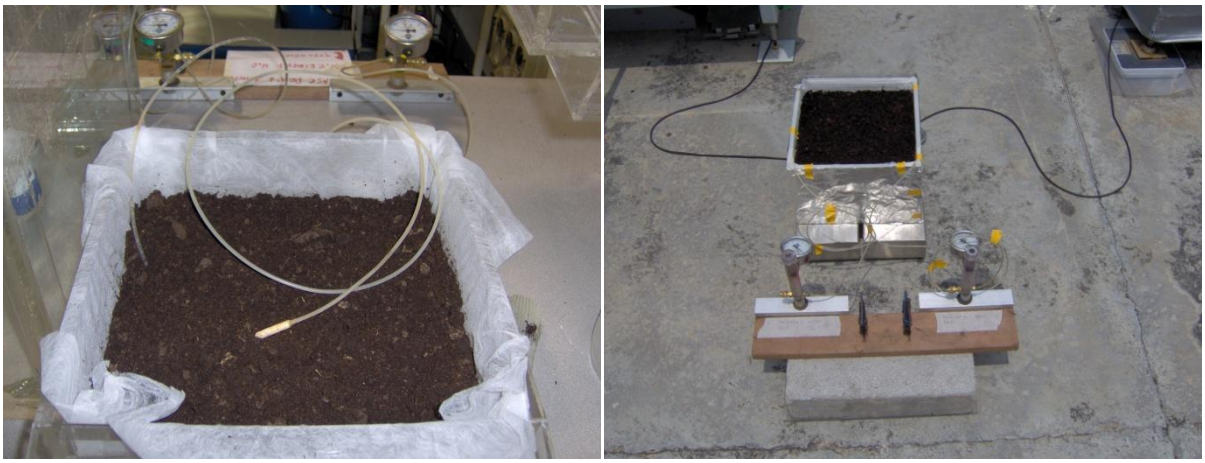

Figure 44. Evaporation experiment set-up

5.3.3.4 Analysis methodology

The hydraulic properties of the soil samples were determined by inverse modelling of two One-step outflow (OSO), five Multi-step outflow (MSO) and a continuous evaporation experiment. Every outflow experiment has three series of optimization conditions: series A, B and C. In the A-series, θr, α and n are free parameters in the parameter vector **b**. In the series B and C, K_s respecitively K_s and l are added to the free parameters in the optimized parameter vector **b**. Parameter determination with the evaporation experiment has been limited to a three-parameter fit A-series optimization condition. Reasons for this choice are mentioned in the result sections hereafter. Based on the recommendations from paragraph 5.3.3.1, the uniqueness of the optimized final parameter vector **b** will be verified by routinely rerun the simulation with 2 different initial parameter estimates. If most of the runs converge to one single parameter vector **b**, it is concluded that this parameter vector represents the global minimum (Durner (a), et al. 1999). An optimization run i counts if the value of the objective function is within 5% of the globally observed minimum for that particular series (0.95 ≤

$SSQ_i/SSQ_{min} \leq 1.05$) and if all parameters are less than 5% off the global minimum values (Durner (a), et al. 1999, p.823).

Table 4. Optimization conditions

Run	Free parameters	Fixed parameters	No. of model runs
	One-step outflow method (h_{bot}=-1000 cm)		
OSO-1A	θ*r*, *α*, *n*	*l=0.5*, K_s*=110 cm/h*	2^3=8
OSO-1B	θ*r*, *α*, *n*, K_s	*l=0.5*	2^4=16
OSO-1C	θ*r*, *α*, *n*, K_s, *l*		2^5=32
OSO-2A	θ*r*, *α*, *n*	*l=0.5*, K_s*=110 cm/h*	2^3=8
OSO-2B	θ*r*, *α*, *n*, K_s	*l=0.5*	2^4=16
OSO-2C	θ*r*, *α*, *n*, K_s, *l*		2^5=32
	Multi-step outflow method (0 cm≥h_{bot}≥-1000 cm)		
MSO-1A	θ*r*, *α*, *n*	*l=0.5*, K_s*=110 cm/h*	2^3=8
MSO-1B	θ*r*, *α*, *n*, K_s	*l=0.5*	2^4=16
MSO-1C	θ*r*, *α*, *n*, K_s, *l*		2^5=32
	Multi-step outflow method (0 cm≥h_{bot}≥-100 cm)		
MSO-2A	θ*r*, *α*, *n*	*l=0.5*, K_s*=110 cm/h*	2^3=8
MSO-2B	θ*r*, *α*, *n*, K_s	*l=0.5*	2^4=16
MSO-2C	θ*r*, *α*, *n*, K_s, *l*		2^5=32
	Multi-step outflow method (0 cm≥h_{bot}≥-100 cm)		
MSO-3A	θ*r*, *α*, *n*	*l=0.5*, K_s*=110 cm/h*	2^3=8
MSO-3B	θ*r*, *α*, *n*, K_s	*l=0.5*	2^4=16
MSO-3C	θ*r*, *α*, *n*, K_s, *l*		2^5=32
	Multi-step outflow method undisturbed sample (0 cm≥h_{bot}≥-200 cm)		
MSO-4A	θ*r*, *α*, *n*	*l=0.5*, K_s*=110 cm/h*	2^3=8
MSO-4B	θ*r*, *α*, *n*, K_s	*l=0.5*	2^4=16
MSO-4C	θ*r*, *α*, *n*, K_s, *l*		2^5=32
	Multi-step outflow method undisturbed sample (0 cm≥h_{bot}≥-100 cm)		
MSO-5A	θ*r*, *α*, *n*	*l=0.5*, K_s*=110 cm/h*	2^3=8
MSO-5B	θ*r*, *α*, *n*, K_s	*l=0.5*	2^4=16
MSO-5C	θ*r*, *α*, *n*, K_s, *l*		2^5=32
	Evaporation experiment		
EVAP-A	θ*r*, *α*, *n*	*l=0.5*, K_s*=110 cm/h*	2^3=8

For all outflow and evaporation experiment runs we use two different initial conditions that were based on tacit knowledge that has been gathered during the experiments (Table 5). Using two initial estimates for every free parameter, 2^n runs have to be performed per experiment per series. For every single experiment this means $2^3+2^4+2^5$=56 runs. The saturated water content θ_s was calculated at the end of every experiment while the saturated permeability K_s was measured with two constant head experiments. The average saturated permeability was high: 26.3 m/d or 110 cm/h. Details and results of the constant head experiments are presented in Appendix 8.

Table 5. Initial conditions for optimizations with the outflow and evaporation experiments

Parameter		Upper boundary	Upper initial condition	Lower initial condition	Lower boundary
	Outflow experiments				
θ*r*	[-]	0.4	0.25	0.1	0
α	[cm^{-1}]	0.5	0.1	0.02	0.01
n	[-]	10	2	1.2	1.01
K_s	[cm h^{-1}]	150	110	50	10/1*
l	[-]	10	0.5	-0.5	-4
	Evaporation experiment				
θ*r*	[-]	0.4	0.3	0.2	0
α	[cm^{-1}]	2	0.2	0.1	0.01
n	[-]	10	2	1.5	1.01

*The lower boundary for K_s has been set to 1 in the MSO experiments 3, 4 and 5

5.3.3.5 Inverse modelling experiment results and discussion

The Tempe Cell outflow experiments and the continuous evaporation experiment were analysed individually. The results of each experiment are presented in a tabular and graphical manner and the mutual differences will be discussed. The Tempe Cell experiment optimization results for the potting soil are listed in Appendix 11. A summary of these results is given in Table 6. The evaporation experiment optimization results for the potting soil are listed in Table 8. The discussion of the results is based on four main topics:

1. The sum of squares of the deviations between modeled and measured data points;
2. The number of runs that converge to the global minimum per series;
3. The appropriateness of the soil water retention function (reflected by a good global fit of the modeled outflow (Durner (a), et al. 1999));
4. The appropriateness of the hydraulic conductivity function (reflected by a good local fit of the modeled outflow (Durner (a), et al. 1999)).

One-step outflow experiment results

Both One-step outflow experiments were characterized by a very low hit-count in all series (Appendix 11). In all six series, only one out of the total of 2^n runs converged to the minimum sum of squares (SSQ) and a lot of simulations did not lead to numerical convergence at all. Based on this low hit-count, it can be concluded that the optimized parameter vector **b**, does not represents the global minimum and therefore is not unique. Treating K_s or *l* as a free parameter hardly improves the overall fit as can be seen in Figure 45 and Appendix 11. The problem of non-uniqueness is probably caused by the fact that these two experiments were *ill-posed*. It was found that the outflow rates of the experiments in the first minutes were extraordinary high. Next to this, air bubbles were present in the conveyance tube between the Tempe Cell and the bulb. Both observations gave clear O-ring leakage indications. O-ring leakages introduce measurement errors in both *Q(t)* and the θ(-1000 cm) data points, therefore increasing the chance of obtaining a non-unique optimization. All Tempe Cell O-rings were replaced after the first two experiments. The absence of air bubbles and the lower initial outflow rates in all posterior experiments have verified the earlier O-ring leakage hypothesis. Because of time-limits and indications that the Multi-step outflow experiment results are superior to the One-step outflow experiment results, no more One-step outflow experiments were performed. A

positive point is that the experience gained at the One-step outflow experiments was of great value for the more complex Multi-step outflow experiments.

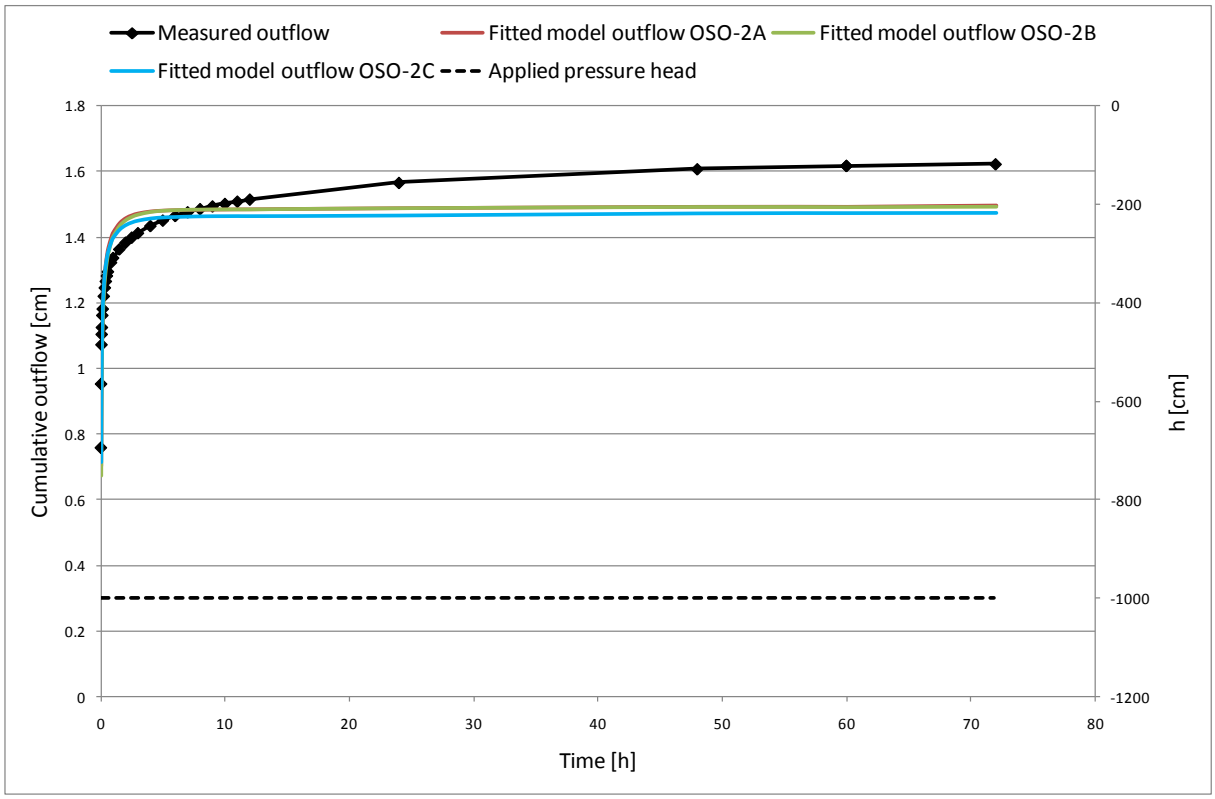

Figure 45. Measured vs. simulated outflow of the One-step outflow series 2A, 2B and 2C

Multi-step outflow experiment results

To facilitate outflow measurement readings during both day and night, the balance was linked to a PC from the start of the first Multi-step outflow experiment. With the use of an adapted data logging software program, continuous readings of the outflow, on a 1-minute time interval, became available. During the first MSO experiment, outflow was initiated after each of the four pressure steps: h=-100 cm, h=-250 cm, h=-500 cm and h=-1000 cm (boundary condition details are given in Appendix 9). Enhancing the flexibility of the hydraulic conductivity function, by allowing K_s to vary, decreases the SSQ to 0.0592. Additional added flexibility, by allowing l to vary, provides no further decrease of the SSQ. The decrease in SSQ between series 1A and 1B can be explained by the lower K_s and higher n in the optimized parameter vector **b** of series 1B compared to 1A. The lower value of K_s introduces a smoother outflow in the first step (h=-100 cm). The higher value of n allows for a greater availability of soil water in the more negative pressure range. A drawback of the parameter differences is the lack of flexibility of series B and C's retention curve in the higher negative pressure ranges. As a result of this, the fitted model outflow underestimates the measured outflow step at the last pressure step (h=-1000 cm) as can be clearly observed in Figure 46. Another conclusion that can be drawn is that the differences in soil water content between h=-100 cm and h=-1000 cm are relatively small compared to the difference in soil water content between h=0 cm and h=-100 cm. Based on this information and the recommendation to design an experiment that covers a wide range of soil water contents, the other Multi-step outflow experiments are preformed in the lower negative pressure ranges. The determination of the hydraulic functions at the water pressure range between h=0 cm and h=-100 cm becomes of main interest for further inverse modelling experiments.

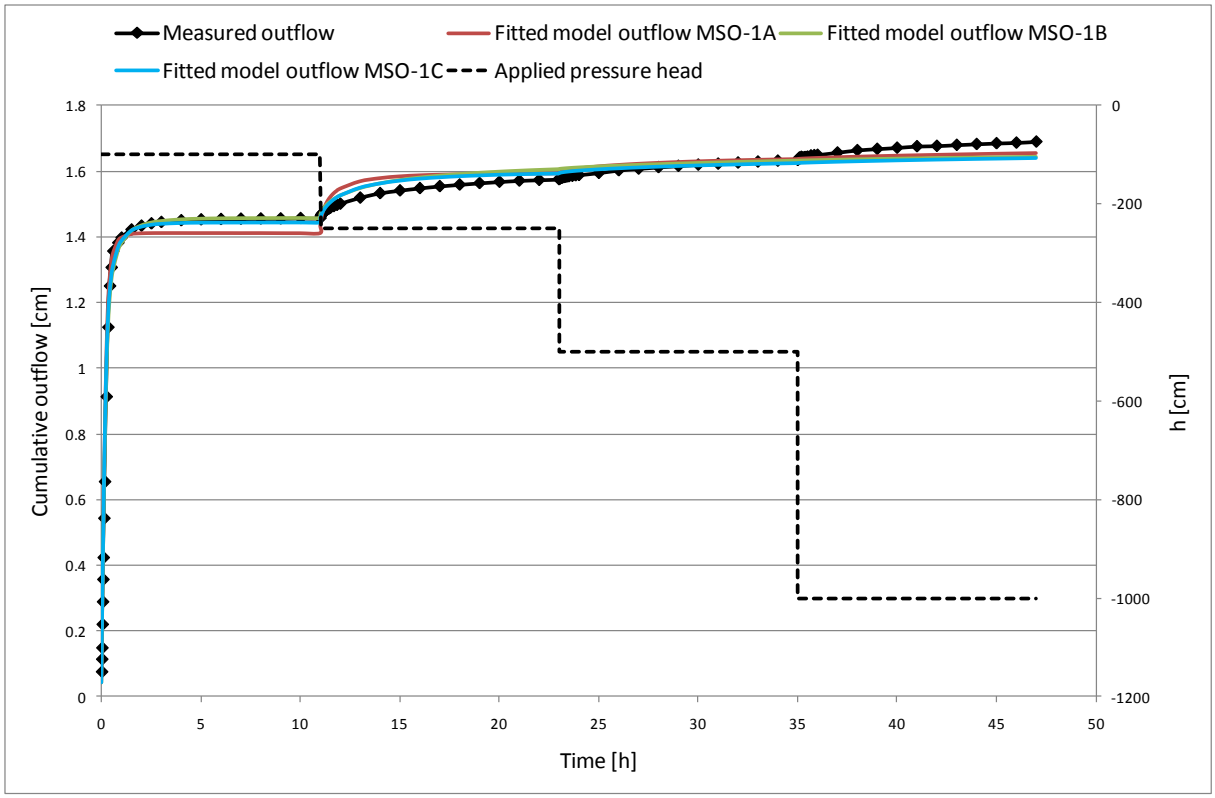

Figure 46. Measured vs. simulated outflow of the Multi-step outflow series 1A, 1B and 1C

Because of very slow interaction between the bulb and the Tempe Cell before the start of the second MSO experiment, the accuracy of the initial pressure head conditions cannot be guaranteed. This presumption was confirmed by the relatively low value of θ_s that has been calculated by oven drying of the Tempe Cell soil sample at the end of the test. Nevertheless, the experiment results are in line with the other outflow experiment results and parameter vectors converge to a global optimum for all three series. Optimization results for MSO-3 are presented in Figure 47. Generally speaking, all series result in reasonable steady state outflow quantities. Independent of the number of free parameters, the deviation between measured and simulated outflow in the first hours of step 1 is quite big. The outflow behavior is much smoother as well, compared to all other outflow experiments. This is most certainly caused by a temporal pressure drop in the system. Pressure variations can be caused by:

1. Pressure line variations (affecting the net cell pressure from the top of the cell);
2. Atmospheric pressure variations (affecting the net cell pressure from the bottom of the cell).

From MSO-4 onwards the pressure line variations have been eliminated by applying pressure from a pressurized air cylinder instead of the standard laboratory pressure line. The remaining atmospheric pressure variations are monitored with an automated pressure logging system. Up to MSO-3, the pressure transducer was only used to set the initial pressure head before the start of every new outflow step. For MSO-4 and MSO-5, the pressure was measured during the entire experiment.

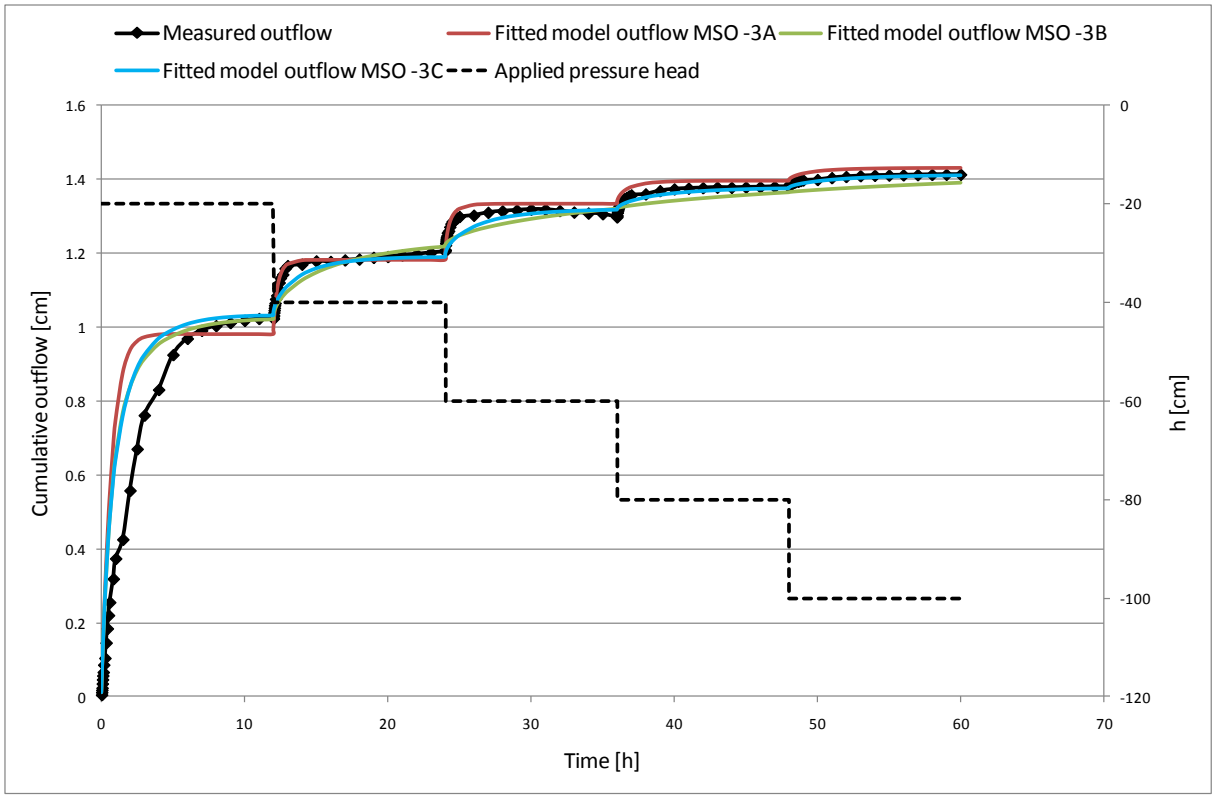

Figure 47. Measured vs. simulated outflow of the MSO series 3A, 3B and 3C

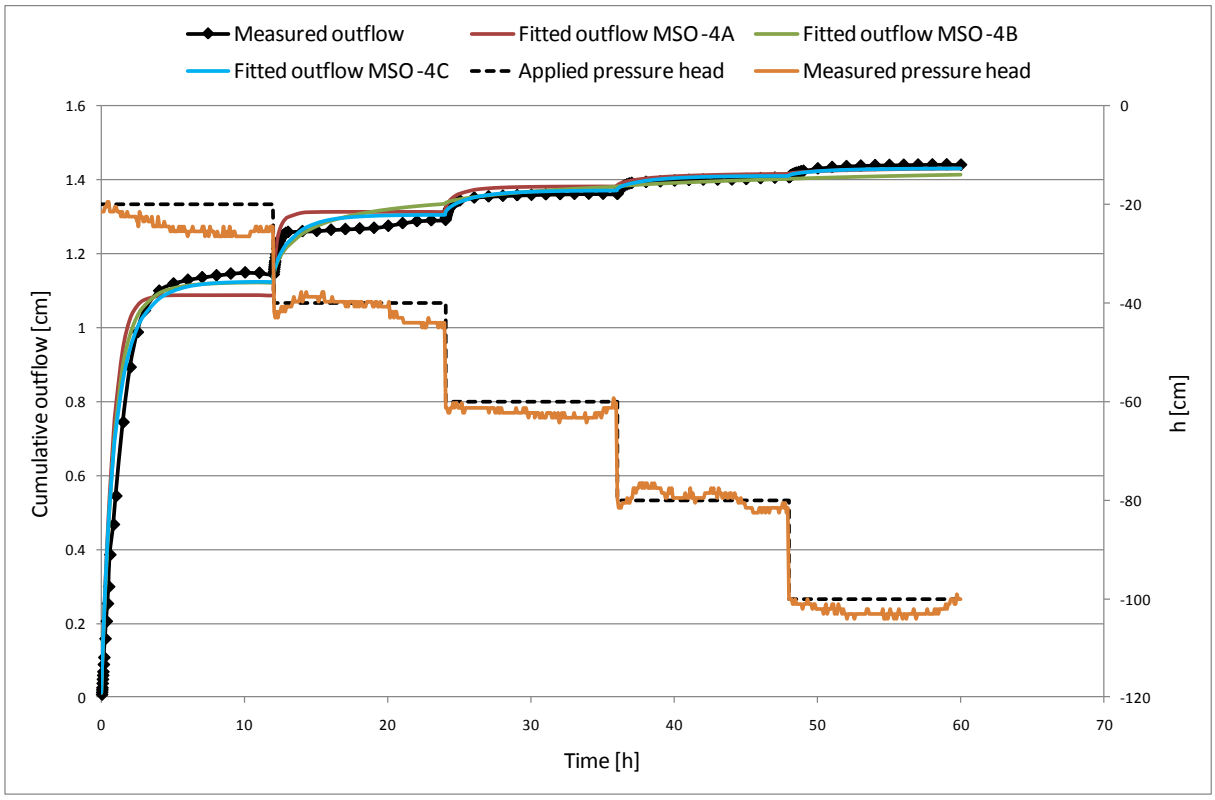

Figure 48. Measured vs. simulated outflow of the MSO series 4A, 4B and 4C and applied (initial) versus measured pressure head

For MSO-4, again all three optimization series results in good global outflow fits (Figure 48). With over 80% of all runs converging to the same optimized parameter vector **b** for series MSO-4A and 4B,

the optimizations are unique as well. The SSQ is almost halved (0.283) when both K_s and *l* are added as free parameters in the optimization process (series MSO-4C). Optimizing both K_s and *l* however, leads to very small unrealistic values for both parameters. Compared to series-A, these low values lead to reduced hydraulic conductivity near saturation, while the hydraulic conductivity is relatively high in the unsaturated part of the soil water content range. These optimization results are in accordance with earlier outflow experiment results from the German silty Jülich soil (Durner (a), et al. 1999). Outflow deviations in the first, second and last pressure step do not give an indication for an inappropriate water retention function. These deviations obviously result from atmospheric pressure variations, that affect the net cell pressure from the water bulb side (bottom of the cell). The atmospheric pressure, which has been measured at the NUS meteo station, varies between 99.9 and 100.4 kPa during the experiment, which corresponds to an absolute pressure variation of 0.5 kPa or 5 cm H_2O. Pressure variations in this order influences the real measured outflow significantly, especially near saturation, where $d\theta/dh$ is relatively high . Finally, based on outflow differences in the first pressure step of MSO-3 and MSO-4, it can be concluded that the undisturbed soil has a slightly higher sand fraction than the prepared samples. The total cumulative outflow after five steps converges in both experiments to 1.4 cm however.

Optimizations in all series of MSO-5 result in low SSQ values (0.075-0.145). The global as well as the local fit of the simulated outflow versus the measured outflow demonstrate the appropriateness of van Genuchten's unimodal non-hysteretic hydraulic functions in this experiment. This particularly good fit could well be the results of the relatively stable pressure head during the experiment runtime (Figure 49). The biggest pressure deviations occur in the third pressure step (h=-100 cm). Since the measured pressure is higher than the simulated lower boundary condition at pressure step three, the outflow that has been calculated in the numerical simulation gives an explainable underestimation of the real outflow. As in MSO-4C, MSO-5C shows a better local fit in the last pressure step. The optimization algorithm generates unrealistic low values for K_s and *l* that result in increased hydraulic conductivity in the unsaturated part (Figure 50). Despite the low SSQ and good global and local fits, the uniqueness of the numerical optimizations have to be questioned. Respectively 3 out of 8, 7 out of 16 and 2 out of 32 runs of different initial conditions converge to the same optimized parameter vector **b** in series MSO-5A, MSO-5B and MSO-5C. The high value of the optimized parameter θ_r (0.38-0.4) decreases the usability of the optimized parameter sets in the dryer water content range. The lower flexibility of the water retention function in the unsaturated spectrum, however improves the fit near saturation. Since the final goal of the unsaturated zone modelling is to accurately simulate green roof outflow, which occurs near saturation, the last feature is far more important than the former one.

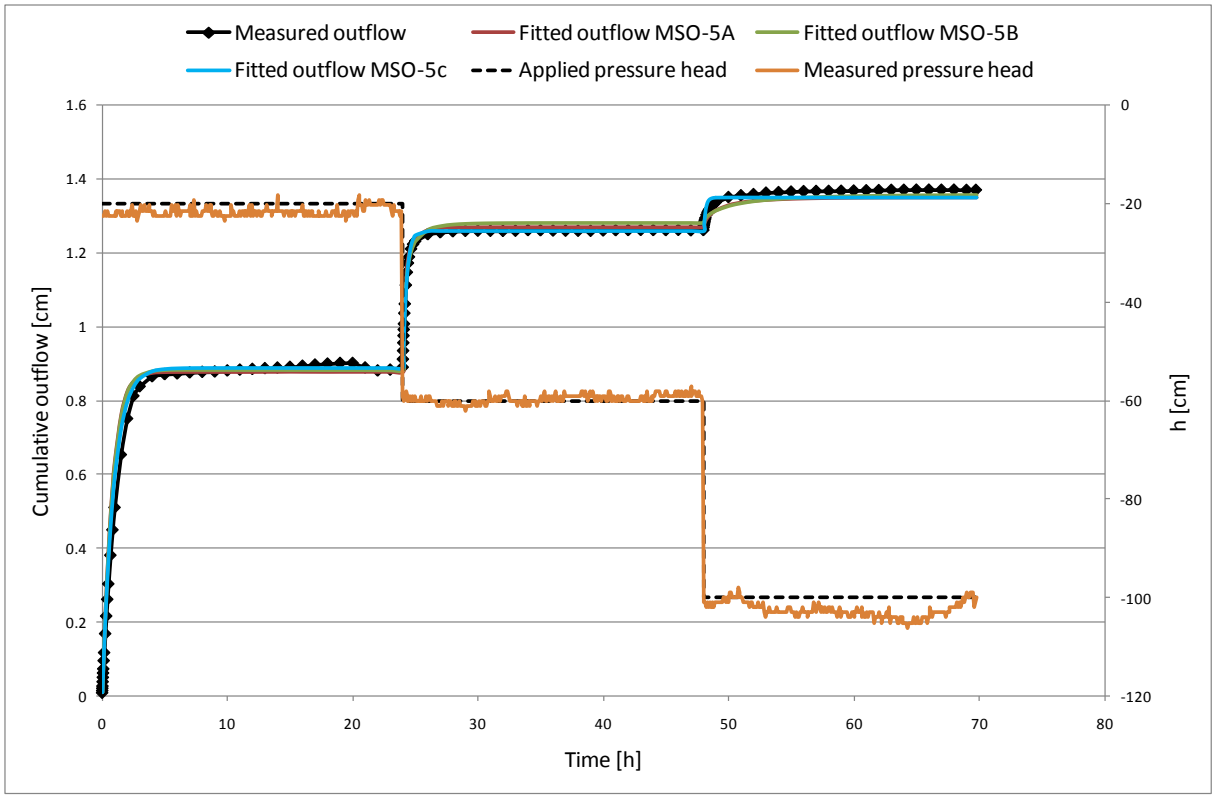

Figure 49. Measured vs. simulated outflow of the MSO series 5A, 5B and 5C and applied (initial) versus measured pressure head

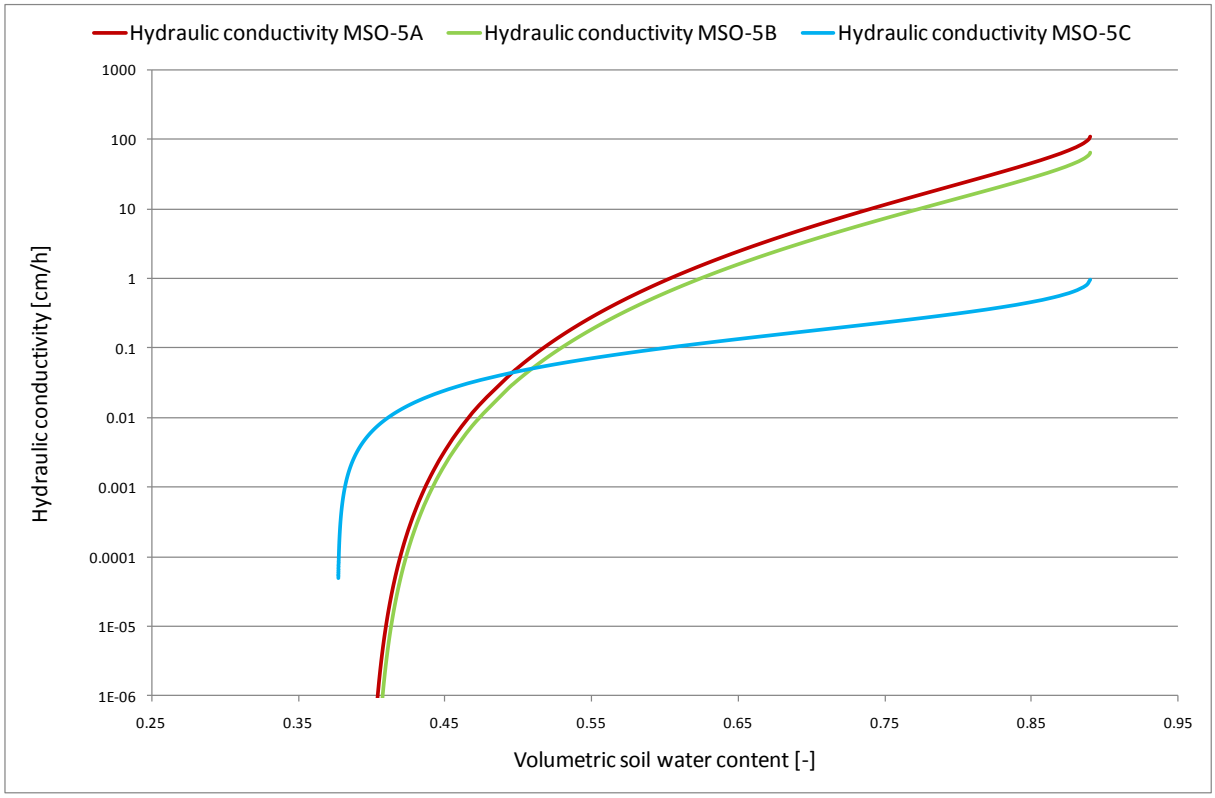

Figure 50. Optimized hydraulic conductivity functions of the MSO series 5A, 5B and 5C

Unlike the One-step outflow experiments, the Multi-step outflow experiments are a good method to establish the soil hydraulic parameters for the soil hydraulic functions. Good global fits between the

measured and simulated outflow characterizes a large part of the evaluated model runs. Although differences between prepared and undisturbed samples were observed, the final optimized parameter vectors **b** of both sample types are in line (Table 6).

Table 6. Summary of the parameter optimization results of outflow experiments

	Min R^2	θ_r	θ_s	α	n	K_s	l
	Prepared soil samples						
OSO-1	0.951	$0.16 \le \theta r \le 0.22$	0.86	$0.02 \le \alpha \le 0.03$	$1.34 \le n \le 1.71$	$44.77 \le K_s \le 110$	$-0.15 \le l \le 0.5$
OSO-2	0.966	$0.22 \le \theta r \le 0.33$	0.89	$0.02 \le \alpha \le 0.04$	$1.38 \le n \le 1.71$	$34.25 \le K_s \le 110$	$0.43 \le l \le 0.5$
MSO-1	0.997	$0.31 \le \theta r \le 0.32$	0.87	$0.03 \le \alpha \le 0.05$	$2.18 \le n \le 2.60$	$20.28 \le K_s \le 110$	$0.24 \le l \le 0.5$
MSO-2	0.996	$0.31 \le \theta r \le 0.31$	0.81	$0.11 \le \alpha \le 0.11$	$1.84 \le n \le 1.88$	$10 \le K_s \le 110$	$-0.46 \le l \le 0.5$
MSO-3	0.995	$0.31 \le \theta r \le 0.33$	0.85	$0.07 \le \alpha \le 0.12$	$1.93 \le n \le 2.50$	$1 \le K_s \le 110$	$-1.44 \le l \le 0.5$
	Undisturbed soil samples						
MSO-4	0.997	$0.30 \le \theta r \le 0.32$	0.81	$0.07 \le \alpha \le 0.11$	$2.25 \le n \le 3.11$	$1 \le K_s \le 110$	$-1.42 \le l \le 0.5$
MSO-5	0.999	$0.38 \le \theta r \le 0.40$	0.89	$0.09 \le \alpha \le 0.11$	$1.98 \le n \le 2.30$	$1 \le K_s \le 110$	$-2.86 \le l \le 0.5$

Allowing K_s and l or both to vary, result in a wide range of parameter values, while predicted model outflow results are only marginally improved. Improved flexibility in the relatively unsaturated soil water content range therefore does not compensate for the loss of a physical meaning of the parameter set. Next to that, the more simple three-parameter fit optimizations give accurate enough results near saturation. Keeping in mind that the final purpose of the green roof model is to simulate outflow, which always occurs near saturation, the choice for a relatively simple model is presumably the best choice here. Soil water retention curves for all inverse experiments series A reveal the heterogeneity between soil samples, but demarcate the parameter vector space **b** to a large extent (Figure 51).

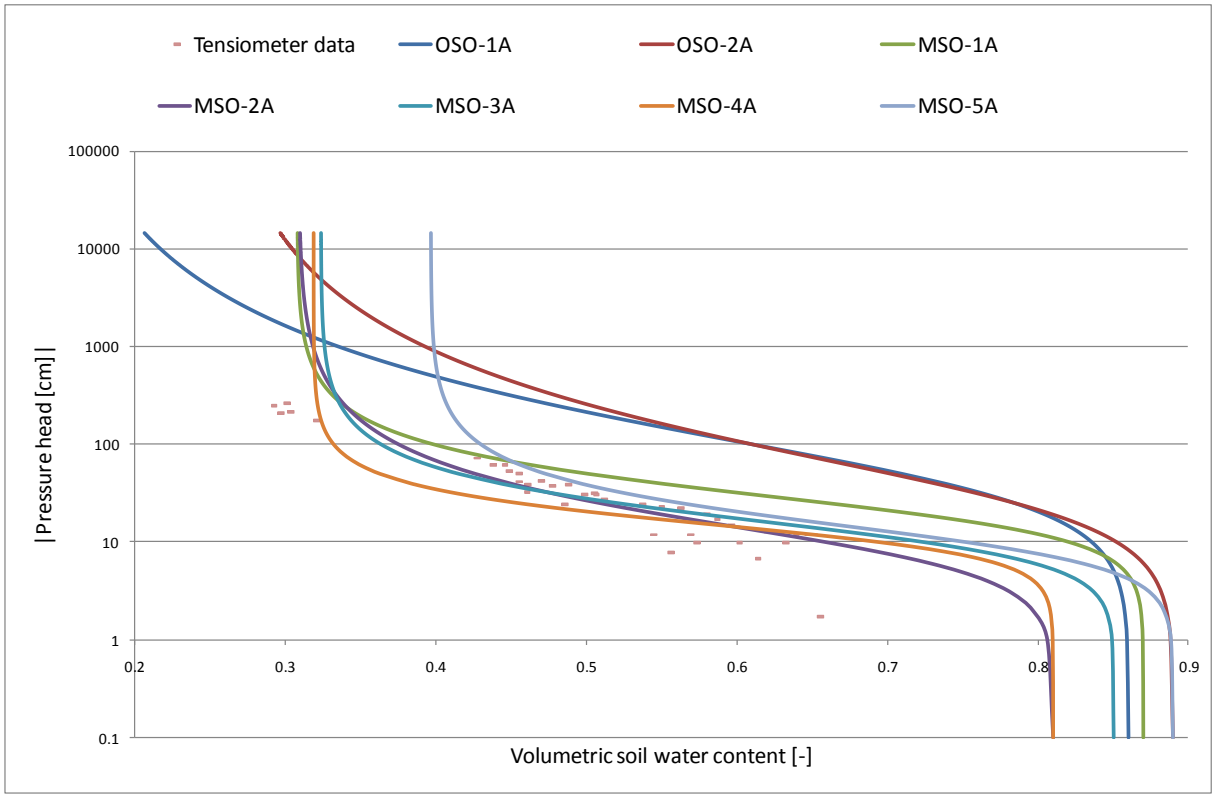

Figure 51. Soil water retention curves for all inverse outflow experiment series A

Evaporation experiment results

The evaporation experiment result section will focus on the four main topics that were introduced earlier: SSQ, uniqueness of the optimized parameter vector **b** and appropriateness of the two hydraulic functions θ*(h)* and *K(h).* Based on the optimization experience and results of the outflow experiments, the choice was made to stick to a three-parameter fit hydraulic optimization model.

The objective function *E(**b**,y)* in the evaporation experiment consists of 300 hourly *Actual Cumulative Surface Flux (ACSF)* [L] measurements and 18 tensiometer measurements from the top tensiometer where *z*=5.5 cm. The *ACSF* is the cumulative value of evaporation minus infiltration over time, which is equal to the change of weight in the experiment. During the total length of the 300-hours experiment, only one small rain event of 3.7 mm occurred on the 26th of February, causing a temporary drop in the *ACSF*-curve. Appendix 10 illustrates that the observed tensiometer measurement fluctuations are caused by temperature variations, a process that was evaluated by Buchter, et al. (1999). In order to reduce measurement errors and thus ill-posedness of the inverse experiment, the inconsistent measurement set from the lower kinked tensiometer was not included in the objective function. Numerical simulations of bare soil evapotranspiration show that an average albedo value α_r [-] of 0.09 minimizes the SSQ: the value of the objective function (Appendix 10). Since HYDRUS-1D only allows a constant albedo value during the evaporation experiment simulations, α_r=0.09 has been chosen for the whole experiment run time. Figure 52 presents the measured and simulated *ACSF* of the evaporation experiment between the February 23 and of March 07, 2010. The simulated *ACSF*-curve is the result of the optimized parameter vector $\mathbf{b}=\{\theta_r, \theta_s, \alpha, n, K_s, l\}^T$ which is shown in Table 7. Parameter identification results are unique since all 8 runs hit the same global minimum. The total SSQ is 10.45. Deviations between the measured and simulated *ACSF* account for 54% of the total SSQ. Deviations between the measured and simulated water pressure heads account for the remaining 46%. The total SSQ of the evaporation experiment is a magnitude larger than the total SSQ of the outflow experiments, which was <1 for all outflow experiments. This can be caused by measurement errors. However, the SSQ, which is a value of the objective function, cannot be directly used to compare optimization results between different inverse experiments because:

1. The objective function (Eq. 5.31) is defined as the sum of all deviations between measured and simulated data. More measurements sets m_y and/or a higher number of data points n_j increase the total SSQ, independent of the goodness of fit;
2. The objective function sums up all *absolute* deviations between measured and simulated data, not the *relative* deviations. This means that certain measurements sets and associated data points can have a big influence on the total SSQ-value, while their relative errors are small compared to other measurement sets. Because the tensiometer dataset *h(t)* has big absolute values (order of three digits [cm]) compared to outflow *Q(t)* or *ACSF(t)* data points (order of one digit [cm]), this measurement set has a large influence on the total SSQ. This example illustrates that the choice for the weighing factors v_j and $w_{i,j}$ also has to be based upon the absolute values of the data points within the datasets. Therefore, weighing factors of 1 and 0.05 were assigned to measurement sets *ACSF(t)* and *h(t)* respectively.

In contrast to the restrictions of the SSQ-value in result evaluation, a discussion which is based on the graphical representation of the measured versus simulated *ACSF(t)* and *h(t)* is a more practical tool. Figure 52 and Figure 53 show a graphical representation of the most important modelling results.

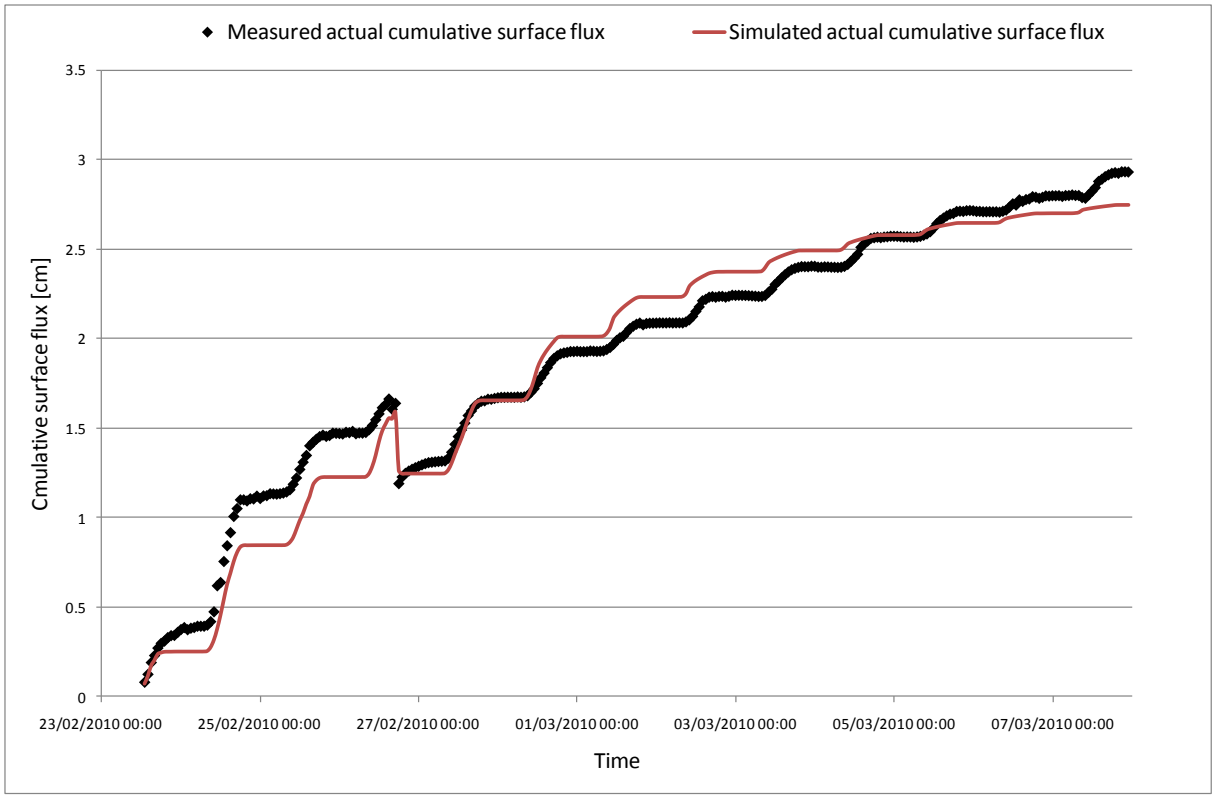

Figure 52. Measured and simulated actual cumulative surface flux of the evaporation experiment

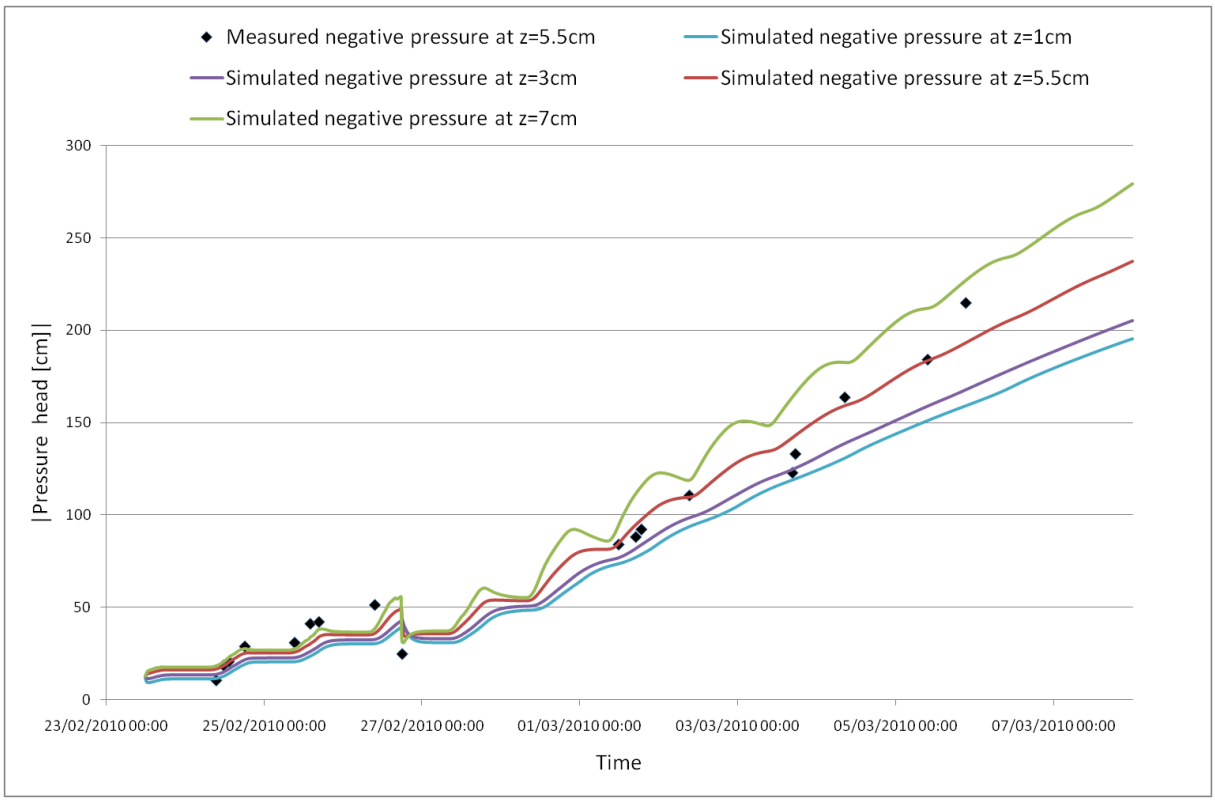

Figure 53. Measured and simulated water pressures heads of the evaporation experiment

The shape of the *ACSF(t)* simulations gives a good general fit (R^2=0.99), which justifies the appropriateness of the soil water retention function. The water pressure head results confirm the model appropriateness. Good correspondence between between tensiometer measurements and

simulated water pressure heads at z=5,5 cm (Figure 53) is clearly visible. Underestimation of the evaporation towards the end of the experiment indicates the lack of flexibility of the water retention function in the very dry soil water range. The same model limitation was found in the outflow experiments. Other local deviations between evaporation measurements and simulations (Figure 52) are discussed in Appendix 10 and are almost certainly caused by:

1. The use of a constant albedo value α_r. A constant albedo value introduces evaporation underestimation in the wet soil water range, where the wet dark soil increases radiation absorption. In the same way, a constant albedo value overestimates evaporation in the dry soil water range, where the dry light soil decreases radiation absorption;
2. Inappropriateness of the Penman-Monteith equation, which was developed by defining the reference evapotranspiration from a reference crop with a height of 0.12 m and an albedo of 0.23 (Allen, et al. 2000), to calculate bare soil evaporation (no crop transpiration and an albedo of 0.09). An example of this imperfection is shown during the first three nights of the experiment, where the equations cannot account for the nightly evaporation processes;
3. Measurement errors in the meteorological input conditions. Temperature, solar radiation, relative humidity, wind and precipitation measurements errors could be introduced by urban structures or spatial variations.

Local deviations between tensiometer measurements and water pressure head simulations (Figure 53) are most certainly caused by sensitivity of the tensiometers to temperature variations, as was mentioned before. Structural dial gauge errors were eliminated by precise dial gauge calibration.

Table 7. Evaporation experiment optimization results for potting soil

Run	**#hits**	**%**	**.SSQ**	**R^2**	**θ*r***	**θ*s***	***α***	***n***	***K_s***	***l***
	Evaporation experiment									
EVAP-A	8/8	100%	10.45	0.99	0.213	0.86	0.23	1.41	110	0.5

Inverse experiment result comparison

Before practical recommendations on the usability of the determined parameter vectors can be given, the optimization results of the outflow and evaporation experiments have to be compared. For that purpose, the optimized parameter vectors **b** and corresponding hydraulic functions of the unique 3-parameter fit inverse experiments MSO-2, MSO-3, MSO-4 and the evaporation experiment will be examined. An overview of all parameter vectors **b** and corresponding hydraulic functions is given in Appendix 11. The parameter vector **b**, which is the result of numerical optimization of the evaporation experiment is presented in Table 7. At first sight one would conclude that these optimization results differ significantly with the outflow experiment optimization results (Table 6). However, the water retention curves that follow from the parameter optimizations of both inverse experiment types show major correspondence, especially at the volumetric water content of interest between θ(h_{seep}) and θ(h=-200 cm). With respect to the final goal of the unsaturated zone model, this is an important and valuable conclusion. The most important differences between outflow and evaporation experiment optimization results are the lower value of the residual moisture content θ_r, the higher value of the bubbling pressure α, and the lower value of the pore-size distribution n in the evaporation experiment. These differences can be observed in Figure 54: the evapotranspiration experiments' water retention curve shows a more gradually volumetric soil water content decline

over increasing absolute pressure heads, with a lower residual water content at θ*r* ≈ 0.2 instead of θ*r* ≈ 0.3. The biggest differences were found in the hydraulic conductivity curves (Figure 55).

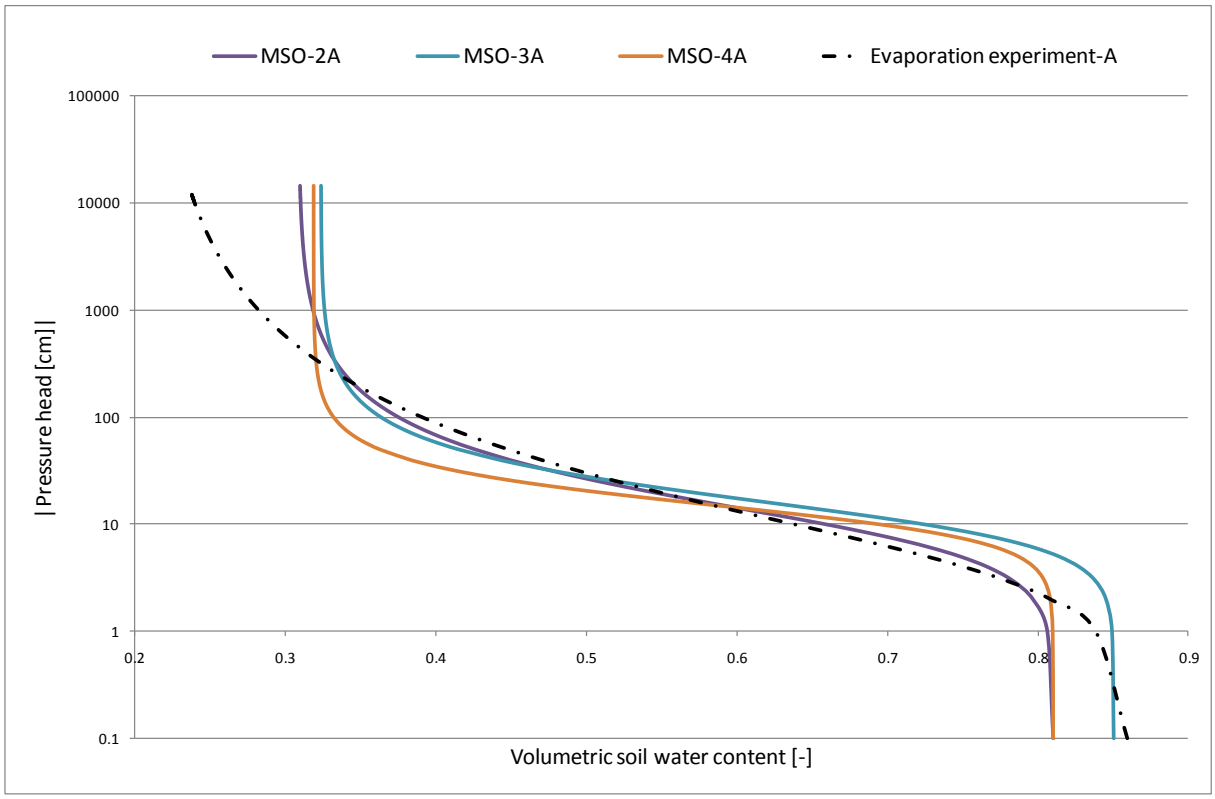

Figure 54. Optimized soil water retention curves of the unique 3-parameter fit inverse experiments

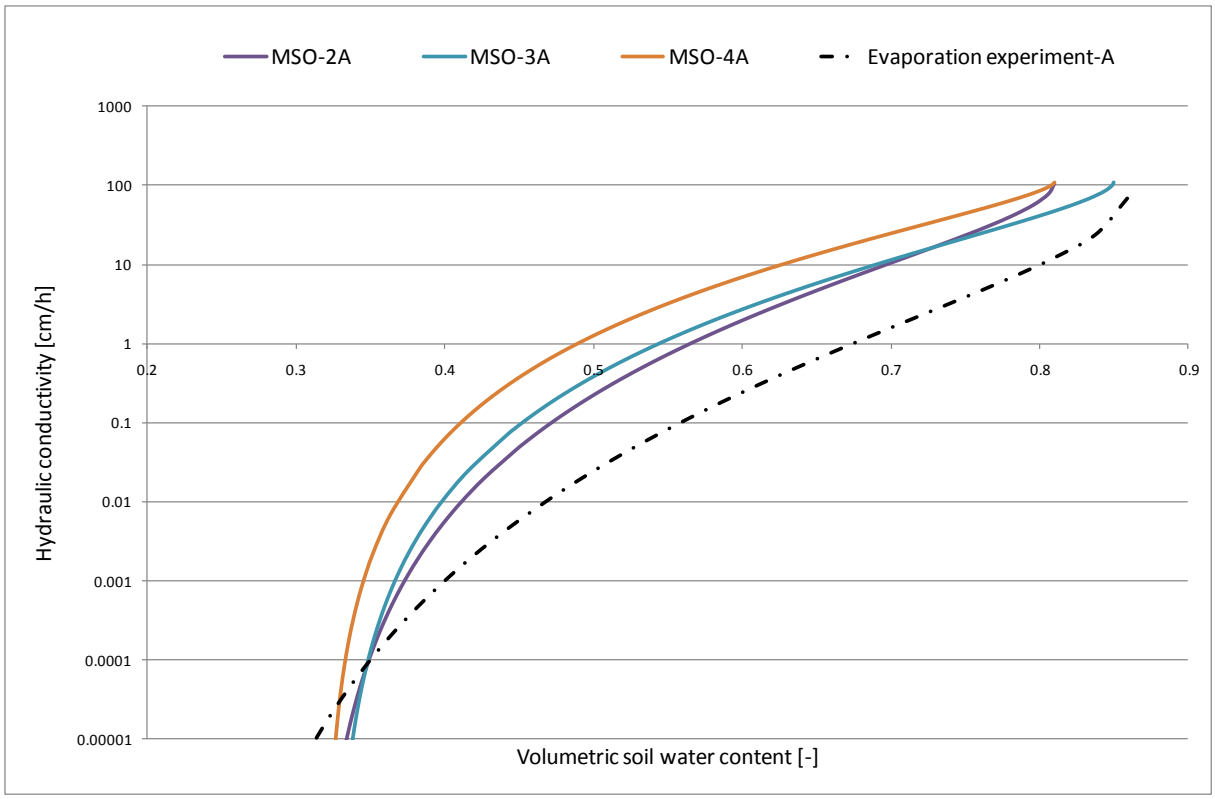

Figure 55. Optimized conductivity curves of the unique 3-parameter fit inverse experiments

Evaporation experiment optimizations result in a hydraulic conductivity curve that lies below the conductivity curves of the Multi-step outflow experiments. Hydraulic conductivity results from MSO-4A give relatively high conductivities, which corresponds to the more sandy content of this undisturbed sample. MSO-2A and MSO-3A show very similar hydraulic conductivity curves, which are positioned just in between the two other curves. Both figures illustrate that despite uniqueness, differences between optimized parameter vectors still exist: a conclusion that was found in other literature as well (Durner (b), Schultze and Zurmuhl 1999).

5.3.3.6 Parameter determination conclusions

Several inverse modelling experiments were carried out under well-defined laboratory and field conditions. The final goal of these experiments was to determine the hydraulic parameters for the soil under investigation: the highly porous and peaty potting soil, which is used for the green-roof experiments in Singapore. Inverse modelling result analyses of three main transient flow experiment types: the One-step and Multi-step outflow experiment and the continuous evaporation experiment, were structured around four topics: the total deviation between measurements and simulations (SSQ), uniqueness of the optimized parameters, and appropriateness of the soil water retention and hydraulic conductivity functions. A large and quick change of the initial boundary condition to h=-1000 cm and O-ring leakages caused ill-posedness of the inverse problem leading to non-uniqueness of the One-step outflow experiment simulations in HYDRUS-1D. Ill-posedness of the inverse problem was reduced in the Multi-step outflow experiments by changing the experimental set-up and procedures. The O-rings were replaced, the gas pressure line was stabilized using gas tanks and data logging devices were implemented in order to be able to continuously measure the outflow and water pressure heads. It was found that, unlike the One-step outflow experiments, the Multi-step outflow experiments are a good method to determine the soil hydraulic parameters for the unimodal non-hysteretic hydraulic functions of van Genuchten. Good global fits between the measured and simulated outflow characterizes a large part of the evaluated model runs. Soil heterogeneity was observed, but the final optimized parameter vectors **b** of both prepared and undisturbed samples are in line. Three out of five 3-parameter fit optimizations yielded unique inverse solutions. Allowing the saturated hydraulic conductivity K_s and the connectivity parameter l to vary, slightly decreased the overall SSQ, but resulted in a wide range of physically meaningless hydraulic conductivity parameter values. Improved flexibility of the hydraulic functions therefore, does not compensate for the loss of reality. Next to that, the more simple 3-parameter fit optimizations give accurate enough results regarding the final green roof field purpose of the parameter determination. Based on earlier recommendations for an optimal inverse experimental design (Durner (b), Schultze and Zurmuhl 1999), a continuous evaporation experiment was performed after the outflow experiments. The evaporation experiment design was based on the Wind Method, but executed under atmospheric instead of laboratory conditions. Results of the unique 3-parameter fit Multi-step outflow and inverse experiment optimizations were compared. It was found that the SSQ cannot be solely used to compare optimization results between different inverse experiments and weighing factors in the objective function have to be well-considered. Comparison of the soil water retention and hydraulic conductivity curves, which are a result of the parameter optimization process in both experiment types, was used as an alternative comparison methodology. The unique 3-parameter fit soil water retention curves show mutual correspondence, especially at the volumetric water content of interest between $\theta(h_{seep})$ and $\theta(h$=-200 cm). Plotted hydraulic conductivity curves proved to be more sensitive for differences in the optimized parameter vectors **b**. During the selection of the initially parameter

vector **b** and consecutive iterations, which will be used for further green roof modelling purposes, these results have to be taken into account. Since the optimized parameter vector **b** of the evaporation experiment has been determined under actual field conditions, this parameter set will be initially used. Good field applicability from these optimized parameters are expected. However, Figure 55 shows that one can hypothesize that the corresponding unsaturated hydraulic conductivity forms the lower boundary of the real hydraulic conductivity.

To summarize, inverse modelling of the Multi-step outflow and evaporation experiments yielded several unique hydraulic parameters for the hydraulic functions. Analysis of the optimized hydraulic functions for the potting soil illustrate that despite uniqueness, differences between optimized parameter vectors still exist. Nevertheless, the results give a good starting point for further green roof outflow simulations and greatly increased awareness and knowledge of the most important soil physics in a controlled, manageable way.

5.4 Model verification

The conversion of the conceptualization into the initial model specification will be checked in the verification part of the model cycle (Verbraeck 2003). In order to ensure that the model does what it is intended to do, we must ascertain whether the model implements the assumptions correctly (Etessami and Gilmore 2008). Model verification differs from model calibration and validation in the sense that model calibration focuses on adjusting the internal model parameter values to obtain a better fit between measurements and simulations and model validation focuses on whether the model results give a good representation of the real results. In paragraph 5.4.1 the model logics will be checked for correctness and consistency. After this, the model output will be checked in paragraph 5.4.2. Important large differences between model simulations and expected model behavior, will be addressed if necessary. The September period will be used in the verification and calibration parts of the model cycle. The December period will finally be used for independent model validation. These months were chosen because of several reasons including data reliability, data completeness, full plant vegetation and event diversity.

5.4.1 Verification of the model logics

The first part of the model verification emphasizes the logics part of the conversion process between the conceptual model and the model specification. Since the HYDRUS-1D model is an existing model for the simulation of water flow in (un)saturated porous media, dimension analysis and debugging techniques are omitted in the verification. A structured walk-through of the HYDRUS-1D manual and source code (Simunek (c), et al. 2008, Simunek (b), Sejna and van Genuchten 2005) gives sufficient confidence in the model logics. The three main components of the model conceptualization: the internal state of the unsaturated porous media, the hydrological processes and the green roof boundaries were successfully converted into a specified model with initial parameters. It is the final goal to verify whether the model specification implements the conceptual ideas correctly under certain assumptions. Because of this, the most relevant assumptions from the model conceptualization and specification are summarized here:

1. One-dimensional vertical flow can sufficiently describe the water flow in green roof media under the sub assumptions that:
    a. Roof gradients are negligibly small;
    b. Soils are homogenously distributed over space and can be characterized by a single set of soil hydraulic parameters;
2. Hydrological fluxes and runoff fluxes are homogenous in space over time;
3. Assumption 1+2: green roof discharge [L^3T^{-1}] can be calculated by multiplying the one dimensional specific discharge [LT^{-1}] with the surface area [L^2];
4. Model applicability is limited between $\theta_r \leq \theta \leq \theta_{seep}$ because of the restrictions that follow from the determination of the soil hydraulic parameters by using inverse modelling techniques;
5. Runoff time from the green roof media bottom to the tipping bucket measurement equipment is negligible;
6. No evaporation occurs on the bottom of the green roof media;
7. Interception storage is regenerated at the rate of potential transpiration;
8. No runoff occurs until the water pressure head drops below a prescribed seepage face pressure value, therefore neglecting preferential flow paths;
9. Unlike the real sedum plants, plant coverage in the model is constant over time and plants do not have internal water storage capacity.

The model logics of the specified model are considered correct under these assumptions. Discussion on the model output verification and model validation have to consider these assumptions as well.

5.4.2 Verification of the model output

The output of the specified model with the initial parameter set will be checked for the September period. Any large differences between model simulations and expected model behavior, will be addressed. This will provide potential leads for model re-specification in the model calibration phase. Overall model output performance will be verified in the output analysis. The influence of the initial condition and the discretization in time and space will be addressed in a seed independence and discretization test., respectively

Model output analysis

Model verification has the goal to ensure that the model does what it is intended to do. Here, that is to give an acceptable accurate simulation of the green roof runoff and therefore:

- Give an acceptable accurate representation of the hydrological fluxes;
- Give an acceptable accurate representation of the internal state of the green roof media.

Although the first model run of the September period finished successfully, the model generated a runoff of over 100 cm, which is almost a tenfold of the total precipitation. After having concluded that this was caused by a wrong input specification of the rainfall (in mm instead of cm), this output error was fixed and the model was successfully tested unintended under an extreme condition. Model output of the initial specification is presented in Figure 56. The model overestimates the overall runoff, but is close to the two green roof runoff measurement values. Transpiration and evaporation fluxes are nicely represented in the model simulations. One would expect that

transpiration exceeds evaporation on a highly vegetated soil media. Next to this it is hypothesized that the total simulated evapotranspiration is too low, given the runoff over prediction. Because of this, the ratio between evaporation and transpiration and the total evapotranspiration sum will be examined in the model calibration part. The two bottom graphs of Figure 56, *h(t)* and θ*(t),* show that the model correctly calculates the internal state of the green roof. The pressure and soil water content decrease over time during dry periods, and increase during rainfall. The differences of *h(t)* and θ*(t)* over the soil depth, represented by the nodes in Figure 56, are correctly calculated as well.

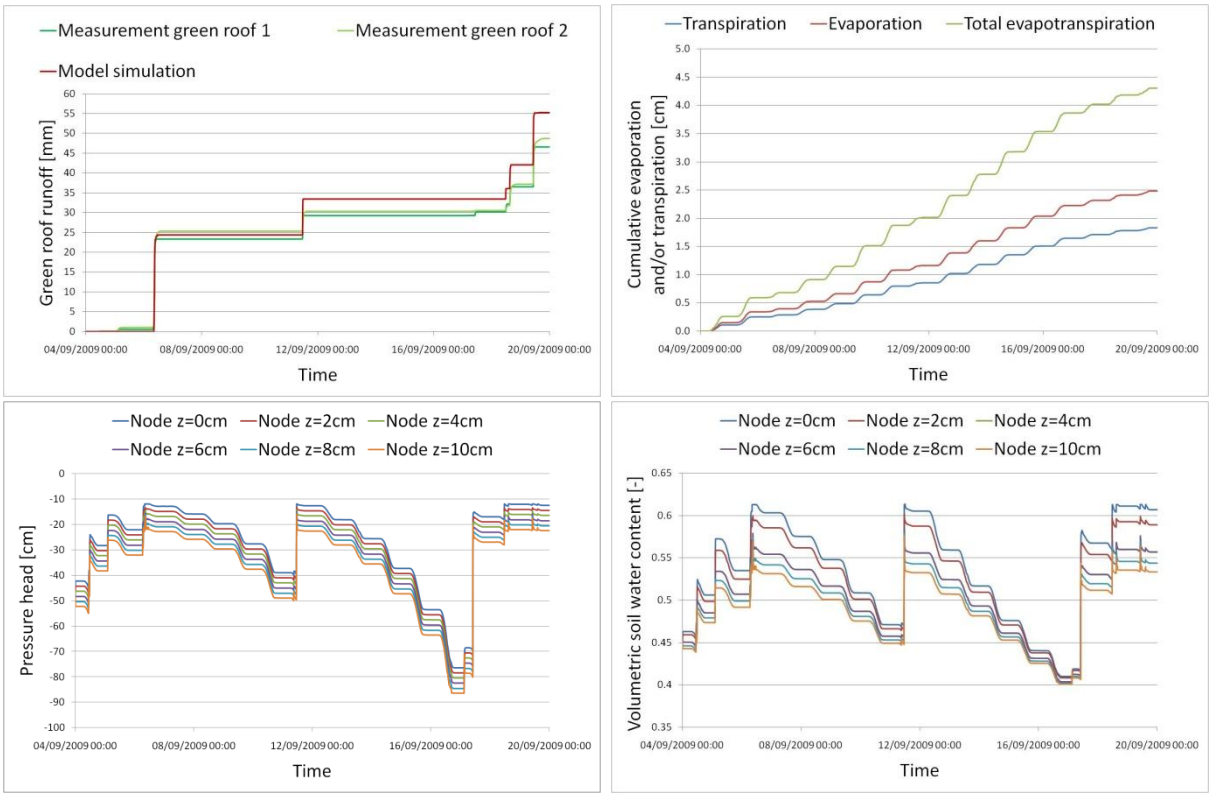

Figure 56. Model output of the initially specified model

Seed independence test

The influence of the seed on the simulation results can be verified by running the model with different seed values (Etessami and Gilmore 2008). The seed or initial value of the simulation model is specified as a volumetric water content over the soil media. Two model runs with seeds θ(t=0)=0.45 and θ(t=0)=0.55 show that the simulation results do depend on the value of the seed until the moment of saturation of the real green roof platforms (Figure 57). Because the seed is an estimated value of the internal state of the green roof platform, the model results can only be evaluated after saturation of the green roof platform and green roof model. This determines the run-in period of the model.

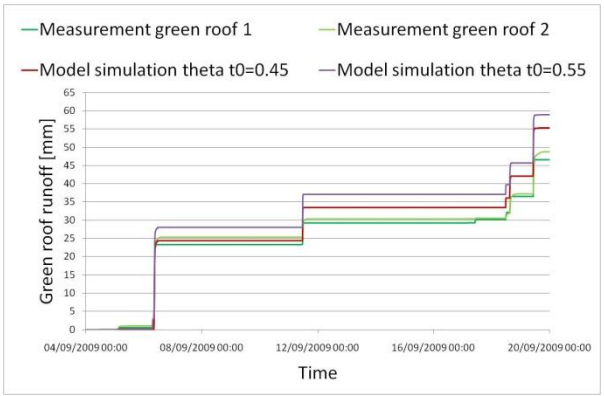

Figure 57. Seed independence test results

Discretization test

A numerical solution of Richards differential equation (Eq. 5.8) in HYDRUS is obtained by using a fully implicit finite difference scheme, which is solved iteratively with a Picard solution method (Simunek (c), et al. 2008). The model runtime and the stability and accuracy of the numerical solution were tested under several combinations of discretization in space and time. The test results are presented in Appendix 12. Based on these test results and formulated considerations, the initial discretization in space (Δx=0.12 cm) is a good balance between runtime, stability and runoff accuracy. The initial discretization in time ($\Delta t_{initial}$=0.001 min, Δt_{min}=0.0001 min and Δt_{max}=1min) gives good stability and accuracy. A smaller time step does result in unnecessary prolonged runtimes, without increased stability or accuracy. Beven (2001) suggests not to use a larger time step because the model might get instable in case of sharp wetting fronts in extreme conditions. Indeed, some numerical instability is introduced when the model is run with a large initial time step $\Delta t_{initial}$=1 min (Appendix 12).

.

5.5 Model calibration

It was shown in the verification phase of the model cycle, that the model does what it is intended to do under the initial specification and assumptions. Before the model can be used to reliably simulate green roof runoff at acceptable accuracy, it is necessary to go through a stage of model parameter calibration. Model calibration focuses on adjusting the internal model parameter values to minimize the residuals between measurements and simulations. For the green roof model in HYDRUS, the goals of the parameter calibration are to:

- Calibrate a model that gives acceptable simulation results by identifying possible changes in the parameter specification that have a positive influence on the model performance;
- Highlight the restrictions of the model performance.

It is not the goal to find one optimum parameter set or correct model specification because of the following arguments:

- The total number of model parameters is >20. A complicated optimization algorithm should be developed to automatically find the 'optimum parameter set'. This is not achievable within the available research time;
- Input and measurement data is not error-free, causing ill-posedness of the optimization;
- The concept of an optimum parameter set in hydrological modelling can be rejected. The concept of *equifinality* advocates that many parameter sets can give a reasonable good fit to measurement data (Beven 2001, p.22);
- To find an optimum parameter set is not a goal on its own.

Thus, the model performance is defined as the capability to generate model simulations that are an acceptable accurate representation of the real green roof measurements. The model calibration is performed in 3 steps:

1. Analyze the accuracy of the initial parameter specification;
2. Determine the sensitivity and feasible parameter range of the parameters;
3. Iteratively adjust the parameter specification to a final calibrated model with acceptable accuracy.

5.5.1 Calibration methodology

Assessing the accuracy of the initial parameter specification, the parameter sensitivity and the accuracy of the final calibrated parameter specification generally requires a quantitative measure of performance and/or goodness of fit (Beven 2001). A well performing model of the green roof runoff at platform scale gives an acceptable accurate representation of:

1. Cumulative runoff magnitude over the entire observed period;
2. Cumulative runoff on event scale;
3. Peak discharge on event scale;
4. Peak discharge timing on event scale;
5. Base flow conservation on event scale.

These requirements are translated into so called *variables*. Variables differ from the *performance indicators*, in the sense that they are not a measure of the green roof performance, only of the model performance relative to a measured value of the same variable. The newly introduced variables are:

1. q_{tot} [L]. This variable is a measure for cumulative runoff over the entire observed period;
2. q_c [L]. This variable is a measure for cumulative runoff on event scale;
3. q_{peak} [LT^{-1}]. This variable is a measure for the peak discharge on event scale;
4. tt_{peak} [T]. This variable is a measure for the time to peak relative to the rainfall peak;
5. q_{bf180} [L]. This variable is a measure of the cumulative base flow runoff from the time of the last recorded rainfall until 180min after the last recorded rainfall.

Besides these variables, the modelling efficiency E_{NS} [-] of Nash and Sutcliffe will be used as a goodness of fit measure of the model on event scale (Beven 2001, Krause, Boyle and Base 2005). This goodness of fit measure is defined as:

$$E_{NS} = 1 - \frac{\sigma_\varepsilon^2}{\sigma_0^2} = 1 - \frac{\sum_{t=1}^{T}(y_j^* - y_j)^2}{\sum_{t=1}^{T}(y_j^* - \widehat{y_j^*})^2} \qquad \text{[Eq. 5.32]}$$

where σ_ε^2 is the sum of the absolute squared differences between the measured (y_j^*) and simulated (y_j) values. σ_0^2 is the variance of the measured values during the simulation period. Here $\hat{y}_j^*$ is the average of the measured values. The efficiency has the value 1 for a perfect model fit. When the efficiency value is 0, in other words $\sigma_\varepsilon^2 = \sigma_0^2$, the model is said not to be better than a one-parameter model that gives a prediction of the mean of the measurements for all time steps (Beven 2001, p.225). Negative efficiency values can give indications for a non-behavioural model.

Last but not least, the model performance will be analyzed qualitatively too, by inspection of individual event hydrographs. This is done because quantitative measures of performance or goodness of fit cannot catch indications for all hydrograph characteristics and irregularities in the model output. The calibration methodology thus focuses on a combination of quantitative and qualitative performance measures. These performance measures will be used to asses the accuracy of the initial model specification, the sensitivity of changes in parameters to changes in the model performance and to asses the accuracy of the final model specification.

5.5.2 Accuracy of the initial parameter specification

According to the introduced calibration methodology, the accuracy of the model simulations under initial parameter specification will be examined. The parameter values of the initial specification are presented in Appendix 13. The model performance discussion is divided into two main parts:

1. Quantitative measure of performance, which includes an analysis of:
    a. performance variables q_{tot} , q_c , q_{peak} , tt_{peak} , q_{bf180} ;
    b. modelling efficiency E_{NS};
2. Qualitative measure of performance, which includes individual event hydrograph inspection.

Quantitative measure of performance: performance variables

The measured cumulative green roof runoff equals 45.99 mm for green roof platform 1 (GR1) and 47.66 mm for green roof platform 2 (GR2). The simulated value for q_{tot} equals 58.60 mm. These values are the sum of the runoff between the end of the run-in period (September 5, 23:59) and September 19, 23:59. It can be concluded that the model over predicts the runoff over the entire period with 20-30%. Based on an evaluation of the cumulative runoff performance variable q_c on event scale, the over prediction of the runoff is a structural imperfection of the initially specified model. This observation holds for all events except for the September 17, 03:06 event (no runoff), the September 17, 10:11 event (small preferential flow amounts), and the September 19, 14:31 event (base flow from previous rainfall). The under prediction of the time to peak is expressed in the values for the tt_{peak} variable, which are too small for almost every event. Premature soil saturation in the model simulations also cause the value q_{peak} to be too high, as compared to the measurements of both green roof platforms, except for the September 06 event, where the simulated runoff peak is in range with the measurements. The differences between measured and simulated values of the last two variables are again a results of the lack of the model to give a good description of the real green roof behaviour. Because this error is a structural one, it could be hypothesized that this is caused by an under estimation of the outgoing hydrological fluxes and not by a too small representation of the available storage, because the residual soil water content is not reached during the entire runtime of the model simulations. In absence of surface runoff, the under estimated hydrological fluxes are equal to the sum of interception, evaporation and transpiration. Last, the simulated values for the variable q_{bf180} are significantly lower than the measured values, which indicates the lack of the initially specified model to correctly represent the falling limb of the green roof hydrograph.

Quantitative measure of performance: modelling efficiency

A second quantitative measure of performance that has been examined for the September, 2009 period is the Nash-Sutcliffe modelling efficiency. Measured and simulated runoff values per time step were used for y_j^* and y_j respectively. According to this model efficiency, the goodness of fit is perfect for the September 17, 03:06 event (no runoff) and the September 19, 14:31 event (no runoff for GR1). For the 31.21 mm rainfall event of September 06, the goodness of fit equals 0.83, which is a good fit. However, for almost all other events, the value for E_{NS} approaches zero or is even negative. This implies, that the model performance is equal or worse than a one-parameter model that gives a prediction of the mean of the observations for all time steps (Beven 2001, p.225). A disadvantage of the Nash-Sutcliffe modelling efficiency is that it gives an overestimation of the model performance during peak flow and an underestimation of the model performance during low flow conditions (Krause, Boyle and Base 2005). Just as for the optimization algorithm that was used before (Eq. 5.31),

this has to do with the fact that the differences between measured and simulated values are squared. This is one of the reasons to incorporated other performance measures in the model calibration as well. Nevertheless, it is the aim to increase the modelling efficiency during the model calibration process.

Qualitative measure of performance: hydrograph inspection

Hydrographs of the eight events between September 06 and September 19 were inspected. The results of this inspection yield a qualitative measure of performance. Hydrographs from the September 06 and September 19, 10:15 events are presented in Figure 58. All other September event hydrographs can be found in Appendix 13. An advantage of a qualitative hydrograph analysis is that one can directly observe the differences between the green roof measurements and the model simulation. The mutual differences between both green roofs can be observed as well.

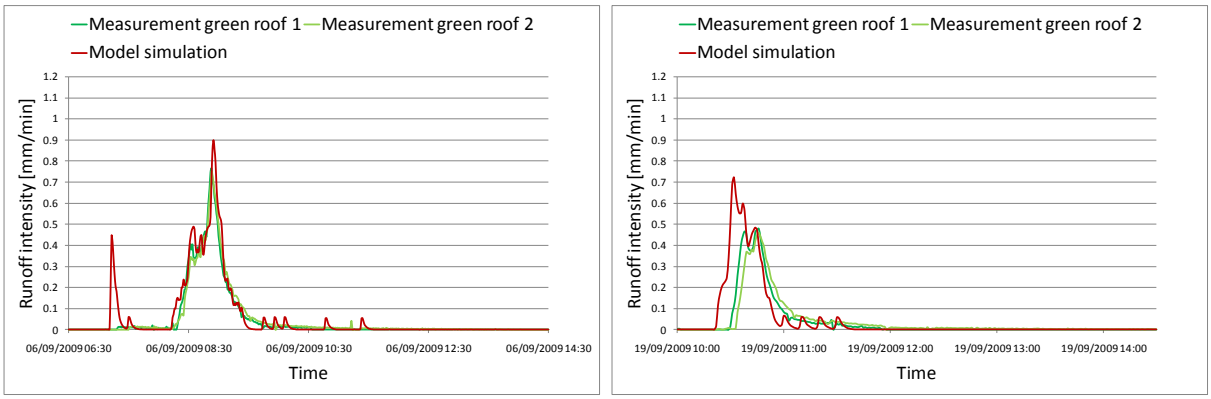

Figure 58. Measured and simulated hydrographs for September 06 and September 19.

The results of the hydrograph analysis corresponds to the performance variables and modelling efficiency results. The overall response of the model simulations is reasonably good, but runoff starts too early, peaks are too high, the time to peak is too low and a precise representation of the base flow is lacking. Two additional points of interest for the model calibration follow from the hydrograph inspection. First, the hydrograph peak over prediction is not only caused by premature soil saturation, as can be observed in the September 19 hydrograph in Figure 58, but is over predicted as well when the measured and simulated runoff peaks coincide, as can be observed in the September 06 hydrograph in Figure 58. This is caused by a too large unsaturated conductivity *K* at the specified seepage face h_{seep} of -12 cm. Second, small peaks can be observed in most of the September hydrographs. This is an artefact of the 1-minute rainfall input interval, which shows the limitations of the use of discrete rainfall specification in hydrological models that focus on effects with small timescales.

Conclusions on the accuracy of the initial parameter specification

The conclusions of the performance measure analysis for the initially specified model are:

1. The model simulations under predict the sum of the outgoing “evaporative” fluxes (evaporation, transpiration and interception);
2. The model simulations over predict the runoff peak;
3. The model simulations under predict the green roof base flow;
4. Discrete rainfall input specification reduces the accuracy of the model simulations.

5.5.3 Sensitivity analysis

In the previous paragraph, the accuracy of the green roof simulations were compared with green roof experiment measurements. Based on the model requirements that were listed in paragraph 5.5 and the quantitative and qualitative measures of performance analysis conclusions in paragraph 5.5.2, three areas of model improvement are suggested:

1. Calibrate model parameters to reduce the under prediction of the outgoing hydrological fluxes;
2. Calibrate model parameters to reduce the over prediction of the runoff peaks;
3. Calibrate model parameters to reduce the under prediction of the green roof base flow.

In order to achieve the suggested model improvements as efficiently as possible, a basic sensitivity analysis will be carried out. Sensitivity analysis aims to quantify the changes in the values of certain parameters to changes in the model performance measures. The sensitivity can be expressed as:

$$S_i = \frac{dZ}{dx_i} \qquad \text{[Eq. 5.33]}$$

where S_i is the sensitivity index with respect to parameter i with value x_i , and Z is the value of a model performance measure. Here, those are the introduced variables and the Nash-Sutcliffe modelling efficiency. The relative change in Z will be evaluated as the value x_i for each of the evaluated parameters is changed in succession with 10 percent (dx_i = 10%), while keeping all other parameter values at their initially specified value. It is the final goal of the sensitivity analysis to highlight the parameters for which the model performance is more sensitive when they change. Calibration of the right sensitive parameter should lead to efficient model improvements, while obtaining the final parameter specification. The parameters that were tested for sensitivity can be divided into four classes:

1. Soil hydraulic parameters;
2. Soil depth and seepage face;
3. Feddes' root water uptake parameters
4. Meteorological parameters.

Model performance measure sensitivity will be evaluated for four out of the eight rainfall-runoff events in the September period: September 06, September 11, September 18, 14:53 and September 19, 10:15.

Sensitivity for the soil hydraulic parameters

Four unique soil hydraulic parameter sets were independently determined with inverse modelling techniques in paragraph 5.3.3. The hydraulic parameter set from the evaporation experiment was used in the initial parameter specification for the model verification and calibration. In order to reduce the calibration complexity, the sensitivity of the parameters for the soil water retention function (θ_r, θ_s , α, n) will not be evaluated here. As a starting point for the sensitivity analysis, the change in model performance for the three remaining unique hydraulic parameter sets were evaluated. These are the multi-step outflow parameter sets MSO-2A, MSO-3A and MSO-4A. The relatively small improvement in q_{tot} (0.04-1.02% less cumulative runoff) and some small reductions in

q_c do not compensate for the reduced model performance that is expressed in the remaining performance variable values of all three parameters sets. On event scale, q_{peak} increases 14-57%, tt_{peak} reduces with 1-2 minutes and q_{bf180} reduces with 46-74% (Appendix 13). The modelling efficiency reduces as well for all four events and all three parameter sets. The reduced model performance for the parameter sets that were determined with the multi-step outflow experiments can all be assigned to an over prediction of the unsaturated hydraulic conductivity, as can be observed in Figure 55. Based on this evaluation, the initially specified soil hydraulic parameters of the evaporation experiment are adopted. The sensitivity of the model performance to changes in K_s and l were addressed in the sensitivity analysis, because q_{peak} is over predicted in the model with the evaporation experiment parameters as well. The sensitivity index S_i is low with respect to q_{tot}, q_c and tt_{peak} for both parameters. The performance variable q_{peak} is almost three times more sensitive to changes in K_s ($0.1 \leq S_i \leq 0.53$) than to changes in l ($-0.03 \leq S_i \leq -0.16$). Changes in K_s also lead to a more efficient improvement in E_{NS} and q_{bf180}. The sensitivity of these three performance measures is only higher with respect to changes in the soil depth and the seepage face, but since the feasible parameter ranges are very limited for those two parameters, calibration of K_s and l are more suitable to improve the simulation accuracy of runoff peaks and base flow.

Sensitivity for the soil depth and seepage face

Next, the sensitivity of the model performance measures to a 10% change in the soil depth z and seepage face h_{seep} were evaluated. The performance variables q_{tot} and q_c for the September 06 event cannot be evaluated because the 10% increase in both parameter values increased the run-in period up to the September 11 event. Based on the sensitivity indexes for the three remaining events ($-0.01 \leq S_i \leq -0.02$), one can conclude that the cumulative runoff is not sensitive with respect to changes in the soil depth and the seepage face. This result justifies the hypothesis that the runoff over prediction by the model is caused by an underestimation of the outgoing hydrological fluxes and not by a too small representation of the available storage. The sensitivity index for q_{peak} is relatively high for changes in the soil depth ($-0.28 \leq S_i \leq -0.72$) and the seepage face ($0.46 \leq S_i \leq 2.09$). The sensitivity indexes for q_{bf180} and the modelling efficiency E_{NS} are high as well, which is a result of the high sensitivity index for q_{peak}. Despite the high sensitivity of most model performance measures with respect to changes in the soil depth and seepage face, the small feasible parameter range for both parameters limit the calibration possibilities for these parameters to a large extent.

Sensitivity for the root water uptake parameters

Sensitivity for the root water uptake parameters cannot be tested with a standard 10% parameter change. The initially specified values for *p2H, p2L* and *p3* are -300 cm, -1000 cm and -2000 cm respectively. Since the simulated water pressure head range lies between -12 cm and +/- -80 cm, the actual transpiration rate is never limited during the runtime of the model simulation ($\alpha(h)=1$ in Eq. 5.29). A 10% change in the values for *p2H, p2L* and *p3* does not change this. The values for *p2H, p2L* and *p3* were changed to -30 cm, -40 cm and -60 cm respectively, in order to reduce the actual root water uptake because of water stress. While having almost no influence on the value for q_c after a short dry weather period, the cumulative runoff q_c is increased after a long dry weather period, like during the September 11 event (+6.1%). Changes in the root water uptake parameters hardly change the other performance variables and modelling efficiency. The very conditional sensitivity and the lack of knowledge about the distribution between evaporation and transpiration reduce the calibration possibilities for the root water uptake parameters.

Sensitivity for the meteorological parameters

Last, the sensitivity of the model performance measures to a 10% change in three meteorological parameters; *SCF,* α_r and *a* were evaluated. The sensitivity indexes of all performance measures were low with respect to changes in the interception constant *a*. The performance variables q_{tot} and q_c are medium sensitive for changes in the values for the soil cover fraction and albedo. q_{tot} changes -0.15% and 0.2% for a 1% increase in the values for *SCF* and α_r respectively. Sensitivity indexes for q_c vary between $-0.30 \leq S_i \leq 0.00$ and $0.01 \leq S_i \leq 0.42$ with respect to a change in the *SCF* and α_r parameter values. The peak discharge variable is conditionally sensitive to changes in *SCF* and α_r. Only for those cases where the model simulations over predict q_{peak} because of too early saturation during high rainfall intensities, as is the case for the September 11 event, will changes in these parameters effectively reduce the peak discharge errors with respect to the measurements. The influence of a change in *SCF* or α_r does not affect the time to peak and hardly changes the base flow. The modelling efficiency is medium sensitive to a change in *SCF* and α_r. The combination of medium sensitivity to the performance variables q_{tot} , q_c , q_{peak} and goodness of fit measure E_{NS} with the relatively large feasible parameter range creates calibration possibilities to increase the hydrological fluxes and reduce the overall over prediction of the runoff.

Conclusion

The influence of a standard change in several model parameters to a change in the five performance variables and the Nash-Sutcliffe modelling efficiency were expressed in terms of the sensitivity index S_i . The potential calibration properties of a certain parameter are a function of the sensitivity index S_i with respect to a performance measure and the feasible parameter range. Table 8 shows the calibration opportunities that follow from the sensitivity analysis. Green cells show good calibration potential, orange cells show medium calibration potential and red cells show limited or no calibration potential. The possibilities to influence the performance variable tt_{peak} might be underestimated because the simulation output values are only available on a 1-minute time interval.

Table 8. Summary of the sensitivity analysis results

	K_s		*I*		*z*		h_{seep}		*RWU*		*SCF*		α_r		*a*	
	S_i	Parameter range	S_i	Parameter range	S_i	Parameter range	S_i	Parameter range	S_i	Parameter range	S_i	Parameter range	S_i	Parameter range	S_i	Parameter range
q_{tot}	- -	+	- -	++	- -	- -	- -	- -	+/-	+	+	+	+	+	- -	+/-
q_c	- -	+	- -	++	- -	- -	- -	- -	+/-	+	+	+	+	+	- -	+/-
E_{ns} *GR1*	+/-	+	-	++	+	- -	+ +	- -	-	+	+	+	+	+	- -	+/-
E_{ns} *GR2*	+/-	+	-	++	+	- -	+ +	- -	-	+	+	+	+	+	- -	+/-
q_{peak}	+	+	+/-	++	++	- -	+ +	- -	-	+	+/-	+	+/-	+	- -	+/-
tt_{peak}	- -	+	- -	++	-	- -	-	- -	- -	+	- -	+	- -	+	- -	+/-
q_{bf180}	+/-	+	+/-	++	+	- -	+	- -	-	+	-	+	-	+	- -	+/-

5.5.4 Obtaining the final parameter specification

The accuracy of the model simulations under the initial parameter specification were addressed in paragraph 5.5.2. Several opportunities to efficiently improve the model simulation performance were identified in the sensitivity analysis in paragraph 5.5.3. Based on these two previous steps, the HYDRUS model can now be improved by means of model calibration. This was done by iteratively changing the parameter values while monitoring the performance measures of the three suggested model improvement areas, which were:

1. Calibrate model parameters to reduce the under prediction of the outgoing hydrological fluxes;
2. Calibrate model parameters to reduce the over prediction of the runoff peaks;
3. Calibrate model parameters to reduce the under prediction of the green roof base flow.

First, the main parameter changes will be described per improvement area. Second, the accuracy of the iteratively adjusted final parameter specification will be presented. The report structure of the second part is based on the structure that was used in the accuracy analysis of the initial parameter specification in paragraph 5.5.2.

5.5.4.1 Determination of the final parameter specification

The final parameter specification has been established by manually adjusting the model parameters, while keeping track of the model performance measure changes. This iterative process is time consuming, since the response surface is very complex for a multiple parameter model. Normally, parameter calibration is based on an optimization of the complex multiple parameter response surface with an algorithm. It was said that because of the available research time and the idea of equifinality, there is no aim to strive for an optimum parameter set. Rather, it is the goal to calibrate a model that gives acceptable simulations by identifying possible changes in the parameter specification that have a positive influence on the model performance and to highlight the restrictions of the model.

Reduction of the under prediction of the outgoing hydrological fluxes

The under prediction of the outgoing hydrological fluxes can be efficiently reduced by changing the meteorological parameters *SCF* and α_r. After that, the less sensitive root water uptake parameters are adjusted. Changes in the outgoing hydrological fluxes were evaluated by comparison of the performance variables q_{tot} and q_c between green roof measurements and simulations. In the final parameter set *SCF* has been changed from 0.43 to 0.95, which basically means that the vegetation fraction of the soil cover is 95%. Green roof soil cover photos in Appendix 3, also visualize that a 95% *SCF* is physically more correct. This increases the transpiration fluxes in the simulations. The albedo value α_r has been lowered to 0.16 in order to increase the potential evaporation and transpiration fluxes. Feddes root water uptake parameters were iteratively lowered to *p2H*=-40 cm, *p2L*=-60 cm and *p3*=-100 cm. This parameter change reduces the actual transpiration between -40 cm and -100 cm: a process that depends on the potential transpiration flux when the soil dries up (Feddes, et al. 1988). Finally, a bug was found in the HYDRUS code with respect to the interception parameter *a*. The interception equation (Eq. 5.17) is based on a 1-day time step, while the time step of the model is 1-minute. Till so far interception was underestimated by a factor 24*60=1440. This also explains the low sensitivity indexes for all performance measures with respect to changes in this parameter,

as was found in the sensitivity analysis. The 1.8 mm maximum interception can be obtained by multiplying *a* in Eq. 5.17 by a factor 1440. According to Eq. 5.21 this yields a value *a*=401 for a *SCF* of 0.95 (*LAI*=6.47).

Reduction of the over prediction of the runoff peaks and under prediction of the base flow
The sensitivity analysis showed that the over prediction of the runoff peaks and the under prediction of the base flow can be changed most efficiently by changing the parameter values of the saturated hydraulic conductivity K_s and the empirical pore-connectivity parameter *l*. Either lowering the parameter value for K_s or increasing *l* can potentially lead to the desired performance measure changes. Other studies show that setting K_s as a matching point in the hydraulic conductivity function (Eq. 5.16) indeed leads to an overestimation of the unsaturated hydraulic conductivity of about one order of magnitude on average (Schaap and Leij 2000), because K_s is sensitive to macropore flow, whereas unsaturated flow occurs in the soil matrix (Schaap and Leij 2000, p.844). The choice was made to change nothing but the empirical pore-connectivity parameter *l*, in order not to reject the measurement results from the hydraulic conductivity experiments (Appendix 7). Peak and base flow performance were found to be most optimal when *l* was changed to a value of 2.85 instead of 0.5. This change resulted in a hydraulic conductivity *K* of 1 cm/min at h_{seep}= -12 cm. An increase in *l* can be understood as a correction factor that causes a steeper drop in hydraulic conductivity than lower values for *l* (Schaap and Leij 2000). Earlier studies found that *l* varied between -8.73 and 371 (Yates, et al. 1992, Schaap and Leij 2000), but hydraulic conductivity data for peat or potting soils were not found in these articles. Nevertheless, these results show that neither K_s nor *l* can be interpreted as a completely physically meaningful parameter. The seepage face and soil depth were not changed in order to stick to their reliably measured values and to reduce calibration complexity. Besides this, the changes in *l* already increase the performance to an acceptable level of accuracy.

5.5.4.2 Accuracy of the final parameter specification

Again, the discussion on the accuracy of the final parameter specification will be divided into two main parts:

1. Quantitative measure of performance which includes an analysis of:
    a. performance variables q_{tot} , q_c , q_{peak} , tt_{peak} , q_{bf180} ;
    b. modelling efficiency E_{NS};
2. Qualitative measure of performance which includes individual event hydrograph inspection.

Quantitative measure of performance: performance variables
The cumulative simulated runoff over the entire simulation period between September 5, 23:59 and September 20, 23:59 equals 52.03 mm. The structural over prediction of the runoff is reduced from 20-30% under the initial specification to 9-13% under the final parameter specification (Figure 59).
The structural over prediction of the event based cumulative runoff q_c is reduced as well. Still, a structural runoff over prediction can be observed when a runoff event follows relatively short after another runoff event. Even under extreme parameterization, the model is not able to regenerate water storage potential as quickly as observed in the measurements.

Under prediction of the hydrological fluxes within one day after another runoff event might be caused by the following aspects:

1. Swelling and shrinking characteristics of the soil;
2. Evaporation during night (illustrated in the September 19, 10:15 event);
3. Temporary water storage in the sedum leaf pores.

All of these aspects cannot be incorporated into the model. An over prediction of the transpiration and evaporation fluxes does compensate for the short term under prediction of the real outgoing fluxes on the long term. Despite the fact that this increases simulation accuracy on the long term, the model overestimates the runoff by 1-2 mm when runoff events follow-up within one day. The over prediction of the peak discharge variable q_{peak} is almost totally gone under the final parameter specification. The change in *I* also took away a large part of the discrete rainfall specification effects.

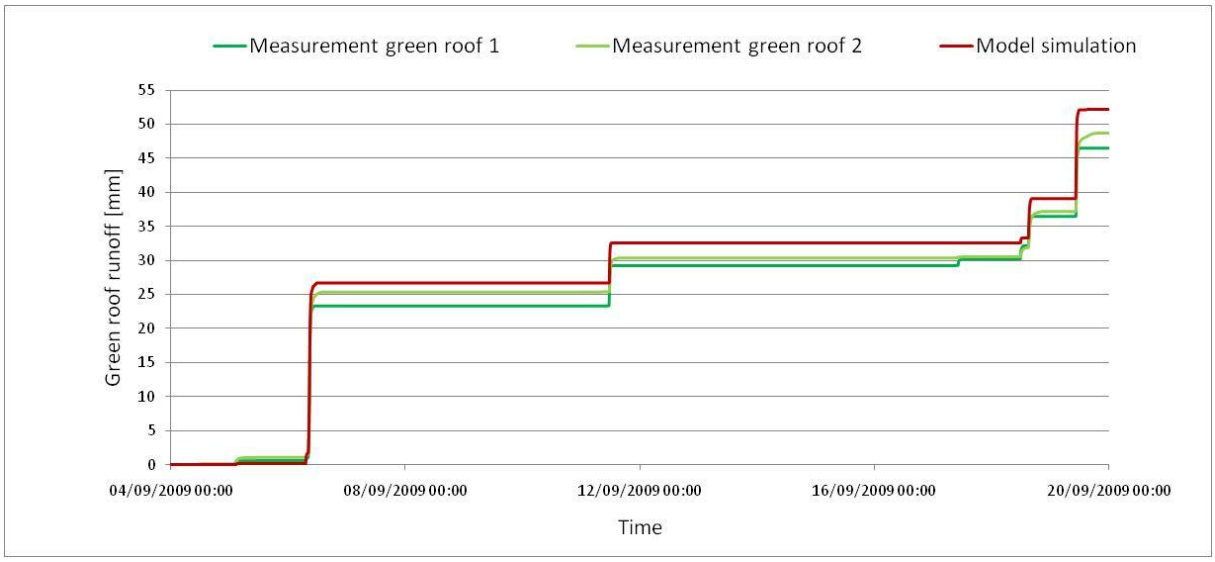

Figure 59. Cumulative measured vs. simulated runoff q_{tot} for the September 2009 period.

On top of that, where the model failed to give a good description of the base flow performance variable under the initial specification, this has now become one of the strongest points of the simulation. The simulated values for q_{bf180} are in harmony with the measurements from green roof 1. The clogging or delaying mechanism in green roof platform 2, which was hypothesized in paragraph 4.4.6 can now be accepted. Last, the under estimated values for the performance variable tt_{peak} have been corrected because of runoff and peak discharge simulation improvements.

Quantitative measure of performance: modelling efficiency

The Nash-Sutcliffe modelling efficiency values under the initial parameter specification were only good for the September 06 event and small or negative for all other events, which implied that the model performance was equal or worse than a one-parameter model that gives a prediction of the mean of the observations for all time steps (Beven 2001, p.225). The values for E_{NS} have improved significantly under the final parameter specification. With respect to the measurements from green roof 1, the modelling efficiencies for runoff events are all positive ($0.5 \leq E_{NS} \leq 0.88$). E_{ns} values with respect to green roof 2 measurements are positive for all events with $q_c \geq 1$ mm ($0.07 \leq E_{NS} \leq 0.92$). E_{NS} is negative for the two very small runoff events, but under prediction of the model performance

during small runoff events was already indicated as a weak point regarding this performance measure. To resume: a great overall improvement of the modelling efficiency has been achieved.

Qualitative measure of performance: hydrograph inspection

Hydrographs of the eight events between September 06 and September 20 were inspected. Now, the improvement of the model simulations with respect to the initial parameter specification can be visualized. Hydrographs from the September 06, September 18, 14:53 and September 19, 10:15 events are presented in Figure 60. The left side of this figure shows the hydrographs under initial parameter specification and the right graphs under final parameter specification. All other September event hydrographs can be found in Appendix 13. Quantitative and qualitative performance measure results are consistent here in the sense that the model is improved on all three model improvement areas. First, premature soil saturation is reduced as can be observed in all three events in Figure 60.

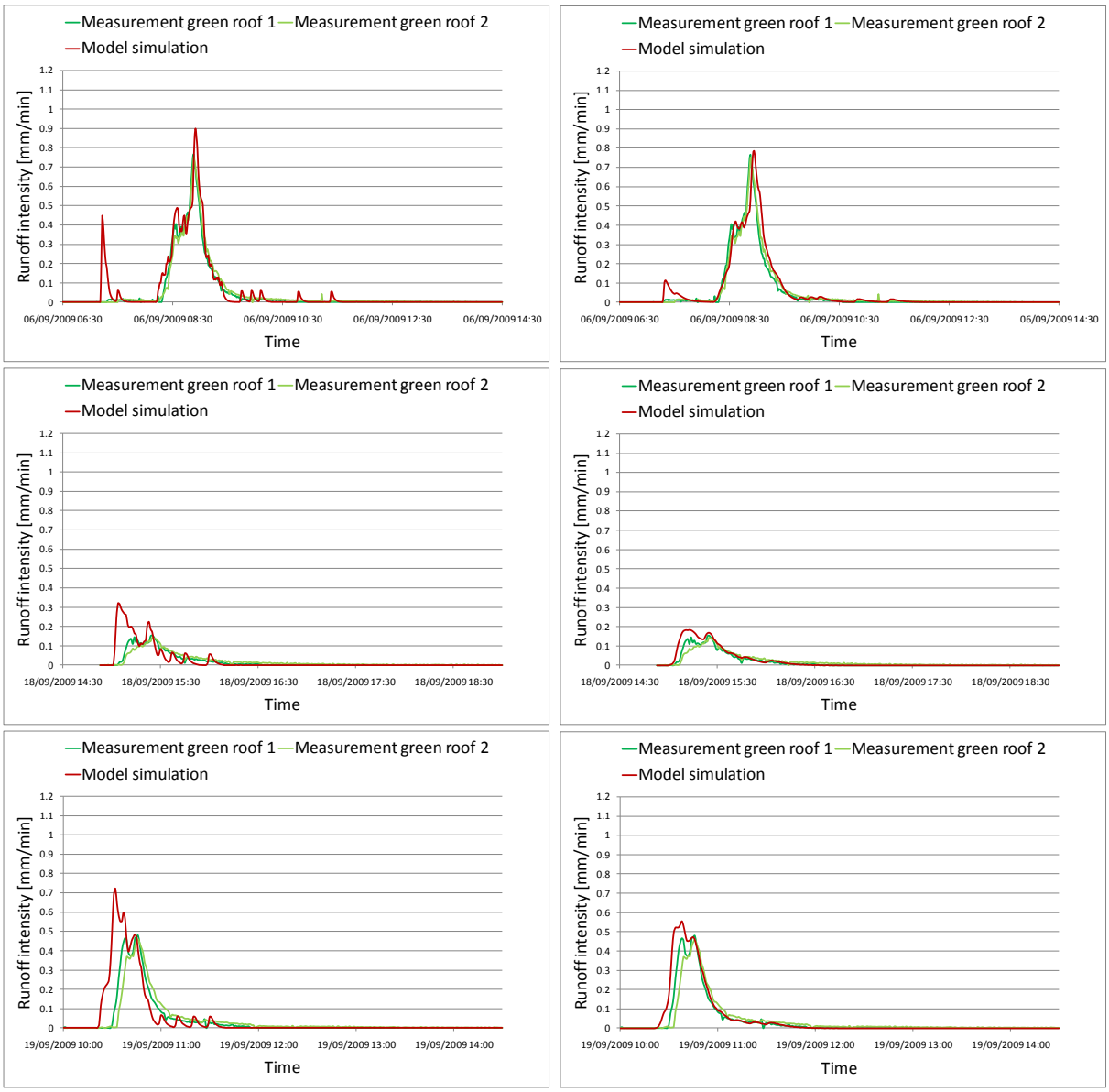

Figure 60. Model simulation result differences between the initial and final parameter specification.

Second, the structural over prediction of the runoff peaks has almost disappeared under the final specification. Other improvements are visualized as well: the small peaks that are an artefact of the rainfall discretization over time are smoothened out. Last, an accurate description of the falling limb of the model simulation hydrographs increases the usability of the model to predict base flow conservation of green roofs. The hydrographs also illustrate the main shortcoming of the model: an over prediction of the green roof runoff when events quickly follow-up.

Conclusions

The accuracy of the model simulations have improved significantly under the final parameter specification. The under prediction of the outgoing hydrological fluxes has been reduced to a large extent. Next, the initial over prediction of the runoff peak, the under prediction of the green roof base flow and the effects of the discrete rainfall input specification were eliminated up to a large extent. The main goal of the model calibration is achieved because identified changes in the parameter specification increased the model accuracy to an acceptable level for all performance measures. The main restriction of the model performance is an over prediction of the green roof runoff when events quickly follow-up. An over prediction of the transpiration and evaporation fluxes does compensate for the short term under prediction of the real outgoing fluxes on the long term.

5.6 Model validation

Model validation is defined here as the task of demonstrating that the model gives a reasonable representation of the real system measurements (Etessami and Gilmore 2008). A reasonably well performing model of the green roof runoff at platform scale gives an acceptable accurate representation of the cumulative runoff, peak discharge, time to peak and base flow measurements. Common approaches for model validation are expert knowledge, theoretical results/analysis and real system measurements (Etessami and Gilmore 2008). Because green roof measurements at platform scale are available, the validation approach is based on comparing the model simulation output with real system measurements. The model validation differs from the model calibration in the sense that the parameters will not be adjusted anymore. It is the goal to test the model performance outside the calibration period in paragraph 5.6.1. The validation period runs from December 01 until December 31. This chapter and the small-scale analysis Part will be wrapped up with conclusions and a discussion on the applicability and restrictions of the green roof rainfall-runoff model in paragraph 5.6.2.

5.6.1 Validation of the December period output values

The output from the model simulations will be compared to real system measurements of the green roof platforms. The model validation report part is, according to the structure that was used in the model calibration, divided into two main parts:

1. Quantitative measure of performance which includes an analysis of:
    a. performance variables q_{tot} , q_c , q_{peak} , tt_{peak} , q_{bf180} ;
    b. modelling efficiency E_{NS};
2. Qualitative measure of performance which includes individual event hydrograph inspection.

Quantitative measure of performance: performance variables

The measured cumulative green roof runoff equals 104.58 mm for green roof platform 1 and 127.13 mm for green roof platform 2. The simulated value for q_{tot} equals 147.99 mm. These values are the sum of the runoff between the end of the run-in period (December 02, 23:59) and December 31, 23:59. The over prediction of the runoff is 42 and 16% for GR1 and GR2 respectively.

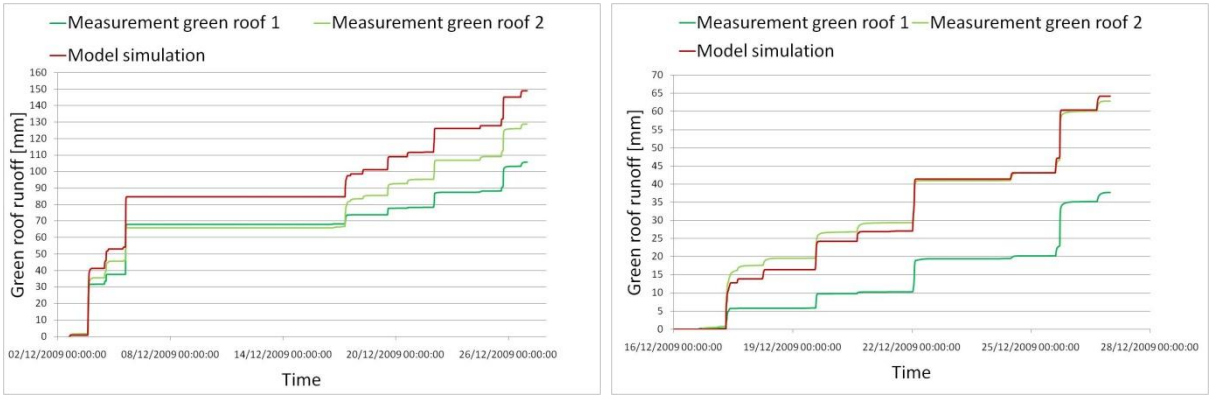

Figure 61. Cumulative measured vs. simulated runoff q_{tot} for the December 2009 period.

The 16% over prediction of the simulated cumulative runoff q_{tot} compared to the measurements from GR 2 is mainly caused by a tipping bucket measurement error during the December 05 event. Measured cumulative runoff from this platform is about 11 mm too low during this particular event. Cumulative runoff of the model simulation and GR1 coincide from December 16 onwards as can be observed from the right graph in Figure 61. Large differences between the simulated runoff and measured runoff from GR1, especially after December 16, are visible as well. The most likely cause for these structural differences are data recording errors on GR1 in December (paragraph 4.4.6). In order to assess the simulation accuracy at individual event scale, performance variables of four single events were analyzed (Table 9). Again, the model simulations over predict q_c when runoff events quickly follow-up. The measured values q_c from GR2 exceed the values for GR1. An over prediction of the value for q_c is visible for the model simulations, but is in line with the measurements from GR2. The simulated values for the peak discharge and the time to peak are accurate. The negative values of the tt_{peak} variable in the measurements of the December 13 event, indicate slight time synchronization differences between rainfall tipping bucket and the runoff balance logging applications. This time lag is decently corrected in the model simulations and the representation of the base flow conservation in the simulations is in range with the measurements. Again, better correspondence is found with the measurements from platform 2.

Quantitative measure of performance: modelling efficiency

Based on the high Nash-Sutcliffe modelling efficiency values ($0.68 \leq E_{NS} \leq 0.86$) from the four analyzed events in December, one can conclude that the simulations can be classified as behavioural with respect to the green roof platform 2 measurements. Some non-behavioural aspects seem to emerge when one reads the Nash-Sutcliffe modelling efficiency values for the same four events ($-3.44 \leq E_{NS} \leq 0.79$) with regard to green roof platform 1. It is more likely though that the data recording errors on green roof platform 1 cause the difference between the simulations and measurements. Nevertheless some non-behavioural aspects always occur in a model, as was already concluded in the model calibration and validation.

Table 9. Individual event values for the quantitative performance measures.

		Measurements GR1	Measurements GR2	Final specification validation model
Overall	q_{tot}	104.6	127.1	148.0
03/12 13:50 P=42.16mm ADWP=0.9d Wet	q_c	30.56	33.92	40.40
	E_{ns} *GR1*			0.78
	E_{ns} *GR2*			0.84
	q_{peak}	0.67	0.62	0.74
	tt_{peak}	-00:02	-00:02	00:02
	q_{bf180}	0.00	0.56	0.25
17/12 7:15 P=16.94 mm ADWP=0.24d Wet	q_c	5.40	15.32	12.82
	E_{ns} *GR1*			-3.44
	E_{ns} *GR2*			0.68
	q_{peak}	0.19	0.61	0.63
	tt_{peak}	00:06	00:03	00:06
	q_{bf180}	0.00	1.13	0.26

		Measurements GR1	Measurements GR2	Final specification validation model
Overall	q_{tot}	104.6	127.1	148.0
19/12 13:02 P=11.21mm ADWP=0.36d Medium wet	q_c	3.94	6.96	7.82
	E_{ns} *GR1*			0.25
	E_{ns} *GR2*			0.88
	q_{peak}	0.16	0.20	0.24
	tt_{peak}	00:49	00:50	00:52
	q_{bf180}	0.00	0.60	0.15
25/12 14:35 P=22.18mm* ADWP=1.29d Medium wet	q_c	14.57	16.48	17.29
	E_{ns} *GR1*			0.79
	E_{ns} *GR2*			0.86
	q_{peak}	0.91	1.00	0.99
	tt_{peak}	00:04	00:04	00:05
	q_{bf180}	2.46	2.72	1.66

*: Event is a combination of two consecutive events

Qualitative measure of performance: hydrograph inspection

Measured and simulated runoff intensities over time are graphically presented in Figure 62. Overall, the simulated hydrographs are in range with the measurements.

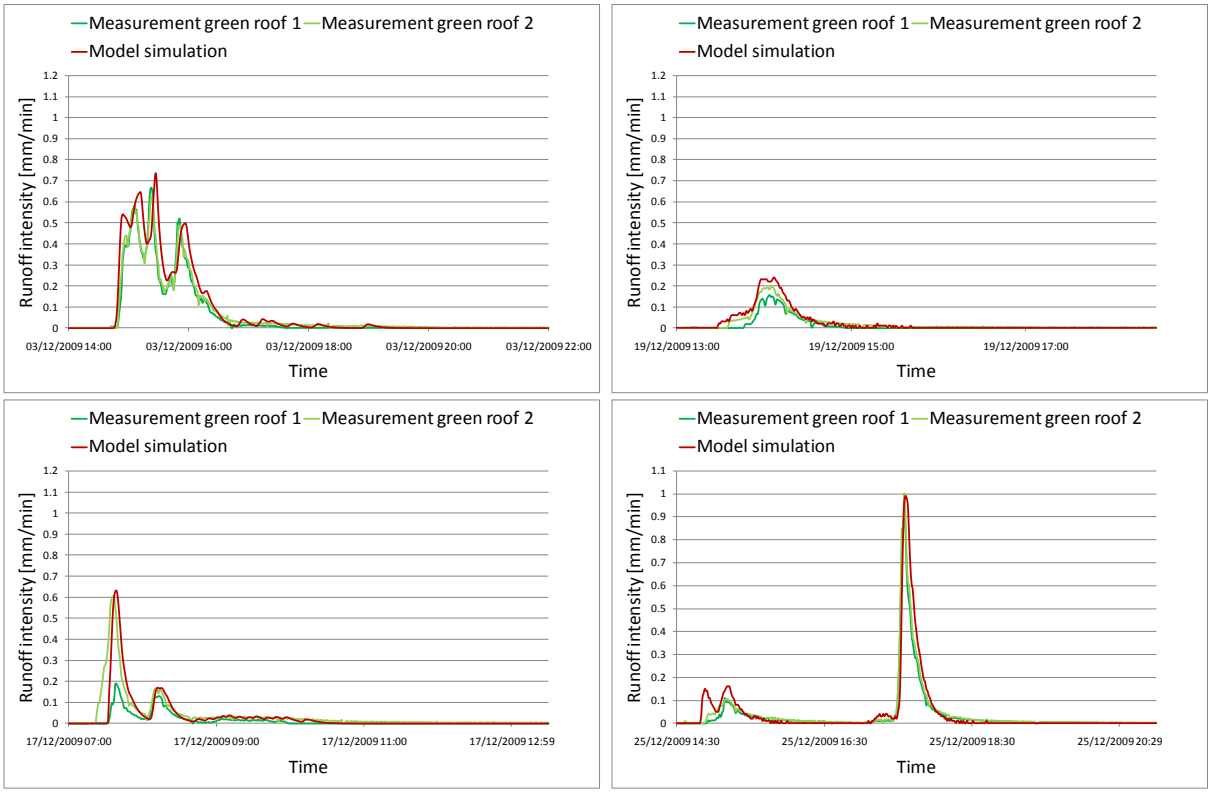

Figure 62. Measured and simulated hydrographs from the model validation period.

Simulated values for the performance measures do better correspond with the measured hydrographs of green roof platform 2 while the simulated hydrographs showed a better fit with the measured hydrographs from platform 1 in the calibration period of September. As was reported in paragraph 4.4.6, data recording errors induced by a tilted tipping bucket are almost certainly the most important cause of the poor fit between model results and green roof 1 measurement results in the December period. Clear examples of better correspondence with measurements from platform 2 are visualized in the December 17 and December 19 hydrographs in Figure 62. Next, structural delays between all local peaks of the simulated and measured runoff in the December 03 event hydrograph give indications for a four minute time difference between the rainfall tipping bucket and the runoff balance logging application. This is positive feedback though, because it means that the model performance might be underestimated. No other points, than the ones which were already mentioned in the quantitative performance measure analysis, arise from the hydrograph inspection.

Discussion on the predictive power of the HYDRUS model vs. simple regression

Model simulation results of twelve rainfall-runoff events in September, 2009 and December, 2009 have shown that the model gives a reasonable representation of the real system measurements. Based on hydrograph inspection, the values of the performance variables q_{tot} , q_c , q_{peak} , tt_{peak} and q_{bf180} as well as the values of the modelling efficiency E_{ns} , it can be concluded that the HYDRUS model gives an acceptable accurate representation of the cumulative runoff, peak discharge, time to peak and base flow measurements. Figure 63 also shows that the physically based HYDRUS-1D model can better predict the green roof retention performance than the simple regression equations that were used in Chapter 4. Ideally, model predicted retention performance values are on the line y=x in Figure 63. Although there are only twelve rainfall-runoff events tested with the HYDRUS-1D model, both graphs show that the retention performance of green roofs cannot be described by simple regression where the retention is expressed as a linear (retention=f(P)) or logarithmic (retention=f(ADWP)) equation. HYDRUS model predicted retention performance values have a better fit with the measured retention performance values of green roof 2. Still, the predictive power of the HYDRUS model is much larger on both platforms compared to the simple regression equations. This means we can adopt the hypothesis of paragraph 5.1: *"The physically based HYDRUS-1D model can better predict the green roof rainfall-runoff performance than the simple regression equations that were used in Chapter 4".* It would be interesting to compare model predictions of the HYDRUS model with model predictions of other runoff generation models (for all four performance indicators and more rainfall events). Regarding the available time, this is a recommendation for future research.

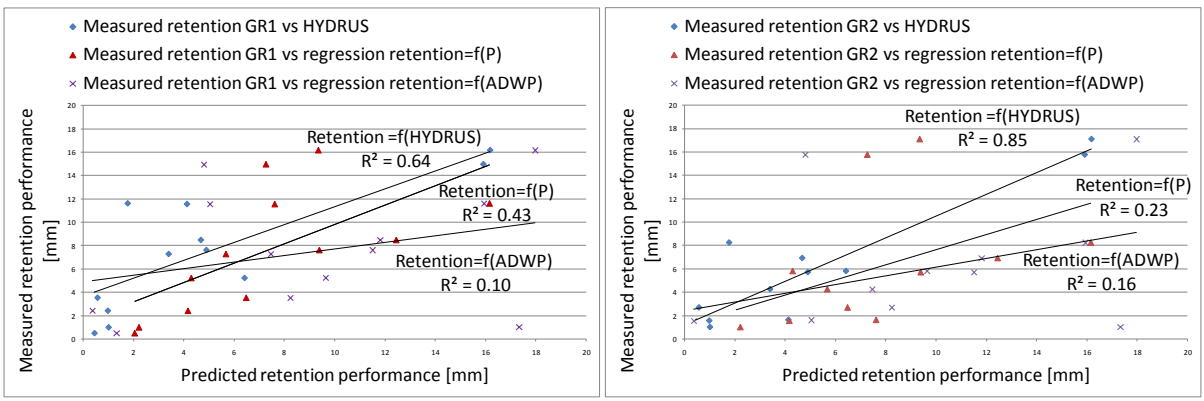

Figure 63. Predictive power of the HYDRUS model vs. simple regression equations

5.6.2 Conclusions on the applicability and restrictions of the green roof rainfall-runoff model

This chapter started with a description of the theoretical and practical goals behind the setup of a modelling approach for the simulation of green roof rainfall-runoff. A model cycle was introduced and has been followed step by step. A simplified conceptualization of the real green roof system was first introduced. Three main components were included: an internal state, hydrological processes and green roof system boundaries. This concept has been specified in the second step of the model cycle. The internal state of the green roof model over time is described by the Richards equation and the non-hysteretic unimodal pore-size model of van Genuchten. Special interests went out to the specification of the soil hydraulic parameters for the hydraulic functions. Four unique optimized parameter vectors were determined using inverse modelling of transient flow experiments. One and multi-step experiments were performed in the lab and a continuous evaporation experiment was performed under field conditions. Despite uniqueness of four determined parameter vectors, mutual differences were found, especially with respect to the hydraulic conductivity function *K(h)*. Results from the optimized soil water retention functions θ*(h)* showed a high level of correspondence.

The conversion of the conceptualization into the initial model specification was checked by verification of the model logics and output. First, all model assumptions from the previous model steps were summarized. An acceptable accurate description of the hydrological fluxes and the internal state of the green roof media under the initial parameter specification gave enough trust to proceed to the model calibration. Identification of parameter changes that can positively influence the model performance was the main goal of the iterative model calibration process. Possible model limitations were highlighted. The idea of one optimum parameter set was rejected because of time constraints, the idea of equifinality and ill-posedness of the measurements. Efficient opportunities to improve the model performance, with respect to the model performance under the initial parameter specification, were identified with a sensitivity analysis and an established feasible range for every parameter. An evaluation of the model performance under the finally calibrated parameterization yielded several positive results. The green roof model is able to give accurate simulations of the green roof runoff over time, the peak discharge, the time to peak and the base flow on event scale in the calibration period of September. The cumulative runoff simulations also closely follow the measured values, but one structural restriction of the model performance has been found. Model simulations tend to over predict the green roof runoff when events quickly follow-up. An over prediction of the transpiration and evaporation fluxes does compensate for the short term under prediction of the real outgoing fluxes on the long term.

The model validation results of the December 2009 period were in line with the calibration results from the September period of the same year. Overall, the model output gives a good representation of the real green roof measurements. Hence, the established green roof model in HYDRUS-1D meets both modelling goals. First it provided a better understanding of the hydrological processes and the soil physics in a green roof media. Second, the introduced model concept can serve as an accurate tool to generate green roof runoff under several meteorological conditions at (sub)catchment-scale. More research is suggested in the swelling and shrinking characteristics of the soil media, evapotranspiration dynamics during day and night and sedum leaf water storage. The outcome of this research can contribute to a better understanding why the present model over predicts the green roof runoff when events quickly follow-up and can finally lead to improved model results.

Part 3 Large-scale green roof analysis

Figure 64. Rendered photo of green roof implementation at the Sunset Way subcatchment

Part 3 presents an assessment of the effects of large-scale green roof implementation on the rainfall-runoff in Singapore. A subcatchment of the Western Catchment that discharges into the Sungei Ulu Pandan canal will be used as a case study. A quantification of the combined hydrological effects of green roof implementation within this demarcated area is initiated by the interests of SDWA and the PUB. Those interests were introduced in chapter 1 and chapter 3 of this report. The goals of this research Part that are derived from those interests are:

1. Quantify the combined hydrological effects of large-scale green roof implementation in the Sunset Way subcatchment;
2. Assess the contribution large-scale green roof implementation can make within Singapore's ABC Waters Programme;
3. Identify generic recommendations for the implementation of green roofs in tropical urbanized catchments.

In order to achieve these goals, a detailed one-dimensional routing model has been developed for the simulation of subcatchment-wide green roof implementation. The contribution of large-scale green roof implementation on the rainfall-runoff will be explored by scenario analysis under extreme and normal meteorological conditions. In the end, conclusions from this Part will help to improve decision making regarding the implementation of extensive green roofs within sustainable stormwater drainage system designs.

Chapter 6 presents a methodology and an analysis of large-scale green roof implementation in the Sunset Way subcatchment in Singapore. The remaining subquestions of the research will be answered based on the analysis results. Chapter 7 includes the overall conclusions and recommendations of the thesis research.

6 Singapore case study large-scale green roof analysis

6.1 Introduction

This chapter presents a quantitative assessment of the effects of large-scale green roof implementation in the Sunset Way subcatchment in Singapore. Paragraph 6.2 describes the methodology of the analysis. The presented scaled-up simulation approach for green roofs is innovative in the field of urban water management because of its high level of distribution and the integration of the physically based green roof model output within the applied routing model at subcatchment-scale. The effects of large-scale green roof implementation will be evaluated based on a scenario analysis. Here, a base case scenario representing the existing situation, will be compared to a green roof scenario with maximum potential green roof coverage. Within the available time of the research, the effects of green roofs will be determined under two types of meteorological conditions that are relevant to urban water management in Singapore:

1. Extreme (design) meteorological conditions;
2. Average meteorological conditions.

Hypothesized effects of green roofs during these meteorological conditions are derived from Singapore's ABC Waters Programme and will be used as the research hypotheses for further large-scale green roof analyses in this chapter. Hypothesized effects of green roofs in Singapore are:

1. Peak discharge and water level reduction and detention during extreme meteorological conditions;
2. Non-natural water level variation reduction during average meteorological conditions.

All analysis results will be presented in paragraph 6.3. The influence of model assumptions and practical implications of the obtained analysis results for the water management strategy in Singapore and tropical urbanized areas in general, will be discussed in paragraph 6.4.

6.2 Methodology

This paragraph consists of a number of subparagraphs. The contents of these subparagraphs give a description of the study area, the different coverage scenarios that will be analyzed, the model schematization process in SOBEK and the meteorological test conditions for the model simulations.

6.2.1 Case-study area description

At coordinates $1^0$19'22.33"N and $103^0$46'12.67"O the case-study area, from now on referred to as Sunset Way subcatchment, is located on the eastern part of the main Western Catchment in Singapore. The Sunset Way subcatchment is part of the Upper Pandan catchment (Figure 65). Having only one discharge point into the Sungei Ulu Pandan canal, this subcatchment is a well demarcated study area. Just like the rest of the Upper Pandan catchment, the Sunset Way subcatchment land use is characterized by a mix of paved zones including buildings, roads, parking lots, and unpaved zones such as parks and gardens (PUB Singapore (b) 2007). Besides this, a commercial area with shops and several food courts is located within the subcatchment. The residential buildings in the area all belong to Singapore's Housing & Development Board. HDB's extensive green roof pilot projects are an extra reason why this area has been selected for investigation. Since 84% of all residential

buildings in Singapore are HDB owned, these typical residential areas offer a great potential for extensive green roof implementation.

Available information from the PUB

Geographic information about land use, large drains and building footprints were obtained from the PUB. A detailed description of the drainage and sewer system are HDB owned, confidential and therefore not available for study purposes. Based on a discussion with the Catchment and Waterways Department on March 03, 2010, critical information about the study area has been obtained (Appendix 14). Maps of the building footprint, contour lines, subcatchment demarcation and main drainage system were collected. Drainage and sewer system are separated in Singapore. Excessive rainwater in the case study area is collected in the drainage system and routed to one outflow canal (for dimensions: see Appendix 15) that discharges into the Sungei Ulu Pandan canal.

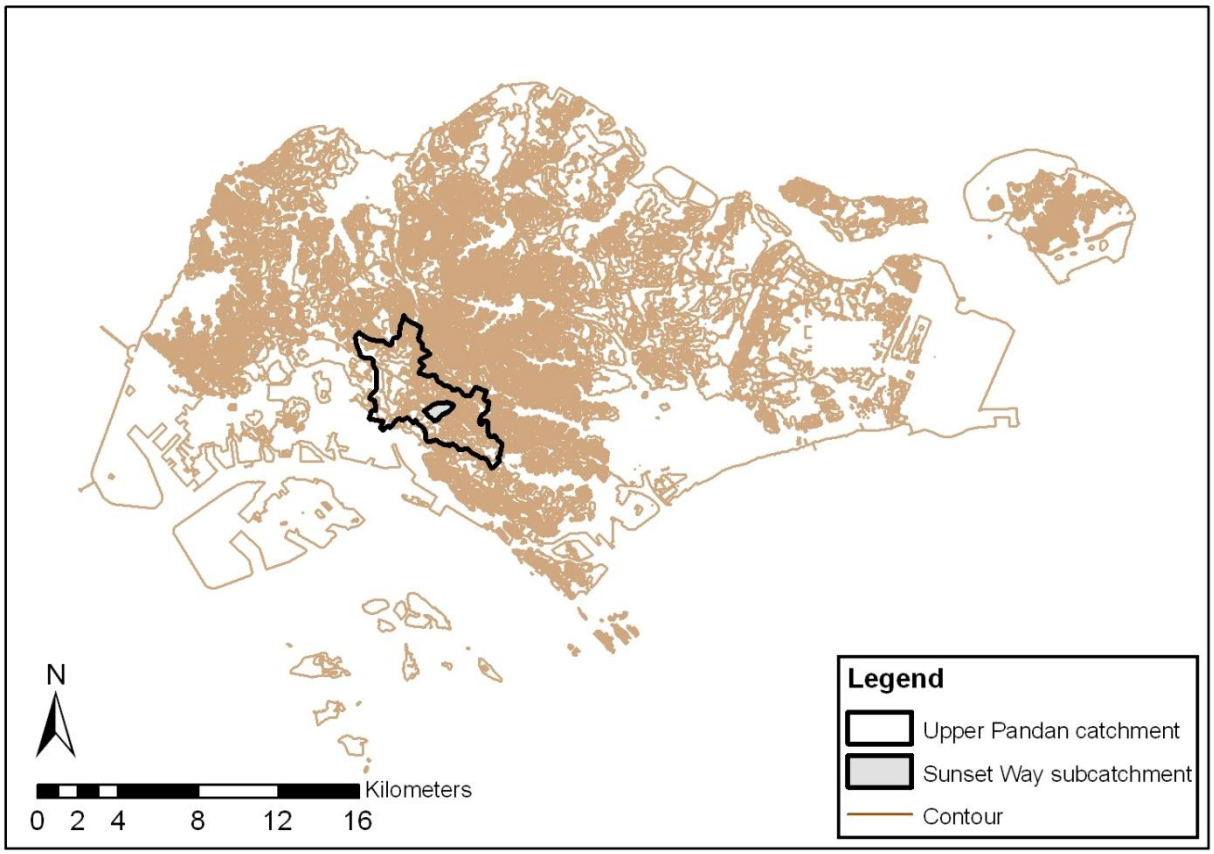

Figure 65. Location of the Upper Pandan catchment and the Sunset Way subcatchment.

Available information from fieldwork

An excessive two week field work in the area has been carried out to map all missing, but relevant characteristics of the subcatchment. The fieldwork strategy aimed to map the elevation distribution over the area, the catchment demarcation and the entire drainage system. Additional insight into the drainage principles of this area were obtained by visual inspection and discussions with local contractors. Gathered information from the fieldwork has been used during the implementation phase of the subcatchment model at Deltares. Some critical observations from the fieldwork are presented in Appendix 15. A conceptual representation of the drainage area of the Sunset Way subcatchment has been made (Figure 66). This representation is based on the available information

from the PUB and the fieldwork. The final subcatchment demarcation has been determined. For further research purposes the drainage area is assumed to be 9.4 ha and has been split up into five different types of land use. Those land use types are: buildings, roads, permeable pavement, other paved areas and parks and gardens. Table 10 summarizes the surface areas per land use type for the entire subcatchment. All roof areas from buildings in the subcatchment sum up to a total of 1.76 ha, which means that roofs cover 18.8% of the total subcatchment surface area. All rooftops in the area are flat and assumed to be available for extensive roof greening. Since the average surface area gradient (1:100) is larger than the design requirements for small and medium drain bed slopes (1:200 – 1:300), drop structures are very common hydraulic structures in the area. All areas in Figure 66, which are not coloured, fall outside the subcatchment's demarcation and do not discharge into the main outflow canal of the area.

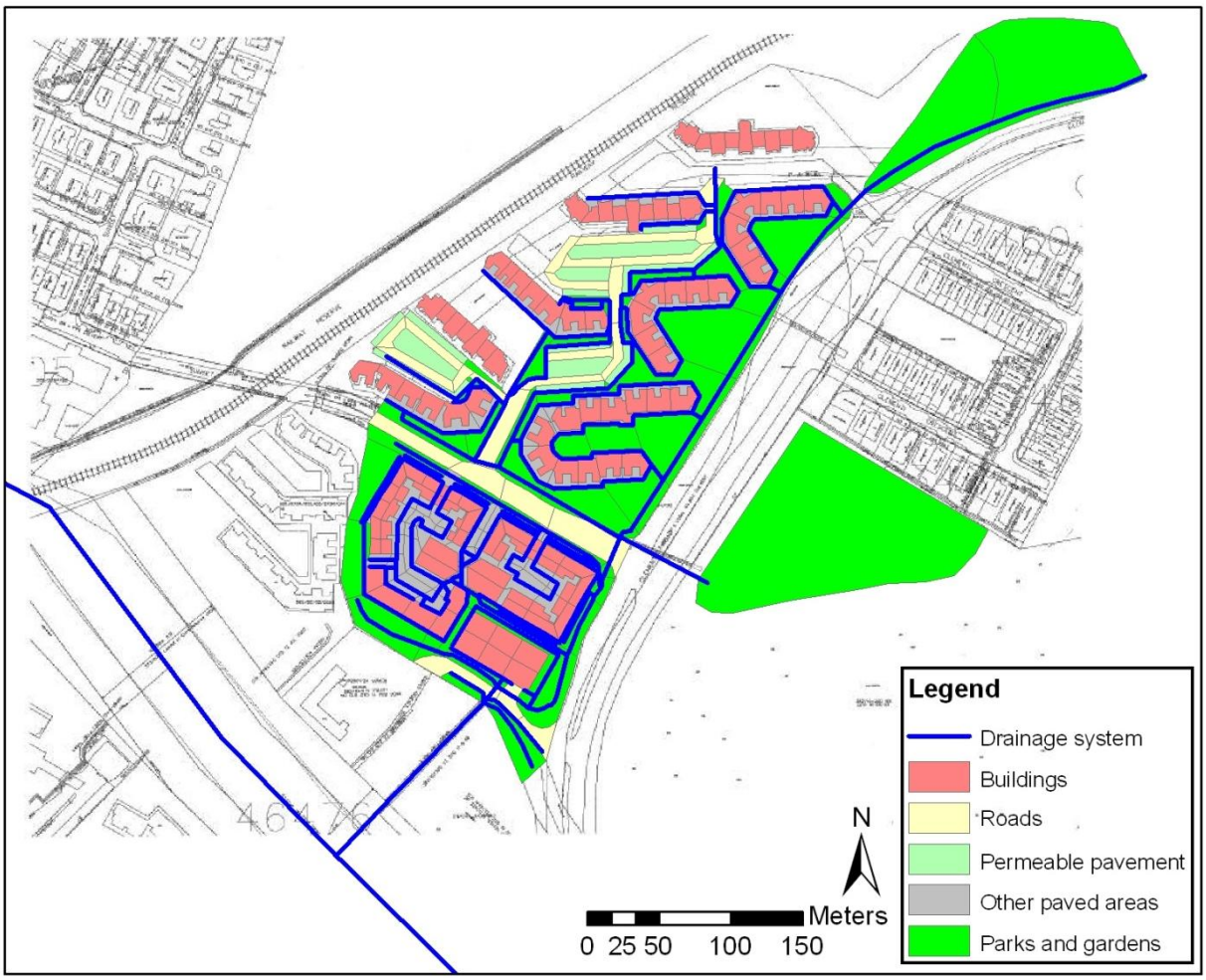

Figure 66. Conceptual representation of the Sunset Way subcatchment.

Table 10. Summary of surface areas per land use type.

Land use type	Surface area	Percentage
Buildings (roof area)	1.76 ha	18.80%
Roads	0.89 ha	9.51%
Permeable pavement	0.44 ha	4.70%
Other paved areas	1.26 ha	13.46%
Parks and gardens	5.01 ha	53.53%
Total area	9.36 ha	100%

6.2.2 Green roof coverage scenarios

Two coverage scenarios are used in the analysis of large-scale green roof implementation on the rainfall-runoff within the Sunset Way subcatchment. The current situation will be represented by a base case scenario. Here 0% of the total roof area will used for roof greening. A 100% extensive green roof implementation will be represented in the green roof scenario. Fragmented green roof scenarios with 0-100% coverage are recommended for green roof analyses at an even larger scale, but are not evaluated within this research. Instead, obtaining a good first impression of green roof potential at a larger than experiment-scale is the main objective here.

6.2.3 Model schematization in SOBEK-1D

Based on the conceptualized representation of the Sunset Way subcatchment (Figure 66), a model was built in SOBEK (Deltares 2009) by Deltares (Vergroesen 2010). This model combines the rainfall-runoff (RR) and the one-dimensional flow (1DFLOW) modules of the software program and has been specifically designed for the aim of this research. The RR module acts as a pre-processor for the 1DFLOW module and features a representation of the hydrological processes and surface runoff delays on various types of paved and unpaved areas. The 1DFLOW module features a representation of the canal hydrodynamics and computes the water levels and flows within the drainage system.

Building the drainage system network

The model representation of the subcatchment's drainage system in SOBEK consists of two main network components:

1. Nodes that represent the rainfall-runoff processes on paved and unpaved surface areas;
2. Nodes that represent the hydrodynamic processes in the drainage system network.

For modelling purposes, the total drainage area of the subcatchment has been subdivided according to the information about the spatial distribution of the different land use types (Figure 66). For all five normal land use types, the runoff that flows into the drainage system network is calculated according to the standard RR module in SOBEK. Buildings, roads and other paved areas are represented by a paved area node (red square in Figure 67) with a 1 mm water storage reservoir. When rainfall occurs on paved area's, inflow to the drainage system is initiated when the storage reservoir is filled. Storage on paved areas is regenerated in the model by evaporation. Permeable pavement, parks and gardens are represented by an unpaved area node (green square in Figure 67). Unpaved nodes are schematized using two storage reservoirs: a storage reservoir on the surface and a storage reservoir in the ground. When the rainfall intensity exceeds the infiltration capacity, the remaining water is stored on the surface. When the surface storage is exceeded, inflow to the drainage system is initiated. Drainage from the groundwater reservoir to the drainage system will occur as the groundwater level is higher than the open water level. A full description of the water balance principles of the SOBEK RR module can be found in the SOBEK manual (Deltares 2009).

Hydrodynamic processes in the drainage system network are schematized with the standard 1DFLOW module node package. The schematized drainage system (Figure 68) consists of a distributed network of connection nodes, branches, manholes, pipes and boundary nodes. The runoff from all (un)paved areas are collected in this drainage system network and the 1DFLOW module calculates the water levels and flow velocities in the canal system.

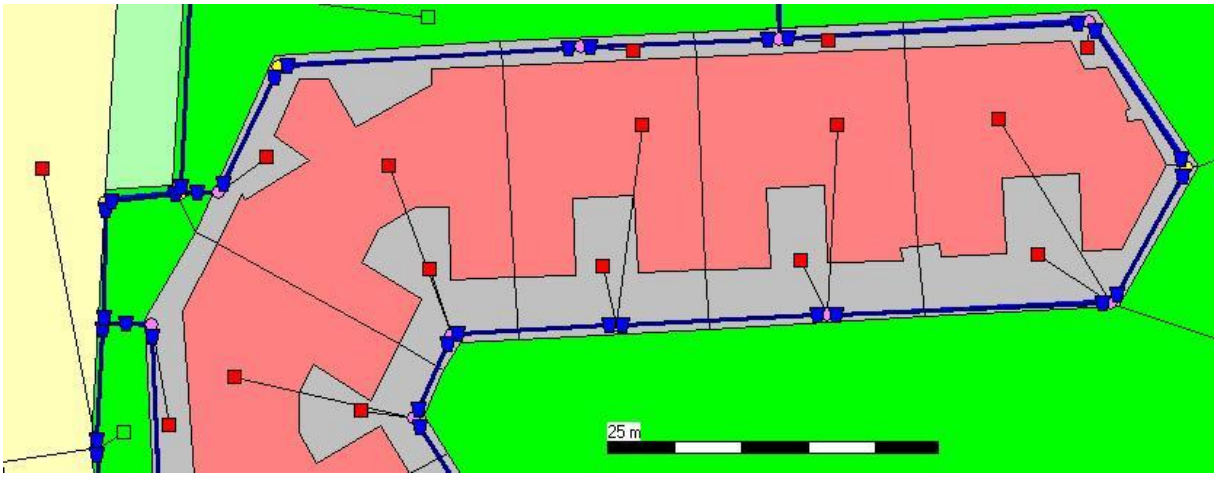

Figure 67. Typical part of the drainage network schematization in SOBEK.

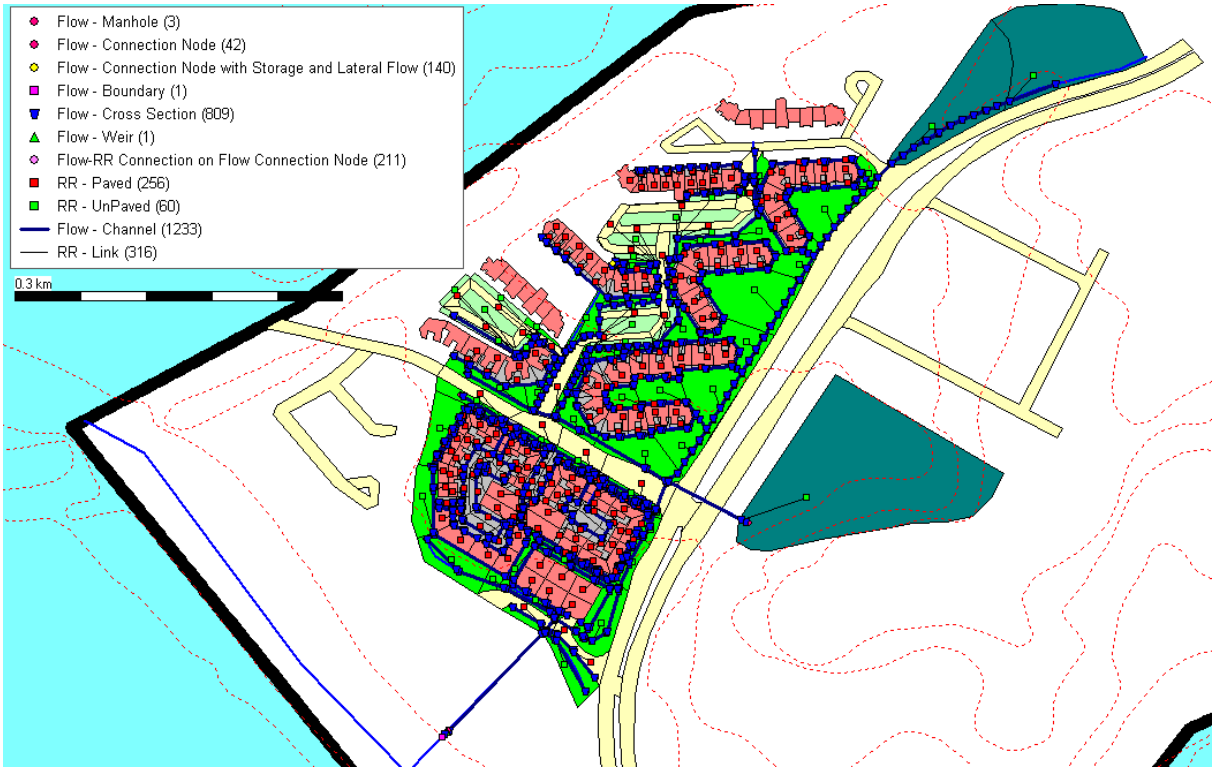

Figure 68. Overview of the model schematization in SOBEK.

Model setup strategy for simulation of scenarios

Standard SOBEK RR and 1DFLOW modules are used in base case scenario simulation runs. In terms of the standard urban water management model setup, which was presented in Figure 15, the RR module of SOBEK is the runoff generation model. Flow routing to the drainage network is incorporated for in the surface runoff delay calculations of the RR module. The 1DFlow module incorporates flow routing in the drainage system (Figure 69). Because green roof processes cannot be accurately described by the RR module of SOBEK, the HYDRUS model will act as a runoff generation model for the building surfaces with implemented green roofs in the green roof scenario simulation runs (Figure 70). Pre-processed outflow from the HYDRUS model will be coupled to all building paved nodes in the SOBEK schematization. Subsequently, the storage of all building nodes are reduced to 0 mm for green roofs. This is done to avoid double counting of the storage potential,

which is already incorporated for in the HYDRUS simulations. Runoff generation on all other paved and unpaved surface areas within this scenario are accounted for by the standard RR module of SOBEK. As usual, flow routing to the drainage system is incorporated for by the SOBEK RR module and routing in the drainage system is described by the 1DFLOW module of SOBEK.

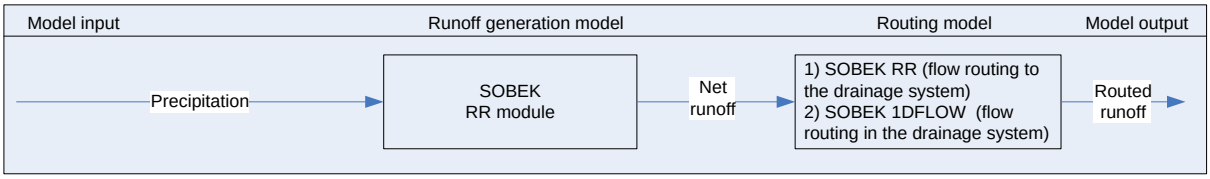

Figure 69. Model setup for the base case scenario runs

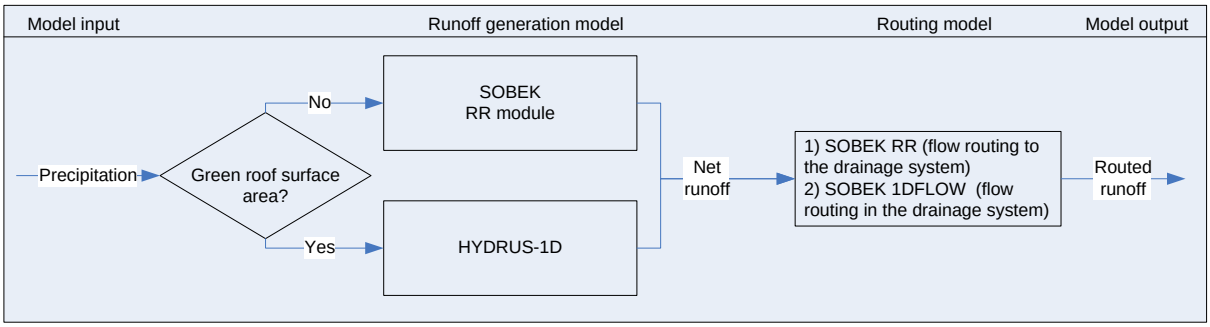

Figure 70. Model setup for the green roof scenario runs

Model assumptions

The SOBEK model which will be used to asses the effects of large-scale green roof implementation in the Sunset Way subcatchment in Singapore has been setup by Deltares within the project context of SDWA's Centre for Aquatic Science 'Pandan Canal' research programme (Vergroesen 2010, SDWA 2010). Within the context of this research, the SOBEK model and its underlying assumptions are adopted. It is worth mentioning the main assumptions, because they have to be incorporated when results and conclusions about large-scale effects of green roofs are deduced from modelling practices in the rest of this chapter:

1. The total subcatchment drainage area equals 9.4 ha;
2. All roof surface areas from buildings (1.76 ha) are available for roof greening;
3. Rainfall-runoff from all rooftops and other surface areas discharge into the drainage system;
4. Normally, drainage and sewer systems are physically separated in Singapore. No information was available about possible sewer overflow locations in the area. Therefore, it is assumed that there is no interaction between both systems;
5. Delay of surface runoff depends on the average distance to the inflow location of the drainage system, the slope and the geometry of the catchment. At paved areas this is incorporated for in the runoff factor *c* [1/min] and at unpaved areas this is incorporated for in the Ernst drainage resistance *W* [d]. A full description of the surface runoff principles at (un)paved nodes can be found in the SOBEK manual (Deltares 2009). Table 11 presents the values for the implemented runoff factors and drainage resistances at (un)paved areas.
   Single parameter values for the runoff delay at paved nodes can be justified, since the paved areas are divided into equal parts of typically 100-200 m^2. Runoff delays of smaller and larger areas are assumed to average out. Runoff factors for standard and green roofs are assumed

to be equal. This assumptions is justified by Berghage, Beattie, et al. (2009): "The vertical component is responsible for the initial abstraction and runoff delay, while the lateral flow component of green roofs appears to be similar to other roofing systems". Adopted parameter values resulted from experimental work and runoff simulations, which are not part of this research (Vergroesen 2010).

6. Initial groundwater levels in the unpaved areas are equal to the initial water level of the corresponding drainage canal;
7. The model has not been calibrated nor validated with real system measurements, because the required measurements were not available. Within this research the model is assumed to be validated by Deltares' expert knowledge. Expert knowledge is one of the validation approaches suggested by Etessami and Gilmore (2008. This validation procedure generally involves careful inspection of model output, model behaviour, tracing and animation.

Table 11. Adopted runoff delay parameters at (un)paved areas at the Sunset Way subcatchment.

Land use type	**Slope**	**Nodal area**	**Runoff factor**	**Drainage resistance**	**Surface storage**	**Infiltration capacity**
Buildings (roof area)	<4%	Typically 100-200 m^2	0.7 [1/min]	-	1 mm	-
Roads	>4%	Typically 100-200 m^2	0.8 [1/min]	-	1 mm	-
Permeable pavement	<4%	Typically 100-200 m^2	-	0.002 [1/d]	2 mm	1 mm/hr
Other paved areas	<4%	Typically 100-200 m^2	0.6 [1/min]	-	1 mm	-
Parks and gardens	<4%	<1000 m^2	-	0.002 [1/d]	2 mm	2mm/hr
Parks and gardens	<4%	>1000 m^2	-	0.005 [1/d]	2 mm	2mm/hr

Despite the fact that the model has been set up with best efforts, these assumptions indicate that the model is a simplified representation of reality. The influence that these assumptions might have on the analysis results will therefore be addressed in a later discussion. The scope of the model use and intensions are adapted on the identified assumptions as well: it is an exploratory means to analyze the effects of large-scale green roofing in the specified subcatchment.

6.2.4 Meteorological test conditions

Meteorological test conditions have been selected under which the hypothesized hydrological effects of large-scale green roof implementation can be assessed. Peak discharge and water level reduction and detention during design storms at subcatchment-scale will be tested under extreme meteorological conditions. The potential contribution of green roofs with respect to non-natural water level variation reduction will be tested under average, normal conditions, because these effects occur on a longer time-scale.

Extreme meteorological test conditions
With respect to the extreme meteorological conditions, two test series will be used:

1. A design storm with a 5 year return period (T=5);
2. The November 19, 2009 flood storm.

For the design of drainage systems in Singapore, return periods (T) are included in the code of practice on surface water drainage (PUB Singapore (a) 2000). The outlet drain of the subcatchment has been designed for a storm with a return period of T=5 years (Appendix 14). The rainfall pattern of this design storm has been established by PUB and is presented in Appendix 16. Besides the prevailing rainfall conditions, another factor appeared to be of main importance for the effectiveness of green roofs: the antecedent soil water condition. Based on this experimental work conclusion that was reported in chapter 4, the HYDRUS model will be run under the T=5 years event with an initial soil water content that varies between 0.25 and 0.55. The pre-processed rainfall-runoff results of this simulation, which will be coupled to SOBEK, are presented in Appendix 16.

A second event that was selected as an extreme test condition is the November 19, 2009 storm that caused flooding in some parts of Singapore. This event was chosen as a practical illustration of green roof effectiveness under extreme meteorological conditions that did actually occur in Singapore. The influence of a rainfall pattern that differs from the design storm can be analyzed. During the storm, flood waters on street reached knee level in the Bukit Timah area (Channelnewsasia.com 2009). This event had a total rainfall depth of 97 mm. The rainfall pattern and the pre-processed rainfall-runoff results from the HYDRUS model are presented in Appendix 16. Just as for the design storm simulations, added value of the HYDRUS model is proven here, since experiment measurements were not available in the month of November due to malfunctioning of the data loggers.

Average meteorological test conditions
On an experiment-scale, the effects of 1 m^2 extensive green roof platforms on the rainfall-runoff were analyzed during four monthly periods in July, September and December, 2009 and March/April, 2010. Based on the conclusion from chapter 4, practical advantages of green roofs should be assessed at (sub)catchment-scale under the same meteorological conditions. With the HYDRUS and SOBEK modelling tools, this analysis can be performed under all available meteorological conditions. Here, the scaled-up effects of green roofs will be tested under the prevailing “average” meteorological conditions of the September, 2009 period. More or longer time series unintentionally increase analysis time, while the contribution of non-natural water level variation reduction can already be assessed in this period, which contains a variety of rainfall events and drought periods. Different meteorological conditions are recommended if the analysis goals differ from the ones set in the ABC Waters Programme.

6.3 Large-scale green roof analysis results

Analysis results of the combined hydrological effects of large-scale green roof implementation in the Sunset Way subcatchment are reported in this paragraph. Subparagraph 6.3.1 focuses on the effectiveness during extreme meteorological conditions. Simulation results during average meteorological conditions will be presented in subparagraph 6.3.2. Depending on the test conditions

and corresponding hypothesized effects, appropriate variables and performance indicators will be presented and differences between the base case scenario and green roof scenario will be discussed. *All presented large-scale green roof results refer to a 12 cm extensive green roof design only.* Addressed performance indicators were introduced in paragraph 2.6.1.5. Because the runoff, peak discharge and base flow are not a specific discharge anymore, like it was assumed in the 1 m^2 roof small-scale platform analysis, new variables for the green roof analysis at subcatchment scale are:

1. Q_{tot} [m^3]. This variable is a measure for cumulative runoff over the entire observed period;
2. Q_c [m^3]. This variable is a measure for cumulative runoff on event scale;
3. Q_{peak} [m^3/s]. This variable is a measure for the peak discharge on event scale;
4. TT_{peak} [min]. This variable is a measure for the time to peak relative to the rainfall peak;
5. Q_{bf180} [m^3]. This variable is a measure of the cumulative base flow runoff from the time of the last recorded rainfall until 180 min after the last recorded rainfall.

6.3.1 Effects of green roofs under extreme meteorological test conditions

HYDRUS simulations show that, depending on the initial roof media wetness, green roofs can retain 4-41 mm of the 111.3 mm T=5 years design storm (Appendix 16). Although green roofs retain up to 37% of the total rainfall depth, these simulations reveal that even under the driest antecedent roof conditions, a 12 cm extensive green roofs is not able to retain enough water to effectively reduce or delay the peak discharge of this design storm (Appendix 16). SOBEK simulation results at subcatchment scale are presented in Table 12. This table presents the cumulative runoff volume, peak discharge and detention variables of the base case scenario and seven green roof scenarios with different initial soil water contents. Besides this, performance indicators for the runoff reduction, peak discharge reduction and extra detention are shown at all green roof scenarios relative to the base case scenario.

Table 12. Effects of large-scale green roofing under a T=5 years design storm.

Scenario	**Total green roof area**	**Initial soil water content**	**Cumulative runoff volume Q_{tot}**	**Runoff reduction ASRPI**	**Peak discharge Q_{peak}**	**Peak discharge reduction PDPI**	**Time to peak tt_{peak}**	**Extra detention DPI**
	[ha]	**[-]**	**[m^3]**	**[m^3 , %]**	**[m^3/s]**	**[m^3/s, %]**	**[min]**	**[min]**
Base case scenario	0	-	9944.40	-	4.22	-	5	-
Green roof scenario 1	1.76	0.25	9238.32	706.08 6.78%	4.15	0.07 1.67%	6	1
Green roof scenario 2	1.76	0.3	9344.07	600.33 5.76%	4.19	0.03 0.68%	5	0
Green roof scenario 3	1.76	0.35	9450.99	493.31 4.74%	4.19	0.03 0.45%	5	0
Green roof scenario 4	1.76	0.4	9556.75	387.65 3.72%	4.20	0.02 0.43%	5	0
Green roof scenario 5	1.76	0.45	9663.03	281.37 2.70%	4.20	0.02 0.43%	5	0
Green roof scenario 6	1.76	0.5	9769.18	175.22 1.68%	4.20	0.02 0.43%	5	0
Green roof scenario 7	1.76	0.55	9873.96	70.44 0.77%	4.20	0.02 0.43%	5	0

At the lower limit of the initial green roof soil water content (θ(t=0)=0.25), green roofs provide just over 700 m^3 of additional storage for a design storm with 10417 m^3 of rainfall (9.36 ha*111.3 mm). Cumulative runoff volumes of scenarios 2 - 7 show that additional storage decreases with increasing initial soil wetness. At the upper limit of the initial soil wetness, green roofs only provide 70 m^3 of extra storage. Green roofs thus provide a varying runoff reduction of 0.77 – 6.78%, relative to the base case scenario. Because green roofs get saturated before the peak moment of the design storm, peak discharge reduction and detention are very limited for all green roof scenarios relative to the base case scenario (Table 12). Runoff peaks in the outflow canal of the subcatchment vary between 4.15 and 4.20 m^3/s, while the peak discharge for the base case scenario is only slightly higher: 4.22 m^3/s. Time to peak of the runoff under the green roof scenarios are equal to the time to peak of the runoff for the base case scenario, except for green roof scenario 1 which provides an extra minute of detention. It should be mentioned that presented time to peak values are relative to the time to peak of the design storm. However, a 5 minute time to peak value does not represent the time of concentration of the subcatchment, since not all areas are contributing to the outflow canal discharge before the rainfall intensity of the design storm decreases again after t=2 hours.

Figure 71 and Figure 72 illustrate the limited influence of green roofs on the peaks and peak detention of the discharge and water levels at the main outflow canal. Under initially dry conditions, green roofs are able to reduce the water levels and discharge to some extent, but depending on the degree of wetness, discharge and water level values of all green roof scenarios will converge to base case scenario values.

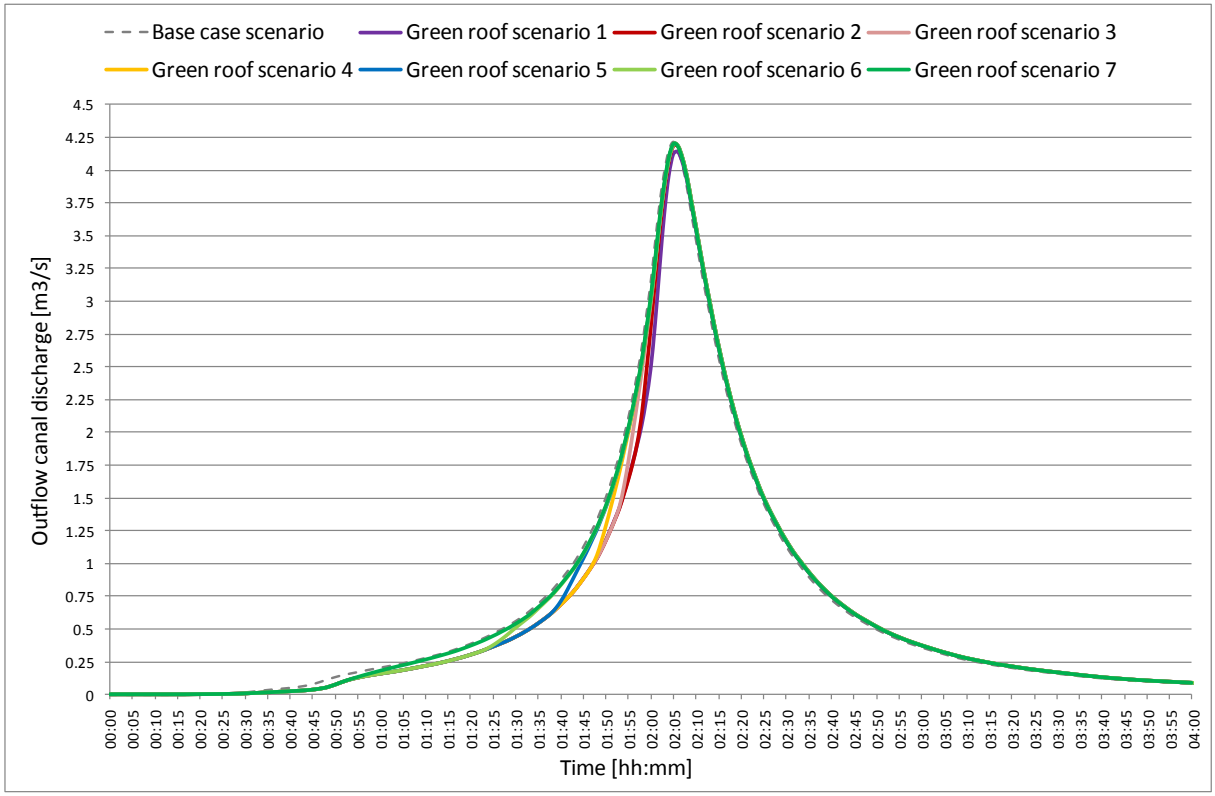

Figure 71. Scenario hydrographs of the design storm at the main outflow canal.

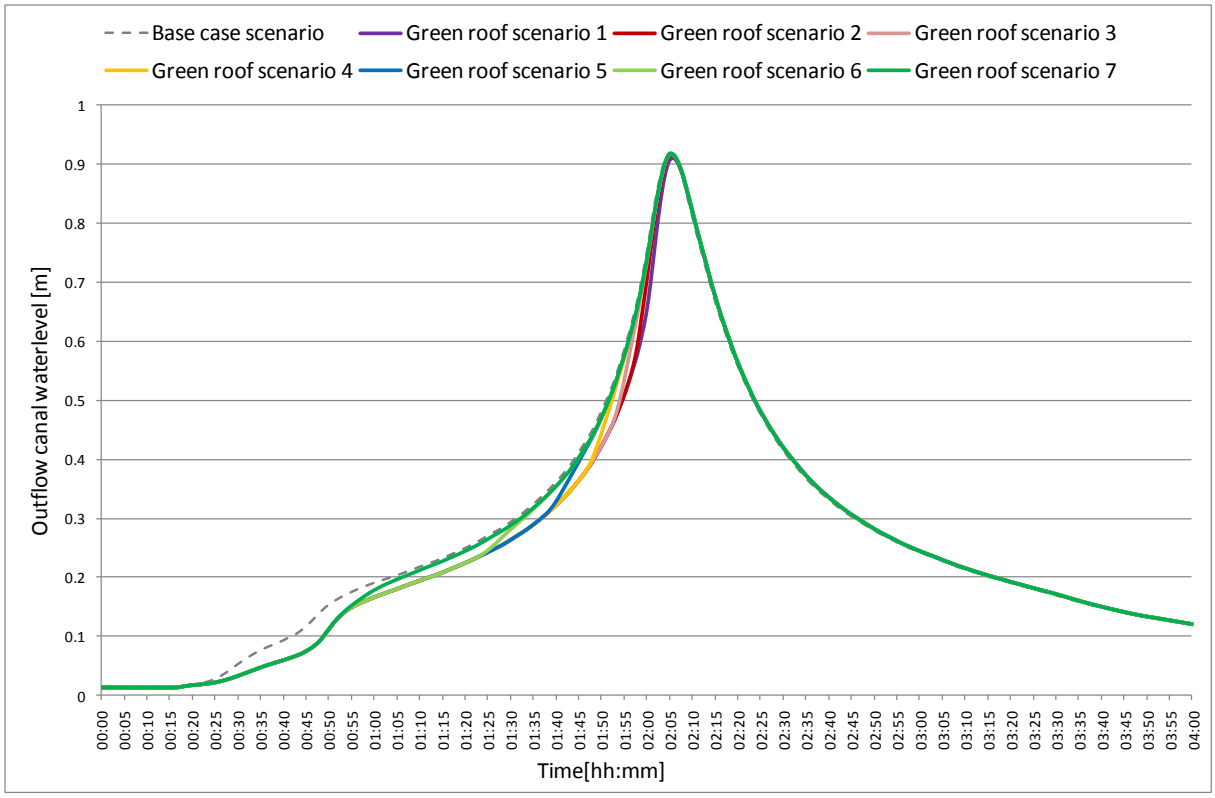

Figure 72. Scenario water levels of the design storm at the main outflow canal.

When the SOBEK model simulations are run under the meteorological conditions of the November 19, 2009 flood storm, similar effects are observed (Table 13). Green roof runoff simulations in HYDRUS as well as the SOBEK routing model simulations were run from November 12 onwards in order to fulfil the run-in period requirement. Rainfall on November 17 and November 18, decreased the green roof storage potential, prior to the flood storm of November 19, to 1.7 mm (Appendix 16). Because of this, cumulative outflow q_c from green roofs for this event equals 95.3 mm, while the total rainfall equals 97 mm in this flood storm which has a duration of 3.5 hours. At subcatchment-scale, just as for the design storm, runoff intensities and water levels of the green roof scenario closely follow the base case scenario after saturation of the green roof media. This is illustrated in Figure 73. Simulation results indicate that green roofs could not have prevented flooding under these meteorological conditions.

Table 13. Effects of large-scale green roofing under the November 19, flood storm.

Scenario	**Total green roof area**	**Initial soil water content**	**Cumulative runoff volume Q_{tot}**	**Runoff reduction ASRPI**	**Peak discharge Q_{peak}**	**Peak discharge reduction PDPI**	**Time to peak tt_{peak}**	**Extra detention DPI**
	[ha]	**[-]**	**[m^3]**	**[m^3,%]**	**[m^3/s]**	**[m^3/s,%]**	**[min]**	**[min]**
Base case scenario	0	-	8448.50	-	3.55	-	7	-
Green roof scenario	1.76	0.6	8443.97	4.53 0.05%	3.56	0.01 -0.29%	7	0

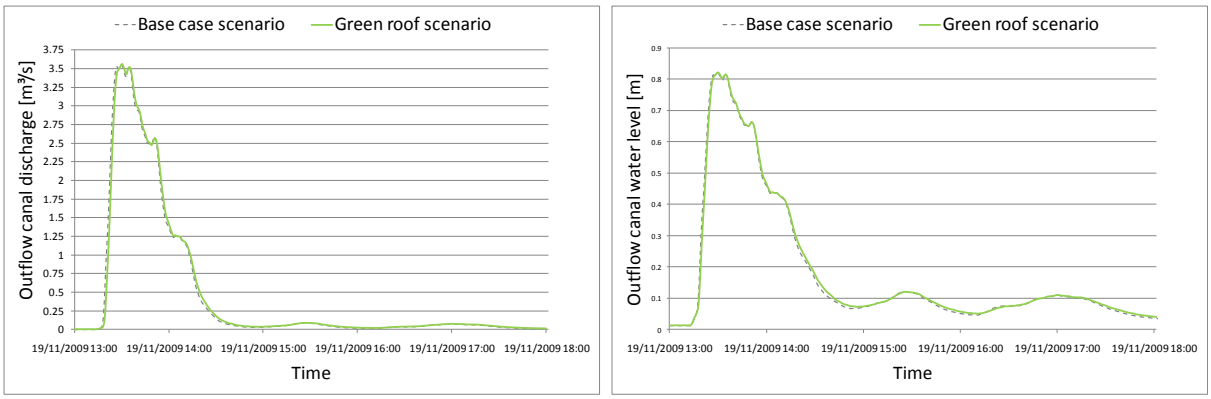

Figure 73. Scenario hydrographs and water levels of the November 19, flood storm at the main outflow canal.

The hypothesized effects of large-scale green roof implementation were stated in the introduction of this chapter. Based on the presented scenario simulation results it can be concluded that the effects of large-scale implementation of the 12 cm extensive green roof design on peak discharge and water level reduction and detention during extreme meteorological conditions is very limited. Two identified main causes for these limited effects are:

1. A 12 cm extensive green roof is often saturated at the time of the rainfall peak during an extreme event;
2. Effects of green roofs are diluted because of the limited building coverage.

The first main cause can be split up into two underlying sub causes: the influence of rainfall characteristics and the influence of antecedent soil water conditions of the green roofs. In the case of the Singapore T=5 years design storm, large rainfall volumes prior to the actual rainfall peak, saturate the extensive green roofs in the rising limb of the design storm. When green roofs reach this point of saturation, runoff reduction and delays cease. Because of this, green roofs hardly decrease the discharge and water level peaks in the subcatchment. Any runoff reduction prior to the peak of the rainfall, could beneficially reduce the impact of such extreme events on the downstream side of the catchment however. To test this, an analysis that integrates the effect of green roofs at an even larger than subcatchment scale is recommended. Independent of the shape and volume of the rainfall event, extensive green roofs can also get saturated prior to the rainfall peak because of wet antecedent roof conditions. Green roof effectiveness can reduce because of this effect, even when the peak of the extreme rainfall event occurs relatively early in the rainfall time series. This was observed in the simulation of a flood storm that actually occurred on November 19, in Singapore.

Second, green roof effects are diluted at subcatchment-scale because the building coverage of the study area is only 19%. While green roofs retain up to 37% of the total rainfall depth of a T=5 years design storm under the driest initial conditions, they can only maximally reduce the runoff volume with 7%, relative to the base case scenario. Similar dilution effects occur for the peak discharge reduction and peak detention during extreme events. Based on this result, it is recommended to implement green roofs on locations with relatively high building coverage.

6.3.2 Effects of green roofs under average meteorological test conditions

To asses the contribution of green roofs to non-natural water level variation reduction, scenario simulations were run in SOBEK under the actual meteorological conditions of September 4-20, 2009. Again, green roof rainfall-runoff has been pre-processed with the HYDRUS model. Large-scale green roof simulation results for the September period are presented in Table 14 (b). These simulation results confirm the observed dilution of green roof effects in the subcatchment, compared to the small-scale green roof effects (Table 14 (a)). Dilution is reflected in the reduced values for all four performance indicators. The ASRPI ratio in the large-scale green roof scenario is much lower than the ASRPI ratio that was measured on experiment-scale. Basically, the same holds for all other three performance indicators. The conditional runoff reduction and desynchronizing effect of green roofs that was measured on experiments-scale, translates into reduced peak discharges at subcatchment-scale. When the runoff time to peak of the subcatchment in the green roof scenario is compared to the base case scenario, hardly any differences can be observed. These results underline that green roof experiment performance cannot be directly translated into overall catchment performance.

With respect to the hypothesized effects of green roofs during average meteorological conditions in Singapore, two variables are of main importance: the peak discharge and the base flow. If green roofs are effectively able to reduce the peak discharge and conserve the base flow, they can contribute to more regulated flows, which is a goal of the ABC Waters Management Strategy.

Green roof experiments results in paragraph 4.4.3 showed that dynamic complexity of rainfall depth and intensity distribution over time as well as the antecedent soil water content of the green roof determine the peak discharge performance. The same argumentation holds for the peak discharge reduction at subcatchment-scale. Additionally, the effects are smoothened out because of the dilution effect, which was introduced in the previous paragraph. Peak discharge results of the September period events are presented in Table 14 (b). Figure 74 shows that green roofs can effectively reduce the peak discharge in the case of a long antecedent dry weather period. This effect ceases however, when the green roof storage capacity is quickly exceeded during an event. Underlying causes for early green roof saturation were discussed in the previous paragraph.

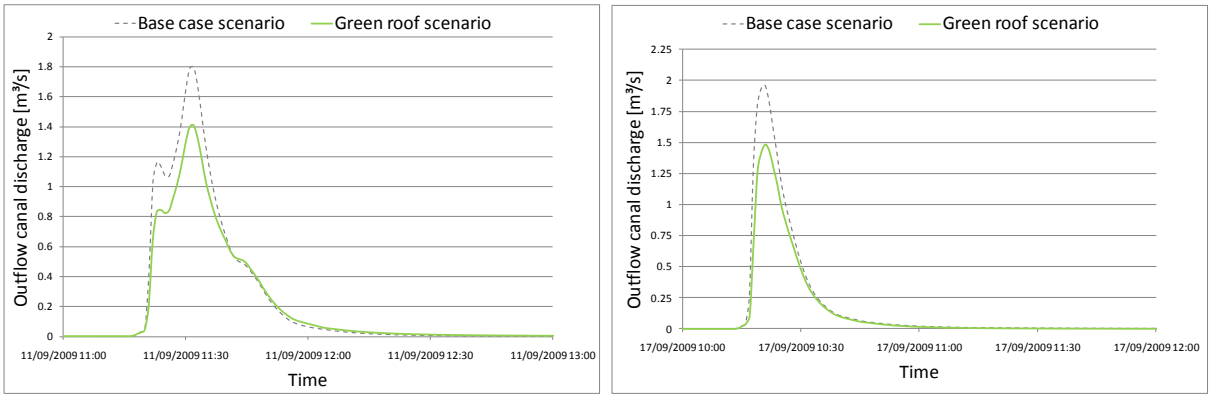

Figure 74. Scenario hydrographs of the September 11 and September 17, 10:11 event.

	Rainfall P [mm]	Cumulative runoff q_c [mm]		ASRPI ratio [%]	Peak discharge q_{peak} [mm/min]		PDPI ratio [%]	Time to Peak tt_{peak} [hh:mm]		DPI [min]	Base Flow q_{bf180} [mm]		BFPI [mm]
		Reference roof	Green roof		Reference roof	Green roof		Reference roof	Green roof		Reference roof	Green roof	
06/09/2009 06:36	31.21	29.06	26.54	8.07	0.99	0.78	21.21	-00:03	00:04	7	0.05	0.22	0.17
11/09/2009 11:13	22.06	20.53	5.88	66.41	1.84	0.40	78.26	00:11	00:18	7	0.03	0.81	0.78
17/09/2009 03:06	1.00	0.5	0.00	50.00	0.04	0.00	100.00	00:04	-	-	0.39	0	-0.39
17/09/2009 10:11	15.91	14.36	0.00	90.26	2.23	0.00	100.00	00:03	-	-	0.00	0	0
18/09/2009 11:37	7.14	6.58	0.73	81.93	1.03	0.06	94.17	00:03	00:17	14	0.59	0.73	0.14
18/09/2009 14:53	6.75	6.11	5.78	4.89	0.38	0.18	52.63	00:01	00:11	10	0.28	0.34	0.06
19/09/2009 10:15	13.59	13.14	13.03	0.81	0.77	0.56	27.27	00:00	00:08	8	0.07	0.39	0.32
19/09/2009 14:31	0.50	0.06	0.06	0.00	0.01	0.00	100.00	00:28	00:19	-9	0.06	0.04	-0.02

(a) Small-scale green roof runoff simulation results compared to measured reference roof runoff

	Rainfall P [mm]	Cumulative runoff Q_c [m^3]		ASRPI Ratio [%]	Peak discharge Q_{peak} [m^3/s]		PDPI Ratio [%]	Time to Peak TT_{peak} [hh:mm]		DPI [min]	Base Flow Q_{bf180} [m^3]		BFPI [mm]
		Base case	GR scenario		Base case	GR scenario		Base case	GR scenario		Base case	GR scenario	
06/09/2009 06:36	31.21	2341.49	2295.34	1.58	1.10	1.09	0.91	00:05	00:06	1	24.12	29.27	5.15
11/09/2009 11:13	22.06	1815.55	1553.87	12.67	1.80	1.41	21.67	00:15	00:15	0	87.61	112.23	24.62
17/09/2009 03:06	1.00	6.93	2.03	5.24	2E-03	5E-04	75.00	00:43	-00:04	-47	15.16	5.61	-9.55
17/09/2009 10:11	15.91	1252.76	995.69	17.26	1.96	1.48	24.49	00:08	00:08	0	25.06	21.69	-3.37
18/09/2009 11:37	7.14	473.73	370.89	15.39	0.80	0.56	30.00	00:08	00:09	1	164.95	154.72	-10.23
18/09/2009 14:53	6.75	358.68	353.11	0.88	0.22	0.22	0.00	00:25	00:25	0	38.82	44.42	5.6
19/09/2009 10:15	13.59	980.61	981.12	-0.04	0.77	0.74	3.90	00:10	00:10	0	37.77	46.31	8.54
19/09/2009 14:31	0.50	3.26	3.25	0.02	8E-04	8E-04	0.00	00:54	01:10	16	7.89	7.63	-0.26

(b) Large-scale green roof scenario simulation results compared to base case scenario simulations (9.37 ha)

Table 14. Comparison of small and large-scale green roof runoff simulation results.

A conservation of the base flow is the second hypothesized main effect of green roofs that could contribute to a reduction of non-natural water level variations in Singapore's stormwater drainage system. Measurement results at experiments-scale showed that green roofs generate a base flow volume of up to 3 litres/m^2 after the last recorded rainfall. It was concluded that they cannot replace the natural function of groundwater however. Large-scale simulation results show that, in line with the small-scale simulation results, green roofs cannot provide additional base flow for events that are totally or almost totally retained by the soil media. This is reflected in the negative BFPI values in Table 14 (b). An example of this effect is the September 17, 10:11 event, which is shown in the right graph of Figure 74. If the green roof gets saturated during the event, minor base flow conservation effects are observed. An example of this base flow conservation effect in the subcatchment is presented in the left graph of Figure 74. Although hardly visible, an additional 24.62 m^3 of runoff is delayed after the last recorded rainfall, relative to the base case scenario without green roofs.

Observed peak discharge reduction and base flow conservation provided by green roofs in the subcatchment do reduce the water level variation to some extent. Figure 75 shows a continuous representation of the water levels in the main outflow canal of the subcatchment during the entire simulation run time. A limited influence of the proposed large-scale extensive green roof implementation with respect to the hypothesized effects, can be derived from this graph. Just as for the base case scenario, the main outflow canal is still mostly dry under the green roof scenario. The peak flow reduction is often significant though.

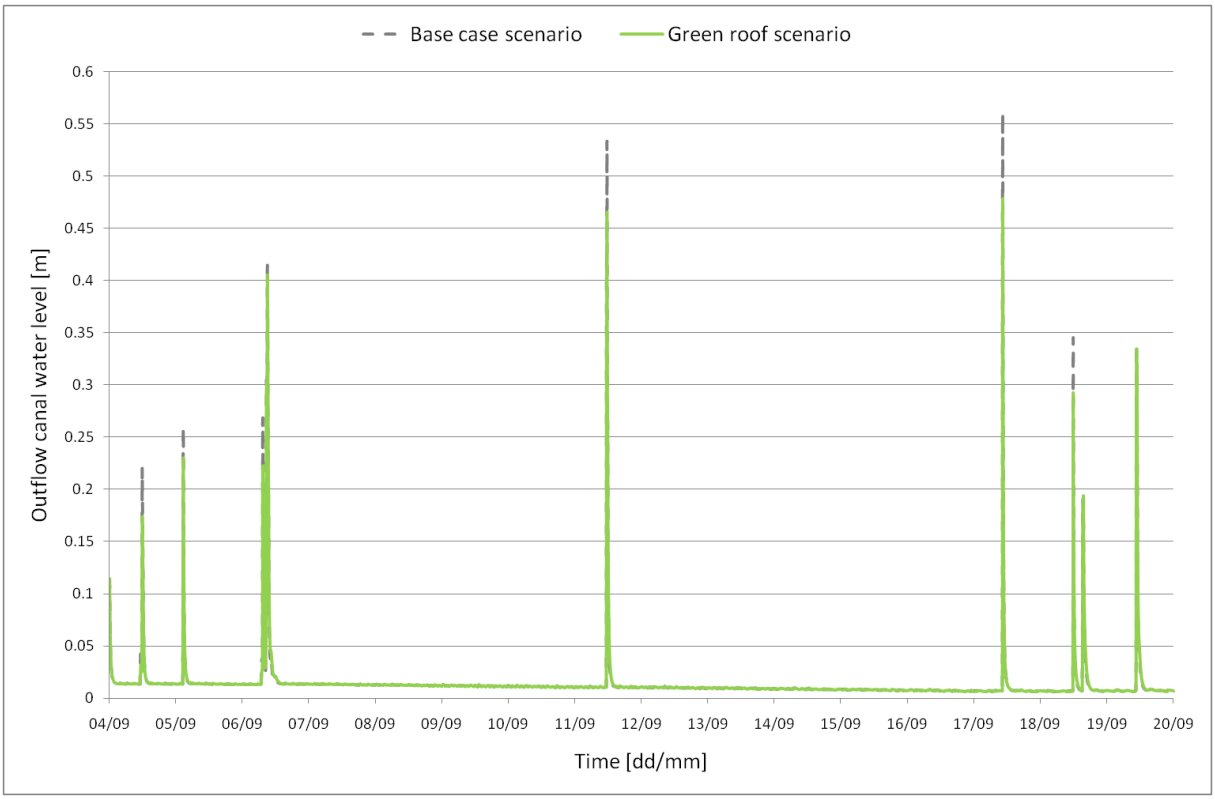

Figure 75. Simulated water levels in the main outflow canal for the entire September period.

6.4 Discussion and conclusions

The case study results demonstrate that the proposed model simulation approach is an appropriate methodology to quantify the effects of green roofs at subcatchment-scale. When the case study results are thoughtfully interpreted, the contribution of green roofs within Singapore's ABC Waters Programme can be assessed and generic recommendations for the implementation of green roofs in tropical urbanized catchment can be provided. Together, these conclusions form an answer to the main research question. Before this can be done, it is important to discuss the influence of the adopted assumptions on the simulation results.

6.4.1 Influence of model assumptions on model results

Seven model assumptions were reported in subparagraph 6.2.3. How the assumptions influence the large-scale green roof simulation results is visualized in Figure 76. This hierarchical tree diagram gives an overview of the main contributing factors that influence the stormwater drainage system runoff simulations. The assumptions influence the calculated values of the contributing factors on several positions, indicated with an orange circle and labelled with a corresponding assumption number. Green roof runoff generation, which is simulated in HYDRUS under all the assumptions discussed in chapter 5, are visualized with a green circle, but will not be addressed again in this discussion. The diagram directly reveals that assumptions were made in almost every operational factor. Operational factors are the factors lowest in hierarchy, and are generally located on the edge of the research demarcation.

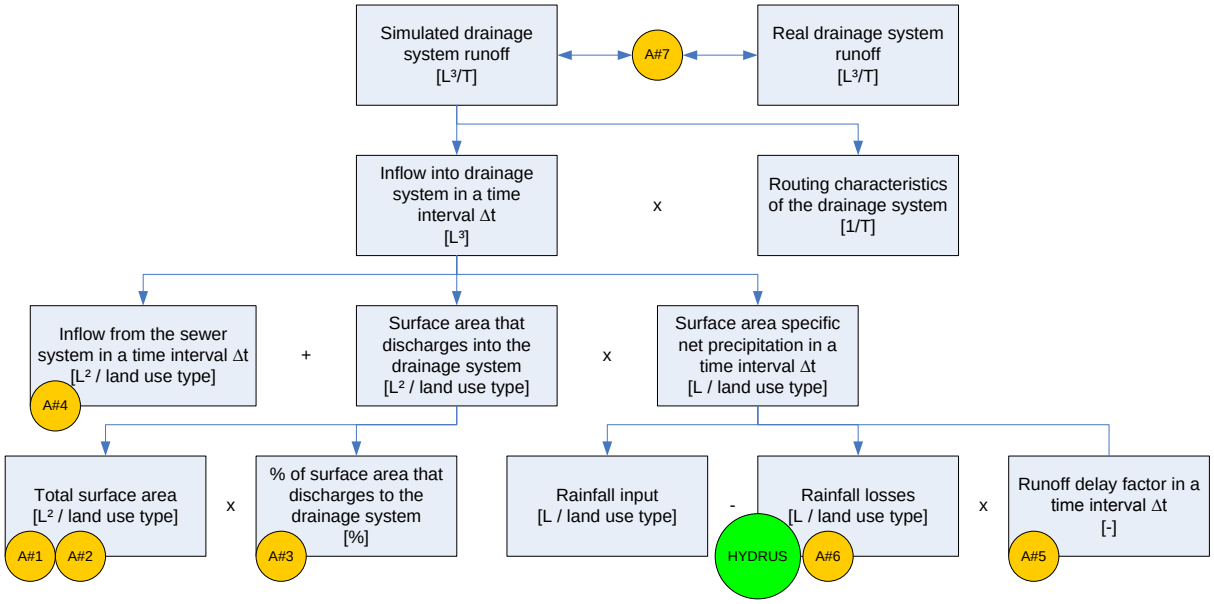

Figure 76. Tree of factors that influence the drainage system runoff simulations at subcatchment-scale

Assumptions 1 and 2: The total subcatchment drainage area is assumed to be 9.4ha and all roof surface areas from buildings are considered to be available for roof greening in the green roof scenario. Deviations from the true catchment demarcation and available surface area for roof greening will introduce errors in the absolute and relative contribution of the six distinguished land use types to the total outflow. Although some basic GIS data was available, it is recommended to improve the GIS data to reduce the runoff deviations that evolve from the overall and internal land use demarcation errors within the representation of the subcatchment.

Assumption 3 and 4: Within the research it was assumed that rainfall-runoff from all rooftops and other areas discharges into the drainage system. Domestic wastewater was assumed to be the only inflow to the sewer system and it was assumed that there was no interaction between both systems. In relatively young HDB complex areas, this assumption holds. In Singapore's older HDB areas, drainage and sewer system appeared to be less well separated and sewer overflows can exist. The Sunset Way HDB area turned out to be an older HDB area. This means that the percentage of building surface area that discharges into the drainage system has been overestimated in the model, because parts of the building surface area discharges into the sewer system in the real world. The real effects of green roofs on the rainfall-runoff in the subcatchment are therefore probably even more diluted. Potential advantages of green roofs to reduce combined sewer overflows in old HDB areas are neglected in the current model simulation results. It follows from this discussion that green roof effects will differ in old and new areas. It is recommended to keep these differentiated effects in mind when green roofs are going to be implemented in Singapore's HDB areas.

Assumption 5: Adopted runoff factors and drainage resistances are based on experimental work and runoff simulations, which are not part of this research (Vergroesen 2010). A simplified classification of the surface runoff delay factors per land use type cannot take all dynamic delay processes into account. A more elaborate study of green roof delay effects that occur with up-scaling may be required. Usually, this kind of accuracy is not fulfilled however for any of the other (un)paved area land use types in present SOBEK simulation activities .

Assumption 6: Because measurements of the groundwater levels in the area are lacking, and because it is to complex to incorporate them into the available simulation tools, it was assumed that the groundwater levels in the unpaved areas are equal to the initial water levels of the corresponding drainage canal. Because drainage canals are mostly dry throughout the year, inflow from unpaved areas is possibly underestimated. In order to improve the simulation accuracy of unpaved area runoff characteristics, more groundwater related research has to be performed. It is a question however, whether the clayey soil types in Singapore with low infiltration rates, are an important enough factor for additional research efforts with respect to this goal. It is probably more efficient to spend valuable research time on the rainfall losses that occur on paved areas, green roofs and the surface losses that occur on unpaved areas, rather than to look at the groundwater storage reservoir.

Assumption 7: The simulation model was assumed to be validated by Deltares' expert knowledge. There were no measurements available to calibrate the internal model parameters and to validate the model under all assumptions. Appropriate water level or discharge measurements at the outflow canal are definitely recommended for these types of simulations. This certainly holds if the model simulations will be used for different purposes as it was used for in this case study: an exploratory means to analyze the effects of large-scale roof greening in the specified subcatchment.

Additional, implicit assumptions: Figure 76 reveals that there are two operational factors left that influence the simulated drainage system runoff, but which miss one or more assumptions: the rainfall input and the routing characteristics of the drainage system. The list of assumptions should be supplemented with at least two more assumptions. First, it was assumed that a homogeneous rainfall distribution over the area correctly represents the real rainfall. Second, the routing characteristics were assumed to be described by the de Saint Venant equations (Deltares 2009).

6.4.2 Contribution of green roofs within Singapore's ABC Waters Programme

ABC's Waters Programme objective is to symbiotically integrate Singapore's parks, reservoirs, waterways, recreation infrastructures and facilities (PUB Singapore (e) 2009, p.5). Implementation of green roofs is one of the ABC Waters design features within the ABC Waters Management Strategy. Together with all other design features, green roofs are piloted in order to contribute to a more sustainable stormwater drainage system with regulated flows and lower peaks (Figure 19).

A good understanding of the green roof functioning is important. Experimental results of this research indicate that green roofs do not exactly function the way ABC Waters Design Guidelines (PUB Singapore (e) 2009) and several studies (van Woert, et al. 2005, Moran, Hunt and Jennings 2004) suppose. The presented extensive green roof design did not just absorb water and slowly release it over a period of time. The following general functions of extensive green roofs followed from experiment analysis and the case study simulation at subcatchment-scale:

- *Retention* is the primary function of green roofs. Rainfall is retained until the maximum storage capacity of the green roof;
- *Detention and peak discharge* reduction is provided by green roofs until the moment of soil saturation. After this moment, green roof peak detention is limited to 1-2 minutes and runoff intensities closely follow the rainfall intensities;
- *Base flow conservation* by green roofs is not provided for rainfall events that are totally or almost totally retained by the soil media. If green roofs get saturated during the rainfall event, minor base flow conservation effects are observed for up to 3 hours after the last recorded rainfall.

It was hypothesized that green roofs are able to contribute to a sustainable stormwater drainage system because of two main hydrological (blue) effects:

1. Peak discharge and water level reduction and detention during extreme meteorological conditions;
2. Non-natural water level variation reduction during average meteorological conditions.

Based on the analysis results it can be concluded that the combined hydrological effects of large-scale extensive green roof implementation on the rainfall-runoff in Singapore are limited. It can act as a part which can contribute to a more sustainable stormwater drainage system, but is not able to mimic predevelopment site hydrology. Green roofs are able to reduce the peak water discharges as long as the soil media is able to retain the rainfall. Under average, normal weather conditions green roofs are able to lower peaks under this consideration, but the peak reduction is diluted because buildings cover only a limited part of the site area. The case study that was used in this research is a typical HDB area. The *building coverage* in this area is 18%. Because of the rainfall depth, intensity and shape of Singapore's current design storm, a 12 cm extensive green roof design does not provide a demonstrable peak discharge reduction and detention in the outlet drain of the case study area. Any retention prior to the design storm peak could potentially reduce flood damage in downstream area. This can be seen as the main advantage of extensive green roofs under present meteorological design conditions. However, further research still has to prove these hypothesized advantages. Under average, normal meteorological conditions, extensive green roofs provide negligible

improvements in base flow and water level conservation during dry weather periods. Green roofs cannot replace the natural function of groundwater, which provide the total flow of the recession curve until the next period of rainfall in natural situations. If for example green roofs have to provide a base flow of 0.1 m^3/s during a one-day dry spell in the case study area, they should provide 8640 m^3 of base flow per day, which equals 49 cm of rainfall (8640 m^3/17600 m^2 of green roof area). Independent of the design, green roofs can never deliver this base flow because these amounts of rainfall are never available. The discussed key capabilities and limitations are summarized in Table 15.

Table 15. Green roof capabilities and limitations.

Considerations	**Green roof capabilities**	**Green roof limitations**
Flood control (extreme meteorological conditions)	-Retention potentially reduces flood damage in downstream areas	-Negligible peak reduction and detention under present PUB design conditions
Regulation of flows (average meteorological conditions)	-Conditional peak water level reduction in the drainage system	- Negligible improvements in base flow and water level conservation during dry weather periods

`

Some additional recommendations with respect to the assessment of the green roof contributions towards a sustainable stormwater drainage system are:

1. The unilateral design requirements that follow from the Code of Practise (PUB Singapore (a) 2000) introduce a bias in the determination of green roof effects under design conditions. Because green roof effectiveness, among others, does depend on 1) the timing of the peak within the event and 2) the amount of rainfall, extreme event analysis should preferably incorporate design storms with variable shapes (timing of the peak) as well as a correct quantity of precipitation. Variable shapes of a design storm are recommended because the capability of green roofs to effectively reduce the peak of an event increases when the peak intensity of the design event is timed in the beginning of the storm and decreases when the peak is situated in the end of the storm. A correct quantity of precipitation, especially before the peak of the design storm becomes more important than in present design calculations, because the effectiveness of green roofs (and other LID measures) is not only a function of the precipitation peak, but of the available storage too. This means that the effect of green roofs under extreme conditions cannot be assessed with a T=5 years design storm, with only one peak and dubious quantities of precipitation. As an alternative for future design purposes, the Sifalda-storm modified by Arnell is recommended by van de Ven (2007). This design storm is constructed of a uniformly distributed centre part, which is derived from a point of the rainfall duration curve, and a rainfall before and after that. Complete time series computations can be recommended as a second good alternative, because those have to be available for the calculation of the Sifalda-storm parameters as well (van de Ven 2007).
2. The case study area is a 9.4 ha subcatchment that discharges into the Sungei Ulu Pandan Canal via the main outflow canal. Although large-scale green roofs are not able to reduce and delay the peak discharge during extreme design conditions, any runoff substraction prior to the maximum discharge reduces water volumes in the downstream part of the catchment. Under the most advantageous scenario, the runoff reduction is 7% under a T=5 years design

storm. This effect is site specific. It is recommended to assess the combined effects of green roof implementation on discharges and water levels in the Sungei Ulu Pandan Canal.

3. To enhance the contribution of green roofs to a sustainable stormwater drainage system in Singapore, green roof design fundamentals should be reconsidered and adapted to the proposed hydrological effects and site specific requirements. As a supplement to the ABC Waters Design Guidelines, several recommendations for the implementation and the design strategy of green roofs in Singapore are presented in Table 16 and Table 17 respectively.
4. Whereas this research focuses on the isolated quantitative hydrological effects of green roofs, the ABC Waters philosophy aims to integrate effects of design features in the blue, green and orange systems. The overall assessment of green roofs contribution towards a City of Gardens and Water should integrate all advantages and disadvantages of green roofs, including effects on water and air quality, aquatic flora and fauna, cooling effects, safety, recreational value, education and social interaction, roof life expectancy and construction and maintenance cost.

Table 16. Implementation strategy recommendations.

Implementation strategy recommendations	**Function**
• Prioritize green roofs in areas with high building coverage	• Reduction of the dilution effect
• Prioritize green roofs in new HDB areas that fully discharge into the drainage system	• Reduction of the dilution effect
• Prioritize green roofs on locations that optimally influence the runoff hydrograph	• Cost-efficient peak discharge reduction
• Perform research on the quantitative and qualitative effects of green roofs within old HDB areas that partly discharge into the sewer system	• Reduction of uncertainty in green roof contribution towards a sustainable stormwater drainage system

Table 17. Design recommendations.

Design recommendations	**Function**
• Add additional layer depth (if permitted within the construction)	• Additional storage capacity of green roofs after long dry spells
• Add extra delay facilities in the soil media, the drainage layer or the conveyance structure of green roofs (delay facilities shall be designed to prevent mosquito breeding)	• Additional peak reduction, base flow and water level conservation
• Choose a drought resistant, low maintenance plant specifies (see Appendix 3 for more information about the maintainability of green roofs in Singapore)	• Prevention of plant mortality and reduction of costs

6.4.2 Understanding of green roof effects in tropical urbanized catchments and the possibilities for a technology transfer to the rest of the world

Limited knowledge on the quantitative hydrological effects of green roof implementation in tropical regions of the world was one of the main reasons to use Singapore as a case study within this research. The research results do not only help to assess the contribution of large-scale green roof implementation towards a sustainable urban environment in Singapore, but can also contribute to the goal of Singapore's Inter-Ministerial Committee on Sustainable Development (IMCDS) to build Singapore into a knowledge hub in the latest technology and services that can help cities to grow in a sustainable, environmentally friendly way (IMCSD 2009).

Research results show that hydrological effects of green roofs depend on several site specific factors such as the size of the area, slopes, land use, building coverage, present drainage system design, weather conditions and more. Because of this, results of this research cannot be directly translated into concrete recommendations for roof greening in tropical urbanized catchments. Nevertheless, gained fundamental knowledge on the hydrological effects of large-scale green roof implementation on the rainfall-runoff in Singapore can contribute to a more sustainable development of stormwater draining systems in other tropical urbanized areas because:

1. The general functioning of extensive green roofs in the tropics was assessed (retention, peak discharge reduction, detention and base flow conservation);
2. A methodology was presented which can be used to simulate green roof effects under meteorological conditions at any location;
3. Capabilities and limitations of green roof implementation towards a sustainable stormwater drainage system were clarified;
4. Implementation strategy recommendations were identified;
5. Design opportunities that can improve the green roof effectiveness were identified.

An extra advantage of the presented model simulation approach, which is based on model coupling of the runoff generation model: HYDRUS-1D, to an existing routing model: SOBEK, is that it also creates theoretical and practical spin-offs for the development of green roofs, as one of the LID measures that can contribute to sustainable stormwater drainage systems in the rest of the world:

1. The physical background of the HYDRUS model provided insight in required additional research for green roof rainfall-runoff measurements and modelling practices (see recommendations in paragraph 7.4);
2. The methodology can be easily used to simulate the large-scale green roof effects of different designs in climates were the hypothesized hydrological effects are even bigger, because of lower design storm peaks and precipitation quantities (such as the Netherlands).

The promotion and international exchange of the knowledge, ideas and recommendations that followed from this study can contribute to help build sustainable stormwater drainage systems in other tropical cities and the rest of the world. Promotion of additional research, pilot projects and communication between various stakeholders such as planning authorities, engineers, private building companies, water boards and the public can further enhance decision making about green roofs and other LID measures within the concept of a sustainable urban environment.

7 Conclusions and recommendations

The different study activities of this research progressed via three main Parts. In Part 1, the project context was established based on an extensive theoretical literature review and a Singapore case study exploration. Singapore's ABC Waters Programme, an analysis of experiment measurements and green roof model simulations at experiment and subcatchment-scale form the skeleton of the research analysis activities in the two remaining Parts. This chapter describes how the different study activities contribute to a final answer to the main research question.

This chapter has been divided into four paragraphs. A recap of the research objectives and applied research approach are presented in paragraph 7.1. Answers to the subquestions are presented in paragraph 7.2. Provided answers to all three subquestions function as a foundation for the final answer to the main research question of this thesis in paragraph 7.3. Recommendations derived from the research conclusions are given in paragraph 7.4.

7.1 Recap of the research objectives and approach

The hydrological effects of urbanization affect the rainfall-runoff regime of many cities in the world. While traditional stormwater drainage systems are often able to effectively serve the function of flood control, they increase downstream peak flows and do not provide a habitat to support a healthy aquatic ecosystem. In order to improve this situation, water managers introduced the concept of Low Impact Development. The goal of this concept is to maintain or re-establish predevelopment site hydrology. Based on the knowledge gap in the understanding of quantitative hydrological effects of green roofs in the tropics, Singapore's ABC Waters Programme Strategy and the experimental green roof research programme as a part of SDWA's research agenda, Singapore was chosen as a case study for this research. The main objectives of the research were to:

1. Analyze the quantitative hydrological effects of green roofs on the rainfall-runoff in Singapore;
2. Determine the quantitative hydrological contribution of large-scale green roof implementation to sustainable stormwater drainage systems in Singapore.

Coupled to Singapore's goal to establish itself as a hub for development of sustainable solutions, this research also had the intention to contribute to an improved sustainable development of sustainable stormwater draining systems in other tropical urbanized areas. To achieve these goals, a research approach was set up, which combines green roof experiment measurements with green roof model simulations. This research approach consisted of two main components:

1. Small-scale green roof analysis;
2. Large-scale green roof analysis.

Small-scale green roof analysis

An approach to measure and simulate the rainfall-runoff processes that occur on 1 m^2 experiment platforms was set up. This facilitates the green roof analysis at subcatchment-scale, later on in the research. The green roof rainfall-runoff measurements that were analyzed in this research originate from the experiment set-up that is part of SDWA's Aquatic Science Centre 'Pandan Canal' research initiatives. Runoff from an extensive green roof platform and a reference roof were analyzed and compared for 66 rainfall events in four periods of one month. A second green roof platform with less

available rainfall-runoff events was used to assess heterogeneity effects between both green roof platform results. The green roof platforms consist of a 12 cm soil media and a drought resistant Sedum Mexicanum vegetation layer. Retention, peak discharge reduction, detention and base flow variables and performance indicators were used to quantify the hydrological effects of green roofs on the rainfall-runoff. The experimental analysis of green roof rainfall-runoff measurements resulted in a better understanding of green roof processes, functioning and performance under varying tropical meteorological conditions.

An unsaturated zone model for the simulation of green roof rainfall-runoff was conceptualized and specified in the physically based HYDRUS-1D simulation software, which numerically solves the Richards equation for water flow in variably saturated porous media. Initial model parameterization was based on literature values and several lab and fieldwork experiments. A research focus point was the determination of the soil hydraulic parameters, for the hydraulic functions of van Genuchten, by inverse modelling of controlled transient flow experiments. Several performance measures were introduced to monitor the model accuracy during the model improvement phase. Finally, the model was successfully calibrated and validated with green roof platform measurements.

Large-scale green roof analysis
A 9.4 ha subcatchment of the Western Catchment that discharges into the Sungei Ulu Pandan canal was used as a case study in order to quantify the hydrological effects of large-scale green roof implementation on the rainfall-runoff in Singapore. A conceptualized representation of the subcatchment was set up with information from Singapore's PUB and by conducting excessive field work. Based on this conceptualized representation of the Sunset Way subcatchment, a model was built in SOBEK by Deltares to quantify the effects of large-scale green roof implementation within the subcatchment. With respect to the hypothesized hydrological contributions of large-scale green roof implementation to sustainable stormwater drainage systems in Singapore, the effects of green roofs were determined under two types of meteorological conditions: extreme meteorological (design) conditions and the actual meteorological conditions of September, 2009. Discharge and water level results of a base case scenario representing the existing situation, were compared to a green roof scenario with maximum potential green roof coverage. In the green roof scenario, pre-processed green roof runoff from the HYDRUS model was coupled to the SOBEK model for an accurate simulation of the scaled-up green roof effects.

7.2 Answers to subquestions

Conclusions of this study will be presented in paragraph 7.3. First, the three subquestions that lead to an answer of the main research question are sequentially answered. These are:

1. **"What are the effects of green roofs on the rainfall-runoff on experiment-scale and how can we model them?"**
2. **"What are the effects of large-scale green roof implementation on the rainfall-runoff in the Sunset Way subcatchment in Singapore?"**
3. **"Which green roof strategy and programme should Singapore choose?"**

The answer to the first subquestion is derived from the small-scale green roof analysis that was reported in Part 2 of this report. The second and third subquestion are answered by the large-scale green roof analysis that was reported in Part 3 of this report.

1. **"What are the effects of green roofs on the rainfall-runoff on experiment-scale and how can we model them?"**

Small-scale green roof platform measurements

Green roof measurement results show that on average, extensive green roofs score well on all four performance indicators. As was derived from the literature review, green roof effectiveness on the rainfall-runoff was determined by the following performance indicators:

- Retention performance indicator relative to rainfall (RPI) and a reference roof (ASRPI);
- Peak discharge performance indicator (PDPI);
- Detention performance indicator (DPI);
- Base flow performance indicator (BFPI).

The green roof platform retained 339 mm out of the 595 mm rainfall (57%) over the four measurement periods. Compared to the reference roof, which retained 105 mm of the rainfall, this means an additional retention of 234 mm (39% of the rainfall sum). The average peak discharge of the green roof rainfall-runoff events was reduced 64% compared with the reference roof, and the average time to peak of the green roof hydrograph appeared 37 minutes after the rainfall peak and 34 minutes after the reference roof peak. The green roof platforms provided extended base flow runoff for up to three hours after the last recorded rainfall. In the first hour after the rainfall stopped, green roofs provided 0.2 liters/m^2 of extra runoff on average. An extra 0.21 liters/m^2 of runoff is provided between one and three hours after the last recorded rainfall. It was concluded that the *average* experiment performance indicator values do not give practical implications whether green roofs are an effective stormwater management solution for the tropics and Singapore specifically. It was found that in order to be able to draw valid conclusions, one should consider that:

1. Practical effectiveness of green roofs should be based on individual event analysis rather than on an average performance;
2. Green roof experiment performance cannot be directly translated into overall catchment performance.

The following general functions of extensive green roofs were derived from experiment analysis:

- *Retention* is the primary function of green roofs. Rainfall is retained until the maximum storage capacity of the green roof;
- *Detention and peak discharge* reduction is provided by green roofs until the moment of soil saturation. After this moment, green roof peak detention is limited to 1-2 minutes and runoff intensities closely follow the rainfall and reference roof intensities;
- *Base flow conservation* by green roofs is not provided for rainfall events that are nearly or totally retained by the soil media. If green roofs get saturated during the rainfall event, minor base flow conservation effects were observed for up to 3 hours after the last rainfall.

Based on the obtained general understanding of the green roof functioning, it can be concluded that event-based green roof performance mainly depends on the antecedent soil wetness of the roof

media as well as the rainfall depth and intensity. The maximum measured retention depth by the green roof platform equalled 32.19 mm for a 36.83 mm rainfall event on July 05, 2009.

Small-scale green roof rainfall-runoff modelling

A modelling approach for the simulation of green roof rainfall-runoff is presented in chapter 5 of this report. The runoff generation model set up was structured around an iterative model cycle. First, the green roof was conceptualized by three main components:

1. The internal state of the unsaturated soil media;
2. Green roof boundaries;
3. Hydrological processes.

The internal state of the green roof model over time is described by the Richards equation and the non-hysteretic unimodal pore-size model of van Genuchten. A research focus point was the determination of the soil hydraulic parameters for van Genuchten's hydraulic functions. Four unique optimized parameter vectors were determined using inverse modelling of transient flow experiments. One-step and multi-step experiments were performed in the lab and a continuous evaporation experiment was performed under field conditions. Despite the fact that four determined parameter vectors were unique, mutual differences were found, especially with respect to the hydraulic conductivity function *K(h)*. Results from the optimized soil water retention functions θ*(h)* showed a high level of correspondence. The upper boundary was described by an atmospheric boundary condition with surface runoff. The lower boundary was modelled by using a seepage face boundary condition. Precipitation, interception, evaporation and transpiration are incorporated in the standard HYDRUS-1D model equations. Meteorological data from the NUS weather station was used as model input to calculate the hydrological fluxes. Sequentially, the model was verified and internal model parameters were adjusted in order to decrease the residuals between the model simulations and green roof platform measurements. Besides an event based qualitative hydrograph inspection, several quantitative variables of performance and a goodness of fit were introduced to support the model optimization process. Those were (runoff units in mm or l/m^2):

1. q_{tot} [mm]. This variable is a measure for cumulative runoff over the entire observed period;
2. q_c [mm]. This variable is a measure for cumulative runoff on event scale;
3. q_{peak} [mm/min]. This variable is a measure for the peak discharge on event scale;
4. tt_{peak} [min]. This variable is a measure for the time to peak relative to the rainfall peak;
5. q_{bf180} [mm]. This variable is a measure of the cumulative base flow runoff from the time of the last recorded rainfall until 180 min after the last recorded rainfall;
6. E_{ns} [-]. The Nash-Sutcliffe modelling efficiency.

Efficient calibration opportunities to improve the model performance were identified with a sensitivity analysis and an established feasible parameter range for every model parameter. Finally the green roof runoff generation model was validated with green roof measurements that were not used in the calibration phase. It can be concluded that the model gives accurate simulations of the green roof runoff over time, the peak discharge, the time to peak and the base flow on event scale. A limitation of the model is that it tends to over predict the green roof runoff when events quickly follow-up. The model is incapable to describe the real swelling and shrinking characteristics of the

soil, evaporation during night and temporary water storage in the sedum leafs. Overall, model simulations gave a good representation of the green roof measurements. The modelling goals were met because a better understanding of the hydrological processes and the soil physics in a green roof media was obtained. Furthermore, the introduced model concept can be used as an effective tool to simulate the scaled up green roof effects under several meteorological conditions at subcatchment-scale.

2. **"What are the effects of large-scale green roof implementation on the rainfall-runoff in the Sunset Way subcatchment in Singapore?"**

The hydrological effects of large-scale green roof implementation in the Sunset Way subcatchment were quantified with model simulations at subcatchment-scale according to the modelling approach that was presented in paragraph 7.1 of this chapter. Variables that were used in the results section of the large-scale green roof analysis were:

1. Q_{tot} [m^3]. This variable is a measure for cumulative runoff over the entire observed period;
2. Q_c [m^3]. This variable is a measure for cumulative runoff on event scale;
3. Q_{peak} [m^3/s]. This variable is a measure for the peak discharge on event scale;
4. TT_{peak} [min]. This variable is a measure for the time to peak relative to the rainfall peak;
5. Q_{bf180} [m^3]. This variable is a measure of the cumulative base flow runoff from the time of the last recorded rainfall until 180 min after the last recorded rainfall.

Large-scale green roof effects under extreme meteorological conditions
The hypothesized effects of green roofs on the peak discharge and water level reduction and detention during extreme meteorological conditions were tested under a T=5 years design storm and the 97 mm flood storm of November 19, 2009. Scenario simulation results showed that the actual effects of large-scale green roof implementation on peak discharge, water level reduction and detention during extreme meteorological conditions is very limited. Depending on the initial soil water content of the green roof scenario under design storm conditions, green roofs provide a variable runoff reduction in the main outflow canal of 70 -706 m^3, which is a reduction of 1-7% compared to the base case scenario, which represents the existing situation. Runoff reduction was negligible under the actual meteorological conditions of the November 19, 2009 flood storm. Under both extreme meteorological test conditions, peak discharge & water level reduction and detention provided by green roofs was negligible. The effects of a large-scale 12 cm extensive green roof implementation under extreme conditions are limited because of the following causes:

1. Green roofs are often saturated at the time of the rainfall peak during an extreme event;
2. Effects of green roofs are diluted because of the limited building coverage.

Singapore's current unilateral design requirements introduce a bias in the determination of green roof effects under design conditions. It was concluded that the effect of green roofs under extreme conditions cannot be assessed with the current single Singaporean T=5 years design storm, because the effectiveness of green roofs does depend on the timing of the peak within the event and the amount of rainfall before, during and after the design storm.

Large-scale green roof effects under average meteorological conditions

The hypothesized effects of extensive green roofs on non-natural water level variation reduction were tested under the actual meteorological conditions of September, 2009. With respect to the hypothesized effects, the main output variables of interest were the peak and base flow discharge and water levels in the main outflow canal. Model simulations showed that green roofs can effectively reduce the peak discharge in the case of a dry initial soil media, but this effect ceases after the moment of soil saturation. Green roof scenario simulations also showed that green roofs cannot provide additional base flow for events that are almost or totally retained by the soil media. If the green roofs get saturated during a rainfall event, minor base flow conservation effects were observed. Because it was shown that the main outflow canal is still mostly dry in the green roof scenario, it can be concluded that the considered 12 cm extensive green roofs provide negligible improvements in non-natural water level reduction at subcatchment-scale.

3. "Which green roof strategy and programme should Singapore choose?"

The main hydrological capabilities and limitations of large-scale green roof implementation were quantified in the Sunset Way subcatchment. The case study analysis results show that the hypothesized hydrological goals of the ABC Waters Management Strategy cannot be achieved with a large-scale implementation of 12 cm standard extensive green roofs. However, Singapore's green roof strategy and programme cannot be directly deduced from the obtained results because large-scale green roof effects are site specific, design modifications can improve the green roof functioning and besides hydrological effects, green roofs provide more (dis)advantages. Strategic recommendations for the implementation of large-scale roof greening should be based on an integrated assessment of all beneficial and detrimental effects of green roofs, including effects on water and air quality, aquatic flora and fauna, cooling effects, safety, recreational value, education and social interaction, roof life expectancy and construction and maintenance cost. To enhance the hydrological contribution of green roofs to sustainable stormwater drainage systems in Singapore, green roof design fundamentals and implementation strategy should be reconsidered and adapted to the proposed hydrological effects and site specific requirements. As a supplement to the ABC Waters Design Guidelines, several recommendations for the implementation and the design strategy of green roofs in Singapore were presented. Table 18 gives a summary of these recommendations:

Table 18. Green roof implementation and design strategy recommendations.

Implementation strategy recommendations	**Design recommendations**
• Prioritize green roofs in areas with high building coverage • Prioritize green roofs in new HDB areas that fully discharge into the drainage system • Prioritize green roofs on locations that optimally influence the runoff hydrograph • Perform research on the quantitative and qualitative effects of green roofs within old HDB areas that partly discharge into the sewer system	• Add additional layer depth (if permitted within the construction) • Add extra delay facilities in the soil media, the drainage layer or the conveyance structure of green roofs (delay facilities shall be designed to prevent mosquito breeding) • Choose a drought resistant, low maintenance plant specifies

The research results cannot be directly translated into concrete recommendations for roof greening in tropical urbanized catchments. However the research results can contribute to a more sustainable development of stormwater drainage systems in other tropical urbanized areas because:

1. The general functioning of extensive green roofs in the tropics was assessed (retention, peak discharge reduction, detention and base flow conservation);
2. A methodology was presented which can be used to simulate green roof effects under meteorological conditions at any location;
3. Capabilities and limitations of green roof implementation towards a sustainable stormwater drainage system were clarified;
4. Implementation strategy recommendations were identified;
5. Design opportunities that can improve the green roof effectiveness were identified.

The presented approach which is based on model coupling of a physically based runoff generation model to an existing routing model also created theoretical and practical spin-offs for the development of green roofs, as one of the LID measures that can contribute to sustainable stormwater drainage system development in the rest of the world:

1. The physical background of the HYDRUS model provided insight in required additional research for green roof rainfall-runoff measurements and modelling practices (see recommendations in paragraph 7.4);
2. The methodology can be easily used to simulate the large-scale green roof effects of different designs in climates were the hypothesized hydrological effects are even bigger, because of lower design storm peaks and precipitation quantities (such as the Netherlands).

Hence, the promotion and international exchange of this knowledge, ideas and recommendations can contribute to the development of sustainable stormwater drainage systems in other tropical cities and the rest of the world.

7.3 Conclusions

The answers to the subquestions function as a foundation for the answer to the main research question:

“What is the quantitative hydrological contribution of large-scale green roof implementation to sustainable stormwater drainage systems in Singapore?”

Scenario simulations in the Sunset Way subcatchment in Singapore showed that the combined hydrological effects of large-scale roof greening on the rainfall-runoff in the main outflow canal of the area are limited. First, runoff analysis in the case study area under extreme meteorological conditions showed that extensive green roofs provide a negligible peak reduction and detention under Singapore’s current design storm with a T=5 years return period. However, these results should be carefully interpreted because Singapore’s unilateral design requirements introduce a bias in the determination of the hypothesized green roof effects under design conditions. It was concluded that the effects of green roofs under extreme conditions cannot be assessed with the current single T=5 years design storm, because the effectiveness of green roofs does depend on the

timing of the peak within the event and the amount of rainfall before, during and after the design storm. Nevertheless, green roofs would surely not have prevented flooding under the actual meteorological conditions of the November 19 flood storm. A possible advantage of green roofs under extreme meteorological conditions is the runoff substraction prior to the maximum discharge. However, further research still has to prove whether this could potentially reduce flood damage in areas further downstream. Second, negligible improvements in the reduction of non-natural water level variations were observed when the green roof scenario model simulation results were compared to the base case scenario model simulation results under average meteorological conditions. Peak flow reduction is conditionally significant, but green roofs are particularly not suitable to provide a base flow, which can replace the natural function of groundwater during dry spells.

It can be concluded that the quantitative contribution of large-scale green roof implementation is smaller than was hypothesized. Green roof measurements, which were analyzed in chapter 4 of this thesis, and green roof modelling in HYDRUS-1D, indicated why green roofs do not simply absorb water and slowly release it over a period of time. Most of the detention and peak discharge reduction is only provided by green roofs until the moment of soil saturation. After this moment, green roof peak detention is limited to 1-2 minutes and runoff intensities closely follow the rainfall intensities. Only if green roofs get saturated, minor base flow conservation for up to 3 hours after the last recorded rainfall was measured on experimental platforms. The physical background of the HYDRUS model enabled us to demonstrate why the examined green roofs cannot provide the hypothesized base flow. It was shown that runoff at the bottom of a green roof can be described with a seepage face boundary. As soon as the soil water content drops below the soil water content at which the media can hold the water against the gravitational forces, runoff from the green roof stops. According to the model computations, which are based on a combination of the Richards equation and van Genuchten's unimodal hydraulic functions, the seepage face soil water content point is generally reached within an hour after the last recorded rainfall. Base flow that is prolonged for more than an hour, which has been measured on one of the green roof platforms, is assumed to originate from clogging of the soil media, drainage layer or filter fabric. A factor that reduces the effectiveness of green roofs at subcatchment-scale is the limited building coverage. Because of the corresponding dilution effect, green roof performance at subcatchment-scale cannot simply be derived from green roof performance at experimental-scale.

Result analysis of this research showed that a standalone large-scale implementation of 12 cm extensive green roofs does not significantly contribute to the quantitative hydrological goals of Singapore's ABC Waters Programme. The hydrological contribution of green roofs to sustainable stormwater drainage systems in Singapore can be enhanced when the design fundamentals and implementation strategy are reconsidered and adapted to the proposed hydrological effects and site specific requirements. Several recommendations for the implementation and the design strategy of green roofs in Singapore were identified. These practical recommendations, together with the scientific recommendations that followed from the research, are described in the next paragraph.

7.4 Recommendations

Recommendations that follow from this research can be subdivided into three main categories:

- Scientific recommendations with respect to experiment-scale green roof analysis;
- Scientific recommendations with respect to the large-scale green roof analysis;
- Practical recommendations of green roof implementation for Singapore and tropical urbanized catchments.

Scientific recommendations: experiment-scale green roof analysis

1. Perform additional statistical data-analysis in order to be able to formalize and summarize the rainfall-runoff measurement results at platform-scale;
2. Promote research efforts that aim to quantify the swelling and shrinking characteristics of soil media, evapotranspiration dynamics during night, temporary water storage in sedum leafs and the hydrological influence of a vegetation cover change;
3. Improve the green roof experiment set-up with continuous, automatically logged, weight measurements. Precise weight measurements can help to validate model predicted evaporative hydrological fluxes. Furthermore, aim to minimize the presence of artefacts that can influence the green roof functioning;
4. Compare green roof runoff model predictions of the HYDRUS model with model predictions of other runoff generation models (for all four performance indicators and a large range of rainfall events).

Scientific recommendations: large-scale green roof analysis

5. Collect and use appropriate water level and/or discharge measurements at the outflow canal for the validation of routing models that are used to assess the influence of large-scale roof greening;
6. Improve the GIS data to reduce the runoff deviations that evolve from the overall and internal land use demarcation errors within the model representation of a subcatchment;
7. Assess the impact of runoff reduction of green roofs prior to the peak of a design event at an even larger than subcatchment-scale;
8. Use different meteorological test conditions if the analysis goals differ from the ones set in the ABC Waters Programme;
9. Incorporate design storms with variable shapes (timing of the peak) as well as a correct quantity of precipitation when one wants to assess the effects of green roofs or other LID measures under extreme meteorological (design) conditions, because the effectiveness of these measures does depend on the timing of the peak within the event and the amount of rainfall before, during and after the design storm. Recommended alternative design storm calculations incorporate the Sifalda-storm or are based on complete times series computations.

Practical recommendations

10. Reconsider and adapt green roof design and implementation strategies to the proposed hydrological effects and site specific requirements;
11. Pilot green roofs in different HDB areas. Measure and analyze the hydrological and non-hydrological effects of the green roof implementation, before and after the implementation;

12. Investigate the cooling effects of green roofs. This analysis showed that green roofs provide significant runoff reduction. The green roof platform measurements and the HYDRUS-1D model are perfectly suitable for a study that aims to quantify the cooling effects of green roofs in a tropical urbanized area;
13. Study the combined large-scale effects of green roofs and other LID measures;
14. Integrate all beneficial and detrimental effects of green roofs, including effects on water and air quality, aquatic flora and fauna, cooling effects, safety, recreational value, education and social interaction, roof life expectancy and construction and maintenance cost, when one wants to assess the contribution of green roofs towards a City of Gardens and Water;
15. Promote international exchange of the obtained knowledge, ideas and recommendations to help build sustainable stormwater drainage systems in other tropical cities and the rest of the world.

Literature List

All documents are cited according to the Chicago reference style guidelines

Agsys CRA. *Albedo.* 2009. http://agsys.cra-cin.it/tools/solarradiation/help/Albedo.html (accessed June 07, 2010).

Akker, C. van den, and H. Savenije. *Hydrologie 1.* Delft: Faculteit CITG, 2006.

Allen, R.G., L.S. Pereira, D. Raes, and M. Smith. *FAO irrigation and drainage paper No. 56.* Rome, Italy: Food and Agriculture Organization , 2000.

Assouline, S., and D.M. Tartakovsky. "Unsaturated hydraulic conductivity function based on a soil fragmentation process." *Water resources research*, 2001: 4.

Attorney-General's Chambers. "Sewerage and Drainage Act." *Singapore statutes online.* 15 January 2010. http://statutes.agc.gov.sg/ (accessed February 03, 2010).

Bedient, P.B., C.H. Huber, en B.E. Vieux. *Hydrology and floodplain analysis.* Upper Saddle River, NJ: Prentice Hall, Inc., 2008.

Berghage, R.D., D. Beattie, A.R. Jarett, C. Thuring, en F. Razaei. *Green roofs for stormwater control.* Cincinnati: United States Environmental Protection Agency, 2009.

Berghage, R.D., et al. *Quantifying evaporation and transpirational losses from green roofs and green roof media capacity for neutralizing acid rain.* Pennsylvania: Pennsylvania State University, 2007.

Beven, K.J. *Rainfall-runoff modelling.* Chichester: John Wiley & Sons Ltd., 2001.

Buccola, N. "A laboratory comparison of green-roof runoff." Portland: Portland State University, 21 July 2008.

Buchter, B., C. Hinz, H. Wydler, and H. Fluhler. "Evaluation of temperature and bypass flow sensitivity of tensiometers in a field soil." *Elsevier*, 1999: 281-291.

Busiek, B., B. Deutsch, A. Savineau, M. Sullivan, and H. Whitlow. *The green build-out model: Quantifying the stormwater management benefits of trees and green roofs in Washington, DC.* Washington: Casey Trees and Limno Tech, 2007.

Cantor, S.L. *Green roofs in sustainable landscape design.* New York: W.W. Norton & Company, Inc., 2008.

Carter, T. L., en T.C. Rasmussen. *Hydrologic behavior of vegetated roofs.* Athens: Journal of the American Water Resources Association, 2006.

Channelnewsasia.com. *Singapore news; Heavy rains causes knee-high floods in Bukit Timah.* 19 November 2009. http://www.channelnewsasia.com/stories/singaporelocalnews/view/1019285/1/.html (accessed February 02, 2010).

Cheney, S. *Singapore news; Flash floods in various parts of Singapore.* 05 April 2009. http://www.channelnewsasia.com/stories/singaporelocalnews/view/420283/1/.html (accessed February 02, 2010).

CISC. *NYC green roof tax abatement.* 15 December 2009. http://blog.cunysustainablecities.org/2009/03/nyc-green-roof-tax-abatement/ (accessed September 16, 2010).

Corbett, E.S., and R.P. Crouse. *Rainfall interception by annual grass and chaparral.* Research paper, Berkeley, California: Forest and Range Experiment Station, 1968.

Cuen, R.H. *Hydrologic Analysis and Design.* New Jersey: Pearson Education, Inc., 2004.

Deltares. *SOBEK; About SOBEK.* 2009. http://delftsoftware.wldelft.nl/ (accessed December 14, 2009).

Deutsch, B., M. Sullivan, H. Whitlow, and A. Savineau. *Re-greening Washington DC: A green roof vision based on quantifying storm water and air quality benefits.* Washington: Casey Trees ans Limno-Tech, 2005.

Durner (a), W., E. Priesack, H. Vogel, and T. Zurmuhl. *Determination of parameters for flexible hydraulic functions by inverse modelling.* Riverside, Califnornia: University of California, 1999.

Durner (b), W., B. Schultze, and T. Zurmuhl. *State-of-the-art in inverse modelling of inflow/outflow experiments.* Riverside, California: University of California, 1999.

Durner (c), W., U. Jansen, and S.C. Iden. "Effective hydraulic properties of layered soils at the lysimeter scale determined by inverse modelling." *European Journal of Soil Science*, 2008: 11.

Elliot, A.H., en S.A. Trowsdale. „A review of models for low impact urban stormwater design." *Elsevier*, 2005: 12.

EPA, US. *Low Impact Development.* Washington, DC: Office of water, 2000.

Etessami, K., and S. Gilmore. "Model validation and verification." *Computer science 4 & MSC: modelling and simulation.* 2008. http://www.inf.ed.ac.uk/teaching/courses/ms/notes/note14.pdf (accessed July 12, 2010).

Feddes, R.A., P. Kabat, P.J.T. van Bakel, J.J.B. Bronswijk, and J. Halbertsma. "Modelling soil water dynamics in the unsaturated zone-state of the art." *Journal of Hydrology*, 1988: 69-111.

Gemeente-Rotterdam. *Rotterdam betaalt mee aan uw groene dak.* 2009.

Google. *Google Earth.* Singapore, 12 November 2009.

Green, T.W., Z. Paydar, H.P. Cresswell, and R.J. Drinkwater. *Laboratory outflow technique for measurement of soil water diffusivity and hydraulic conductivity.* Technical report, Australia: CSIRO, 1998.

Green-buildings.com. *Green roof costs: what is the cost per square meter?* 2008. http://www.green-buildings.com/content/78335-green-roof-cost (accessed January 27, 2010).

Greenroofplants.com. *Sedum Mexicanum.* 2010. http://www.greenroofplants.com/Catalogweb/Sedum_mexicanum.htm (accessed February 17, 2010).

Gribbin, J.E. *Introduction to hydraulics and hydrology.* New York: Thomson Delmar Learning, 2007.

Gromaire-Mertz, M.C., S. Garnaud, A. Gonzales, and G. Chebbo. "Characterization of urban runoff pollution in Paris." *Water Science and Technology*, 1999: 1-8.

Hillel, D.H. *Introduction to Soil Physics.* Amherst, Massachusetts: Academic Press, 1982.

Hilten, R.N., T.M. Lawrence, and E.W. Tollner. "Modelling stormwater runoff from green roofs with HYDRUS-1D." *Elsevier*, 2008: 6.

Hoong, C.L. *The Singapore green plan 2012.* Singapore: Ministry of Environment, 2002.

Hopmans, J.W., J. Simunek, N. Romano, and W. Durner. *Inverse methods.* Madison WI: Soil Science Society of America, 2002.

Hopmans, J.W., T. Vogel, and P.D. Kobelik. "X-ray tomography of soil water distribution in one-step outflow experiments." *Soil Science Society America*, 1992: 255-262.

Hutchinson, D., P. Abrams, R. Retzlaff, and T. Liptan. *Stormwater monitoring two ecoroofs in Portland, Oregan, USA.* Chicago: Greening Rooftops for Sustainable Communities, 2003.

IMCSD. *A lively and liveable Singapore: strategies for sustainable growth.* Singapore: Ministry of Environment and Water Resources and Ministry of National Development, 2009.

InfE'de. *Ruwenbos.* 2010. http://www.infede.nl/projecten/foto-pags/fotopag-ruwenbos.htm (accessed September 16, 2010).

Joshi, U.M., and A.J.J. Vergroesen. *Green roof runoff experiments in Singapore.* NOVATECH, 2010.

Kidd, J. *Optimum green roof for Brisbane.* MSc thesis, Brisbane: University of Queensland, 2005.

Kjeilen, Tore. *Looklex Encyclopedia.* 2009. http://i-cias.com/e.o/ziggurat.htm (geopend November 17, 2009).

Klimaatinfo.nl. *Het klimaat van Singapore.* 2010. http://www.klimaatinfo.nl/singapore/ (accessed February 01, 2010).

Kodesova, R. "Determination of hydraulic properties of unsaturated soil via inverse modelling." *College lecture on Soil Physics .* Trieste: Czech University of Agriculture, 2003. 221-230.

Köhler, M., and M. Schmidt. *Water quality benefits.* Berlin: roofscapes.com, 2003.

Köhler, M., M. Schmidt, F.W. Grimme, M. Laar, and F. Gusmao. "Urban Water Rentention by Greened Roofs in Temperate and Tropical Climate." *Scientific Contributions for Sustainable Development, Vol 2*, 2001: 12.

Krause, P., D.P. Boyle, and F. Base. “Comparison of different efficiency criteria for hydrological model assessment.” *Advances in Geosciences*, 2005: 89-97.

Laar, M., and F.W.M. Grimme. “Thermal comfort and reduced flood risk through green roofs in the tropics.” *The 23rd Conferrence on Passive and Low Energy Architecture .* Geneva, Switzerland: University of Applied Sciences, Cologne, Germany, 2006. 4.

Lanks, B. *Part 2: The Green Roof.* 17 September 2008. http://www.metropolismag.com/story/20080917/part-2-the-green-roof (geopend December 08, 2009).

Leopold, L.B. *Hydrology for urban land planning; A guidebook on the hydrologic effects of urban land use.* Washington: United States Department of the Interior, 1968.

LID-centre. *The low impact development center, Inc.* 12 November 2009. http://www.lowimpactdevelopment.org/ (geopend November 17, 2009).

Mandal, U.K., K.S.S. Sarma, U.S. Victor, and N.H. Rao. “Profile Water Balance Model for Irrigated and Rainfed Systems.” *Agronomy Journal 94*, 2002: 8.

Mansell, M.G. *Rural and urban hydrology.* London: Thomas Telford Publishing, 2003.

Marsalek, J., B. Jiminez-Cisneros, M. Karamouz, P-A. Malmquist, J. Goldenfum, and B. Chocat. *Urban water cycle processes and interactions.* Paris: UNESCO, Taylor & Francis, 2008.

Marshall, T.J., J.W. Holmes, and C.W. Rose. *Soil physics.* Cambridge: Cambridge University Press, 1999.

Martin, B.K. *The dynamic stormwater response of a green roof.* MSc thesis, Guelph: University of Guelph, 2008.

Mentens, J., M. Hermy, en D. Raes. *Extensieve groene daken.* Brochure, Brussel: Agentschap voor Natuur en Bos, 2002.

Metropolismag.com. *Greenroof timeline.* 11 September 2006. http://www.metropolismag.com/story/20060911/green-roof-timeline (geopend November 18, 2009).

Moran, A., B. Hunt, en G. Jennings. *A North Carolina field study to evaluate green roof runoff quantity, runoff quality, and plant growth.* Raleigh: North Carolina State University, 2004.

Neuman, S.P., E. Bresler, P. Kowalik, and R.A. Feddes. “Finite difference and finite element simulation of field water uptake by plants.” *Hydrological Sciences Bulletin*, 1976: 81-98.

NUS geography Weather Station. *Weather station information.* 2010. http://courses.nus.edu.sg/course/geomr/front/fresearch/metstation/info01.htm (accessed February 18, 2010).

Parker, J.C., J.B. Kool, and M.T. van Genuchten. “Determining soil hydraulic properties from one-step outflow experiments by parameter estimation:II. Experimental studies.” *Soil Science Society America*, 1985: 1354-1359.

PC-PROGRESS. *HYDRUS-1D for windows.* 2008. http://www.pc-progress.com/en/Default.aspx?hydrus-1d (geopend December 13, 2009).

Pittery, Maartje, and Joost Vorstenbosch. *Handleiding daktuinen.* Amsterdam: Gemeente Amsterdam Dienst Ruimtelijke Ordening, 2004.

Pluhowski, E.J. *Urbanization and its effect on stream temperature.* Baltimore: John Hopkins University, 1968.

Post, D.E., et al. “Predicting soil albedo from soil color and spectral reflectance data.” *Soil Science Society of America Journal*, 2000: 1027-1034.

Prowell, Eric Schommer. *An analysis of stormwater retention and detention of modular green roof blocks.* MSc thesis, Athens: University of Georgia, 2006.

PUB Singapore (a). *Code of Practise on surface water drainage.* Singapore: Public Utilities Board, 2000.

PUB Singapore (b). *Western Catchment Masterplan.* Singapore: Public Utilities Board, 2007.

PUB Singapore (c). *ABC Waters Master Plan 2008.* Singapore: Public Utilities Board, 2008.

PUB Singapore (d). *Local catchment; the first national tap.* 2008. http://www.pub.gov.sg/water/Pages/LocalCatchment.aspx (accessed February 02, 2010).

PUB Singapore (e). *ABC Design Guidelines.* Singapore: Public Utilities Board, 2009.

PUB Singapore (f). *About us.* 2008. http://www.pub.gov.sg/about/Pages/default.aspx (accessed February 03, 2010).

Rotterdam, Gemeente. *Groene daken programma.* 12 November 2008. http://www.rotterdam.nl/smartsite2198164.dws (accessed December 07, 2009).

Savenije, H.H.G. *Hydrology of catchments, rivers and deltas.* Delft: TU-Delft, faculty of Civil Engineering, 2007.

Schaap, M.G., and F.J. Leij. “Improved prediction of unsaturated hydraulic conductivity with the Mualem-van Genuchten model.” *Soil Science Society of America*, 2000: 64:843-851.

SDWA. *Centre for Aquatic Science Research - Pandan.* 2010. http://www.sdwa.nus.edu.sg/index.php?option=com_content&view=article&id=61:project-pandan&catid=38:research-programmes&Itemid=109 (accessed February 02, 2010).

SEC. *2100F soilmoisture probe operating instructions.* Santa Barbara, California: Soil Moisture Equipment Corporation, 2009.

—. *Tempe Pressure Cell operating instructions.* Santa Barbara, California: Soilmoisture Equipment Corporation, 1995.

SEMP. *Tropical Storm Alisson 2001: The worst urban flood in US history.* May 21, 2005. http://www.semp.us/publications/biot_reader.php?BiotID=215 (accessed October 02, 2010).

SEPA. *Sustainable Urban Drainage Systems.* 2010. http://www.sepa.org.uk/water/water_regulation/regimes/pollution_control/suds.aspx (accessed October 01, 2010).

Simply Jean. *Orchard Road Floods.* 16 June 2010. http://blog.simplyjean.com/2010/06/16/orchard-road-floods/ (accessed Oktober 02, 2010).

Simunek (a), J., O. Wendroth, and M.T. van Genuchten. "Parameter estimation analysis of the evaporation method for determining soil hydraulic properties." *Soil Science Society America*, 1998: 894-905.

Simunek (b), J., M. Sejna, and M. van Genuchten. *Code for Simulating the One-Dimensional Movement of Water, Heat and Multiple Solutes in Variably Saturated Porous Media.* Prague: PC-Progress, 2005.

Simunek (c), J., M. Sejna, H. Saito, M. Sakai, and M.Th. van Genuchten. *The HYDRUS-1D sofware package for simulating one-dimensional movement of water, heat, and multiple solutes in variably-saturated media.* Software Manual, Riverside, California: Department of Environmental Sciences University of California Riverside, 2008.

Singapore Government. *Statistics Singapore.* 2009. http://www.singstat.gov.sg/stats/keyind.html#popnarea (accessed February 01, 2010).

Stovin, V., N. Dunnett, and A. Hallam. "Green roofs - getting sustainable drainage off the ground." *NOVATECH*, 2007: 8.

Taylor, Brian, en D.A. Gangnes. *Method for quantifying runoff reduction of green roofs.* Portland: Magnusson Klemencic Associates, 2004.

Thompson, S.A. *Hydrology for water management.* Rotterdam: Balkema, 1999.

Tielrooij, F., J. van Dijk, J.de Blecourt-Maas, A. van de Ende, G.A. Oosterbaan, en H.J. Overbeek. *Waterbeleid voor de 21e eeuw.* Den Haag: Ministerie van Verkeer en Waterstaat, 2000.

UN. *Meeting the urban challenges.* Sevilla: UN-habitat , 2008.

Universities Space Research Association. *Reflectivity in remote sensing.* 2007. http://space.hsv.usra.edu/TRESTE/07_annual_workshop_presentations/07workshop_docs/07workshop_TMCC/Reflectivity%20in%20Remote%20Sensing.pdf (accessed June 07, 2010).

USDA. *Urban hydrology for small watersheds.* Washington DC: United States Department of Agriculture, National Resources Conservation Service, 1986.

USEPA. *Reducing Urban Heat Islands: Compendium of Strategies.* Washington: U.S. Environmental Protection Agency, 2008.

van de Ven, F.H.M. *Watermanagement in Urban Areas.* Delft: TU-Delft, 2007.

van Genuchten (a), M.T. “A closed-form equation for predicting the hydraulic conductivity of unsaturated soils.” *Soil Science Society America*, 1980: 892-898.

van Genuchten (b), M.T., and D.R. Nielsen. “On describing and predicting the hydraulic properties of unsaturated soils.” *Annales Geophysicae*, 1985: 615-627.

van Woert, N.D., D.B. Rowe, J.A. Andresen, C.L. Rugh, R.T. Fernandez, and L. Xiao. “Green roof stormwater retention: effects of roof surface, slope, and media depth.” *Journal of Environmental Quality*, 11 May 2005: 9.

Velazquez, L.S. *Travels in Landscape architecture.* October 2003. http://www.greenroofs.com/archives/sg_oct03.htm (geopend November 18, 2009).

Verbraeck, A. *Discrete modellen.* Delft: Faculty of Technology, Policy and Management, TU-Delft, 2003.

Vergroesen, A.J.J. *Development of an integrated approach and modeling instrument for urban water systems .* Delft: TU-Delft, Deltares, 2010.

Ward, R.C., en M. Robinson. *Principles of hydrology.* London: Mc Graw-Hill Book Company, 1990.

Washington County Maryland. *Best Management Practices .* 2010. http://www.washco-md.net/public_works/engineering/swmstruct.htm (accessed September 16, 2010).

Watson, W.P. *Annual rainfall for U.S. states.* 2006. http://www.betweenwaters.com/etc/usrain.html (geopend December 10, 2009).

Wong, T.S.W., and C. Chen. "Use of kinematic wave method to assess effects of urban development on flood peak changes." *New Directions for Surface Water Modelling* (New Directions for Surface Water Modelling), 1989: 93-102.

Worldclimate.com. *Macritchie Res., Singapore.* 2008. http://www.worldclimate.com/cgi-bin/data.pl?ref=N01E103+2100+4869201G1 (accessed February 01, 2010).

WTCB. *Groendaken.* Brussel: Wetenschappelijk en Technisch Centrum voor het Bouwbedrijf, 2006.

Yates, S.R., M. Th. van Genuchten, A.W. Warrick, and F.J. Leij. “Analysis of measured, predicted, and estimated hydraulic conductivity using the RETC Computer Program.” *Soil Science Society of America* , 1992: 56:347-354.

Appendix 1 Green roof PI literature values

Researchers	Location	Green roof type and growing media depth	Monitoring period and # precipitation events	RPI	PDPI	DPI (min in relation to normal roofs)
(Carter and Rasmussen 2006)	Athens, USA	-Extensive -76.2 mm	-12 months -31 prec. events	-88% (light rain <2.54 cm) -54% (medium storms 2.54-7.62 cm) -48% (large storms >7.62 cm) -39-100% (precipitation event scale)	-depends on precipitation depth -0-80% peak discharge reduction (p.1269)	-17.9 min (average) -5 min (minimum) -120 min (maximum)
(van Woert, et al. 2005)	Detroit, USA	-Extensive -25 mm	-430 days -83 prec. events	-96% (light rain <2 mm) -83% (medium rain 2-6 mm) -52% (heavy rain >6 mm) -61% (for the total period)	-no information	-15 min (light rain) -5 min (medium rain) - <5 min (heavy rain)
(Stovin, Dunnett and Hallam 2007)	Sheffield, UK	-Extensive -80 mm	-3 months -11 events	-34%	-57% (average)	-no information
(Berghage, Beattie, et al. 2009)	Rock Springs, USA	-Extensive -85 mm	-11 months -111 events	-52,7% (green roofs) -14,1% (flat asphalt roof) -29,7% (media-only roof)	-59% (average based on 8 events >0.5 inch)	-no information
(Hutchinson, et al. 2003)	Oregon, USA	-Extensive -100-130 mm	-15 months -unknown # events	-69% (for the total period)	-no information	-no information
(Prowell 2006)	Athens, USA	-Extensive -100 mm	-12 months -70 events	-43% (for the total period) -67% (precipitation event scale)	-58% (p. 74)	-18 min (median times)
(Moran, Hunt and Jennings 2004)	North Carolina, USA	-Extensive -50-100 mm	-9 months	-60% (for the total period)	-85%	-no information

Appendix 2 Comparison of different loss & delay models

Model	Primary author or organization	Green roof research that use the model	Physical background of the model	Advantages	Disadvantages
Curve-number method	-United States Department of Agriculture (USDA 1986)	-Carter and Rasmussen (2006)	-Curve numbers were developed from empirical analyses of data from agricultural watersheds (USDA 1986)	-Commonly used model -Efficient and simple to use -Is useful for design purposes	-Antecedent moisture conditions are not taken into account (Prowell 2006, p.10) -Runoff output is very sensitive to small CN changes -Initial abstraction term I_a = 0.2S was found through studies in agricultural watersheds, (USDA 1986) not in urban watersheds -CN procedure is less accurate when runoff is less than 0.5 inch (USDA 1986) -Only applicable for rainfall -Does not account for delays in the runoff generation
Water Balance Model/Reservoir model	-No primary owner	-Martin (2008) -Prowell (2003)	-Mass balance equation: Inputs=Outputs+ΔStorage -Runoff begins when the storage S (field capacity) is exceeded	-Relatively easily applicable -Good way to understand the hydrological response of green roofs	-Supposes homogeneous water content distribution over the soil depth -In reality runoff begins before the field capacity is reached (Prowell 2006) -Model is very site-specific and hard to apply on different locations (labor intensive/not efficient)
Hydrus-1D	-PC-PROGRESS -J. Simunek -M. Sejna -Th. Van Genuchten	-Hilten, et al. (2008)	-HYDRUS numerically solves the Richards' equation for saturated-unsaturated water flow	-Physically the most correct description of the real processes in unsaturated soils -Scientifically verified (PC-PROGRESS 2008) -Public-domain modelling environment	-No total insight in the functioning of the model, model assumptions and mathematics. -HYDRUS appears to over-predict runoff generation during heavy rainfall (Hilten, Lawrence and Tollner 2008)

Appendix 3 Green roof vegetation development

On June 24, 2010, Sedum Mexicanum were freshly planted on green roof platforms 1 and 2. The development of the vegetation cover between July, 2009 and March, 2010 is visualized in the photographs that are presented in this appendix. In absence of any weeds, the vegetation cover in July and September, 2009 is very dense. First weeds are coming up in December, 2009. This can be seen in the top right corner of Figure (c). In March, 2010 the roof consists of half sedum and half weeds. The 1:100 year dry spell Singapore suffered in the months of January and February, 2010, reduced the sedum vegetation cover significantly. This shows that even extensive green roofs with this type of drought resistant vegetation cover do need maintenance during dry spells in tropical areas. Occasional irrigation and the removal of weeds can help to maintain a fixed, dense vegetation cover.

(a) July, 2009

(b) September, 2009

(c) December, 2009

(d) March, 2010

Appendix 4 Meteorological measurements

Meteorological data which will be used for modelling purposes are collected from the NUS meteo station and the SDWA rain gauge. The NUS meteo station is located on top of building E2, at only 100 meter from the experiment location at building EA (see Figure 21). The meteo station provides free meteorological data to students and the general public. The weather station however does not conform to WMO guidelines for weather stations in open terrain or recommendations for urban areas (NUS geography Weather Station 2010) because it is placed on a small ridge on top of the E2 university building. Atmospheric pressure [kPa], air temperature [^{0}C], relative humidity [%], wind speed [m/s], wind direction [degr], incoming radiation [W/m^2] and rainfall [mm/5min] are logged with a measurement interval of 5 minutes and can be downloaded every week from the NUS weather station website. The advantages of the broad scope of freely available data and the small distance between the meteo station and the experiments outweighs the disadvantage of the meteo station not to meet the WMO guidelines. In order to correct for rainfall measurement errors due to the positioning of measurement instruments and local rainfall differences, a 0.2 mm RG600 Global Water Tipping bucket rain gauge with a GL500-2-1 data logger has been placed next to the experiment platforms on the rooftop of building EA. The data logging measurement interval of this rain gauge has been set to 1 minute. Meteorological data from NUS is available since 2003, while rainfall data from the SDWA rain gauge is available since June 2009.

Rainfall is measured with a Global Water tipping bucket and data logger

Appendix 5 Green roof experiment measurement data

This Appendix gives a data summary of the small-scale green roof experiment platform measurements in Singapore. Information is presented for every rainfall event >0.5 mm in the four specified periods in July, September, December 2009 and March/April 2010.

General event information			Runoff depth [mm]			Peak Discharge [mm/min]			Time to Peak [min]					0-60 min base flow [mm]			0-180 min base flow [mm]		
Event date (+time of first rainfall measurement)	P [mm]	ADWP [d]	Ref	GR1	GR2	Ref	GR1	GR2	Ref -P	GR1 -P	GR2-P	GR1-Ref	GR2-Ref	Ref	GR1	GR2	Ref	GR1	GR2
July 2009																			
05/07/2009 17:20	36.83	6.3	30.66	1.05	4.64	1.21	0.05	0.12	1	48	52	47	51	0.15	-	0.37	0.15	-	0.57
06/07/2009 15:25	2.03	0.9	1.23	0.00	0.00	0.04	-	-	2	-	-	-	-	0.31	-	-	0.34	-	-
07/07/2009 12:50	1.02	0.9	0.21	0.00	0.00	0.04	-	-	-5	-	-	-	-	0.03	-	-	0.05	-	-
07/07/2009 15:55	18.54	0.1	12.19	4.39	6.85	1.11	0.19	0.22	0	35	15	35	15	0.22	0.63	1.83	0.23	0.63	2.23
08/07/2009 11:50	0.51	0.8	0.00	0.00	0.00	-	-	-	0	-	-	-	-	-	-	-	0.00	-	-
11/07/2009 08:00	2.54	2.8	1.021	0.00	0.00	0.12	-	-	0	-	-	-	-	0.18	-	-	0.25	-	-
11/07/2009 11:25	0.76	0.1	0.206	0.00	0.00	0.02	-	-	6	-	-	-	-	0.08	-	-	0.11	-	-
11/07/2009 23:35	0.76	0.5	0.183	0.00	0.00	0.04	-	-	-2	-	-	-	-	-	-	-	-	-	-
15/07/2009 07:10	24.38	3.3	19.44	0.04	0.18	1.12	0.01	0.02	-4	208	6	212	10	0.07	0.02	0.01	0.08	0.02	0.01
September 2009																			
04/09/2009 10:50	6.78	3.0	5.74	0.04	0.08	0.76	0.04	0.01	-3	-48	-48	-45	-45	0.25	-	0.03	0.31	-	0.03
05/09/2009 02:18	6.02	0.6	6.21	0.42	0.77	0.68	0.04	0.04	-3	10	22	13	25	0.40	0.24	0.78	0.42	0.24	0.92
06/09/2009 06:36	31.21	1.2	29.06	22.74	24.12	0.99	0.77	0.75	-3	0	0	3	3	0.05	-	0.31	0.05	0.01	0.49
11/09/2009 11:13	22.06	5.2	20.53	5.91	4.62	1.84	0.27	0.20	11	19	27	8	16	0.03	0.80	1.47	0.03	0.80	1.80
17/09/2009 03:06	1.00	5.7	0.5	0.00	0.00	0.04	-	-	4	-	-	-	-	0.31	-	-	0.39	-	-
17/09/2009 10:11	15.91	0.3	14.36	0.91	0.13	2.23	0.08	0.02	3	8	10	5	7	-	0.09	0.03	-	0.12	0.04
18/09/2009 11:37	7.14	1.1	6.58	1.89	1.07	1.03	0.08	0.04	3	18	22	15	19	0.55	1.54	1.04	0.59	1.57	1.31
18/09/2009 14:53	6.75	0.1	6.11	4.33	4.78	0.38	0.27	0.14	1	13	23	12	22	0.19	0.31	0.88	0.28	0.31	1.29
19/09/2009 10:15	13.59	0.8	13.14	10.06	10.39	0.77	0.48	0.46	0	16	16	16	16	0.07	0.36	0.98	0.07	0.36	1.49
19/09/2009 14:31	0.50	0.2	0.06	0.00	0.25	0.01	-	0.01	28	-	56	-	28	0.06	-	0.22	0.06	-	0.49

General event information			Runoff depth [mm]			Peak Discharge [mm/min]			Time to Peak [min]					0-60 min base flow [mm]			0-180 min base flow [mm]		
Event date (+time of first rainfall measurement)	P [mm]	ADWP [d]	Ref	GR1	GR2	Ref	GR1	GR2	Ref -P	GR1 -P	GR2-P	GR1-Ref	GR2-Ref	Ref	GR1	GR2	Ref	GR1	GR2
December 2009																			
02/12/2009 15:45	4.57	0.13	1.67	0.92	1.23	0.23	0.09	0.04	-1	57	7	58	8	0.05	0.58	0.75	0.07	0.76	1.05
03/12/2009 13:50	42.16	0.92	34.54	30.56	33.72	0.91	0.67	0.63	-39	-2	-2	37	37	0.07	0.00	0.37	0.07	0.00	0.57
04/12/2009 11:13	5.59	0.89	5.02	1.87	3.76	0.31	0.09	0.12	1	13	16	12	15	0.03	0.04	0.69	Overlap of events		
04/12/2009 13:56	5.85	0.11	5.32	4.02	5.29	0.57	0.30	0.30	0	5	5	5	5	0.13	0.67	1.61	Overlap of events		
04/12/2009 16:03	1.45	0.09	0.68	0.00	0.8	0.04	-	0.06	42	-	78	-	36	0.07	-	0.39	0.07	0.00	0.43
05/12/2009 11:29	1.87	0.81	1.37	0.03	0.5	0.11	0.00	0.01	0	119	36	119	36	0.14	0.02	0.23	Overlap of events		
09/12/2009 14:47	1.86	4.00	1.11	0.00	0.00	0.14	-	-	-2	-	-	-	-	0.26	-	-	0.26	-	-
17/12/2009 01:31	1.25	0.44	0.49	0.106	0.00	0.22	0.01	0.01	-1	-2	37	-1	38	0.12	0.00	0.11	0.13	0.00	0.24
17/12/2009 07:15	16.94	0.24	14.12	5.4	14.79	0.86	0.19	0.61	-1	6	3	7	4	0.10	0.00	0.67	0.14	0.00	1.13
17/12/2009 14:16	1.87	0.29	0.89	0.08	0.95	0.16	0.01	0.03	-1	25	9	26	10	0.08	0.05	0.62	0.09	0.05	0.86
18/12/2009 05:15	3.31	0.62	1.83	0.00	1.45	0.06	-	0.04	0	-	4	-	4	0.07	0.00	0.57	0.10	0.00	0.91
19/12/2009 04:26	1.03	0.97	0.47	0.00	0.00	0.03	-	-	39	-	-	-	-	0.09	0.00	0.00	0.15	0.01	0.00
19/12/2009 13:02	11.21	0.36	7.83	3.94	6.64	0.36	0.16	0.20	-1	49	50	50	51	0.02	0.00	0.31	0.02	0.00	0.61
20/12/2009 14:45	5.02	1.07	3.3	0.42	2.02	0.44	0.03	0.08	0	9	10	9	10	0.08	0.05	0.38	0.09	0.08	0.66
21/12/2009 10:43	0.62	0.83	0.19	0.01	0.00	0.06	0.00	-	-1	37	-	38	-	0.10	0.01	0.00	Overlap of events		
21/12/2009 13:09	0.83	0.10	0.00	0.00	0.00	-	-	-	-	-	-	-	-	-	-	-	-	-	-
22/12/2009 00:07	16.41	0.46	13.33	8.67	11.39	0.61	0.34	0.38	-1	4	3	5	4	0.21	1.63	2.24	0.21	1.82	2.40
23/12/2009 13:57	0.62	1.58	0.19	0.00	0.00	0.04	-	-	22	-	-	-	-	0.13	0.00	0.00	Overlap of events		
24/12/2009 05:14	1.65	0.64	0.9	0.04	0.01	0.06	0.00	0.00	21	104	5	83	-16	0.08	0.01	0.00	Overlap of events		
24/12/2009 07:32	6.00	0.10	3.78	0.6	1.87	0.06	0.01	0.03	2	33	30	31	28	0.10	0.26	0.53	0.10	0.36	0.77
25/12/2009 14:35	8.35	1.29	6.84	2.49	3.22	0.66	0.11	0.11	-1	29	30	30	31	0.24	0.88	1.00	Overlap of events		
25/12/2009 17:00	13.83	0.10	12.3	11.39	12.53	1.36	0.91	1.00	-2	4	4	6	6	0.09	1.88	2.15	0.09	2.46	2.72
26/12/2009 14:54	5.79	0.91	4.22	2.08	2.56	0.20	0.04	0.05	0	29	27	29	27	0.29	0.47	0.41	0.31	0.81	0.58

General event information			Runoff depth [mm]			Peak Discharge [mm/min]			Time to Peak [min]					0-60 min base flow [mm]			0-180 min base flow [mm]		
Event date (+time of first rainfall measurement)	P [mm]	ADWP [d]	Ref	GR1	GR2	Ref	GR1	GR2	Ref -P	GR1 -P	GR2-P	GR1-Ref	GR2-Ref	Ref	GR1	GR2	Ref	GR1	GR2
March and April 2010																			
10/03/2010 04:35	21.81	5.5	17.95	NM	1.57	0.77	NM	0.05	-2	NM	156	NM	158	0.14	NM	0.48	0.14	NM	0.64
10/03/2010 12:05	1.03	0.3	0.28	NM	0.33	0.04	NM	0.06	2	NM	88	NM	86	0.03	NM	0.22	0.03	NM	0.24
13/03/2010 16:44	9.35	3.2	6.39	NM	0.00	0.74	NM	-	-1	NM	-	NM	-	0.13	NM	0.00	0.17	NM	0.00
14/03/2010 14:34	32.02	0.9	26.23	NM	15.75	0.99	NM	0.70	-3	NM	127	NM	130	0.07	NM	1.00	0.07	NM	1.42
15/03/2010 14:09	3.11	1.0	2.09	NM	0.15	0.15	NM	0.03	-2	NM	95	NM	97	0.34	NM	0.15	0.41	NM	0.27
18/03/2010 11:18	1.24	2.9	0.22	NM	0.00	0.02	NM	-	-1	NM	-	NM	-	0.04	NM	0.00	Overlap of events		
18/03/2010 13:45	3.52	0.1	2.16	NM	0.00	0.21	NM	-	1	NM	-	NM	-	0.22	NM	0.00	Overlap of events		
18/03/2010 15:33	3.52	0.1	2.63	NM	0.00	0.08	NM	-	-4	NM	-	NM	-	0.16	NM	0.00	0.16	NM	0.00
19/03/2010 14:46	1.02	1.0	0.46	NM	0.00	0.03	NM	-	3	NM	-	NM	-	0.05	NM	0.00	0.05	NM	0.00
19/03/2010 18:01	3.81	0.1	2.57	NM	0.00	0.13	NM	-	-2	NM	-	NM	-	0.16	NM	0.00	Overlap of events		
20/03/2010 08:51	8.13	0.6	7.88	NM	5.01	0.05	NM	0.06	1	NM	232	NM	231	0.19	NM	0.68	0.19	NM	0.76
21/03/2010 14:56	53.60	1.3	50.61	NM	46.05	2.71	NM	1.99	1	NM	15	NM	14	0.21	NM	0.88	0.21	NM	1.24
22/03/2010 15:31	1.02	1.0	0.88	NM	0.00	0.13	NM	-	-3	NM	-	NM	-	0.12	NM	0.00	0.18	NM	0.00
23/03/2010 08:21	16.76	0.7	15.75	NM	12.50	0.80	NM	0.42	25	NM	18	NM	-7	0.13	NM	0.63	0.13	NM	0.93
30/03/2010 15:33	19.45	7.3	17.54	NM	0.06	0.63	NM	0.01	2	NM	11	NM	9	0.27	NM	0.01	0.27	NM	0.02
02/04/2010 04:32	0.62	2.5	0.16	NM	0.00	0.02	NM	-	11	NM	-	NM	-	0.08	NM	0.00	0.08	NM	0.00
02/04/2010 19:46	9.08	0.6	7.51	NM	0.00	0.89	NM	-	3	NM	-	NM	-	0.82	NM	0.00	0.86	NM	0.00
03/04/2010 15:02	2.07	0.8	1.45	NM	0.00	0.03	NM	-	2	NM	-	NM	-	0.30	NM	0.00	0.38	NM	0.00
04/04/2010 06:10	9.51	0.6	8.51	NM	3.04	0.13	NM	0.07	79	NM	92	NM	13	0.22	NM	0.72	0.23	NM	0.87
05/04/2010 14:06	5.83	1.3	4.60	NM	0.96	0.34	NM	0.07	42	NM	45	NM	3	0.77	NM	0.93	Overlap of events		
05/04/2010 17:02	0.62	0.1	0.00	NM	0.00	-	NM	-	-	NM	-	NM	-	0.20	NM	0.17	0.20	NM	0.36
08/04/2010 09:44	6.33	2.7	5.01	NM	0.00	0.62	NM	-	4	NM	-	NM	-	0.61	NM	0.00	0.65	NM	0.00
08/04/2010 18:08	1.24	0.4	0.56	NM	0.00	0.08	NM	-	2	NM	-	NM	-	0.09	NM	0.00	0.12	NM	0.00
09/04/2010 14:21	23.95	0.8	20.67	NM	9.93	1.13	NM	0.78	1	NM	70	NM	69	0.17	NM	0.81	0.17	NM	1.07

NM: no measurement data is available for green roof platform 1 in the March-April period

Appendix 6 Seepage face experiment description

The available storage capacity of a soil under normal conditions is equal to the soil volume multiplied with the empty pore space fraction. The empty pore space fraction is equal to the saturated soil water content θ_s minus the actual soil water content θ at time *t*. Based on van Genuchten's unimodal pore-size distribution model (Eq. 5.9), the maximum storage capacity is equal to the saturated soil water content θ_s minus the residual soil water content θ_r at wilting point. Green roof experiment measurements show that gravity drainage across the bottom of the soil media occurred before the soil becomes saturated (*h*=0 cm). This decreases the available storage capacity of the roof and therefore has to be incorporated into the model.

Experiment goal

The HYDRUS model allows for a specification of a water pressure head other than zero (h_{seep}) for triggering flux across the seepage face (PC-PROGRESS 2008). Determination of this water pressure head at which a flux across the seepage face starts, is the main goal of the seepage face experiment.

Experiment theory

According to the soil water retention theory (Hillel 1982), a water pressure head always corresponds to a soil specific volumetric water content θ. Because it is easier to measure the volumetric soil water content at the moment that runoff starts or ends, two experiments were performed to determine the value for θ_{seep}: the volumetric water content for triggering flux across the seepage face. The value for h_{seep} can directly be obtained from the soil specific soil water retention curve for potting soil afterwards. The two seepage face experiments are:

1. Oven drying of freshly drained in situ soil samples at 105^0C;
2. Direct in situ soil water content measurements with a Time Domain Reflectrometer (TDR).

The volumetric water content θ can be formulated as follows (Hillel 1982):

$$\theta = \frac{V_w}{V_t} \qquad \text{[Eq. A6.1]}$$

where V_w and V_t are the volume of water and the total soil body [L^3]. The volume of water equals:

$$V_w = \left(\frac{M_w - M_{dry}}{\rho_{water}}\right) \qquad \text{[Eq. A6.2]}$$

where M_w is the mass of the wet soil [M], M_{dry} is the mass of the soil after 24h oven drying at 105^0C [M] and ρ_{water} is the density of water [ML^{-3}]. When Eq. A5.2 is substituted into Eq. A5.1 and rewritten, an expression is obtained were the water content is a function of the wet and dry mass, the density of water and a total sample volume:

$$\theta = \frac{M_w - M_{dry}}{\rho_{water} \cdot V_t} \qquad \text{[Eq. A6.3]}$$

This equation is used to calculate θ_{seep} at the first experiment type. The TDR was especially calibrated for potting soil media, and directly shows a value for θ_{seep} on the screen and is easy to use.

Experiment materials
The materials for the oven drying experiments are:

- In situ soil samples from the green roof platform after a runoff event;
- Soil core samplers;
- Laboratory oven;
- Balance.

In situ soil samples from the green roof platform were weighed before and after 24 hours of oven drying at 105 ^{0}C. The volume was determined and the volumetric water content for triggering flux across the seepage face θ_{seep} was determined with Eq. A5.3.


In-situ core sampling activities

Laboratory oven

The materials for the in situ TDR measurements are:

- TDR measurement device.

In situ measurements were performed at the green roof platform. The TDR device consists of a measurement probe and a display unit. A calibrated soil water content value can be read out directly from the display unit, when the probe is placed into the soil.

TDR soil water content measurement probe


TDR display unit

Oven drying experiment results

Three drained out in situ samples of the green roof were taken and oven dried at 105^0C. The average moisture content θ_{seep} has been calculated using Eq. 5.3. The three θ_{seep} values were 0.59, 0.60 and 0.65. The average θ_{seep} value is 0.61, but the results show some spatial variation over the roof.

	Experiment 1	**Experiment 2**	**Experiment 3**
Sample volume [cm^3]	93.1	93.1	104.8
Wet weight of the sample [gr]	124.2	118.8	132.1
Oven dry weight of the sample [gr]	63.9	62.7	70.3
Dry bulk density [gr/cm^3]	0.20	0.19	0.19
θ_{seep} [-]	0.65	0.60	0.59

TDR measurement results

The TDR device was only available in the last week of April 2010. Measurements on April 23 showed that the maximum θ_{seep} was 0.61 while at some points in the green roof 0.52 was measured as the maximum soil water content. On April 26, a soil water content between 0.58 and 0.65 was measured after a rainfall event with small runoff quantities.

Appendix 7 Spatial discretization-profile

The spatial discretization of the green roof experiment model contains of a 12 cm soil with 100 nodes.

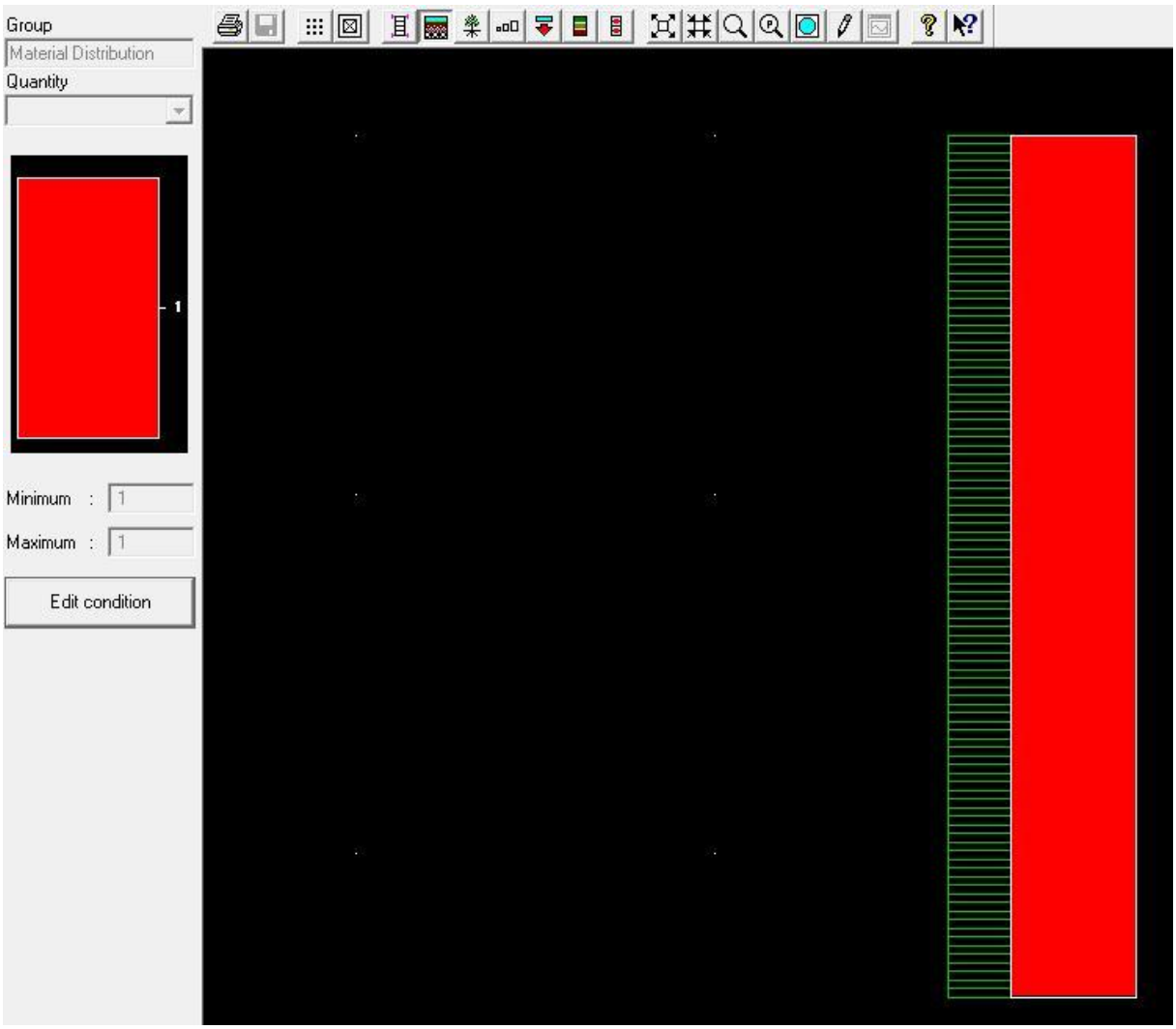

Appendix 8 Potting soil permeability experiments

Experiment goal

Determination of the saturated hydraulic conductivity or permeability K_s, of the potting soil which is used as the growing media in the rooftop experiments at the NUS. K_s is one of the hydraulic parameters which will serve as an input for the HYDRUS-1D model.

Experiment theory

Two types of tests are generally performed to obtain an empirical value for the saturated coefficient of permeability. These are the constant head permeability test and the falling head permeability test. In this experiment the constant head permeability test procedure will be used because first estimates provide information that the permeability of potting soil will exceed 10^{-4} cm/s. When a constant water head is provided on a permeameter, K_s can be calculated according to Darcy's law:

$$Q = K \cdot A \cdot \frac{\Delta h}{L} \qquad \text{[Eq. A8.1]}$$

where Q is the discharge [L^3T^{-1}], K stands for the permeability [LT^{-1}], A is the cross sectional area of flow [L^2], Δh is the constant head difference [L] and L is the length of the soil column [L]. Derived from Darcy's law, the permeability can be expressed in the remainder of available terms, together with the relation between water volume V and discharge Q (Q=V/t):

$$K = \frac{V \cdot L}{A \cdot t \cdot \Delta h} \qquad \text{[Eq. A8.2]}$$

where K is the permeability [LT^{-1}], V is the flow through water volume during experiment [L^3], L is the length of the soil column [L], A is the cross sectional area of flow [L^2], t is the experiment flow through time [T] and Δh is the constant head difference [L]. The saturated coefficient of permeability can be measured when the soil is totally saturated during the flow through time of the experiment.

Experiment materials

The experimental set-up consists of the following components:

- Constant head permeameter;
- Precise measuring jug with a volume of 2 litre;
- A water input tube connected to the drinking water tap;
- An excess outflow tube to keep a constant head and which is connected to the sink;
- A soil column of 22 cm potting soil with a filter fabric sheet, a 5 cm drainage layer on the bottom, a filter fabric sheet and a 3 cm drainage layer on top. Two big rocks were put on the soil column to prevent floating of the soil and drainage material. It is to be assumed that these rocks do not influence the permeability of the soil.


Experiment results

The table in this appendix shows the experiment results of the permeability experiments.

The rows represent volume measurements at certain time *t* [min'sec]. In experiment 1, 800 ml was flown out of the permeameter in 15'24 at constant head difference Δh of 34 cm and in experiment 2 1300 ml was flown out in 17'37 at a constant head difference Δh of 42.5 cm. K_s has been calculated accordingly. The average K_s for the potting soil is (24.7+28.0)/2 = 26.3 m/d or 110 cm/h.

	Experiment 1		**Experiment 2**	
	V [ml]	**t [min'sec]**	**V [ml]**	**t [min'sec]**
Volume measurement 1	0	0'00	0	0'00
Volume measurement 2	100	1'52	200	2'38
Volume measurement 3	200	3'56	300	4'04
Volume measurement 4	300	5'49	400	5'26
Volume measurement 5	400	7'50	600	8'00
Volume measurement 6	500	9'50	800	10'45
Volume measurement 7	600	11'44	1100	15'10
Volume measurement 8	700	13'33	1300	17'37
Volume measurement 9	800	15'24		
Total volume	800		1300	
Δh	34 cm		42.5cm	
A (D=5 cm)	19.63 cm^2		19.63 cm^2	
L	22 cm		22 cm	
Total t	15'24		17'37	
K_s	24.7 m/d		28.0 m/d	

Appendix 9 Inverse modelling outflow experiments

Experiment materials

The outflow experiment set-up is based on existing technical operating instructions for outflow experiments with Tempe Pressure Cells (SEC 1995, Green, et al. 1998). This experiment set-up has been used by several other scientists to determine the soil hydraulic parameters of soils (Durner (a), et al. 1999, Parker, Kool and van Genuchten 1985). The experiment set-up description in this appendix gives an overview of the used materials, methodology and input for the numerical simulations. The experimental set-up consists of the following main components:

- Soil Moisture Equipment Corp. Tempe Pressure Cell, type #1450. A 30 mm high brass cylinder with a 85 mm diameter has been used;
- Prepared (OSO#1, OSO#2, MSO#1-3) or undisturbed (MSO#4-5) soil samples;
- A Pressure line. A regulated gas pressure line has been used for all experiments except for MSO#4 and MSO#5. In these experiments a tank with compressed gas has been used to reduce pressure variations;
- Pressure transducer. The pressure transducer measures the actual pressure and is used to monitor the cell pressure at the start and during the experiments;
- Outflow tube and water collection bulb to collect the outflow water;
- Data loggers for the balance readings and pressure transducer measurements.

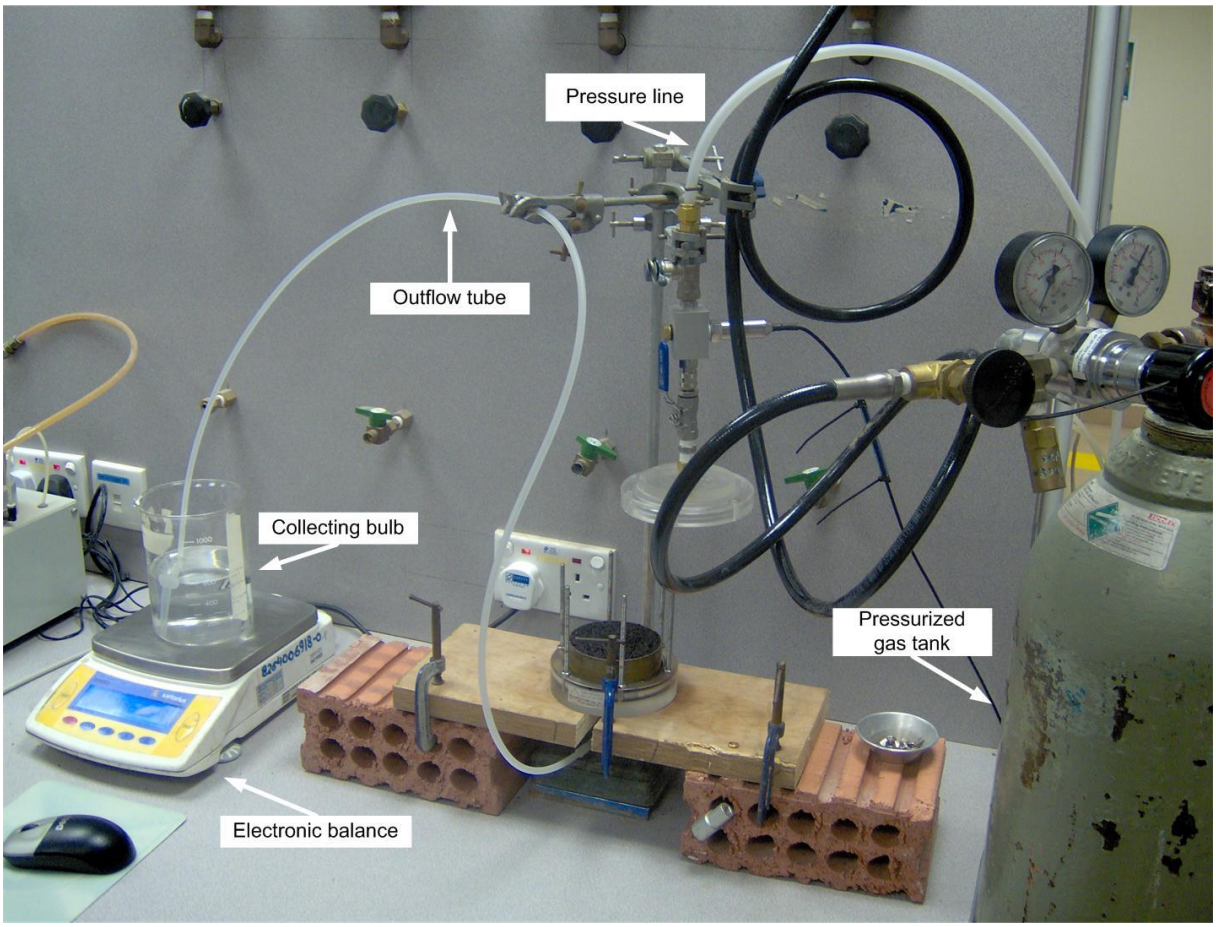

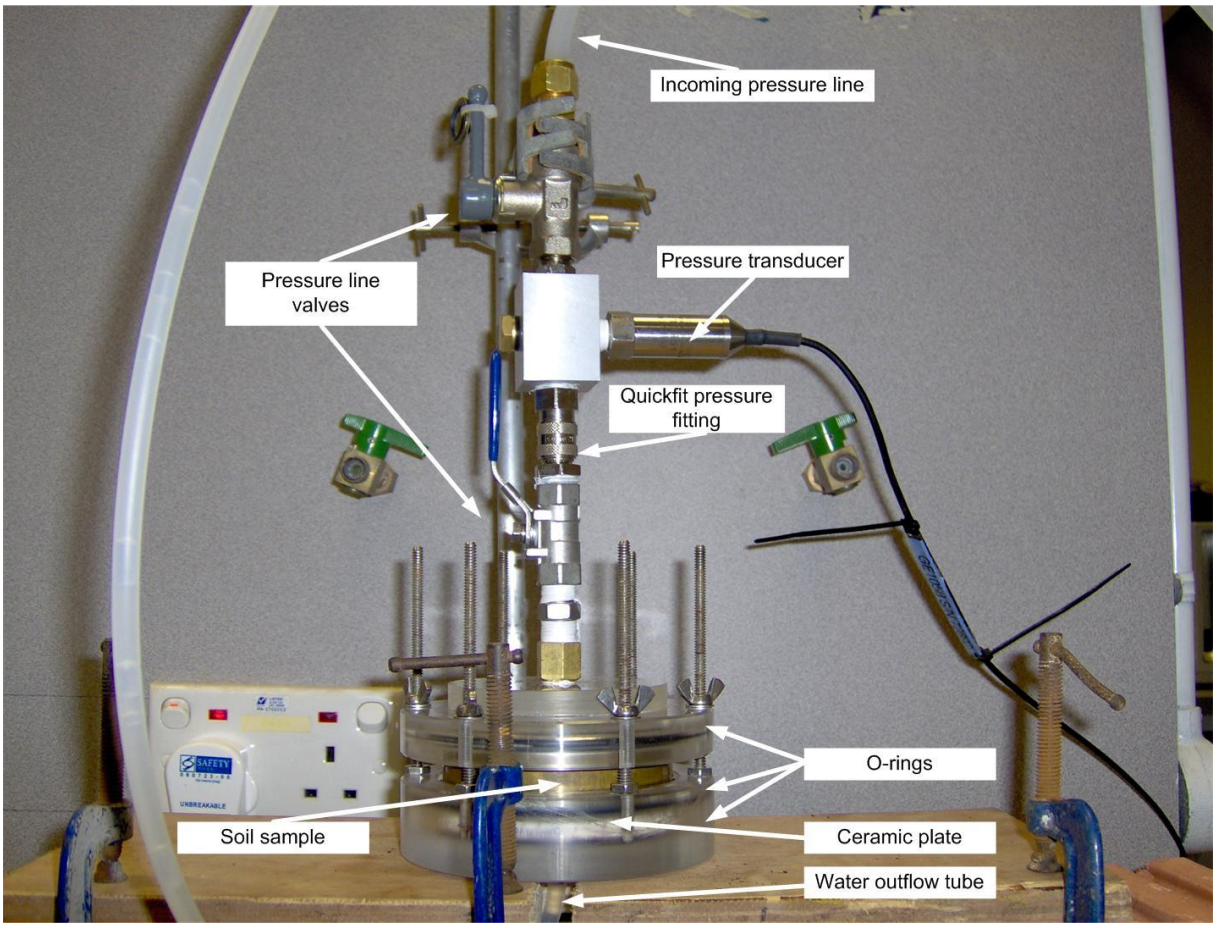

Experiment methods

The experimental methodology is based on technical operating manuals for the use of Tempe Pressure Cells (SEC 1995, Green, et al. 1998). The following process cycle was performed for every outflow experiment and consists of 7 main sub processes:

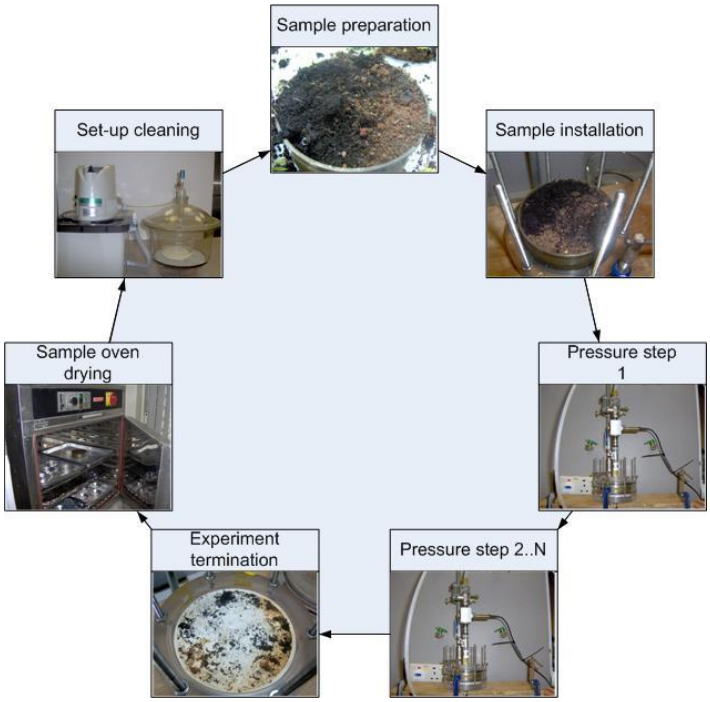

1. Sample preparation: placement of the soil sample in the brass cylinder;

2. Sample installation: insertion of the soil sample in the Tempe Cell and initial wetting;

3-4. Pressure steps 1..N: pressure steps are initiated by changing the pressure head and opening of the valves;

5. Experiment termination: after the last pressure step, the sample is removed from the Tempe Cell;

6. Sample oven drying: includes soil sample weighing before and after 24h oven drying at 105^0C;

7. Set-up cleaning: set-up cleaning and saturation and deaeration of the ceramic plate in a vacuum desiccator.

Experiment input for the numerical simulation

The following table shows the experiment input for the numerical simulations in HYDRUS-1D for all performed experiments:

- 2 One-step outflow experiments (OSO-1 and OSO-2);
- 3 Multi-step outflow experiments with prepared soil samples (MSO-1, MSO-2 and MSO-3);
- 2 Multi-step outflow experiments with undisturbed soil samples (MSO-4 and MSO-5).

Run	**Initial conditions**	**Boundary conditions**	**Measurement set m_y**	**Number of data points n_j**	**Weight of the data points**
OSO-1	$h(z,t) = h_i(z)$ $t = 0, 0 \le z \le L$	top $q(z,t) = 0$ $t > 0, z = L$	q(t)	21	1
		bottom $h(z,t) = -1000$ cm $0 \le t \le 72, z = 0$	θ(-1000 cm)	1	1
OSO-2	$h(z,t) = h_i(z)$ $t = 0, 0 \le z \le L$	top $q(z,t) = 0$ $t > 0, z = L$	q(t)		
		bottom $h(z,t) = -1000$ cm $0 \le t \le 72, z = 0$	θ(-1000 cm)	1	1
MSO-1	$h(z,t) = h_i(z)$ $t = 0, 0 \le z \le L$	top $q(z,t) = 0$ $t > 0, z = L$	q(t)	107	1
		bottom $h(z,t) = -100$ cm $0 \le t \le 11, z = 0$ $h(z,t) = -250$ cm $11 \le t \le 23, z = 0$ $h(z,t) = -500$ cm $23 \le t \le 35, z = 0$ $h(z,t) = -1000$ cm $35 \le t \le 47, z = 0$	θ(-100 cm) θ(-250 cm) θ(-500 cm) θ(-1000 cm)	4	1
MSO-2	$h(z,t) = h_i(z)$ $t = 0, 0 \le z \le L$	top $q(z,t) = 0$ $t > 0, z = L$	q(t)	192	1
		bottom $h(z,t) = -20$ cm $0 \le t \le 20, z = 0$ $h(z,t) = -40$ cm $20 \le t \le 46, z = 0$ $h(z,t) = -60$ cm $46 \le t \le 70.08, z = 0$ $h(z,t) = -80$ cm $70.08 \le t \le 94, z = 0$ $h(z,t) = -100$ cm $94 \le t \le 118, z = 0$	θ(-20 cm) θ(-40 cm) θ(-60 cm) θ(-80 cm) θ(-100 cm) θ(-250 cm) θ(-500 cm) θ(-1000 cm)	8	10

Run	Initial conditions	Boundary conditions	Measurement set m_y	Number of data points n_j	Weight of the data points
MSO-3	$h(z,t) = h_i(z)$ $t = 0, 0 \le z \le L$	top $q(z,t) = 0$ $t > 0, z = L$	q(t)	134	1
		bottom $h(z,t) = -23.5$ cm $0 \le t \le 12, z = 0$ $h(z,t) = -37$ cm $12 \le t \le 24, z = 0$ $h(z,t) = -51$ cm $24 \le t \le 36, z = 0$ $h(z,t) = -80$ cm $36 \le t \le 48, z = 0$ $h(z,t) = -100$ cm $48 \le t \le 60, z = 0$	θ(-23.5 cm) θ(-37 cm) θ(-51 cm) θ(-80 cm) θ(-100 cm) θ(-250 cm) θ(-500 cm) θ(-1000 cm)	8	10
MSO-4	$h(z,t) = h_i(z)$ $t = 0, 0 \le z \le L$	top $q(z,t) = 0$ $t > 0, z = L$	q(t)	156	1
	UNDISTURBED SOIL SAMPLE	bottom $h(z,t) = -24.5$ cm $0 \le t \le 12, z = 0$ $h(z,t) = -43.9$ cm $12 \le t \le 24, z = 0$ $h(z,t) = -61.2$ cm $24 \le t \le 36, z = 0$ $h(z,t) = -81.6$ cm $36 \le t \le 48, z = 0$ $h(z,t) = -100$ cm $48 \le t \le 60, z = 0$ $h(z,t) = -194.9$ cm $60 \le t \le 68, z = 0$	θ(-24.5 cm) θ(-43.9 cm) θ(-61.2 cm) θ(-81.6 cm) θ(-100 cm) θ(-194.9 cm)	6	10
MSO-5	$h(z,t) = h_i(z)$ $t = 0, 0 \le z \le L$	top $q(z,t) = 0$ $t > 0, z = L$	q(t)	116	1
		bottom $h(z,t) = -20$ cm $0 \le t \le 24, z = 0$ $h(z,t) = -60$ cm $12 \le t \le 48, z = 0$ $h(z,t) = -100$ cm $24 \le t \le 69.75, z = 0$	θ(-20 cm) θ(-60 cm) θ(-100 cm)	3	10

Appendix 10 Inverse modelling evaporation experiment

Experiment materials

The evaporation experiment is based on the Wind Method (Simunek (a), Wendroth and van Genuchten 1998). The main difference between both experiments is that the Wind Method evaporation experiment is a laboratory inverse experiment while the evaporation experiment in this research was carried out under field conditions: on the same rooftop as the green roof platforms in Singapore. The evaporation experiment was performed in the dry month of February between February 23, 2010 and March 08, 2010 (t_{total} = 18000 minutes). During these 18000 minutes, the pressure head was monitored at selected times t_j at two different depths z_i (1.5 and 5.5 cm from the bottom of the 10 cm soil layer). The total weight of the soil tray was measured on a 2-second time interval. The experimental set-up consists of the following main components:

- 2 Soil Moisture Equipment Corp. tensiometers, type 2100F. A tensiometer consists of a porous ceramic cup with a 6 mm diameter and 25 mm length, a 1.8 m long nylon tube which connects the tensiometer body with the ceramic cub that is submerged in the potting soil, and a dial gauge that allows negative pressure readings from 0 – 100 centibar (1 centibar = 0.01 bar or 1 kPa or 10.2 cm H_2O);
- 2 balances, which are connected to a PC with data logging system;
- A tray with a 5 cm drainage layer and a 10 cm potting soil layer;
- An aluminium reflection layer to minimize sideways heating up of the soil sample.

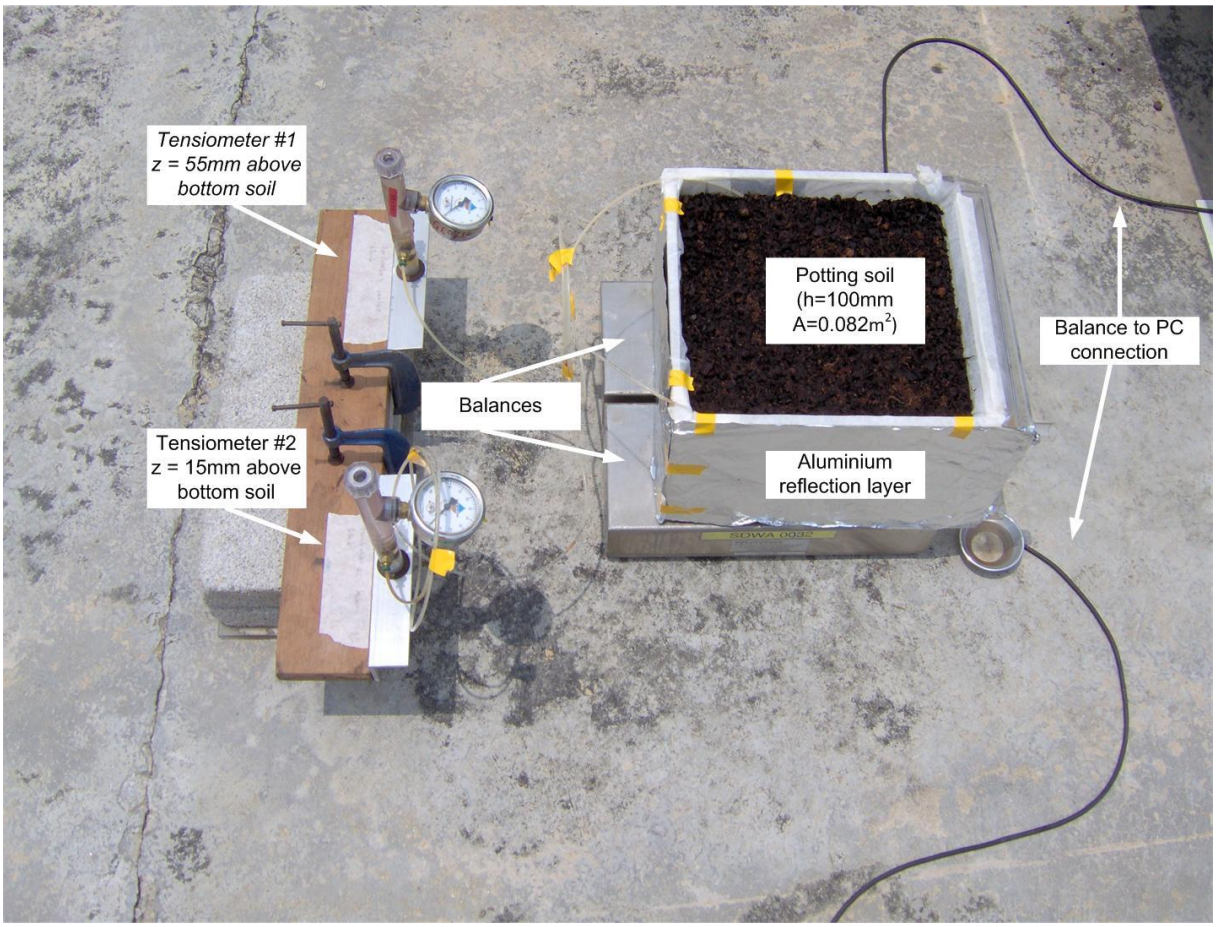

Experiment methods

The evaporation experiment is a specific transient flow experiment where measured water pressure heads and measured evaporation values will be compared to numerically optimized values of the pressure heads and measured evaporation in HYDRUS-1D which correspond to an optimized hydraulic parameter vector **b**. The following steps were performed in the evaporation experiment:

1. Tensiometer preparation: before placing the tensiometers in the tray with potting soil, the ceramic cups were deaerated in an ultrasonic bath. Next, both tensiometers were prepared according to the operating instructions from the Soilmoisture Equipment Corporation (SEC 2009). This includes removing any excess air from the tensiometer tube and dial gauge with a vacuum desiccator;

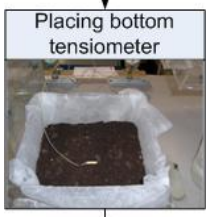

2. Placing the bottom tensiometer: after preparation of the tray with a 5 cm drainage layer and a filter fabric, the first tensiometer is placed at 1.5 cm from the soil bottom. The bottom tensiometer had a kink in the nylon tube near the ceramic cup, which might affect the tensiometer readings;

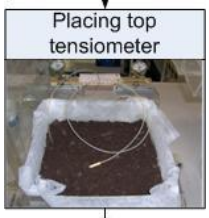

3. Placing the top tensiometer: the top tensiometer is placed 4 cm higher than the bottom tensiometer, at 5.5 cm from the soil bottom. The top tensiometer was in good shape;

4. Topping off with soil: on top of the top tensiometer, 4.5 cm soil was placed;

5. Initial wetting of the soil: the evaporation experiment tray has been wetted with an artificial rain simulator in the lab. The initial wetting was terminated at θ_{seep} = 0.61. This is the moisture content at which the soil starts draining to the drainage layer;

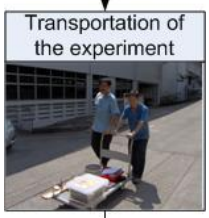

6. Transportation: the evaporation experiment set-up was transported after preparation and initial wetting. During transportation and installation, the experiment set-up was covered to prevent early evaporation;

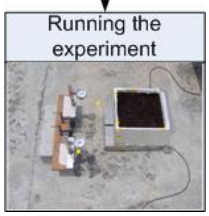

7. Running the experiment: the evaporation experiment ran between 23 February 2010, 12:00 and 07 March 2010, 23:59. During the experiment the water pressure heads were monitored at selected times. The total experiment weight has been logged automatically on a 2-second time interval.

Experiment input for the numerical simulation

The following table shows the evaporation experiment input for the numerical simulations in HYDRUS-1D:

Run	**Initial conditions**	**Boundary conditions**	**Measurement set m_y**	**Number of data points n_j**	**Weight of the data points**
EVAP	$\theta(z,t) = \theta_i(z)$ $t = 0, 0 \le z \le L$	top $q(z,t) = q_{evap}(t)$ $t > 0, z = L$	*ACSF(t)*	300 (1 data point per hour)	1
		bottom $q(z,t) = 0$ $t > 0, z = 0$	*h(t)*	18	1

where θ_i is the initial soil water content [-], z is the vertical coordinate positive upwards [L], q is the flux density [LT^{-1}] and q_{evap} is the time-variable evaporation rate imposed at the soil surface [LT^{-1}] (Simunek (a), Wendroth and van Genuchten 1998, Hopmans, Simunek, et al. 2002).

Measurement set AC*SF(t)* is the actual cumulative surface flux (infiltration/evaporation -/+). In absence of rainfall, or in periods when the cumulative evaporation exceeds the cumulative infiltration, A*CSF(t)* is always positive. For the numerical optimization 300 A*CSF(t)* data points were used. The A*CSF(t)* values were calculated from balance measurements. Measurement set *h(t)* consists of tensiometer readings. For the numerical optimization 18 tensiometer reading s from the top tensiometer with *z*=5.5 cm were used. The bottom tensiometer readings showed non-consistent values. This is probably caused by a kink in the nylon tube of the bottom tensiometer. Based on the recommendations in paragraph 5.3.3.1 to minimize measurement errors of data in the objective function E(**b**,y), only tensiometer data from the top tensiometer were added to the objective function. Severe oscillations in both tensiometers were observed during the day. This is probably caused by temperature differences that affect the tensiometer performance. Buchter, et al. (1999) evaluated the sensitivity of tensiometers in a field soil to temperature. Their results show that temperature changes can introduce errors of several tens of hectopascals (Buchter, et al. 1999). Since 1 hPa is equal to 1 cm H^2O, the introduced error can be in the order of tens of centimetres. Errors in the order of tens of centimetres will definitely have a negative influence on the numerical optimization. Because of the relatively high value of the pore-size distribution parameter *n* for potting soil, small errors in the measured water pressure can lead to wrongly optimized values of the soil hydraulic parameters. This in turn, can lead to ill-posedness of the inverse solution (Hopmans, Simunek, et al. 2002).

Because the top boundary condition is an atmospheric boundary condition, one has to specify albedo values which account for the solar radiation reflectivity. The following table shows wet and dry dark soil albedo literature values:

Literature source	Albedo dry dark soil	Albedo wet dark soil
(Agsys CRA 2009)	0.13	0.08
(Universities Space Research Association 2007)	0.1	0.09
(Post, et al. 2000)	-	0.048
(Allen, et al. 2000)	-	0.05
(Ward and Robinson 1990)	<0.40	>0.05

Albedo values are used to calculate the net solar radiation R_{ns} [MT^{-3}] from measured solar or shortwave radiation R_s [MT^{-3}], according to the following formula (Allen, et al. 2000):

$$R_{ns} = (1 - \alpha_r)R_s \qquad \text{[Eq. A10]}$$

where α_r is the albedo value [-]. Since the albedo value influences the total potential evapotranspiration, a correct representation of this input parameter is important. The albedo value for the evaporation experiment has been established by running simulations for α_r = 0.05, 0.07, 0.09, 0.11, 0.13 and 0.15 under two different sets of initial values in a numerical simulation with three free parameters (θ_r, α and n). The initial values of the series are: series 1(θ_r = 0.2, α = 0.1 and n = 1.5) and series 2 (θ_r = 0.3, α = 0.2 and n = 2). The results of the albedo analysis show that an albedo of 0.09 gives the lowest average deviations between the measured cumulative surface flux and the simulated surface flux (SSQ = 10.45). Both lower and higher albedo values give higher SSQ's, which means that 0.09 is the optimal average value during the whole evaporation experiment.

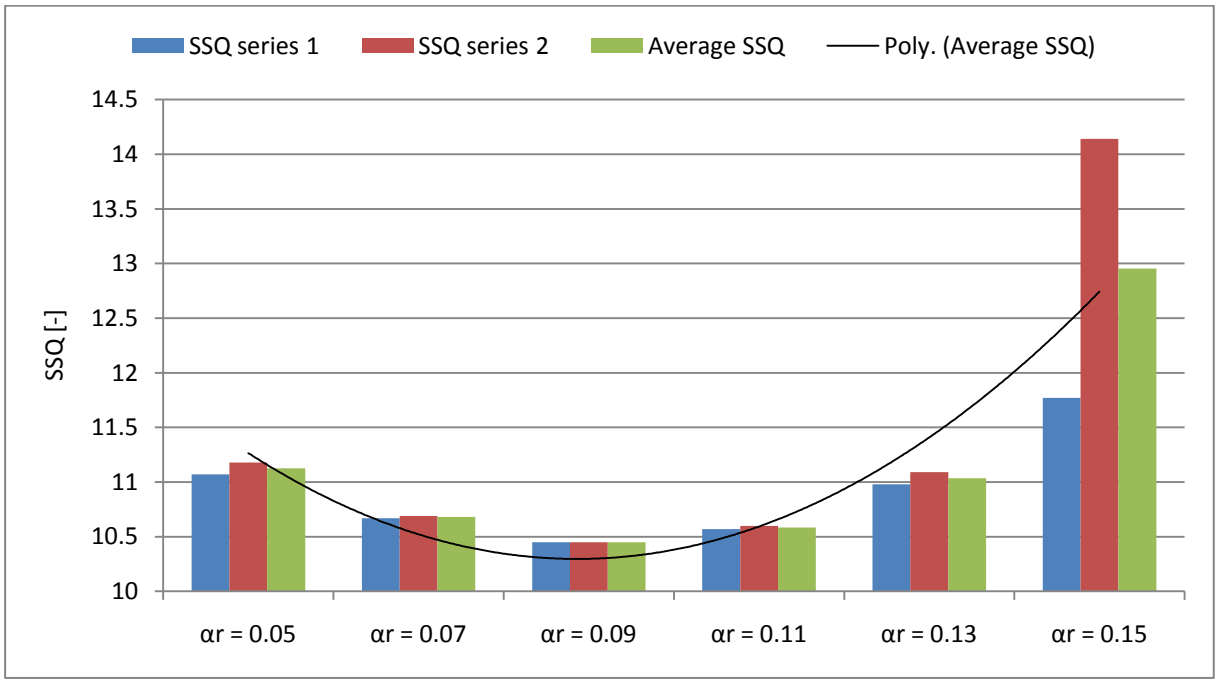

When one takes a closer look at the measured versus simulated actual surface flux, two main conclusions can be drawn:

1. The simulations underestimate the actual cumulative surface flux in the wet range (23th - 27th of February) for all albedo values;
2. Although one constant albedo value is not sufficient to exactly mimic the measured evaporation over time, the absolute error is smaller than 3 mm at any time during the experiment.

It is observed that, independent of the albedo value, the model simulations underestimate the evaporation in the first three days. This indicates too low potential cumulative surface fluxes in this region. Important underlying factors of these deviations could be measurement errors in the meteorological input data and/or evaporation or water (vapor) transport at the lower boundary (the drainage layer). Next, the potential evaporation in this experiment's simulations are based on the Penman-Monteith equation, which was developed by defining the reference evapotranspiration from a reference crop with a height of 0.12 m and an albedo of 0.23 (Allen, et al. 2000). Based on the experiment, the appropriateness of the Penman-Monteith equation to calculate bare soil potential evaporation under tropical conditions, can be questioned.

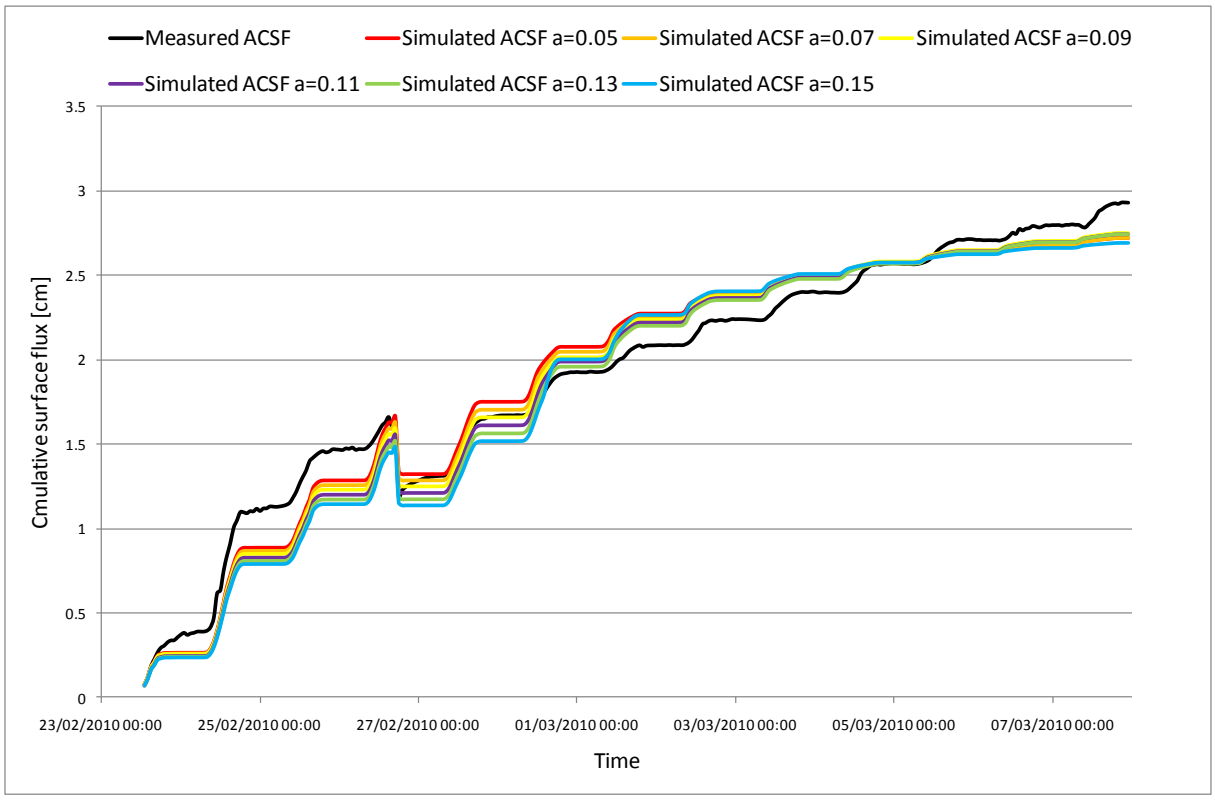

It follows from the evaporation experiment that low albedo values show smaller deviation between measured and simulated evaporation in the wet range. α_r = 0.05 gives the smallest deviations in this range, which correspond to the literature values of wet dark soil. From the 27th of February onwards, the simulations with relatively higher albedo values show better correspondence with the measured cumulative surface flux. Again, these results correspond to the literature values. Despite proved limitations, HYDRUS-1D only allows its users to enter a constant albedo value in simulations of bare soils. An albedo value of 0.09 will be used in the parameter optimizations of this experiment.

Appendix 11 Inverse modelling experiment results

The table in this appendix shows the optimization results for the potting soil. Every row represents one series of optimizations that consists of 3^n number of simulation runs. For the series A this gives 2^3 = 8 runs, for the series B this gives 2^4 = 16 runs, and for series C this gives 2^5 = 32 runs. In the columns the following information is presented:

- *# hits*: the number of optimization runs that converges to the global optimum;
- *%:* #hits divided by #runs. If this % is higher than 50%, the series is considered unique;
- *SSQ*: value of the objective function E(**b**,y) being minimized during the optimization process;
- R^2: a measure of the relative magnitude of the total sum of squares associated with the fitted equation, a value of 1 indicates a perfect correlation between the fitted and measured values (Simunek (c), et al. 2008, p.125);
- θ_r, θ_s, *α, n, K_s, l:* optimized hydraulic parameters in the optimized parameter vector **b**. For the series A (3 parameter fit optimization), θ_s, K_s and *l* are fixed parameters. For the series B (4 parameter fit optimization), θ_s and *l* are fixed parameters and for the series C, θ_s is the only fixed parameter. θ_s is always fixed, since it is measured by oven drying of the soil sample at the end of every experiment.

Run	#hits	%	.SSQ	R^2	θr	θs	α	n	K_s	l
	One-step outflow method (h_{bottom}=-1000 cm)									
OSO-1A	1/8	12.5	0.218	0.946	0.14	0.86	0.02	1.42	110	0.5
OSO-1B	1/16	6.3	0.194	0.951	0.16	0.86	0.02	1.50	88.6	0.5
OSO-1C	1/32	3.1	0.164	0.961	0.26	0.86	0.03	1.71	44.8	-0.15
OSO-2A	1/8	12.5	0.136	0.968	0.25	0.89	0.04	1.42	110	0.5
OSO-2B	1/16	6.3	0.1323	0.969	0.22	0.89	0.04	1.38	117.7	0.5
OSO-2C	1/32	3.1	0.1435	0.966	0.33	0.89	0.02	1.71	34.2	0.43
	Multi-step outflow method (0 cm≥h_{bottom}≥-1000 cm)									
MSO-1A	2/8	25	0.08602	0.997	0.31	0.87	0.05	2.18	110	0.5
MSO-1B	1/16	6.3	0.0592	0.998	0.31	0.87	0.03	2.60	20.3	0.5
MSO-1C	3/32	9.4	0.0638	0.998	0.32	0.87	0.04	2.51	35.0	0.24
	Multi-step outflow method (0 cm≥h_{bottom}≥-100 cm)									
MSO-2A	6/8	75	0.6824	0.996	0.31	0.81	0.11	1.84	110	0.5
MSO-2B	14/16	87.5	0.6629	0.996	0.31	0.81	0.11	1.88	10	0.5
MSO-2C	15/32	46.9	0.6366	0.996	0.31	0.81	0.11	1.84	10	-0.46
	Multi-step outflow method (0 cm≥h_{bottom}≥-100 cm)									
MSO-3A	5/8	62.6	0.8351	0.995	0.32	0.85	0.08	2.22	110	0.5
MSO-3B	15/16	93.8	0.6519	0.997	0.33	0.85	0.07	2.50	1.88	0.5
MSO-3C	2/32	6.3	0.4292	0.997	0.31	0.85	0.12	1.93	1	-1.44
	Multi-step outflow method undisturbed sample (0 cm≥h_{bottom}≥-200 cm)									
MSO-4A	7/8	87.5	0.5567	0.997	0.32	0.81	0.08	2.74	110	0.5
MSO-4B	13/16	81.3	0.5189	0.997	0.32	0.81	0.07	3.11	6.0	0.5
MSO-4C	5/32	15.6	0.2843	0.998	0.30	0.81	0.11	2.25	1	-1.42
	Multi-step outflow method undisturbed sample (0 cm≥h_{bottom}≥-100 cm)									
MSO-5A	3/8	37.5	0.1511	0.998	0.40	0.89	0.09	2.22	110	0.5
MSO-5B	7/16	43.8	0.1451	0.999	0.40	0.89	0.09	2.30	65.7	0.5
MSO-5C	2/32	6.3	0.0754	0.999	0.38	0.89	0.11	1.98	1	-2.86
	Evaporation experiment									
EVAP-A	8/8	100	10.45	0.990	0.21	0.86	0.23	1.41	110	0.5

The two figures below give a representation of the optimized hydraulic functions for all three-parameter fit inverse experiments. The first graph represents the soil water retention curves θ*(h)* and the second figure shows the corresponding hydraulic conductivity curves *K*(θ*)*.

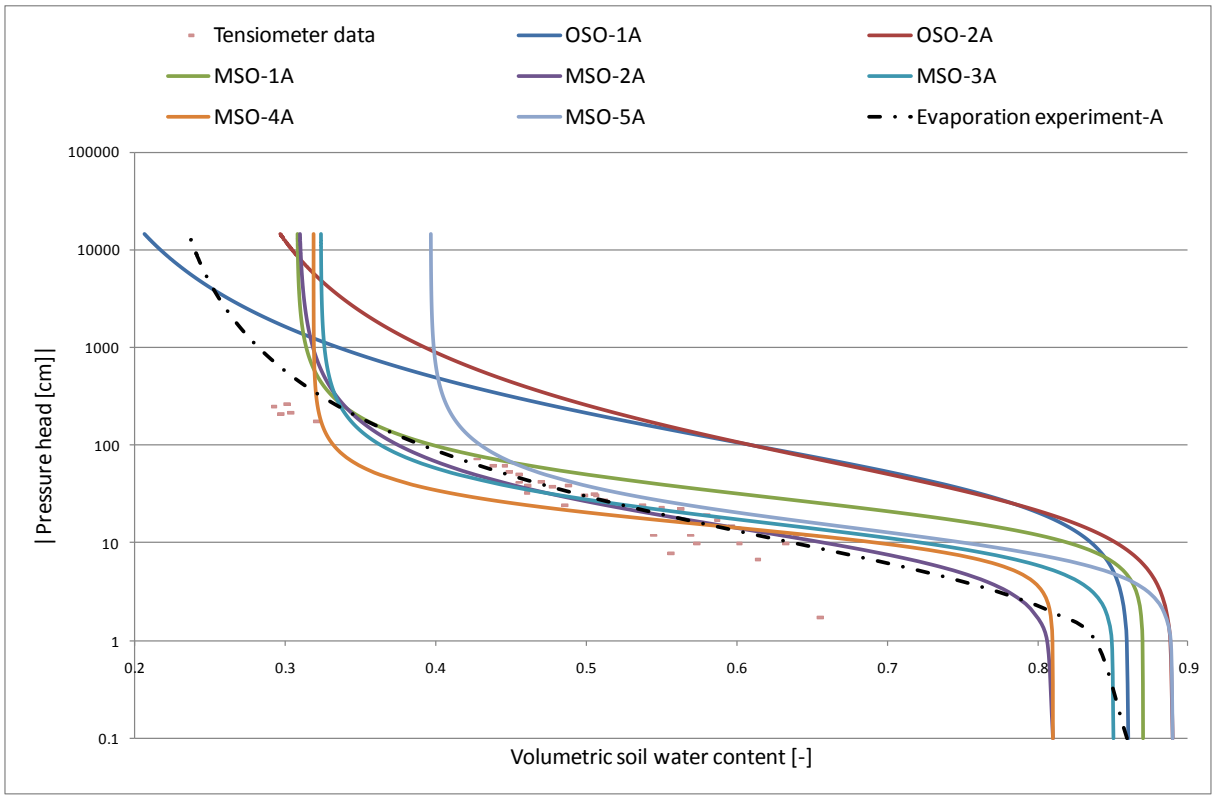

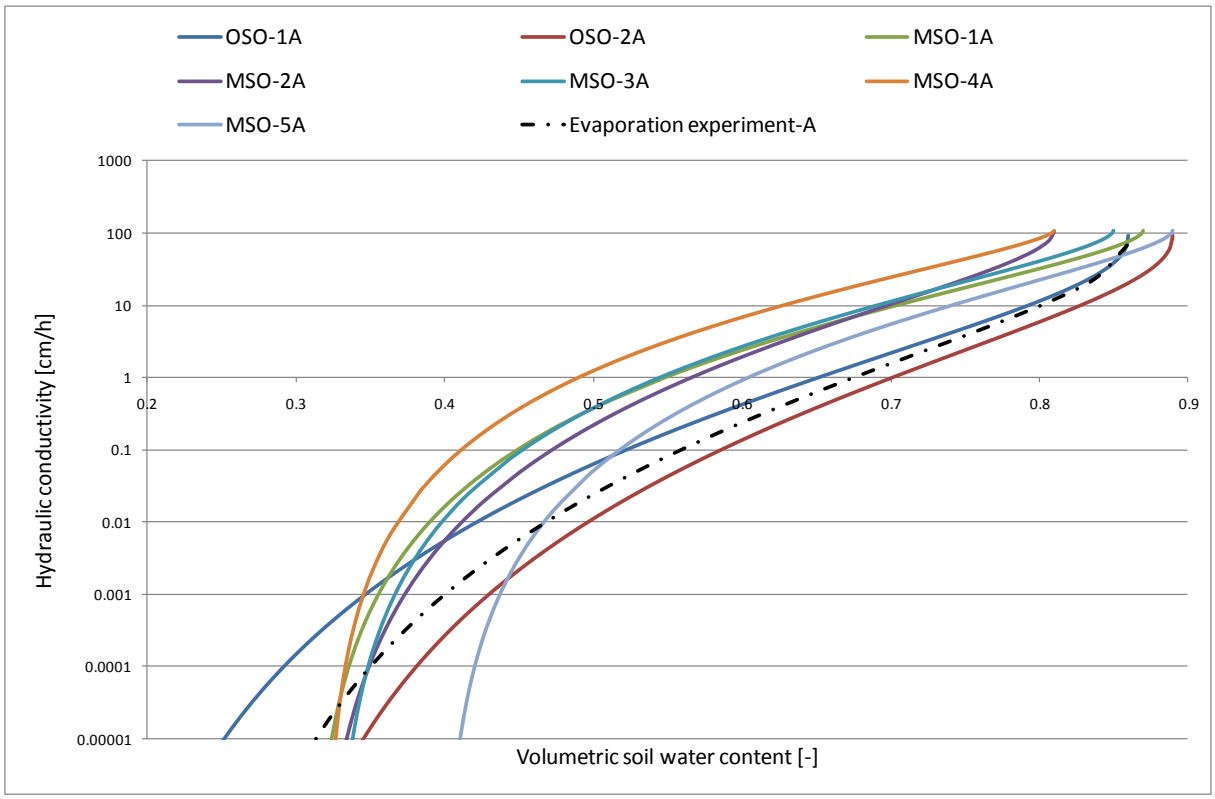

Appendix 12 Discretization test

Discretization in space

The initially specified discretization in space consists of 101 nodes or Δx=0.12 cm (Appendix 7). The influence of a finer and coarser grid distribution on the model runtime, stability and accuracy of the runoff simulations was tested under a constant initial time discretization. Results of this test are:

1. The runtime is low for Δx=1.2 cm and Δx=0.12 cm and almost triples for Δx=0.012 cm;
2. Stability is good for all three space discretization values, but some negative values occur for Δx=1.2 cm, which is an artefact of a too course grid. Negative values occur for Δx=0.012 cm, as well, which means that the domain of dependence of the PDE is moving towards the discrete domain of dependence (Courant, Friedrichs, Lewy condition: $c_n \Delta t \leq \Delta x$);
3. The cumulative outflow values are similar for all discretizations, with a maximum difference of 1%. At event scale, green roof simulation hydrographs of the September 11, 2009 event are very similar for all nodal densities. Two small negative values for the Δx=1.2 cm discretization can be observed.

Based on these considerations the initial discretization in space (Δx=0.12 cm) is a good balance between runtime, stability and runoff accuracy.

Space discretization		**Time discretization**			**Output**		
#nodes	**Δx [cm]**	**$\Delta t_{initial}$ [min]**	**Δt_{min} [min]**	**Δt_{max} [min]**	**Runtime [s]**	**Stability check**	**Cum. outflow [mm]**
11	1.2	0.001	0.0001	1	23.5	Stable	55.25
101	0.12	0.001	0.0001	1	28	Stable	55.26
1001 (max)	0.012	0.001	0.0001	1	71	Stable	54.74

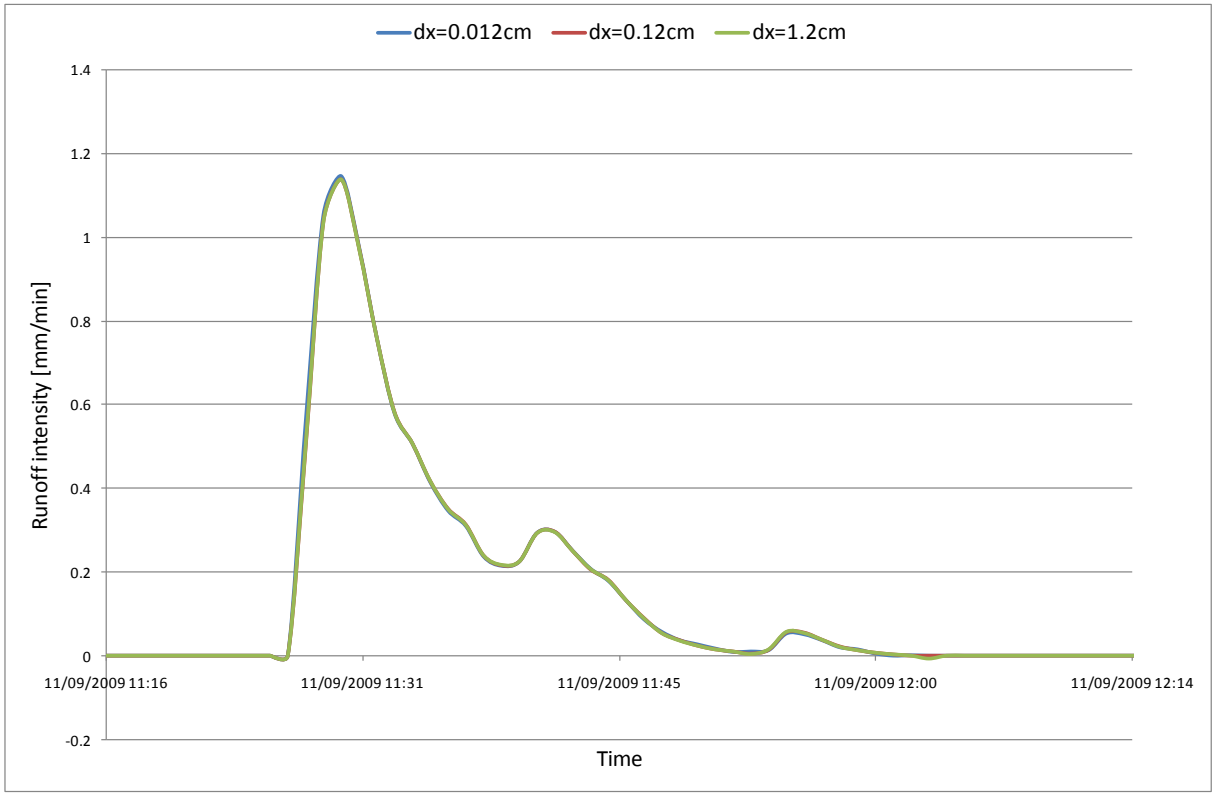

Discretization in time

Discretization in time starts with a prescribed initial time increment $\Delta t_{initial}$. The time step is automatically adjusted at each time level according to prescribed rules. Basically, this comes down to increasing the time step Δt by a predetermined constant (1.3) if the number of iterations ≤ 3, and decreasing the time step by a constant 0.7 if the number of iterations ≥ 7. The lower and upper time step limits are specified as Δt_{min} and Δt_{max}. The influence of a smaller and larger initial, minimum and maximum time step on the model runtime, stability and accuracy of the runoff simulations was tested under a constant initial discretization in space (Δx=0.12 cm). Results of this test are:

1. The runtime is in the order of 27-28 s for all time discretization values, except for the smallest time discretization with $\Delta t_{initial}$=0.0001, which has a long runtime of 77 s;
2. The numerical solution is stable for all time values and rapidly converges to a satisfactory tolerance value. For $\Delta t_{initial}$=1, the maximum number of iterations increases to 10, and some numerical instability arises as can be observed in the hydrograph of September 11, 2009. For $\Delta t_{initial}$=0.0001 this number decreases, but at the cost of an increased runtime;
3. All numerical model simulations lead to comparable cumulative outflow values. At event scale, the green roof simulation hydrograph of September 11, 2009 looks very similar for the four smallest discretizations. A negative value and more wiggles show that the domain of dependence of the PDE is moving towards the discrete domain of dependence for $\Delta t_{initial}$=1 (Courant, Friedrichs, Lewy condition: $c_n \Delta t \leq \Delta x$). This instability leads to decreased accuracy.

Time discretization			**Space discretization**		**Output**			
$\Delta t_{initial}$ [min]	**Δt_{min} [min]**	**Δt_{max} [min]**	**#nodes**	**Δx [cm]**	**Runtime [s]**	**Stability check**	**Cum. outflow [mm]**	**Max number of iterations before convergence**
1	0.1	1000	101	0.12	27	Stable	55.26	10
0.1	0.01	100	101	0.12	27.5	Stable	55.27	5
0.01	0.001	10	101	0.12	27.5	Stable	55.27	5
0.001	0.0001	1	101	0.12	28	Stable	55.26	5
0.0001	0.00001	0.1	101	0.12	77	Stable	55.26	2

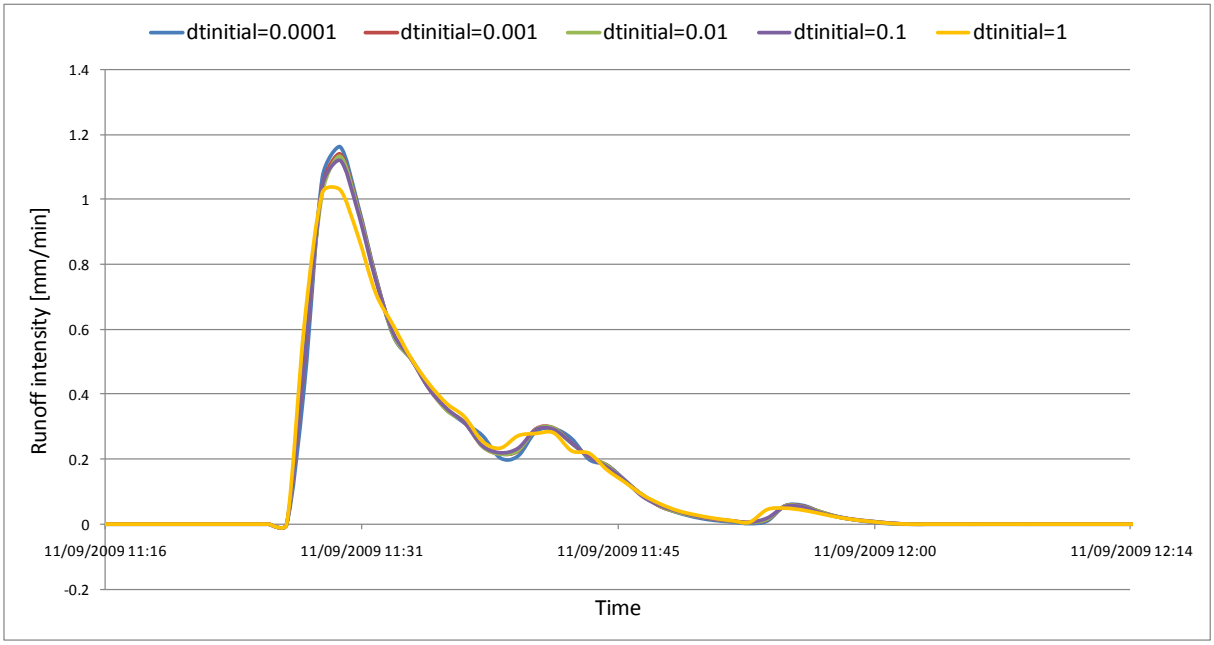

Appendix 13 HYDRUS-1D model calibration

This appendix includes input values for the model run parameters, performance measure values from the initial parameter specification, results from the sensitivity analysis and performance measure values from the final parameter specification.

Model parameter specification for verification, sensitivity analysis and calibration model runs

The following table shows the parameter specification for the different verification (V-1), calibration (C-1..C-N) and sensitivity analysis (S-1..S-N) model runs.

Model run	**Initial condition**	**Soil depth**	**Soil hydraulic parameters**						**Seepage face**		**Root water uptake parameters**					**Meteorological parameters**		
	θ_0		θ_r	θ_s	α	n	K_s	l	θ_{seep}	h_{seep}	*P0*	*P0pt*	*P2H*	*P2L*	*P3*	*SCF*	α_r	*a*
	[-]	[cm]	[-]	[-]	[1/cm]	[-]	[cm/min]	[-]	[-]	[-]	[cm]					[-]	[-]	[mm]
V-1 Initial specification	0.45	12	0.21	0.86	0.23	1.41	110	0.5	0.61	-12	0	-12	-300	-1000	-2000	0.43	0.23	1.50
C-1 Initial specification	0.48	12	0.21	0.86	0.23	1.41	110	0.5	0.61	-12	0	-12	-300	-1000	-2000	0.43	0.23	1.50
S-1 MSO-2A	0.48	12	0.31	0.81	0.11	1.84	110	0.5	0.61	-13	0	-13	-300	-1000	-2000	0.43	0.23	1.50
S-2 MSO-3A	0.48	12	0.32	0.85	0.08	2.22	110	0.5	0.61	-17	0	-17	-300	-1000	-2000	0.43	0.23	1.50
S-3 MSO-4A	0.48	12	0.32	0.81	0.08	2.74	110	0.5	0.61	-14	0	-14	-300	-1000	-2000	0.43	0.23	1.50
S-4 Soil depth	0.48	13.2	0.21	0.86	0.23	1.41	110	0.5	0.61	-12	0	-12	-300	-1000	-2000	0.43	0.23	1.50
S-5 K_s	0.48	12	0.21	0.86	0.23	1.41	121	0.5	0.61	-12	0	-12	-300	-1000	-2000	0.43	0.23	1.50
S-6 *l*	0.48	12	0.21	0.86	0.23	1.41	110	0.55	0.61	-12	0	-12	-300	-1000	-2000	0.43	0.23	1.50
S-7 h_{seep}	0.48	12	0.21	0.86	0.23	1.41	110	0.5	0.67	-8	0	-8	-300	-1000	-2000	0.43	0.23	1.50
S-8 Feddes	0.48	12	0.21	0.86	0.23	1.41	110	0.5	0.61	-12	0	-12	-30	-40	-60	0.43	0.23	1.50
S-9 SCF	0.48	12	0.21	0.86	0.23	1.41	110	0.5	0.61	-12	0	-12	-300	-1000	-2000	0.47	0.23	1.31
S-10 α_r	0.48	12	0.21	0.86	0.23	1.41	110	0.5	0.61	-12	0	-12	-300	-1000	-2000	0.43	0.25	1.50
S-11 *a*	0.48	12	0.21	0.86	0.23	1.41	110	0.5	0.61	-12	0	-12	-300	-1000	-2000	0.43	0.23	1.65
C-2 final specification	0.50	12	0.21	0.86	0.23	1.41	110	2.85	0.61	-12	0	-12	-40	-60	-100	0.95	0.16	401*

*: A bug in the interception calculation was found and described in paragraph 5.5.3.1

Performance measure values from the initial parameter specification

This table gives a representation of the performance variables and the modelling efficiency for all eight events with more than 0.5 mm rainfall between September 06 and September 20, 2009 under the initial parameter specification.

		Measurements GR1	Measurements GR2	Initial specification calibration model
Overall	q_{tot}	46.0	47.7	58.6
06/09 06:36 P=31.21mm ADWP=1.2d Wet	q_c	22.74	24.30	27.75
	E_{ns} *GR1*	-	-	0.83
	E_{ns} *GR2*	-	-	0.83
	q_{peak}	0.77	0.75	0.89
	tt_{peak}	00:00	00:00	00:02
	q_{bf180}	0.01	0.49	0.22
11/09 11:13 P=22.06mm ADWP=5.2d Dry	q_c	5.91	4.96	9.06
	E_{ns} *GR1*	-	-	-2.33
	E_{ns} *GR2*	-	-	-9.59
	q_{peak}	0.27	0.20	1.14
	tt_{peak}	00:19	00:27	00:13
	q_{bf180}	0.80	1.80	0.20
17/09 03:06 P=1.00mm ADWP=5.66d Dry	q_c	0	0	0
	E_{ns} *GR1*	-	-	-
	E_{ns} *GR2*	-	-	-
	q_{peak}	0	0	0
	tt_{peak}	-	-	-
	q_{bf180}	0	0	0
17/09 10:11 P=15.91mm ADWP=0.3d Dry	q_c	0.96	0.14	0
	E_{ns} *GR1*	-	-	-
	E_{ns} *GR2*	-	-	-
	q_{peak}	0.08	0.02	0
	tt_{peak}	00:08	00:10	00:00
	q_{bf180}	0.12	0.04	0

		Measurements GR1	Measurements GR2	Initial specification calibration model
Overall	q_{tot}	46.0	47.7	58.6
18/09 11:37 P=7.14mm ADWP=1.06d Medium wet	q_c	1.92	1.34	2.62
	E_{ns} *GR1*	-	-	-9.04
	E_{ns} *GR2*	-	-	-46.09
	q_{peak}	0.08	0.04	0.47
	tt_{peak}	00:18	00:22	00:06
	q_{bf180}	1.57	1.31	0.31
18/09 14:53 P=6.75mm ADWP=0.14d Wet	q_c	4.33	5.20	5.98
	E_{ns} *GR1*	-	-	-0.63
	E_{ns} *GR2*	-	-	-1.72
	q_{peak}	0.27	0.14	0.32
	tt_{peak}	00:12	00:23	00:02
	q_{bf180}	0.31	1.29	0.22
19/09 10:15 P=13.59mm ADWP=0.8d Wet	q_c	10.06	10.91	13.12
	E_{ns} *GR1*	-	-	0.29
	E_{ns} *GR2*	-	-	-0.38
	q_{peak}	0.48	0.46	0.72
	tt_{peak}	00:16	00:16	00:02
	q_{bf180}	0.36	1.49	0.22
19/09 14:31 P=0.50mm ADWP=0.18d Wet	q_c	0	0.53	0.07
	E_{ns} *GR1*	-	-	-
	E_{ns} *GR2*	-	-	-4.05
	q_{peak}	0	0.01	0.02
	tt_{peak}	-	00:56	00:17
	q_{bf180}	0	0.49	0.07

Here q_{tot} is the cumulative runoff over the entire observed period [mm], q_c is the cumulative runoff on event scale, q_{peak} is the peak discharge on event scale [mm/min], tt_{peak} is the time to peak relative

to the rainfall peak [hh:mm], q_{bf180} is a measure for the base flow 180 min after the last recorded rainfall. E_{ns} is the Nash-Sutcliffe modelling efficiency with respect to the green roof measurements. The following figures give a representation of the green roof hydrographs for all 8 events with more than 0.5 mm rainfall between September 06 and September 20, 2009. Every single figure includes hydrographs of the two green roof platform measurements and the model simulation.

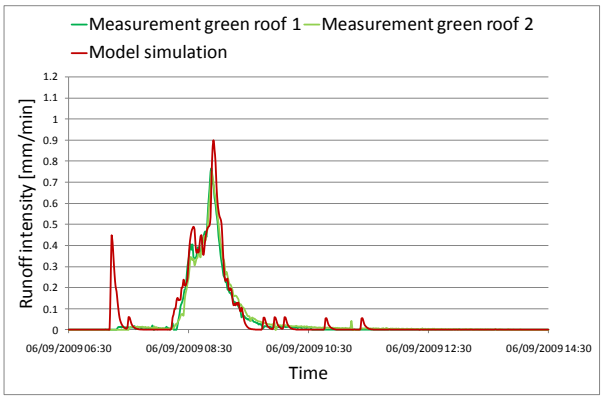

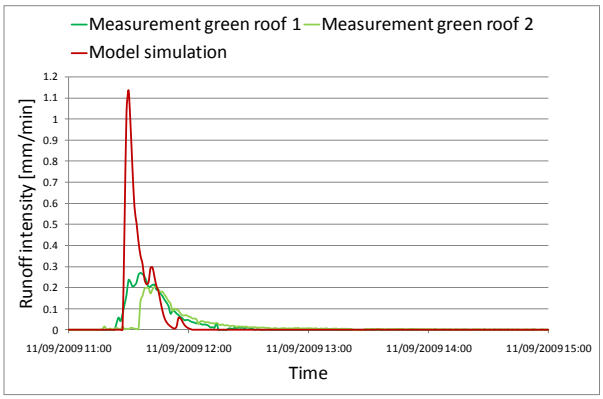

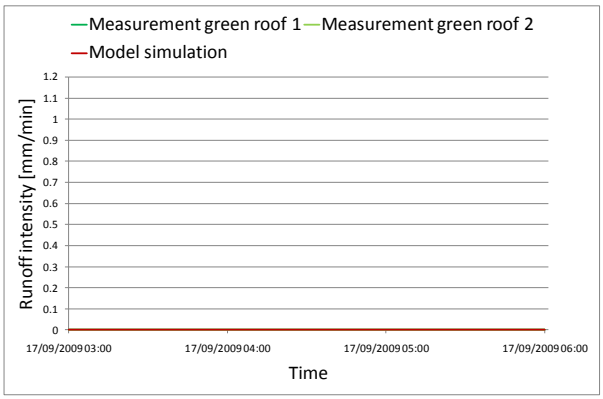

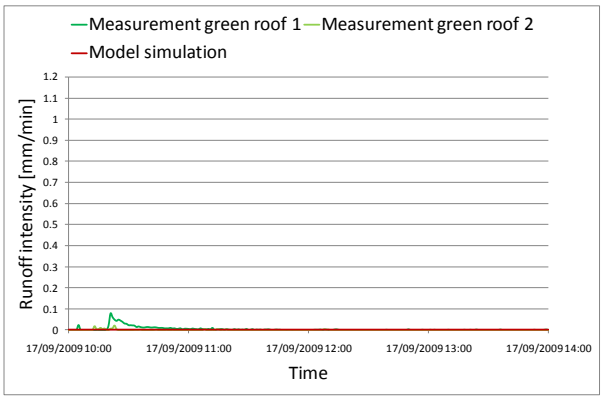

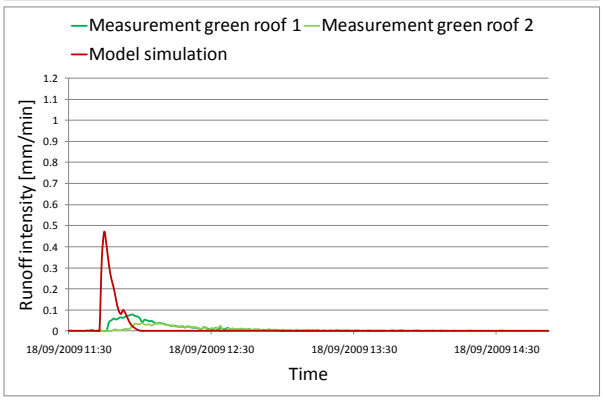

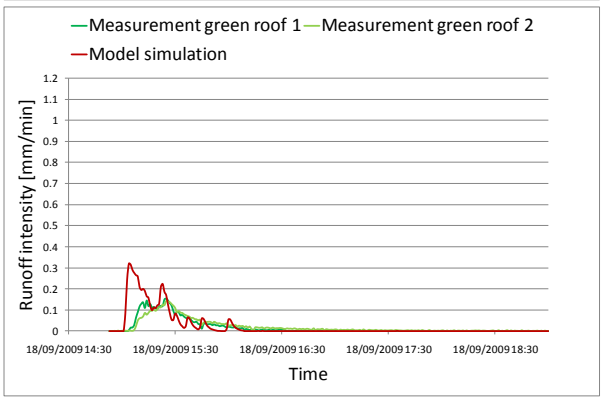

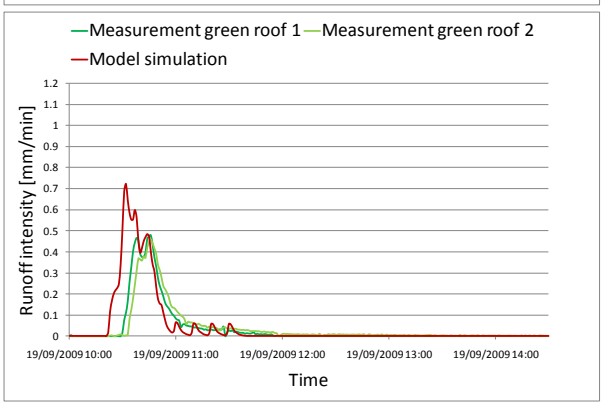

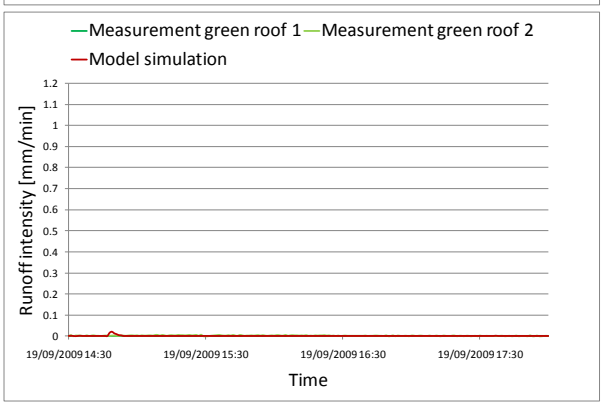

Sensitivity analysis: determination of the feasible parameter ranges

The potential calibration possibilities of a certain parameter is a function of the sensitivity of the model performance measures to changes in the parameter and the feasible parameter range. The following decisions have been made with regard to the feasible parameter ranges of the four identified classes:

1. Soil hydraulic parameters: 4 unique parameters sets that were calibrated with inverse modelling of outflow and evaporation experiments. The feasible parameter range for K_s and l were established with an estimated lower and upper bound;
2. Soil depth and seepage face: lower and upper bound values from experiment measurements;
3. Feddes' root water uptake parameters: estimated lower and upper bound values;
4. Meteorological parameters: estimated lower and upper bound values.

1. Feasible parameter ranges for the soil hydraulic parameters:

Parameter	**Initial specification EVAP-A**	**MSO-2A**	**MSO-3A**	**MSO-4A**
θr [-]	0.21	0.31	0.32	0.32
θs [-]	0.86	0.81	0.85	0.81
α [1/cm]	0.23	0.11	0.08	0.08
n [-]	1.41	1.84	2.22	2.74
K_s [cm/min]	110	110	110	110
l [-]	0.50	0.50	0.50	0.50

And for testing the individual sensitivity to changes in K_s and l:

Parameter	**Initial specification**	**Lower bound**	**Upper bound**
K_s [cm/min]	110	25	200
l [-]	0.5	-4	+4

2. Feasible parameter ranges for the soil depth and seepage face:

Parameter	**Initial specification**	**Lower bound**	**Upper bound**
z [cm]	12	10	15
θ_{seep} [-]	0.61	0.52	0.65

Lower and upper bound values for θ_{seep} originate from the performed seepage face experiments (Appendix 6). h_{seep} needs to be calculated based on van Genuchten's soil water retention function and thus depends on the specified set of hydraulic parameters.

3. Feasible parameter ranges for Feddes' root water uptake parameters:

Parameter	**Initial specification**	**Lower bound**	**Upper bound**
p2H [cm]	-300	-30	-8000
p2L [cm]	-1000	-40	-12000
p3 [cm]	-2000	-60	-24000

Lower and upper bound values for p2H, p2L and p3 were based on the root water uptake database in HYDRUS.

4. Meteorological parameters:

Parameter	Initial specification	Lower bound	Upper bound
SCF [-]	0.43	0.1	0.95
α_r [-]	0.23	0.05	0.25
a [mm]	1.5	0.5	5

Lower and upper bound values for *SCF* were estimated between 0.1 (10% plant vegetation) and 0.9 (95% plant vegetation). Lower and upper bound albedo values were estimated between α_r = 0.05 (bare wet soil) and α_r = 0.25 (full vegetation cover). Lower and upper bound values for the interception constant were estimated between 0.5 mm (low interception storage) and 5 mm (very high interception storage).

Sensitivity analysis: sensitivity index results

The following tables present the sensitivity analysis results. Here q_{tot} is the cumulative runoff over the entire observed period [mm], q_c is the cumulative runoff on event scale, q_{peak} is the peak discharge on event scale [mm/min], tt_{peak} is the time to peak relative to the rainfall peak [hh:mm], q_{bf180} is a measure for the base flow 180 min after the last recorded rainfall. E_{ns} is the Nash-Sutcliffe modelling efficiency with respect to the green roof measurements.

Performance variable and Nash-Sutcliffe modelling efficiency values are presented for the 4 different unique parameter sets (initial run C-1, S-2, S-3 and S-4), a 10% change in the values for K_s and *I* (S-4 and S-5), a 10% change in soil depth *z* and seepage face h_{seep} (S-6 and S-7), a changed set of root water uptake parameters (S-8) and a 10% change in the Soil Cover Fraction *SCF*, albedo α_r and interception constant *a (*S-9, S-10 and S-11).

Sensitivity indexes S_i are presented only for the sensitivity analysis model runs with a standard 10% parameter value change. This sensitivity index can therefore not be calculated for the different unique parameter sets and Feddes root water uptake parameters. The sensitivity index for the rest of the parameter change has been calculated according to Eq. 5.33.

		C-1 Initial specification calibration model	S-1 MSO-2A	S-2 MSO-3A	S-3 MSO-4A	S-4 K_s +10%	S-5 I +10%	S-6 z +10%	S-7 h_{seep} +10%	S-8 Root water uptake parameters	S-9 SCF +10%	S-10 α_r +10%	S-11 a +10%
Overall	q_{tot} [mm]	58.60	58.58	58.12	58.00	58.61	58.59	58.42	54.84	61.78	57.74	59.76	58.60
06/09 06:36 P=31.21mm ADWP=1.2d Wet	q_c [mm]	27.75	27.78	27.78	27.67	27.75	27.75	27.55	23.94	27.74	27.64	27.85	27.75
	S_i q_c [-]					0.00	0.00	-0.07	-1.37		-0.04	0.04	0.00
	E_{ns} $GR1$[-]	0.83	0.74	0.71	0.72	0.83	0.83	0.85	0.93	0.83	0.84	0.83	0.83
	S_i E_{ns} $GR1$ [-]					-0.06	0.01	0.22	1.13		0.08	-0.09	0.00
	E_{ns} $GR2$ [-]	0.83	0.69	0.67	0.67	0.82	0.83	0.85	0.91	0.83	0.84	0.82	0.83
	S_i E_{ns} $GR2$ [-]					-0.10	0.03	0.32	1.02		0.09	-0.09	0.00
	q_{peak} [mm/min]	0.90	1.02	1.03	1.03	0.91	0.90	0.86	0.94	0.90	0.90	0.90	0.90
	S_i q_{peak} [-]					0.10	-0.03	-0.38	0.46		0.01	0.01	0.01
	tt_{peak} [hh:mm]	00:02	00:01	00:01	00:01	00:02	00:02	00:02	00:01	00:02	00:02	00:02	00:02
	S_i tt_{peak} [-]					0.00	0.00	0.00	-5.00		0.00	0.00	0.00
	q_{bf180} [mm]	0.22	0.11	0.05	0.09	0.22	0.22	0.22	0.21	0.22	0.22	0.22	0.22
	S_i q_{bf180} [-]					-0.18	0.05	0.09	-0.46		-0.09	-0.05	-0.05
11/09 11:13 P=22.06mm ADWP=5.2d Dry	q_c [mm]	9.06	9.08	9.12	9.16	9.06	9.05	9.05	9.08	9.61	8.77	9.44	9.05
	S_i q_c [-]					0.00	-0.01	-0.01	0.02		-0.31	0.42	0.00
	E_{ns} $GR1$[-]	-2.33	-4.81	-5.16	-5.25	-2.53	-2.28	-1.92	-3.37	-3.08	-2.03	-2.87	-2.33
	S_i E_{ns} $GR1$ [-]					0.85	-0.23	-1.77	4.45		-1.29	2.31	-0.01
	E_{ns} $GR2$ [-]	-9.59	-13.74	-14.33	-14.48	-9.98	-9.48	-8.72	-11.55	-11.26	-8.87	-10.80	-9.58
	S_i E_{ns} $GR2$ [-]					0.41	-0.12	-0.90	2.04		-0.75	1.27	-0.01
	q_{peak} [mm/min]	1.14	1.50	1.53	1.54	1.16	1.13	1.07	1.27	1.18	1.11	1.17	1.14
	S_i q_{peak} [-]					0.15	-0.04	-0.57	1.12		-0.22	0.30	0.00
	tt_{peak} [hh:mm]	00:13	00:11	00:11	00:11	00:13	00:13	00:13	00:12	00:13	00:13	00:13	00:13
	S_i tt_{peak} [-]					0.00	0.00	0.00	-0.77		0.00	0.00	0.00
	q_{bf180} [mm]	0.20	0.10	0.06	0.08	0.19	0.20	0.21	0.18	0.20	0.19	0.19	0.20
	S_i q_{bf180} [-]					-0.10	0.10	0.72	-0.62		-0.05	0.00	0.00

		C-1 Initial specification calibration model	S-1 MSO-2A	S-2 MSO-3A	S-3 MSO-4A	S-4 K_s +10%	S-5 I +10%	S-6 z +10%	S-7 h_{seep} +10%	S-8 Root water uptake parameters	S-9 SCF +10%	S-10 α_r +10%	S-11 a +10%
18/09 14:53 P=6.75mm ADWP=0.14d Wet	q_c [mm]	5.98	5.97	5.93	5.92	5.98	5.98	6.00	5.97	5.98	5.97	6.01	5.98
	$S_i\ q_c$ [-]					0.00	0.00	0.02	-0.01		-0.02	0.04	0.01
	$E_{ns}\ GR1$[-]	-0.63	-1.88	-1.98	-2.02	-0.73	-0.61	-0.41	-1.07	-0.63	-0.62	-0.66	-0.64
	$S_i\ E_{ns}\ GR1$ [-]					1.50	-0.45	-3.61	6.90		-0.17	0.32	0.05
	$E_{ns}\ GR2$ [-]	-1.72	-3.43	-3.58	-3.66	-1.84	-1.68	-1.42	-2.28	-1.72	-1.70	-1.75	-1.72
	$S_i\ E_{ns}\ GR2$ [-]					0.73	-0.21	-1.75	3.29		-0.08	0.18	0.02
	q_{peak} [mm/min]	0.32	0.49	0.50	0.50	0.34	0.31	0.30	0.39	0.32	0.32	0.32	0.32
	$S_i\ q_{peak}$ [-]					0.53	-0.16	-0.72	2.09		-0.03	0.06	0.03
	tt_{peak} [hh:mm]	00:02	00:01	00:01	00:01	00:02	00:02	00:03	00:02	00:02	00:02	00:02	00:02
	$S_i\ tt_{peak}$ [-]					0.00	0.00	5.00	0.00		0.00	0.00	0.00
	q_{bf180} [mm]	0.22	0.11	0.07	0.08	0.21	0.22	0.22	0.20	0.22	0.22	0.22	0.21
	$S_i\ q_{bf180}$ [-]					-0.09	0.05	0.14	-0.51		0.00	0.00	-0.05
19/09 10:15 P=13.59mm ADWP=0.8d Wet	q_c [mm]	13.12	13.06	13.01	13.14	13.12	13.12	13.13	13.13	13.13	13.12	13.13	13.13
	$S_i\ q_c$ [-]					0.00	0.00	0.01	0.00		0.00	0.01	0.01
	$E_{ns}\ GR1$[-]	0.29	-0.26	-0.30	-0.32	0.24	0.30	0.39	0.08	0.28	0.29	0.28	0.28
	$S_i\ E_{ns}\ GR1$ [-]					-1.54	0.44	3.66	-7.14		-0.01	-0.03	-0.02
	$E_{ns}\ GR2$ [-]	-0.38	-1.00	-1.04	-1.07	-0.43	-0.36	-0.24	-0.63	-0.38	-0.38	-0.38	-0.38
	$S_i\ E_{ns}\ GR2$ [-]					1.51	-0.43	-3.68	6.68		0.00	0.03	0.02
	q_{peak} [mm/min]	0.72	0.90	0.93	0.93	0.73	0.72	0.69	0.81	0.72	0.72	0.72	0.72
	$S_i\ q_{peak}$ [-]					0.14	-0.06	-0.48	1.18		0.00	-0.01	0.00
	tt_{peak} [hh:mm]	00:02	00:00	00:00	00:00	00:02	00:02	00:02	00:01	00:02	00:02	00:02	00:02
	$S_i\ tt_{peak}$ [-]					0.00	0.00	0.00	-5.00		0.00	0.00	0.00
	q_{bf180} [mm]	0.22	0.11	0.06	0.08	0.22	0.22	0.23	0.21	0.22	0.22	0.22	0.22
	$S_i\ q_{bf180}$ [-]					-0.09	0.09	0.46	-0.46		0.05	0.05	0.05

Performance measure values from the final parameter specification

This table gives a representation of the performance variables and the modelling efficiency for all 8 events with more than 0.5 mm rainfall between September 06 and September 20, 2009 under the final parameter specification.

		Measurements GR1	Measurements GR2	Final specification calibration model
Overall	q_{tot}	46.0	47.7	52.03
06/09 06:36 P=31.21mm ADWP=1.2d Wet	q_c	22.74	24.30	26.54
	E_{ns} *GR1*	-	-	0.88
	E_{ns} *GR2*	-	-	0.92
	q_{peak}	0.77	0.75	0.78
	tt_{peak}	00:00	00:00	00:04
	q_{bf180}	0.01	0.49	0.22
11/09 11:13 P=22.06mm ADWP=5.2d Dry	q_c	5.91	4.96	5.88
	E_{ns} *GR1*	-	-	0.61
	E_{ns} *GR2*	-	-	0.07
	q_{peak}	0.27	0.20	0.40
	tt_{peak}	00:19	00:27	00:18
	q_{bf180}	0.80	1.80	0.81
17/09 03:06 P=1.00mm ADWP=5.66d Dry	q_c	0	0	0
	E_{ns} *GR1*	-	-	-
	E_{ns} *GR2*	-	-	-
	q_{peak}	0	0	0
	tt_{peak}	-	-	-
	q_{bf180}	0	0	0
17/09 10:11 P=15.91mm ADWP=0.3d Dry	q_c	0.96	0.14	0
	E_{ns} *GR1*	-	-	-0.16
	E_{ns} *GR2*	-	-	-0.07
	q_{peak}	0.08	0.02	0
	tt_{peak}	00:08	00:10	00:00
	q_{bf180}	0.12	0.04	0

		Measurements GR1	Measurements GR2	Final specification calibration model
Overall	q_{tot}	46.0	47.7	52.03
18/09 11:37 P=7.14mm ADWP=1.06d Medium wet	q_c	1.92	1.34	0.73
	E_{ns} *GR1*	-	-	0.50
	E_{ns} *GR2*	-	-	-0.02
	q_{peak}	0.08	0.04	0.06
	tt_{peak}	00:18	00:22	00:17
	q_{bf180}	1.57	1.31	0.73
18/09 14:53 P=6.75mm ADWP=0.14d Wet	q_c	4.33	5.20	5.78
	E_{ns} *GR1*	-	-	0.68
	E_{ns} *GR2*	-	-	0.34
	q_{peak}	0.27	0.14	0.18
	tt_{peak}	00:12	00:23	00:11
	q_{bf180}	0.31	1.29	0.34
19/09 10:15 P=13.59mm ADWP=0.8d Wet	q_c	10.06	10.91	13.03
	E_{ns} *GR1*	-	-	0.82
	E_{ns} *GR2*	-	-	0.45
	q_{peak}	0.48	0.46	0.56
	tt_{peak}	00:16	00:16	00:08
	q_{bf180}	0.36	1.49	0.39
19/09 14:31 P=0.5 0mm ASWP=0.18d Wet	q_c	0	0.53	0.06
	E_{ns} *GR1*	-	-	-
	E_{ns} *GR2*	-	-	-2.41
	q_{peak}	0	0.01	0
	tt_{peak}	-	00:56	00:19
	q_{bf180}	0	0.49	0.04

The following figures give a representation of the green roof hydrographs for all 8 events with more than 0.5 mm rainfall between September 06 and September 20, 2009. Every single figure includes hydrographs of the two green roof platform measurements and the model simulation.

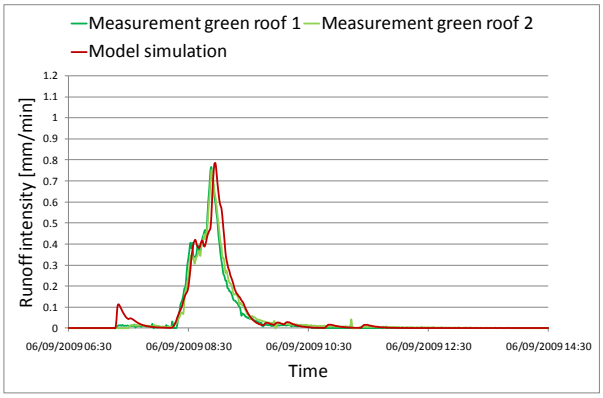

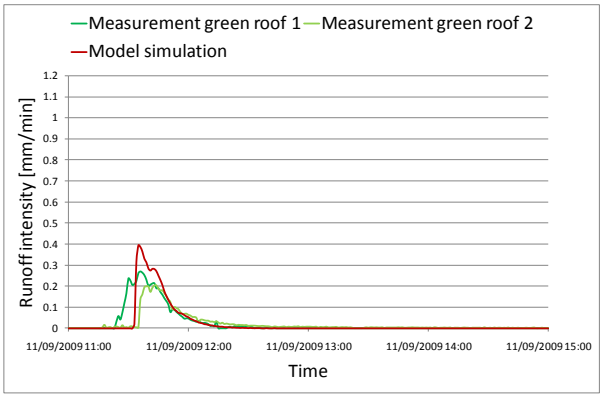

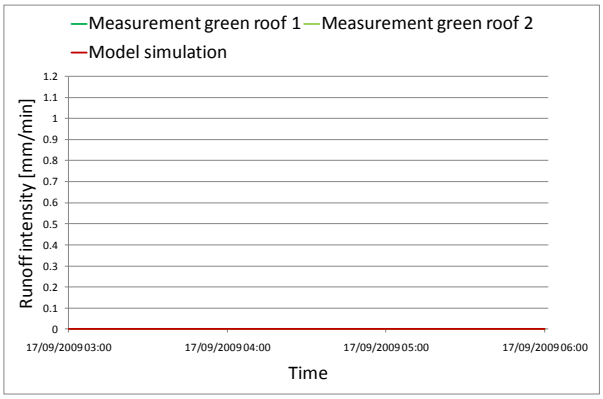

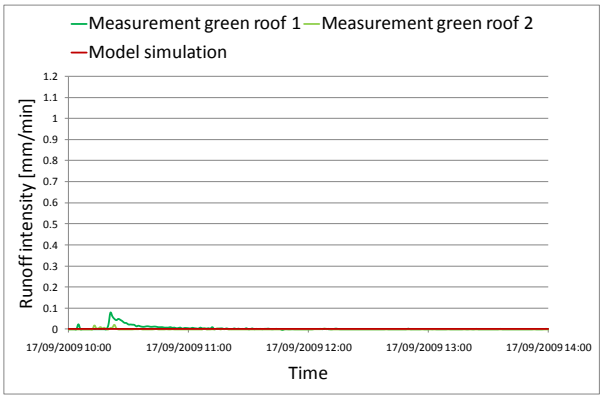

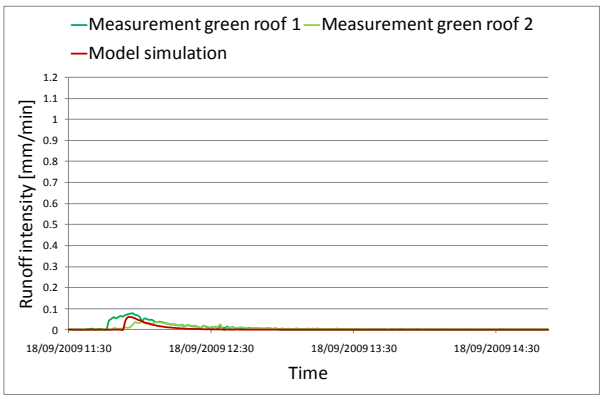

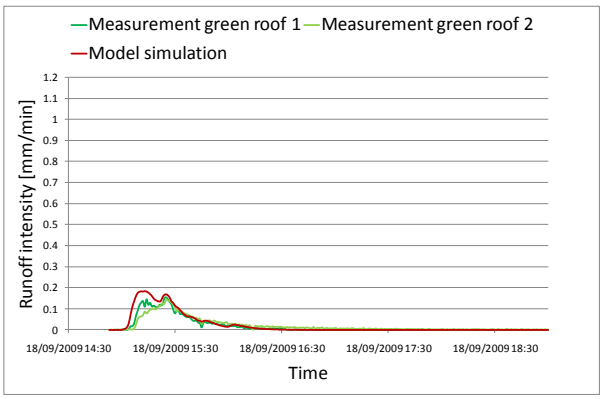

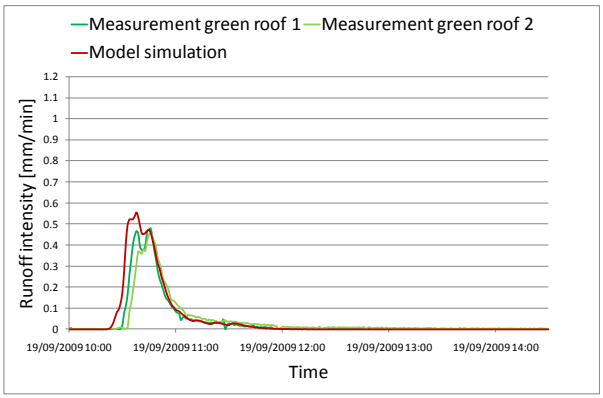

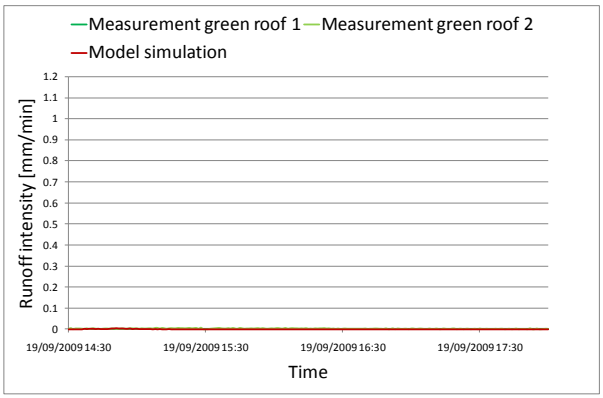

Validation performance measure values and hydrographs

The following table and hydrographs give a quantitative and qualitative representation of the model performance during 4 events within the validation period between December 02, 23:59 and December 26, 23:59 in 2009 under the final parameter specification.

		Measurements GR1	Measurements GR2	Final specification calibration model
Overall	q_{tot}	104.6	127.1	148.0
03/12 13:50 P=42.16mm ADWP=0.9d Wet	q_c	30.56	33.92	40.40
	E_{ns} *GR1*			0.78
	E_{ns} *GR2*			0.84
	q_{peak}	0.67	0.62	0.74
	tt_{peak}	-00:02	-00:02	00:02
	q_{bf180}	0.00	0.56	0.25
17/12 7:15 P=16.94mm ADWP=0.24d Wet	q_c	5.40	15.32	12.82
	E_{ns} *GR1*			-3.44
	E_{ns} *GR2*			0.68
	q_{peak}	0.19	0.61	0.63
	tt_{peak}	00:06	00:03	00:06
	q_{bf180}	0.00	1.13	0.26

		Measurements GR1	Measurements GR2	Final specification calibration model
Overall	q_{tot}	104.6	127.1	148.0
19/12 13:02 P=11.21mm ADWP=0.36d Medium wet	q_c	3.94	6.96	7.82
	E_{ns} *GR1*			0.25
	E_{ns} *GR2*			0.88
	q_{peak}	0.16	0.20	0.24
	tt_{peak}	00:49	00:50	00:52
	q_{bf180}	0.00	0.60	0.15
25/12 14:35 P=22.18mm* ADWP=1.29d Medium wet	q_c	14.57	16.48	17.29
	E_{ns} *GR1*			0.79
	E_{ns} *GR2*			0.86
	q_{peak}	0.91	1.00	0.99
	tt_{peak}	00:04	00:04	00:05
	q_{bf180}	2.46	2.72	1.66

*: Event is a combination of two consecutive events

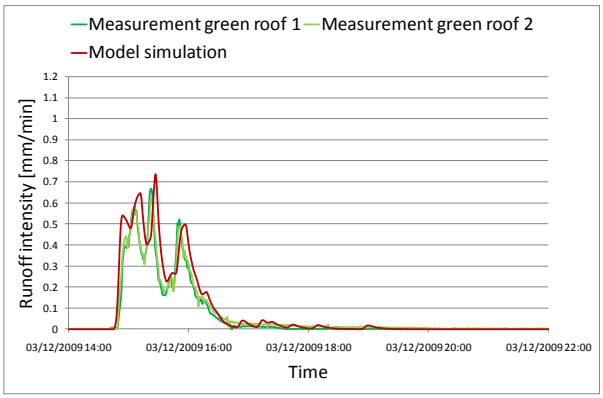

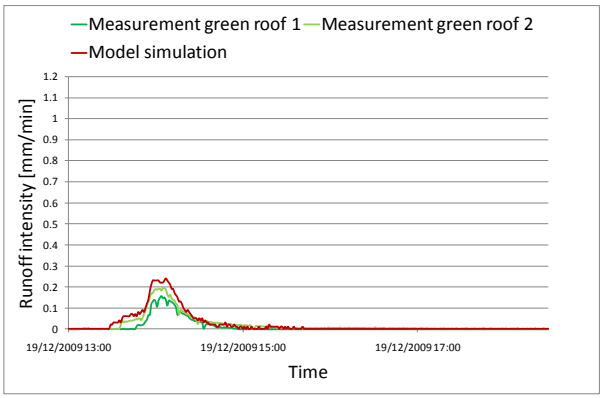

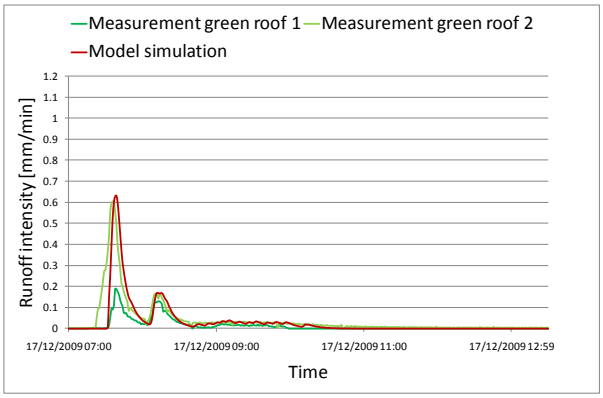

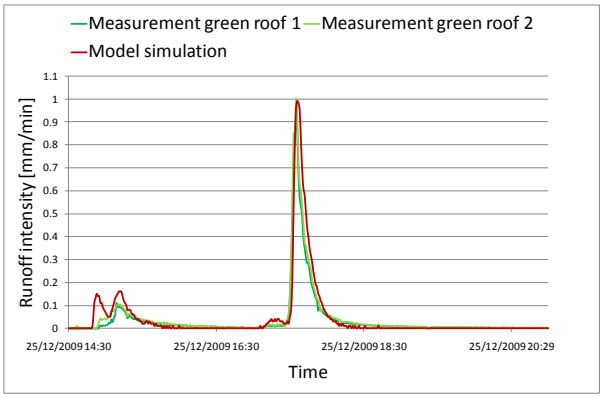

Appendix 14 Minutes of the March 03, 2010 meeting with PUB

This appendix presents the minutes of the meeting at PUB's head office in Singapore. This meeting has been organized to discuss the research goals of the thesis research, to obtain more information about the catchment details, design practices and other information that could be relevant for the research.

Attendees
Mdm. Yeo (PUB)
Mr. Babu (PUB)
Mr. Vergroesen (TU-Delft, SDWA)
Mr. van Spengen (TU-Delft)

Subcatchment details
Several catchment details have been discussed. The following information is worth mentioning:

- The subcatchment drainage system has been designed based on the Code of Practice on surface water drainage (PUB Singapore (a) 2000). The drains are designed with the rational formula in combination with Manning's formula;
- The drainage area of the subcatchment is 20 ha and the main drain is designed according to this total drainage area;
- The time of concentration t_c [T] of the subcatchment equals 17 minutes. This is the sum of the overland flow time t_0 (10 minutes) plus the drain flow time t_d (7 minutes) from the most remote point of the subcatchment to the outlet of the main drain to the Sungei Ulu Pandan canal;
- The return period adopted for the design of the drains equals T=5 years. Based on the rainfall intensity-duration-frequency (IDF) curves for Singapore, this corresponds to such a design storm having a duration equal to the time of concentration with an intensity *I* of 150 mm/hr;
- The runoff coefficient *C* [-]of HDB areas is assumed to be 0.8;
- The slope of small and medium canals is 1:200 – 1:300;
- The Manning roughness coefficient for concrete drains is 0.015;
- No stage-discharge relationship is available for the main drain of the subcatchment;

Available resources
The following resources were made available by PUB for study purposes:

- GIS maps including information on land use, large drains and building footprints.

Maps including the building footprints, contour lines of the subcatchment and the subcatchment demarcation, are presented in the following figures.

Building footprint map of the subcatchment

Map including contour lines, subcatchment demarcation (green dashed line) and outflow point at the main canal (left bottom)

Appendix 15 Sunset Way subcatchment fieldwork findings

This appendix contains the most important findings from the fieldwork in the Sunset Way subcatchment.

Fieldwork activities

The following 5-step strategy has been adopted to map all missing, but relevant characteristics of the subcatchment:

Step 1. Map the real demarcation of the subcatchment;
Step 2. Individually determine which buildings are connected to the drainage system and which buildings are connected to the sewer system;
Step 3. Observe and map all medium and large drain positions and dimensions;
Step 4. Observe and map all small drain positions and dimensions;
Step 5. Verify the fieldwork data with the data that is provided by the PUB.

Information that has been gathered during the fieldwork activities, was captured in several maps. These maps were used to conceptualize the catchment characteristics for later modelling purposes.

Fieldwork findings

Important fieldwork findings per step are:

Step 1. The drainage area of the Sunset Way subcatchment is smaller than 20 ha. All areas which are positioned on the eastern side of the Clementi Road do not discharge into the main outflow canal and therefore fall outside the subcatchment demarcation. The 1.5 ha dog training park area is an exception, since it is connected to the subcatchment with a submerged culvert that crosses the Clementi Road. The actual measured surface area of the subcatchment is 9.4 ha;
Step 2. Several roof surfaces are connected to the sewer network. Other roof surfaces are connected to the drainage network. According to PUB, all roof surfaces should be connected to the drainage network;
Step 3. The positioning and dimensions of all medium and large drains were mapped;
Step 4. The positioning and dimensions of all small drains were mapped;
Step 5. Land use, building footprints and the positioning and dimensions of large drains generally corresponded to the information that was provided by the PUB. Fieldwork data with respect to the positioning and dimensions of medium and small drains cannot be verified with information from PUB. Two major differences between the fieldwork findings and information which was provided by PUB are:
    1. The catchment surface area is 9.4 ha instead of 20 ha;
    2. Not all roof surfaces are connected to the drainage network.

Fieldwork conclusions

The available subcatchment information from PUB has been supplemented with information that has been obtained during the fieldwork period. A conceptual schematization of the subcatchment has been made, based on the available information from PUB and the fieldwork. This conceptual schematization is presented in the figure below. This conceptualization is used for the model schematization in SOBEK.

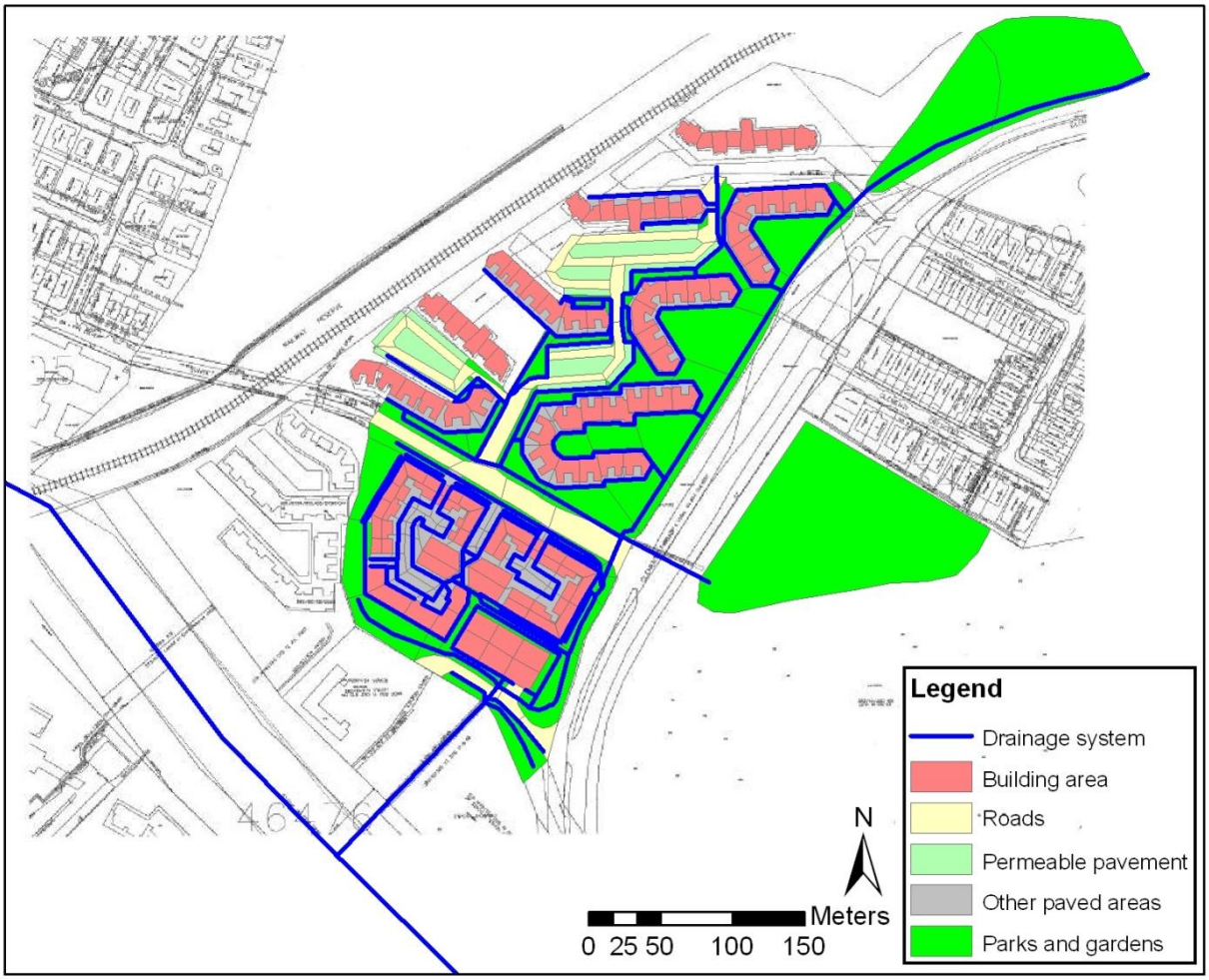

The dimension of the main outflow canal are presented in the following figure:

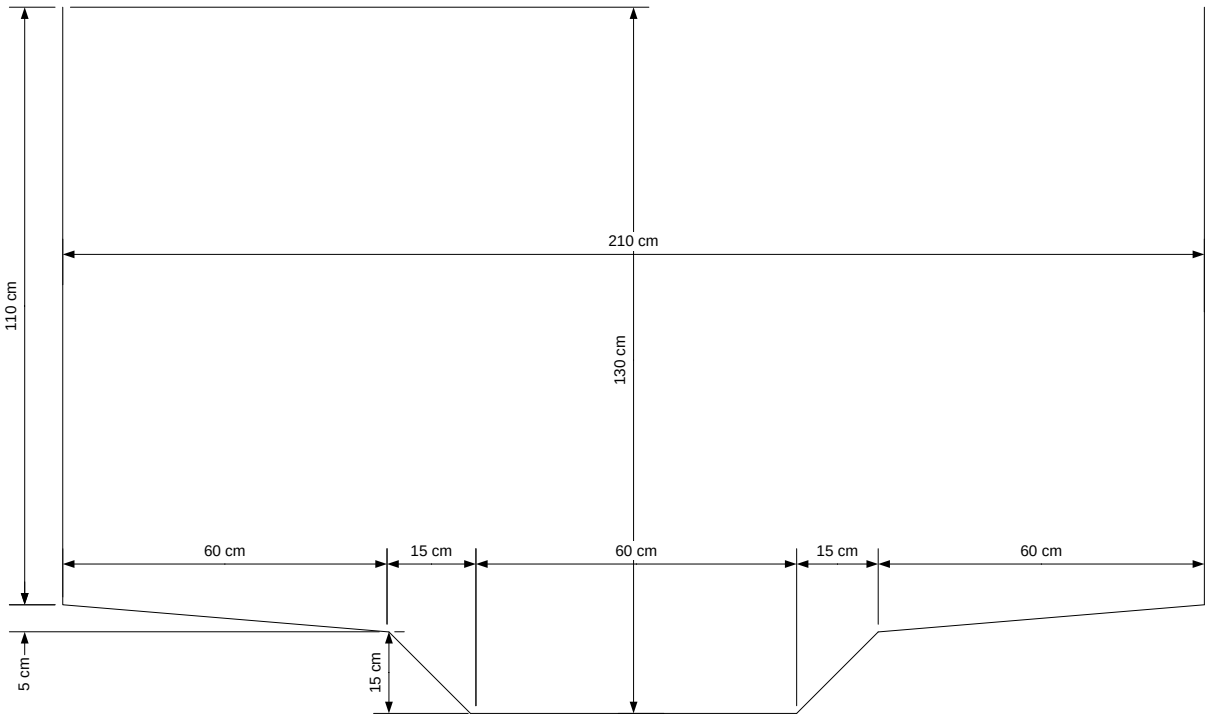

Appendix 16 Meteorological test conditions

Extreme meteorological test conditions: design storm

The following figure includes the rainfall intensities of a storm with a return period of 5 years (T=5). This design storm is used for the design of all outlet drains and secondary facilities in Singapore's catchments. The peak intensity of this design storm equals 3.1 mm/min.

Pre-processed rainfall-runoff from the validated HYDRUS model will be coupled to the SOBEK model. HYDRUS model output hydrographs were calculated for several different initial soil water contents $0.25 \leq \theta \leq 0.55$ under the design storm rainfall intensities. The influence of the initial water content is clearly visualized in the output graph of this simulation. After saturation of the green roof soil media, runoff hydrographs closely follow the design storm rainfall intensities. Even under the driest antecedent roof conditions, a 12 cm extensive green roofs is not able to retain enough water to effectively reduce or delay the peak discharge of the design storm.

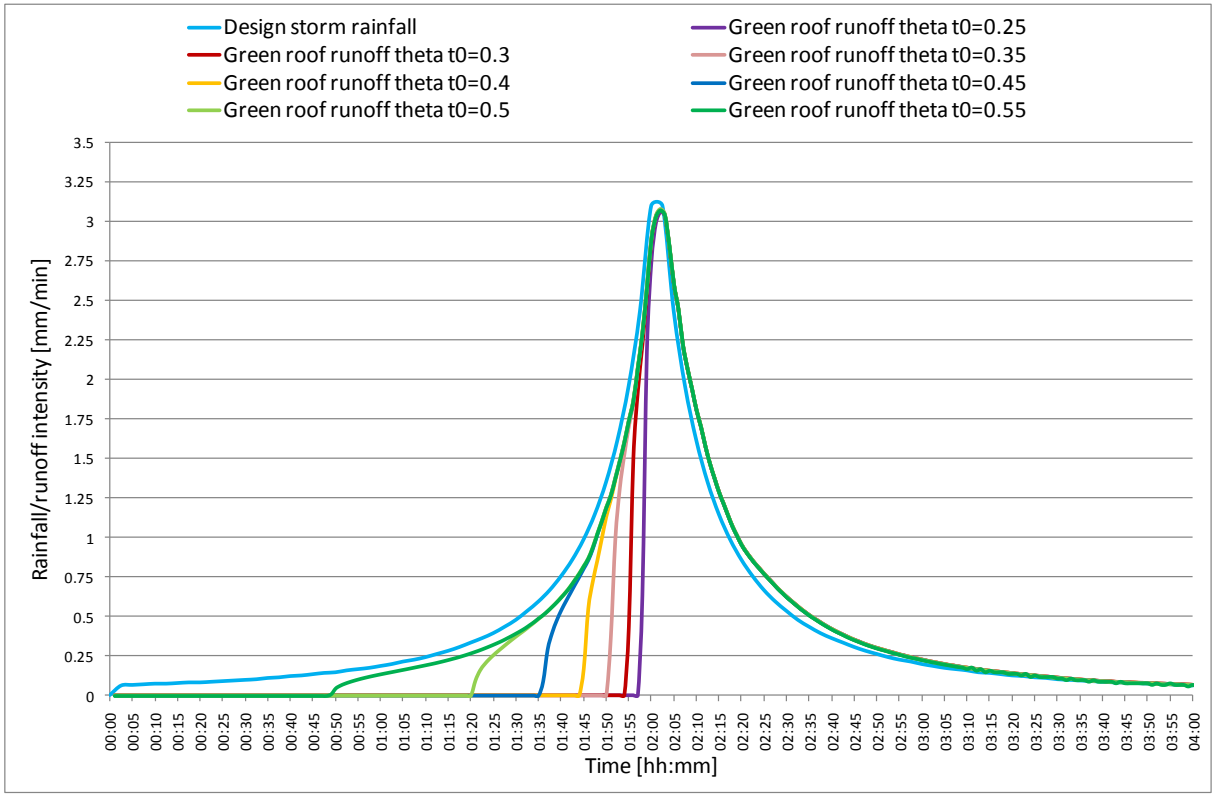

Extreme meteorological test conditions: November 19, 2009 flood storm

At November 19, 2009 97 mm of rain was measured between 13:11 and 17:45. During this 3.5 hours event, peak rainfall intensities raised up to 3 mm/min and caused floods in several parts of Singapore. Again the rainfall intensities and the pre-processed green roof runoff from HYDRUS are presented in one figure. Green roof model simulations were run under measured meteorological conditions from November 12 onwards in order to fulfil the run-in period requirement of the model simulations. Cumulative green roof outflow q_c for this event equals 95.3 mm. A 4.62 mm rain event on November 17 and a 5.89 mm rain event on November 18 decreased the green roof storage potential, prior to the flood storm of November 19, to 1.7 mm. When the soil water content at the bottom of the roof reaches the value of the seepage face at $\theta(h)$ = -12 cm, green roof runoff delays

are reduced up to 1-2 minutes, relative to the rainfall intensities. Just as for the design storm, green roof runoff intensity then closely follows the rainfall intensity.